



Ectonucléotidases, adénosine et transmission synaptique

Marie Gleizes

► To cite this version:

Marie Gleizes. Ectonucléotidases, adénosine et transmission synaptique. Neurosciences [q-bio.NC]. Université Paul Sabatier - Toulouse III, 2017. Français. NNT : 2017TOU30306 . tel-01929938

HAL Id: tel-01929938

<https://theses.hal.science/tel-01929938>

Submitted on 21 Nov 2018

HAL is a multi-disciplinary open access archive for the deposit and dissemination of scientific research documents, whether they are published or not. The documents may come from teaching and research institutions in France or abroad, or from public or private research centers.

L'archive ouverte pluridisciplinaire **HAL**, est destinée au dépôt et à la diffusion de documents scientifiques de niveau recherche, publiés ou non, émanant des établissements d'enseignement et de recherche français ou étrangers, des laboratoires publics ou privés.



THÈSE

En vue de l'obtention du

DOCTORAT DE L'UNIVERSITÉ DE TOULOUSE

Délivré par :

Université Toulouse 3 Paul Sabatier (UT3 Paul Sabatier)

Présentée et soutenue par :
Marie Gleizes

le 22 Novembre 2017

Titre :

Ectonucléotidases, adénosine et transmission synaptique

École doctorale et discipline ou spécialité :
ED CESCO : Neurosciences, comportement et cognition

Unité de recherche :
Centre de recherche Cerveau et Cognition - UMR 5549

Directeur/trice(s) de Thèse :
Lionel NOWAK - Centre de recherche Cerveau et Cognition
Caroline FONTA - Centre de recherche Cerveau et Cognition

Jury :
Myriam ERMONVAL - Institut Pasteur - Rapporteur
Paul SALIN - Centre de recherche en Neurosciences de Lyon - Rapporteur
Bruno CAULI - Institut de Biologie Paris Seine - Examinateur
Bernard FRANCES - Centre de recherches sur la Cognition animale - Président du jury
Lionel NOWAK - Centre de recherche Cerveau et Cognition - Directeur de thèse
Caroline FONTA - Centre de recherche Cerveau et Cognition - Directrice de thèse

THÈSE

En vue de l'obtention du

DOCTORAT DE L'UNIVERSITÉ DE TOULOUSE

Délivré par :

Université Toulouse 3 Paul Sabatier (UT3 Paul Sabatier)

Présentée et soutenue par :
Marie Gleizes

le 22 Novembre 2017

Titre :

Ectonucléotidases, adénosine et transmission synaptique

École doctorale et discipline ou spécialité :
ED CESCO : Neurosciences, comportement et cognition

Unité de recherche :
Centre de recherche Cerveau et Cognition - UMR 5549

Directeur/trice(s) de Thèse :
Lionel NOWAK - Centre de recherche Cerveau et Cognition
Caroline FONTA - Centre de recherche Cerveau et Cognition

Jury :
Myriam ERMONVAL - Institut Pasteur - Rapporteur
Paul SALIN - Centre de recherche en Neurosciences de Lyon - Rapporteur
Bruno CAULI - Institut de Biologie Paris Seine - Examinateur
Bernard FRANCES - Centre de recherches sur la Cognition animale - Président du jury
Lionel NOWAK - Centre de recherche Cerveau et Cognition - Directeur de thèse
Caroline FONTA - Centre de recherche Cerveau et Cognition - Directrice de thèse

REMERCIEMENTS

Je souhaite tout d'abord remercier mes deux directeurs de thèse Lionel Nowak et Caroline Fonta. Merci pour m'avoir donné ma chance en m'acceptant comme stagiaire M2 et pour m'avoir permis de continuer en thèse. Merci pour tous vos conseils, votre disponibilité, merci d'avoir cru en moi. En bref, merci pour tout !

Je remercie Myriam Ermonval et Paul Salin pour avoir accepté le travail de rapporteurs pour cette thèse. Merci également à Bruno Cauli et Bernard Francès pour avoir accepté de faire partie de mon jury de thèse.

Merci à Fanny, ma super collègue de bureau, pour avoir supporté mon caractère de râleuse pendant 3 ans. Merci pour ta bonne humeur permanente, pour la glue sur les mains, pour les debriefs de Game of Thrones, pour ce fameux marquage au Crésyl Violet qui restera gravé dans ma mémoire et bien d'autres choses. Il faudrait bien plus de trois lignes pour résumer ces trois années avec toi !

Merci aussi à Max et Anne-Claire pour tous les fous rires que nous avons pu avoir entre midi et deux et à bien d'autres moments.

Merci à Camille et Emilie pour tous leurs conseils et leur aide sur la gestion d'une lignée de souris. Merci Emilie de m'avoir aidée avec les extractions d'ADN ces derniers mois. Merci aussi à Marie et Céline pour leur aide avec les souris.

Merci aux étudiants du Cerco pour les moments de détente et de convivialité ainsi qu'à tous mes amis pour leur soutien.

Un immense merci à mes parents, mon petit frère, ma grand-mère, ma cousine et à Marco pour leur soutien inconditionnel, merci d'avoir toujours cru en moi.

« Merci » à Microsoft Windows qui a rajouté du challenge dans l'écriture de ce manuscrit en choisissant toujours le meilleur moment pour me faire le « Blue screen of Death ». J'ai retenu la leçon Microsoft, je sauvegarde le moindre mot tapé maintenant !

J'ai passé trois années formidables, un grand merci à tous !

LISTE DES ABREVIATIONS

AC	Adénylate cyclase
ACP	Déoxyadenosine 5'- monophosphonate
ADA	Adénosine déaminase
AdK	Adénosine kinase
ADK	Adénylate kinase
ADO	Adénosine
ADP	Adénosine diphosphate
AMP	Adénosine monophosphate
AMPA	Acide α -amino-3-hydroxy-5-methyl-4-isoxazolepropionic (« α -amino-3-hydroxy-5-methyl-4-isoxazolepropionic acid »)
AMPc	Adénosine monophosphate cyclique
AOPCP	$\alpha\beta$ -méthylène-ADP
aPC	Cortex piriforme antérieur (« anterior piriform cortex »)
ATP	Adénosine triphosphate
CD73	Cluster of différenciation 73
CGL	Cystathionine gamma lyase
CMP	Cytidine monophosphate
cN-I	Nucléotidase cytosolique I ("cytosolic nucleotidase I")
CNT	Transporteur concentratif de nucléoside (« concentrative nucleoside transporter »)
CPA	Cyclopentyladénosine
CPT = 8-CPT	8-cyclopentyl-1,3-dimethylxanthine
DAG	Diacylglycérol
DPCPX	8-cyclopentyl-1,3-dipropylxanthine
ENT	Transporteur équilibratif de nucléosides (« equilibrative nucleoside transporter »)
FSCV	Voltamétrie cyclique à scan rapide (« Fast-scan cyclic voltammetry »)
GABA	Acide γ -aminobutyrique (« γ -aminobutyric acid »)
GAD65	Acide glutamique décarboxylase 65 (« Glutamic acid decarboxylase 65 »)
GAD67	Acide glutamique décarboxylase 67 (« Glutamic acid decarboxylase 67 »)
GMP	Guanosine monophosphate
GPI	Glycosylphosphatidylinositol

GTP	Guanosine triphosphate
HEK	Lignée cellulaire de rein humain (« Human embryonic kidney »)
HPP	Hypophosphatasie
IL-1 β	Interleukine-1 β
IL-6	Interleukine-6
IMP	Inosine monophosphate
IP3	Inositol-3-phosphate
KO	Knock-Out
LCRa	Liquide céphalo-rachidien artificiel
LFP	Potentiel de champs locaux (« Local field potential »)
LOT	Lateral olfactory tract (voir TOL)
NAA	N-acétylaspartate
NAAG	N-acétyl-aspartyglutamate
NBMPR	S-6-(4-nitrobenzyl)mercaptopurine riboside
NBTI	S-(4-Nitrobenzyl)-6-thioinosine
NCS-1	Neuronal calcic sensor-1
NDPK	Nucléoside diphosphate kinase
NMDA	N-méthyl-D-aspartate
NPPase	Nucléotide pyrophosphatase/phosphodiesterase
NT5E	Ecto-5'-nucléotidase
NTPDase	Nucléoside triphosphate diphosphohydrolase
PAP	Prostatic acid phosphatase
PE	Phosphoéthanolamine
Pi	Phosphate inorganique
PIP2	Phosphatidyl-inositol-2-phosphate
PK	Protéine Kinase
PKA	Protéine Kinase A
PKC	Protéine Kinase C
PL	Pyridoxal
PLC	Phospholipase C
PLP	Pyridoxal-5'-phosphate
PNP	Purine nucléoside phosphorylase
pNP-TMP	p-nitrophényl-tri-monophosphate
PPADS	Pyridoxal-phosphate-6-azophényl-2',4'-disulfonate
pPC	Cortex piriforme postérieur (« posterior piriform cortex »)

PPD	Dépression par paire de pulse (« Paired pulse depression »)
PPF	Facilitation par paire de pulse (« Paired pulse facilitation »)
PPi	Pyrophosphate inorganique
PTP	Potentialisation post-tétanique (« Post tetanic potentiation »)
RB2	Reactive Blue 2
RE	Réticulum endoplasmique
REM	Mouvement oculaire rapide (« Rapid eye movement »)
RMN	Résonnance magnétique nucléaire
SAH	S-adénosyl-homocystéine
SAHH	S-adénosyl-homocystéine hydrolase
SAM	S-adénosyl-méthionine
shRNA	Short hairpin ribonucleic acid
SL	Cellule semi-lunaire
SP	Cellule semi-pyramide
STD	Dépression à court terme (« Short term depression »)
STP	Plasticité à court terme ("Short term plasticity")
TCA	Cycle des acides tricarboxyliques (« Tricarboxylic cycle acid »)
TNAP	Phosphatase alcaline non spécifique des tissus (« Tissue Nonspecific Alkaline Phosphatase »)
TOL	Tractus olfactif latéral (voir LOT)
UDP	Uridine diphosphate
UTP	Uridine triphosphate
VNUT	Transporteur vésiculaire de nucléoside (« Vesicular nucleoside transporter »)
XO	Xanthine oxydase

REMERCIEMENTS

LISTE DES ABREVIATIONS

TABLE DES MATIERES

CHAPITRE I : INTRODUCTION GENERALE.....	1
I. L'ADÉNOSINE DANS LE SYSTÈME NERVEUX CENTRAL : FORMATION, TRANSPORT, MÉTABOLISME ET SIGNALISATION.....	3
A. <i>Formation d'adénosine intracellulaire</i>	4
1. A partir des nucléotides.....	4
2. A partir de S-adénosylhomocystéine	4
B. <i>Formation extracellulaire d'adénosine à partir d'ATP extracellulaire</i>	5
1. Libération d'ATP extracellulaire.....	5
2. Les récepteurs à l'ATP	8
a. <i>Les récepteurs P2X.....</i>	8
b. <i>Les récepteurs P2Y.....</i>	12
3. Les ectonucléotidases.....	17
a. <i>Les ecto-nucléosides triphosphates diphosphohydrolases (E-NTPDases)</i>	17
b. <i>Les ecto-nucléotides pyrophosphatases/ phosphodiesterases (E-NPPases) ...</i>	19
c. <i>L'ecto-5'-nucléotidase (NT5E)</i>	20
d. <i>La phosphatase alcaline non spécifique des tissus (TNAP)</i>	22
C. <i>Le transport de l'adénosine</i>	26
1. Les transporteurs de nucléosides équilibratifs (ENT)	26
2. Les transporteurs de nucléosides concentratifs (CNT)	27
D. <i>Le métabolisme de l'adénosine</i>	28
E. <i>Les récepteurs à l'adénosine.....</i>	29
1. Le récepteur A1	31
2. Le récepteur A2a	33
3. Le récepteur A2b	34
4. Le récepteur A3	35
II. ADÉNOSINE ET PLASTICITÉ SYNAPTIQUE À COURT TERME	37
A. <i>La plasticité synaptique à court terme</i>	39
1. La facilitation synaptique à court terme	40
a. <i>Les mécanismes de la facilitation à court terme</i>	40
• <i>Hypothèse du calcium résiduel.....</i>	40

• Saturation des tampons calciques endogènes.....	42
• Senseurs calciques	42
b. Augmentation et potentialisation post-tétanique (PTP).....	43
2. La dépression synaptique à court terme.....	44
a. Les mécanismes présynaptiques de la dépression synaptique	45
• Diminution du stock de vésicules.....	45
• Inactivation des sites de libération.....	45
• Diminution de l'influx calcique.....	45
b. Les mécanismes postsynaptiques de la STD	46
• Désensibilisation des récepteurs postsynaptiques.....	46
3. Les rôles de la plasticité synaptique à court terme	48
4. Les modèles phénoménologiques de la plasticité à court terme.....	49
<i>B. Les effets de l'adénosine sur la plasticité synaptique à court terme.....</i>	51
III. OBJECTIFS DE LA THÈSE ET APPROCHES EXPÉRIMENTALES	52
A. <i>Les objectifs de la thèse</i>	52
B. <i>Les approches expérimentales.....</i>	54
1. Approche métabolomique sur des souris KO pour la TNAP	54
2. Approche électrophysiologique et pharmacologique dans le cortex piriforme de souris wild-type <i>in vitro</i>	55
a. <i>Le cortex piriforme</i>	55
• Pourquoi avoir choisi cette structure d'étude ?	55
• Structure du cortex piriforme	56
• Plasticité dans le cortex piriforme	59
b. <i>Pharmacologie</i>	59
c. <i>Plasticité synaptique à court terme in vitro</i>	59
CHAPITRE III : LES TRAVAUX DE LA THESE	61
A. <i>Identification of altered brain metabolites associated with TNAP activity in a mouse model of hypophosphatasia using untargeted NMR-based metabolomics analysis.</i>	
<i>Thomas Cruz, Marie Gleizes, Stéphane Balayssac, Etienne Mornet, Grégory Marsal, José Luis Millán, Myriam Malet-Martino, Lionel G Nowak, Véronique Gilard, Caroline Fonta. Journal of neurochemistry. 2017;140(6):919-940.....</i>	61
1. Résumé	61
2. Article.....	62

<i>B. Unexpected effect of TNAP and NT5E inhibition suggest that AMP acts as a A1 receptor agonist in the mouse piriform cortex. Marie Gleizes, Caroline Fonta, Lionel G. Nowak. En préparation.</i>	85
1. Résumé	85
2. Article.....	85
<i>C. Prominent facilitation at beta and gamma frequency range revealed with physiological calcium concentration in adult mouse piriform cortex in vitro. Marie Gleizes, Simon P. Perrier, Caroline Fonta, Lionel G. Nowak. PLoS One. 2017;12(8):e0183246.</i>	118
1. Résumé	118
2. Article.....	119
<i>D. Effect of adenosine on short-term plasticity in mouse piriform cortex in vitro: adenosine acts as a high-pass filter. Simon P. Perrier, Marie Gleizes, Caroline Fonta, Lionel G. Nowak. En préparation.</i>	149
1. Résumé	149
2. Article.....	150
CHAPITRE IV : DISCUSSION GENERALE ET PERSPECTIVES.....	171
<i>A. Etude métabolomique</i>	171
<i>B. Etudes électrophysiologiques et pharmacologiques</i>	175
1. Etude de la contribution de la TNAP dans la synthèse d'adénosine dans le cortex piriforme chez la souris adulte.....	175
2. Etude de l'influence du calcium extracellulaire sur la transmission synaptique et sur la plasticité synaptique à court terme dans le cortex piriforme chez la souris adulte.....	182
3. Etude de l'influence de l'adénosine extracellulaire sur la plasticité synaptique à court terme dans le cortex piriforme chez la souris adulte.....	185
CHAPITRE V : CONCLUSION.....	189
CHAPITRE VI : REFERENCES BIBLIOGRAPHIQUES	200
RESUME	

CHAPITRE I : INTRODUCTION GENERALE

Depuis plusieurs années, un des sujets d'étude de l'équipe est l'analyse des fonctions de la phosphatase alcaline non spécifique des tissus (TNAP) dans le système nerveux central. Des mutations du gène qui codent pour cette enzyme chez l'homme conduisent à une maladie: l'hypophosphatasie. Cette maladie est caractérisée par des défauts de minéralisation osseuse, voire selon les mutations, à des crises d'épilepsie sévères conduisant à la mort. Or la TNAP est aussi présente dans le cerveau notamment dans les cellules neuronales chez le rongeur et le primate. A partir du modèle souris KO, la TNAP participe indirectement à la synthèse de divers neurotransmetteurs dont le GABA. La survenue des crises d'épilepsie serait donc due à un défaut dans la synthèse de GABA. Par ailleurs, la TNAP a une fonction d'ectonucléotidase qui lui confère la propriété de déphosphoryler les nucléotides extracellulaires. Cependant, dans le système nerveux, peu d'informations sont disponibles concernant le rôle d'ectonucléotidase de la TNAP. Si tel est le cas, la TNAP pourrait déphosphoryler l'ATP, l'ADP et l'AMP en adénosine. Etant donné son rôle d'inhibiteur présynaptique, l'absence d'adénosine pourrait contribuer à l'apparition des crises d'épilepsie chez les patients hypophosphatasiques par son rôle anticonvulsivant.

Le but de cette thèse est d'identifier, d'une part, si la TNAP est impliquée dans la production d'adénosine dans le cerveau chez la souris avec deux approches complémentaires : une approche métabolomique et une approche électrophysiologique. D'autre part, étudier l'influence de l'adénosine sur la plasticité synaptique de manière à examiner, en miroir, les effets que pourraient entraîner une mutation de la TNAP au niveau fonctionnel.

Dans ce premier chapitre, je développerai les différentes voies et mécanismes conduisant à la présence d'adénosine dans le milieu extracellulaire ainsi que la signalisation associée à ce neuromodulateur (Partie I). Dans la partie II, j'exposerai les différents mécanismes impliqués dans la plasticité synaptique à court terme ainsi que les effets de l'adénosine dans ce type de plasticité

synaptique. La partie III sera consacrée aux objectifs de la thèse et à la présentation des approches expérimentales utilisées afin de répondre aux diverses questions que nous nous sommes posées.

Dans le chapitre II, chaque article sera constitué d'un bref résumé et du manuscrit associé. Ils seront ensuite discutés dans le chapitre III. Pour finir, je conclurai sur l'ensemble des travaux énoncés dans cette thèse dans le chapitre IV.

I. L'ADENOSINE DANS LE SYSTEME NERVEUX CENTRAL : FORMATION, TRANSPORT, METABOLISME ET SIGNALISATION.

L'adénosine joue un rôle central en tant qu'élément de base des acides nucléiques et des molécules de stockage de l'énergie ; elle est le produit de diverses enzymes et c'est un modulateur de l'activité cellulaire. Les effets physiologiques de l'adénosine ont été décrits pour la première fois au niveau du système cardiovasculaire : Drury et Szent-Györgyi (1929) ont mis en évidence une diminution du rythme cardiaque, de la pression artérielle ainsi qu'une dilatation des vaisseaux artériels suite à une injection intraveineuse d'adénosine chez les mammifères.

L'adénosine est produite de façon continue, aussi bien dans le milieu intracellulaire que dans le milieu extracellulaire, essentiellement à partir d'ATP dont le rôle n'est pas uniquement de fournir l'énergie nécessaire au métabolisme des cellules. Ainsi, l'ATP peut être déphosphorylée en ADP, AMP et adénosine par diverses ectonucléotidases présentes à la surface des cellules. La concentration en adénosine extracellulaire est estimée entre 30-300 nM (Latini et Pedata, 2001) et est sensiblement équivalente dans le milieu intracellulaire puisque la plupart des cellules expriment des transporteurs de l'adénosine dits équilibratifs (*voir paragraphe C*).

L'adénosine active des récepteurs purinergiques P1 dont quatre sous-types ont été décrits (A1, A2a, A2b et A3). Dans le système nerveux central, la principale voie par laquelle l'adénosine contrôle les fonctions nerveuses en conditions physiologiques concerne le contrôle de la libération des neurotransmetteurs (Fredholm et al., 2005). En effet, l'activation des récepteurs A1 provoque une inhibition de la libération des neurotransmetteurs tandis que l'activation des récepteurs A2a facilite la libération des neurotransmetteurs. L'adénosine joue ainsi un rôle dans diverses fonctions cérébrales telles que la régulation du cycle sommeil/éveil via l'activation des récepteurs A1 et A2a, tous deux impliqués dans l'induction du sommeil. De plus, en modulant les mécanismes de plasticité synaptique que je détaillerai dans la partie B, l'adénosine contribue aux processus de mémoire et d'apprentissage. L'adénosine est impliquée dans les maladies neurodégénératives telles que la maladie d'Alzheimer, la maladie de Parkinson ou bien la chorée

de Huntington. L'activation du récepteur A1 induisant la production du précurseur soluble du peptide amyloïde et la phosphorylation de la protéine tau ainsi que la présence de ce récepteur au niveau des structures touchées dans cette maladie neurodégénérative suggère que le récepteur A1 joue un rôle dans la pathogenèse de la maladie d'Alzheimer (Angulo et al., 2003). Dans le cas de la maladie de Parkinson, c'est le récepteur A2a qui semble impliqué puisqu'il interagit négativement avec le récepteur à la dopamine D2 (Ongini et Fredholm, 1996)

A. Formation d'adénosine intracellulaire

1. A partir des nucléotides

Au niveau des terminaisons nerveuses, l'ATP peut être formée à partir du glucose capturé dans le milieu extracellulaire, à partir du cycle de l'acide citrique (TCA) et de la glycolyse. Mais l'essentiel de la synthèse de l'ATP se fait via des phosphorylations oxydatives dans les mitochondries (cycle de la respiration mitochondriale). Ainsi, la concentration d'ATP dans le cytoplasme s'élève entre 5 à 10 mM en condition physiologique (Dunwiddie et Masino, 2001 ; Sperlagh et Vizi, 2011). L'ATP ainsi produite est transportée hors de la mitochondrie par des transporteurs de nucléotides. L'ATP est ensuite dégradée par des ATPases en ADP et en AMP par des ADPases (Figure 1). L'AMP est ensuite déphosphorylée en adénosine via une 5'-nucléotidase intracellulaire : la nucléotidase cytosolique I, cN-I (Sala-Newby et al., 1999).

2. A partir de S-adénosylhomocystéine

L'adénosine peut également être produite dans le milieu intracellulaire via le cycle de la méthionine. La méthionine est convertie en S-adénosyl-homocystéine (SAH) au moyen de diverses transférases (Figure 1). La SAH est ensuite hydrolysée en adénosine et homocystéine par la S-adénosyl-homocystéine hydrolase (SAHH) (Broch and Ueland, 1980). Cependant, que ce soit en condition physiologique ou pathologique, lors de l'ischémie par exemple, cette voie ne

contribuerait que marginalement à la production d'adénosine dans le cerveau (Latini et Pedata, 2001).

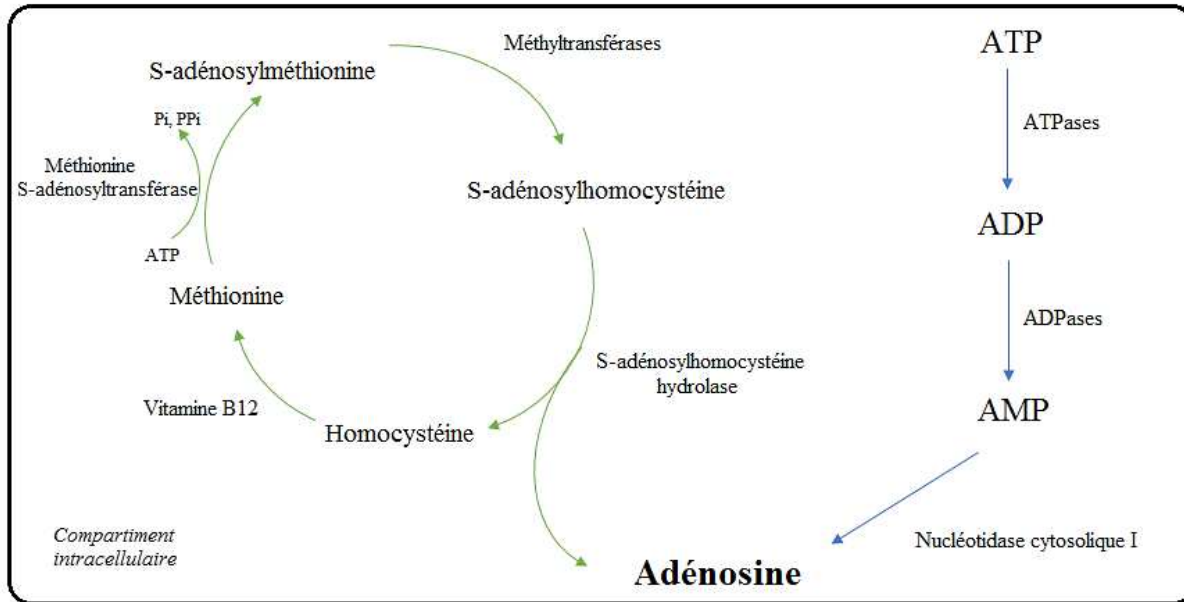


Figure 1 : Schéma récapitulatif de la production d'adénosine intracellulaire. L'adénosine intracellulaire provient en majorité de la dégradation d'ATP intracellulaire (en bleu) mais peut également être produite par le cycle de la méthionine (en vert).

B. Formation extracellulaire d'adénosine à partir d'ATP extracellulaire

L'adénosine peut être libérée en tant que telle par des transporteurs spécifiques (*voir paragraphe C*) au niveau neuronal (Lovatt et al., 2012) et indirectement à partir du métabolisme de l'ATP extracellulaire au niveau neuronal (Pankratov et al., 2007) et glial (Pascual et al., 2005) dont la concentration extracellulaire est de l'ordre du micromolaire (Barsotti et Ipata, 2004). Wall et Dale (2013) ont démontré que ces deux voies contribuent de manière équivalente à la présence d'adénosine au niveau du milieu extracellulaire dans l'hippocampe chez la souris.

1. Libération d'ATP extracellulaire

La libération d'ATP au niveau extracellulaire peut avoir lieu aussi bien au niveau neuronal qu'au niveau glial dont le mécanisme le plus connu est la libération par exocytose dépendante du

calcium (Pankratov et al., 2006). Au niveau neuronal, l'ATP est stockée dans des vésicules de sécrétion synaptiques par l'intermédiaire de transporteurs vésiculaires de nucléotides d'acide nucléiques VNUT (Sawada et al., 2008). Ce transporteur utilise le gradient électrochimique de la pompe à proton H+/ATPase afin de faire entrer l'ATP cytosolique dans la vésicule synaptique (Figure 2) (Lazarowski, 2012). L'ATP peut être stockée dans des vésicules propres ou dans des vésicules mixtes en présence d'autres neurotransmetteurs tels que le glutamate et le GABA (Fields et Stevens, 2000).

L'ATP des astrocytes a plusieurs origines. D'une part, il peut provenir de la recapture du glutamate par les astrocytes au niveau de la fente synaptique via des transporteurs dépendants du sodium et de la synthèse *de novo* du glutamate à partir de glucose. Par la suite, le glutamate est converti en glutamine ou incorporé au cycle des acides tricarboxyliques (TCA) où il va subir diverses réactions (oxydation, régénération ou une dégradation complète) (Dienel, 2013). Par exemple, la dégradation complète du glutamate produit 20 fois plus d'ATP que ce qu'il est nécessaire pour son entrée dans l'astrocyte (Anderson et Swanson, 2000). D'autre part, la production d'ATP dans les astrocytes peut se faire via la glycolyse. Le glucose entre dans les astrocytes via un transporteur (GLUT1) où il est métabolisé en pyruvate par la glycolyse. Le pyruvate entre dans le cycle TCA où il est à son tour métabolisé pour produire de l'ATP (Pellerin et Magistretti, 1994).

La libération de l'ATP par les neurones se fait par la fusion des vésicules à la membrane présynaptique dont le mécanisme repose sur l'association des protéines du complexe SNARE, composé de diverses protéines, et sous l'induction d'un influx calcique (Stout et al., 2002).

Tout comme les neurones, il a été montré que les astrocytes expriment également le complexe SNARE nécessaire à la libération vésiculaire de l'ATP (Zhang et al., 2004). En revanche, la libération d'ATP par les astrocytes est distincte de la libération du glutamate (Zhang et al., 2007). Au niveau glial, l'ATP peut également être libéré par des mécanismes non vésiculaires (Figure 2) comme par exemple, via des canaux chlore en réponse à un étirement de la membrane plasmique de cellules telles qu'un gonflement osmotique (Lazarowski, 2012), via des transporteurs de type

ATP binding cassette (Abraham et al., 1993) ; ou encore via les récepteurs P2X7 qui lorsqu'ils sont activés de façon prolongée se convertissent en un pore non sélectif perméable à diverses molécules y compris l'ATP (Suadicani et al., 2006).

Les connexines et les pannexines sont également impliquées dans la libération non vésiculaire d'ATP (Scemes et al., 2009). En effet, les connexines peuvent s'assembler pour former un hémicanal perméable à l'ATP (Kang et al., 2008). La libération d'ATP par les astrocytes via les connexines se fait en réponse à une diminution de la concentration en calcium dans le milieu extracellulaire (Cotrina et al., 1998). Tout comme les connexines, les pannexines s'assemblent pour former un canal qui lui aussi est perméable à l'ATP. L'activation du récepteur P2X7 par l'ATP entraîne un efflux rapide d'ions K⁺ responsables de l'ouverture du pore formé par la pannexine-1 (Pelegrin et Surprenant, 2006).

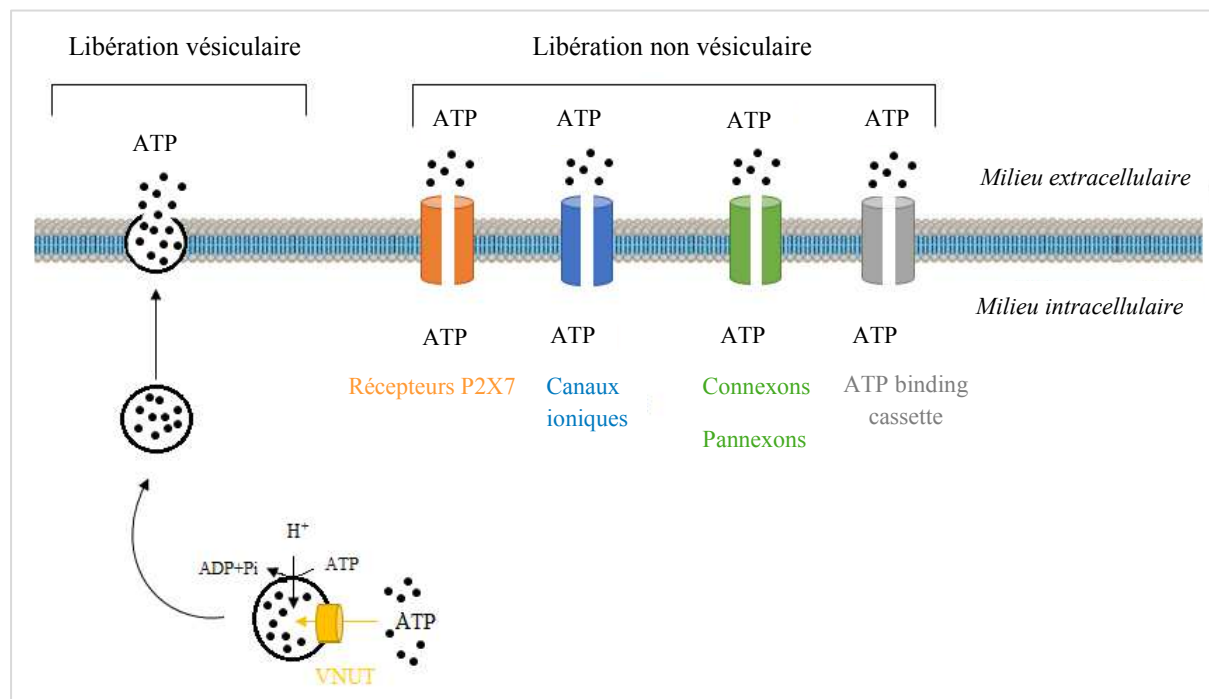


Figure 2 : Schéma récapitulatif des différents acteurs impliqués dans la libération de l'ATP au niveau neuronal et glial. L'ATP peut être libérée dans le milieu extracellulaire de façon vésiculaire ou de façon non vésiculaire par l'intermédiaire de récepteurs P2X7, de canaux ioniques, de connexons et pannexons ou via le transporteur ATP binding cassette.

2. Les récepteurs à l'ATP

Une fois libérée, l'ATP va agir sur des récepteurs purinergiques de type P2X et /ou P2Y présents à la surface des neurones et des cellules gliales (Ralevic et Burnstock, 1998). Les récepteurs P2 sont divisés en deux classes selon que ce sont des récepteurs de types canaux ioniques (P2X) ou qu'ils sont couplés à des protéines G (P2Y) (Abbrachio et Burnstock, 1994). Le Reactive Blue 2, la suramine et le PPADS (Pyridoxal-phosphate-6-azophényl-2', 4'-disulfonate) sont des antagonistes non sélectifs des récepteurs P2X et P2Y et inhibent les courants induits par l'ATP.

a. Les récepteurs P2X

Sept récepteurs P2X (P2X1 à P2X7) ont été clonés et caractérisés chez les mammifères (Ralevic et Burnstock, 1998). Ce sont des récepteurs de type canaux cationiques, perméables aux ions Na^+ , K^+ , Ca^{2+} , dont l'ATP est l'agoniste principal. De manière générale, l'activation des récepteurs suite à la fixation de l'ATP conduit à une augmentation de la concentration en calcium intracellulaire et à la dépolarisation de la cellule (Bean, 1992). C'est un mécanisme de transduction dont la réponse est très rapide (de l'ordre de la milliseconde) puisqu'elle ne nécessite pas la production de messagers secondaires. Par conséquent, ce type de récepteur induit une transmission excitatrice rapide (Bean, 1992). Le tableau 1 récapitule les principales caractéristiques des récepteurs P2X.

Le récepteur P2X1 est exprimé dans diverses structures du système nerveux central chez le rat : l'hippocampe, le cervelet, la moelle épinière, le cortex cérébral et plus précisément dans les neurones pyramidaux des couches V et VI (Florenzano et al., 2008). En revanche, aucune activité n'a été détectée dans le cortex piriforme que ce soit au niveau des fibres ou au niveau des neurones. Ce récepteur jouerait un rôle dans la survie des neurones suite à une lésion du cervelet (Florenzano et al., 2002).

Les récepteurs P2X2, P2X4 et P2X6 sont les sous-types les plus abondants puisqu'ils sont exprimés dans la plupart des structures du cerveau (bulbe olfactif, cortex cérébral, hippocampe, noyau supraoptique, hypothalamus, cervelet, striatum), dans la moelle épinière où ils sont exprimés au niveau postsynaptique, les ganglions du système sensoriel (ganglion trijumeau, ganglion cochléaire, ganglions de la moelle épinière) et au niveau des ganglions autonomes (Nörenberg et Iles, 2000). Les récepteurs P2X2, P2X4 et P2X6 sont également exprimés par les astrocytes et le récepteur P2X4 est aussi exprimé par la microglie (Xu et al., 2016).

Le récepteur P2X3 est uniquement exprimé par certains neurones sensoriels et est absent des neurones du système nerveux central (Ralevic et Burnstock, 1998 ; Collo et al., 1996). En agissant sur le récepteur P2X3 présynaptique, l'ATP favorise la libération de glutamate (Burnstock, 2008).

La localisation du récepteur P2X5 est plus controversée. En effet, Collo et ses collaborateurs (1996) ont conclu, avec des expériences d'hybridation *in situ*, à l'absence d'ARNm du récepteur P2X5 dans le cerveau à l'exception du noyau mésencéphalique, du nerf trijumeau et de la moelle épinière. Cependant, en 2008, Guo et ses collègues ont mis en évidence la présence d'ARNm du récepteur P2X5 dans le cerveau dont la distribution correspond à l'expression de la protéine du récepteur P2X5. En effet, ils ont observé que le récepteur P2X5 est exprimé dans de nombreuses structures du cerveau : hippocampe, bulbe olfactif, cortex piriforme, cortex cérébral, thalamus, hypothalamus. Les résultats ont également confirmé ceux obtenus en 1996 (Collo et al., 1996) au niveau du noyau mésencéphalique, du nerf trijumeau et de la moelle épinière. Aux vues de la distribution de ce récepteur, il est admis que le récepteur P2X5 est impliqué dans la transmission purinergique excitatrice rapide au niveau système olfactif et au niveau de l'hippocampe (Guo et al., 2008).

Le récepteur P2X7 est souvent décrit à part des autres récepteurs P2X dû au fait que l'affinité de ce récepteur pour l'ATP est 100 fois moins élevée que pour les autres récepteurs (Surprenant et al. 1996) et qu'il soit également capable d'agir en tant que pore non-sélectif (Ralevic et Burnstock, 1998). En effet, lorsque ce récepteur est activé de façon prolongée par de fortes concentrations

en ATP, il se convertit en un pore perméable aux ions et à de petites molécules allant jusqu'à 900 Daltons y compris l'ATP. Cette augmentation de la perméabilité induit un changement drastique de la composition ionique intracellulaire des cellules. Par conséquent, une stimulation prolongée du récepteur par de fortes concentrations d'ATP conduit à la mort des cellules (Dubyak et el-Moatassim, 1993). Le récepteur P2X7 est principalement exprimé dans les cellules gliales du système nerveux central et périphérique tels que les astrocytes, les oligodendrocytes, la microglie et les cellules de Schwann (Sperlagh et al., 2006) Il a été initialement rapporté que le récepteur P2X7 est présent dans les neurones de l'hippocampe (Atkinson et al., 2002) et, entre autre, au niveau des terminaisons excitatrices de la moelle épinière (Atkinson et al., 2004). Cependant, la présence du récepteur P2X7 dans ces structures reste très controversée (Sim et al., 2004).

Récepteurs	Agoniste endogène	Localisation dans le système nerveux	Localisation cellulaire	Localisation subcellulaire (neurones)	Rôles	Références
P2X1	ATP	Cortex cérébral, hippocampe, striatum, moelle épinière, cervelet, système sensoriels	Neurones pyramidaux des couches V et VI, cellules gliales.	Pré- et postsynaptique	Survie des neurones suite à une lésion, croissance des neurites	Norenberg et Illes, 2000 ; Florenzano et al., 2002,2008.
P2X2	ATP	Bulbe olfactif, cortex cérébral (cortex piriforme), hippocampe, moelle épinière, ganglions sensoriels et autonomiques.	Neurones et astrocytes.	Pré- et postsynaptique	Transmission sensorielle, facilite la transmission excitatrice	Collo et al., 1996 ; Khakh et al., 2003 ; Kanjhan et al., 1999 ; Rubio et Soto, 2001
P2X3	ATP	Système nerveux périphérique, ganglions racines dorsales	Neurones sensoriels, neurones sympathiques	Pré- et postsynaptique	Transmission stimuli douloureux, favorise la libération de glutamate.	Ralevic et Burnstock, 1998 ; Collo et al., 1996 ; Burnstock, 2008
P2X4	ATP	Bulbe olfactif, cortex cérébral (cortex piriforme), hippocampe, moelle épinière, ganglions sensoriels et autonomiques.	Neurones, astrocytes et microglie	Pré- et postsynaptique	Facilite la transmission synaptique car perméable aux ions calcium	Norenberg et Illes, 2000 ; Collo et al., 1996 ; Xu et al., 2016 ; Baxter et al., 2011 ; Rubio et Soto, 2001
P2X5	ATP	Cortex cérébral (cortex piriforme) bulbe olfactif, hippocampe, thalamus, hypothalamus, moelle épinière	Neurones	Postsynaptique	Transmission purinergique excitatrice rapide	Guo et al., 2008
P2X6	ATP	Bulbe olfactif, cortex cérébral (cortex piriforme), hippocampe, moelle épinière, ganglions sensoriels et autonomiques.	Neurones et astrocytes	Postsynaptique	Fonctionnel si hétéromérisation avec P2X2 et P2X4	Collo et al., 1996 ; Torres et al., 1999 ; Rubio et Soto, 2001
P2X7	ATP > 100 µM	Cortex cérébral, hippocampe, noyaux thalamiques et hypothalamiques, amygdale,	Astrocytes, microglie, oligodendrocytes et cellules de Schwann.	X	Pro-inflammatoire, pro-apoptotique, augmente la libération de neurotransmetteurs excitotoxiques	Surprenant et al., 1996 ; Sperlagh et al., 2006

Tableau 1 : Principales caractéristiques des récepteurs P2X.

a. Les récepteurs P2Y

Les récepteurs P2Y sont des récepteurs couplés aux protéines G. Huit sous-types ont été identifiés : P2Y1, P2Y2, P2Y4, P2Y6, P2Y11, P2Y12, P2Y13 et P2Y14 (Ralevic et Burnstock, 1998). Les protéines G de ces récepteurs sont formées de trois sous-unités : alpha, bêta et gamma. La sous-unité alpha porte le site de liaison avec le récepteur, le site catalytique d'hydrolyse du GTP et le site de liaison avec l'adénylate cyclase (AC). Lorsque le récepteur est activé, la sous-unité alpha se libère du complexe alpha-bêta-gamma et se lie à divers effecteurs : l'adénylate cyclase, des phospholipases et des canaux Ca^{2+} et K^+ (Fredholm et al., 2005).

L'adénylate cyclase est une enzyme membranaire qui produit de l'AMP cyclique (AMPc) à partir d'ATP. L'AMPc est un messager secondaire qui active des protéines kinases (PK) lesquelles phosphorylent diverses molécules qui régulent des voies métaboliques ou la transcription de certains gènes.

La phospholipase C est une enzyme membranaire qui hydrolyse les phospholipides. Elle transforme le phosphatidyl-inositol-2-phosphate (PIP2) en diacylglycérol (DAG) et inositol-3-phosphate (IP3). L'IP3 agit au niveau des stocks intracellulaires de calcium afin de libérer du calcium qui va lui-même agir sur différentes enzymes. Le DAG, quant à lui, stimule la protéine kinase C (PKC). Selon le couplage du récepteur P2Y avec différentes catégories de protéines G, l'activité de l'effecteur (adénylate cyclase, phospholipases ou canaux) est soit stimulée, soit inhibée. Les récepteurs P2Y12, P2Y13 et P2Y14 sont couplés à une protéine Gi (Abbracchio et al, 2006) qui inhibe l'AC et assure l'ouverture des canaux potassiques (*Figure 3*). Les récepteurs P2Y1, P2Y2, P2Y4, P2Y6 et P2Y11 sont couplés à une protéine Gq qui permet l'activation de la phospholipase C et la libération de calcium à partir des stocks intracellulaires (*Figure 3*) (von Kugelgen, 2006 ; Abbracchio et al, 2006). Le tableau 2 récapitule les principales caractéristiques des récepteurs P2Y.

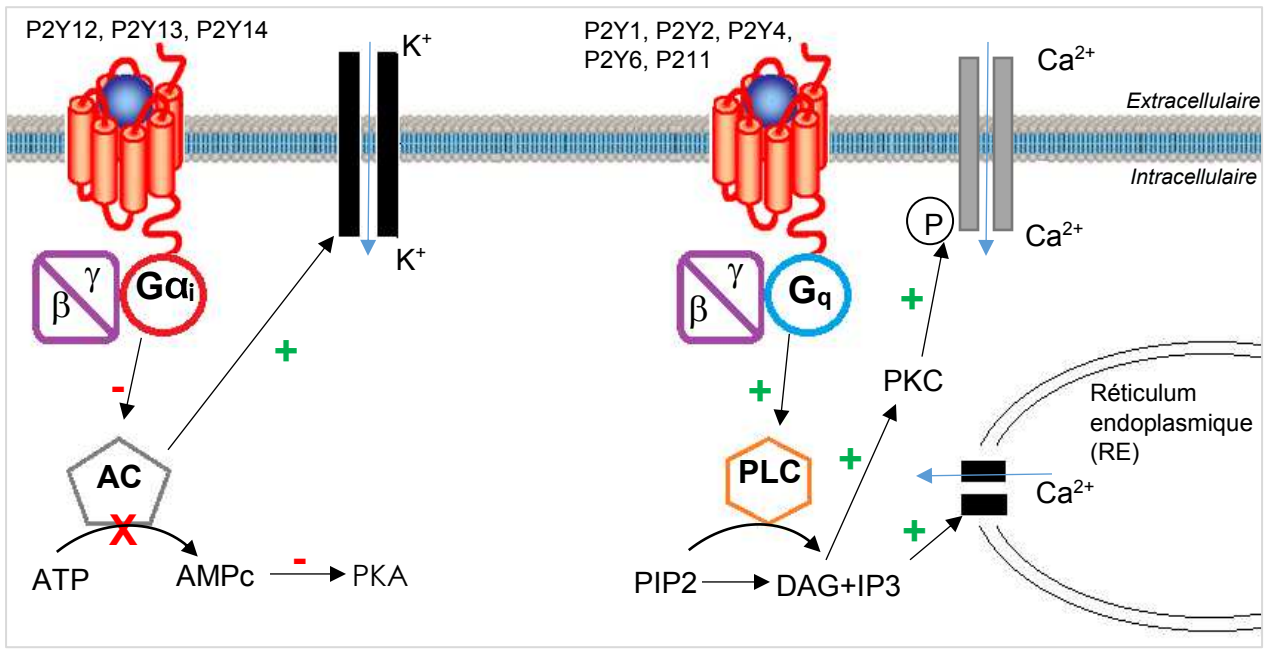


Figure 3 : Représentation schématique des mécanismes de transduction associés à chaque récepteur P2Y. A gauche, la voie de signalisation dépendante de l'AMPc. Suite à l'activation du récepteur, la protéine G_i est activée et induit une inhibition de l'adénylate cyclase (AC) limitant la production de second messager AMPc et empêchant l'activation de la protéine kinase A (PKA). Par ailleurs, l'activation de l'AC provoque l'ouverture des canaux potassiques. A droite, la voie de signalisation dépendante de l'inositol phosphate. Suite à l'activation du récepteur, la protéine G_q est activée et active la phospholipase C (PLC) induisant l'hydrolyse phosphatidyl-inositol-4-5-diphosphate (PIP2) en diacylglycérol (DAG) et inositol-3-phosphate (IP3). L'IP3 permet la libération des stocks de calcium intracellulaire via l'ouverture des canaux calciques du réticulum endoplasmique (RE). Le DAG active la protéine kinase C (PKC) qui provoque l'ouverture des canaux calciques présents au niveau de la membrane plasmique.

Les récepteurs P2Y sont activés par divers nucléotides avec des affinités différentes pour chacun des sous-types. En effet, le récepteur P2Y1 est activé par l'ADP, bien que l'ATP soit un agoniste partiel de ce récepteur. L'ADP est également l'agoniste naturel des récepteurs P2Y12 et P2Y13. Les récepteurs P2Y2 et P2Y4 sont activés par l'ATP et l'UTP avec une affinité équivalente (Abbracchio et al., 2006). Enfin, les récepteurs P2Y6 et P2Y14 sont activés par l'UDP et l'UDP-glucose, respectivement.

Le récepteur P2Y1 est présent dans diverses régions du cerveau telles que le cortex cérébral, l'hippocampe, le cervelet, le putamen, le noyau sous-thalamique et le noyau caudé (King et

Burnstock, 2002). Dans l'hippocampe, le récepteur P2Y1 est localisé au niveau des membranes pré- et postsynaptiques des synapses glutamatergiques (Tonazzini et al., 2007). Le récepteur P2Y1 est impliqué dans la modulation de la transmission synaptique puisqu'il a été montré que ce récepteur inhibe la libération de glutamate dans le cortex cérébral chez le rat (Bennett et Boarder, 2000), au niveau des synapses des collatérales de Schaffer (Mendoza-Fernandez et al., 2000) et dans les terminaisons sensorielles de la moelle épinière (Heinrich et al., 2008). Ce mécanisme d'inhibition semble être médié par le complexe $\beta\gamma$ de la protéine G du récepteur P2Y1 qui inhibe les canaux calciques dépendants du voltage (Gerevich et al., 2004). Ce récepteur est présent au niveau des astrocytes de l'hippocampe où son activation par l'ATP joue un rôle protecteur contre les dommages causés par un stress oxydatif via la libération d'interleukine-6 (Weisman et al., 2012). Il est également localisé au niveau des oligodendrocytes (Moran-Jimenez et Matute, 2000) et des cellules microgliales.

Dans le système nerveux central, le récepteur P2Y2 est localisé dans l'hippocampe, le cortex préfrontal, l'hypothalamus et la moelle épinière (Abbrachio et al., 2006). Il est exprimé dans les neurones où il est localisé au niveau postsynaptique (Choi et al., 2013), dans les astrocytes, la microglie et oligodendrocytes (Ho et al., 1995 ; Boucsein et al., 2003 ; Kirischuk et al., 1995). Au niveau des astrocytes, l'activation de ce récepteur stimule la prolifération et la migration des cellules. En effet, l'activation du récepteur P2Y2 stimule la cascade de signalisation des intégrines qui régulent la réorganisation du cytosquelette des cellules gliales ainsi que la motilité de ces cellules (Weisman et al., 2012).

Le récepteur P2Y4 est localisé dans le bulbe olfactif, le cortex cérébral, l'hippocampe, la moelle épinière et le cervelet (Song et al., 2011). Dans ces régions, le récepteur P2Y4 est exprimé par les astrocytes et au niveau présynaptique dans les neurones de l'hippocampe chez le rat où ce récepteur jouerait un rôle inhibiteur dans la libération de glutamate (Rodrigues et al., 2005).

Le récepteur P2Y6 est localisé dans l'amygdale, le noyau accumbens, le putamen et l'hippocampe où il est exprimé par les neurones pyramidaux (Weisman et al., 2012). L'activation

de ce récepteur au niveau microglial par l'UDP induit la phagocytose des neurones (Neher et al., 2014).

Chez les rongeurs, le récepteur P2Y11 ne semble pas être exprimé (Weisman et al., 2012 : Dreisig et Kornum, 2016).

Les récepteurs P2Y12, P2Y13 et P2Y14 sont essentiellement localisés au niveau des cellules gliales. En effet, le récepteur P2Y12 est localisé au niveau des oligodendrocytes et des cellules microgliales tandis que les récepteurs P2Y13 et P2Y14 sont localisés aux niveau des astrocytes (Sperlagh et al., 2007).

Récepteurs	Agoniste endogène	Localisation dans le système nerveux	Localisation cellulaire	Localisation subcellulaire (neurones)	Rôles	Références
P2Y1	ADP>ATP (agoniste partiel)	Cortex cérébral, hippocampe, cervelet, noyau caudé, putamen	Neurones et astrocytes	Pré- et postsynaptique	Inhibe la libération de glutamate et noradrénaline ; neuroprotecteur dans les astrocytes ; favorise l'elongation axonale	Guzman et al., 2005 ; Weisman et al., 2012 ; Moran-Jimenez et Matute, 2000
P2Y2	ATP=UTP	Hippocampe, hypothalamus, moelle épinière.	Neurones, astrocytes, oligodendrocytes et microglie	Pré- et postsynaptique	Inhibe la libération de glutamate ; prolifération et migration dans les astrocytes.	Choi et al., 2013 ; Weisman et al., 2012 ; Rodrigues et al., 2005
P2Y4	ATP= UTP (souris et rat)	Bulbe olfactif, cortex cérébral (cortex piriforme), hippocampe, moelle épinière et cervelet	Neurones et astrocytes	Pré- et postsynaptique	Inhibe la libération de glutamate et GABA	Song et al., 2011 ; Rodrigues et al., 2005 ; Weisman et al., 2012
P2Y6	UDP>>UTP	Amygdale, noyau accumbens, putamen, l'hippocampe,	Microglie et neurones	ND	Phagocytose des neurones par la microglie	Weisman et al., 2012 ; Neher et al., 2014
P2Y12	ADP	Hippocampe, noyau accumbens, cervelet, ganglion de la corne dorsale	Neurones oligodendrocytes et cellules microgliales	Présynaptique	Inhibe la libération de glutamate et de noradrénaline.	Sperlagh et al., 2007
P2Y13	ADP	Hippocampe, ganglion de la corne dorsale	Oligodendrocytes ; astrocytes et neurones glutamatergiques	Présynaptique	Inhibe la libération de glutamate et noradrénaline ; régule négativement l'elongation axonale	Sperlagh et al., 2007 ; del Puerto et al., 2013
P2Y14	UDP/UDP-glucose	Cortex cérébral, hippocampe, cervelet, thalamus et ganglions de la base, ganglion de la corne dorsale	Neurones et astrocytes	ND	Antinociceptif	Chambers et al., 2000 Sperlagh et al., 2007 ; Puchałowicz et al., 2014

Tableau 2 : Principales caractéristiques des récepteurs P2Y. Le récepteur P2Y11 n'est pas mentionné car il est absent chez les rongeurs. ND : information non disponible.

3. Les ectonucléotidases

L'ATP libérée dans le milieu extracellulaire peut agir directement sur les récepteurs spécifiques P2X et P2Y. L'ATP extracellulaire peut également être dégradée en ADP, AMP et adénosine par des ectonucléotidases. Il existe quatre types d'ectonucléotidases impliquées dans la production d'adénosine dans le système nerveux central : les ecto-nucléosides triphosphates diphosphohydrolases (E-NTPDases), les ecto-nucléotides pyrophosphatases phosphodiésterases (E-NPPases), l'ecto-5'- nucléotidase (NT5E) et la phosphatase alcaline non spécifique des tissus (TNAP). En fonction des enzymes, les ectonucléotidases hydrolysent les nucléosides tri-, di- et monophosphates pour générer des nucléosides diphosphates, monophosphates, de l'adénosine, du pyrophosphate (PPi) et du phosphate inorganique (Pi). Dans cette partie, je ne décrirai que les enzymes responsables de la dégradation des nucléotides extracellulaires permettant la production d'adénosine (Tableau 3).

- a. Les ecto-nucléosides triphosphates diphosphohydrolases (E-NTPDases)

NTPDases 1, 2, 3 et 8 (Zimmermann, 2001)	$\text{ATP} \rightarrow \text{ADP} + \text{Pi}$ $\text{ADP} \rightarrow \text{AMP} + \text{Pi}$
---	--

De manière générale, les NTPDases hydrolysent une grande variété de nucléotides triphosphates (ATP, UTP) et diphosphates (ADP, UDP) avec des affinités différentes et en présence de cations divalents Ca^{2+} ou le Mg^{2+} (Kukulski et al., 2005). De ce fait, les enzymes qui composent cette famille sont également appelées ATPDases, ecto-ADPases, ecto-ATPases ou encore ecto-apyrases. Le produit final des différentes réactions d'hydrolyse est un nucléoside monophosphate : l'AMP ou l'UMP. Chez les mammifères, huit gènes (Entpd chez la souris, ENTPD chez l'Homme) codent pour les protéines de la famille des NTPDases. Ce sont des enzymes membranaires dont quatre ont une orientation extracellulaire (E-NTPDase 1, 2, 3, 8),

tandis que les NTPDases 4 à 7 ont une orientation intracellulaire (Robson et al., 2006). Dans cette partie, seules les NTPDases conduisant à la formation d'AMP extracellulaire, c'est-à-dire les E-NTPDases membranaires 1, 2, 3, et 8, seront décrites (*Figure 4*).

Les E-NTPDases 1, 2, 3 et 8 peuvent être différencierées les unes des autres en fonction de leur affinité pour un substrat donné et donc du produit final de la réaction qu'elles catalysent. La NTPDase1 hydrolyse l'ATP et l'ADP avec une affinité équivalente tandis que la NTPDase3 et la NTPDase8 ont une affinité 2 à 3 fois plus élevée pour l'ATP que pour l'ADP (Kukulski et al., 2005). La NTPDase2 se démarque des autres NTPDases puisqu'elle a une affinité environ 10 fois supérieure pour les nucléosides triphosphates comparé aux nucléosides diphosphates (Kukulski et al., 2005 ; Zimmermann 2001).

La NTPDase1 a une localisation très large au sein du système nerveux central. En effet, l'étude d'immunohistochimie de Wang et Guidotti (1998) sur des tranches de cerveau de rat, a révélé un fort marquage dans les neurones du cortex cérébral, de l'hippocampe et du cervelet ainsi qu'au niveau des cellules endothéliales des vaisseaux sanguins et des cellules gliales.

La NTPDase2 est exprimée au niveau des couches germinales dans le cerveau en développement et dans le cerveau adulte de rat. En effet, l'expression de la NTPDase2 est localisée dans la zone subventriculaire et de la couche subgranulaire du gyrus denté chez la souris adulte (Gampe et al, 2015) où elle est associée aux astrocytes (Braun et al., 2003 ; Langer et al., 2008).

La NTPDase3 est exclusivement localisée dans les neurones, plus précisément dans les terminaisons axonales. Cette localisation suggère un rôle de régulateur des concentrations extracellulaires d'ATP au niveau synaptique (Belcher et al., 2006). Cette enzyme est fortement exprimée dans les neurones des ganglions de la racine dorsale, contrairement aux NTPDases1, 2 et 8, suggérant un rôle de cette ectonucléotidase dans les circuits nociceptifs (Vongtau et al., 2011). De plus, la NTPDase3 est également exprimée au niveau des axones myélinisés cutanés et dans les organes cibles spécialisés qui participent à la sensation tactile (Vongtau et al., 2011).

La NTPDase8 a été détectée dans le foie, le jejunum et le rein mais aucune activité enzymatique n'a à ce jour été révélée dans le cerveau (Bigonnesse et al., 2004 ; Fausther et al., 2007).

b. Les ecto-nucléotides pyrophosphatas/phosphodiésterases (E-NPPases)

NPPases 1, 2 et 3 <i>(Gijsbers et al., 2003)</i>	ATP → AMP + PPi
---	-----------------

Les NPPases catalysent des réactions d'hydrolyse de liaisons pyrophosphate ou phosphodiester de divers composés extracellulaires tels que les nucléotides, les lysophospholipides et les phosphates ester de choline (Zimmermann et al., 2012). Comme pour les NTPDases, l'activité enzymatique des NPPases est dépendante de la présence de cations divalents tels que le Ca²⁺ ou le Mg²⁺. Les NPPs sont des glycoprotéines transmembranaires (Bollen et al., 2000). Seules les NPP1, NPP2 et NPP3 réalisent l'hydrolyse des nucléotides extracellulaires (Goding et al., 2003) tandis que les NPP4 à 7 hydrolysent les lysophospholipides (Yegutkin, 2008).

La réaction générale que catalysent les NPP1 à 3 est l'hydrolyse de l'ATP en AMP et pyrophosphate (PPi). La NPP1 catalyse cette réaction de manière plus efficace que la NPP2 et la NPP3. En effet, Gijsbers et al. (2003) ont mesuré *in vitro* l'activité relative d'hydrolyse des NPP1, 2 et 3 envers le pNP-TMP, un substrat classique des nucléotides phosphodiésterases. Ils ont montré que l'activité enzymatique de la NPP3 et de la NPP2, vis-à-vis de l'hydrolyse du pNP-TMP, était trois fois et six fois inférieure respectivement à celle de la NPP1 (*Figure 4*).

La NPP1, NPP2 et NPP3 ont été détectées dans la plupart des tissus (Bollen et al., 2000). Bjelobaba et ses collaborateurs (2006) ont étudié la localisation de la NPP1 dans le cerveau chez le rat grâce à l'utilisation d'anticorps anti-NPP1. Leurs travaux ont révélé une distribution très répandue de cette enzyme dans la plupart des régions du cerveau avec un marquage intense

au niveau des couches II et IV du cortex cérébral. La NPP1 est aussi présente dans le cortex piriforme, l'hypothalamus et le thalamus. Elle est principalement localisée au niveau des neurones dans différentes régions cérébrales sauf dans les neurones des ganglions de la base qui n'expriment pas la NPP1.

La NPP2 est exprimée au niveau du plexus choroïde et de la zone subventriculaire durant le développement puis son expression diminue à l'âge adulte chez la souris (Savaskan et al., 2007).

Les auteurs ont également mis en évidence que la NPP2 est absente des neurones, des astrocytes et de la microglie mais a été retrouvée dans une lignée précoce d'oligodendrocytes (Savaskan et al., 2007).

La NPP3 (gp130RB13-6) a été initialement identifiée à l'aide d'un anticorps monoclonal en tant que glycoprotéine au niveau d'une sous-population de précurseur neural dans le cerveau de rat (Deissler et al., 1995). Il a été rapporté que la NPP3 est uniquement détectée dans les astrocytes immatures (Blass-Kampmann et al., 1997).

c. L'ecto-5'-nucléotidase (NT5E)

Ecto-5'-nucléotidase (Cusack et al., 1983)	AMP → adénosine +Pi
---	---------------------

L'ecto-5'-nucléotidase est une protéine ancrée à la surface externe de la membrane plasmique par une ancre glycosylphosphatidylinositol (GPI) en position C-terminale. Elle hydrolyse exclusivement les nucléosides-5'-monophosphates (AMP, UMP, CMP, IMP, GMP) et l'AMP est considéré comme le substrat physiologique majeur de cette enzyme (*Figure 4*) (Cusack et al., 1983). Elle peut également exister sous forme soluble dans l'espace extracellulaire suite à l'hydrolyse de l'ancre GPI par une phospholipase C (Vogel et al., 1992).

L'ecto-5'-nucléotidase est aussi considérée comme étant un marqueur de différenciation, ou antigène de différenciation CD73 (cluster of differentiation 73), des lymphocytes T et B (Thomson

et al., 1990). Des souris KO pour cette enzyme ont un métabolisme de l'adénosine réduit comparé à des souris sauvages (Klyuch et al., 2012). En revanche, comme la délétion n'a aucun effet sur l'activité des ecto-ATPases, le métabolisme de l'ATP en AMP des souris KO pour la NT5E n'est pas altéré (Langer et al., 2008). L'ecto-5'-nucléotidase est exprimée dans diverses régions du cerveau : le cortex cérébral, l'hippocampe, le cervelet, la moelle épinière ainsi que dans les ganglions de la base où l'expression de l'enzyme est plus élevée comparé aux autres régions cérébrales (Langer et al., 2008 ; Augusto et al., 2013). Ces résultats ont été confirmés par Kulesskaya et collaborateurs (2013) qui ont étudié la distribution de l'ecto-5'-nucléotidase sur des tranches de cerveau de souris par immunohistochimie. Ils ont révélé un marquage intense au niveau du striatum, du noyau caudé, du putamen, du tubercule olfactif et du globus pallidus, structures localisées dans les ganglions de la base. Par ailleurs, Trieu et al. (2015) ont mis en évidence que la NT5E est présente dans la couche la du cortex piriforme par immunohistochimie. Des modifications de l'activité de cette enzyme ont été observées au cours du développement puisqu'il a été montré que l'activité de l'ecto-5'-nucléotidase augmente avec l'âge (Fuchs, 1991). En effet, durant le développement, l'ecto-5'-nucléotidase est localisée au niveau de la surface des cellules nerveuses migrantes et immatures ainsi qu'au niveau de synapses lors de la synaptogenèse et du remodelage synaptique (Fenoglio et al., 1995). En revanche dans le cerveau adulte, l'enzyme est localisée au niveau des astrocytes et de la microglie (Schoen et Kreutzberg, 1995), des oligodendrocytes et de la myéline (Cammer et al., 1986) ainsi qu'au niveau des neurones (Bjelobaba et al., 2007).

d. La phosphatase alcaline non spécifique des tissus TNAP

TNAP <i>(Demenis et Leone, 2000)</i>	$\text{ATP} \rightarrow \text{ADP} + \text{Pi} \rightarrow \text{AMP} + \text{Pi} \rightarrow \text{adénosine} + \text{Pi}$
--	---

La TNAP est impliquée dans l'hydrolyse de diverses molécules. Elle possède une activité phosphomonoestérase qui lui confère la propriété de déphosphoryler entre autres, le pyrophosphate (PPi), le pyridoxal-5'-phosphate (PLP) et la phosphoéthanolamine qui constituent les trois substrats de la TNAP les plus connus. Ainsi la TNAP est impliquée dans les processus de minéralisation osseuse via l'hydrolyse du PPi en phosphate inorganique (Russel, 1965), dans la voie de synthèse de neurotransmetteurs, tels que le GABA via la déphosphorylation du PLP qui est un cofacteur d'enzymes nécessaires à la synthèse du GABA (Whyte et al., 1985). La TNAP a également une fonction d'ectonucléotidase qui conduit à l'hydrolyse des nucléosides et nucléotides à pH alcalin et physiologique (Demenis et Leone, 2000). Il a été montré que la TNAP hydrolyse l'ATP, l'ADP, l'AMP en adénosine (*Figure 4*) au niveau de la surface épithéliale des voies respiratoires chez l'Homme (Picher et al., 2003) et au niveau de la plaque osseuse (Say et al., 1991).

La phosphatase alcaline est très largement exprimée dans le système nerveux central. L'activité de cette enzyme a été rapportée dans le cortex cérébral, le bulbe olfactif, le thalamus et l'hypothalamus chez le rongeur (Langer et al., 2008). Dans le cerveau chez le primate, la TNAP est associée aux neurones et aux cellules endothéliales (Brun-Heath et al., 2012). Une forte activité phosphatase alcaline a également été mise en évidence au niveau de structures pré- et postsynaptiques du système nerveux central chez le rat (Sugimura et Mizutani, 1979) et chez le primate (Fonta et al., 2004) ainsi qu'au niveau des nœuds de Ranvier (Fonta et al., 2005).

La TNAP est fortement exprimée pendant les stades précoces du développement. En effet, pendant le développement embryonnaire chez la souris, la TNAP est exprimée par des

progéniteurs neuraux dans les zones ventriculaire et subventriculaire qui sont des régions caractérisées par une grande activité de prolifération durant le développement. Kermer et ses collaborateurs (2010) ont montré que l'abolition de la protéine codant pour la TNAP par des ARN interférents dans des cultures de cellules souches neurales réduit la prolifération et la différenciation des neurones suggérant que la TNAP est essentielle dans la prolifération et la différenciation des progéniteurs neuraux.

Si la TNAP est fortement exprimée durant les stades précoces, son activité diminue durant le développement tardif. Cependant elle est toujours exprimée dans les zones ventriculaire et subventriculaire durant les stades adultes (Langer et al., 2007). Ceci suggère que la TNAP contribuerait au développement du système nerveux central via le contrôle de la prolifération, de la migration et de la différenciation neuronale (Ermonval et al., 2009). Le mécanisme par lequel la TNAP régulerait ces fonctions impliquerait la signalisation purinergique. En effet, dans des cultures de neurones de l'hippocampe, il a été montré que la TNAP co-localiserait avec le récepteur P2X7 au niveau des cônes de croissances des axones. En hydrolysant l'ATP extracellulaire, la TNAP empêcherait ainsi l'activation des récepteurs P2X7 impliqués dans l'inhibition de la croissance axonale (Diez-Zaera et al., 2011).

Par ailleurs, Street et al (2013) ont mis en évidence l'expression de la TNAP dans les neurones de la moelle épinière et des ganglions de la corne dorsale grâce à l'hybridation in situ avec des sondes spécifiques de la TNAP, régions dans lesquelles la TNAP hydrolyse l'AMP en adénosine. Dans ces régions, la TNAP serait impliquée dans les circuits de la douleur puisque l'adénosine, via les récepteurs A1, a un effet antidiouleur. De plus, Zhang et coll. (2012) ont étudié la contribution de la TNAP dans la production d'adénosine dans l'hippocampe chez la souris en utilisant un inhibiteur spécifique de la TNAP, le MLS-0038949. Ils ont mis en évidence que la TNAP ne contribuerait de manière significative à la production d'adénosine dans l'hippocampe que chez des souris KO pour la NT5E et non chez des souris sauvages.

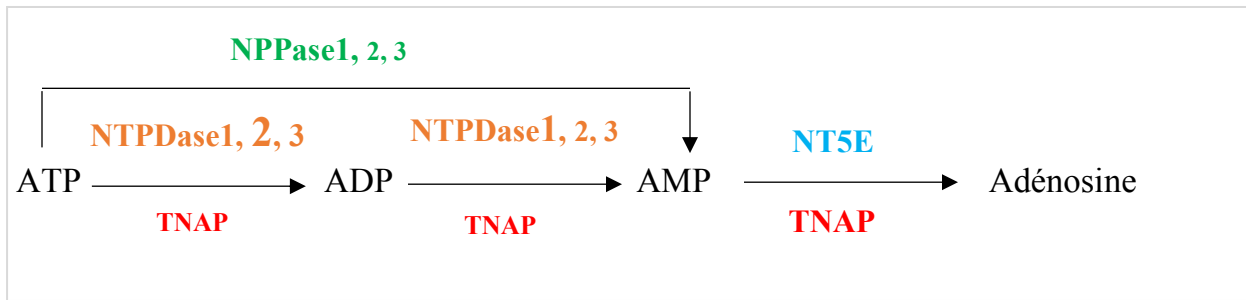


Figure 4 : Schéma récapitulatif des réactions catalysées par les ectonucléotidases responsables de la production d'adénosine extracellulaire dans le système nerveux central.
 Une taille de police différente a été utilisée afin de rendre compte des affinités des enzymes pour chaque substrat. Par exemple, la NTPDase2 a une affinité 10 fois supérieure pour l'ATP par rapport à l'ADP.

Enzymes	Substrat endogène	Réaction chimique	Localisation dans le système nerveux	Localisation cellulaire	Rôles	Références
NTPDase1	ATP=ADP	ATP→ADP+Pi ; ADP → AMP+Pi	Cortex cérébral, hippocampe, cervelet, vaisseaux sanguins, thalamus, caudé putamen	Neurones, cellules endothéliales, microglie	Régule les concentrations en nucléotides/nucléosides extracellulaires	Langer et al., 2008 ; Wang et Guidotti, 1998 ; Kukulski et al., 2005
NTPDase2	ATP>>>ADP	ATP→ADP+Pi ; ADP → AMP+Pi	Hippocampe, gyrus denté (zone sous-ventriculaire et sous granulaire)	Astrocites, progéniteurs neuraux	Régule les concentrations en nucléotides/nucléosides extracellulaires	Langer et al., 2008 ; Gampe et al., 2015 ; Kukulski et al., 2005
NTPDase3	ATP>>ADP	ATP→ADP+Pi ; ADP → AMP+Pi	Hypothalamus, hippocampe, cortex, ganglions racine dorsale	Neurones	Régule les concentrations en nucléotides/nucléosides extracellulaires, rôle dans les circuits nociceptifs	Langer et al., 2008 ; Vongtau et al., 2011 ; Kukulski et al., 2005
NPP1	ATP	ATP→AMP +PPi	Cortex cérébral, hypothalamus, cortex piriforme, thalamus, vaisseaux sanguins	Neurones, cellules endothéliales	Régule les concentrations extracellulaires en ATP, AMP ; rôle dans la minéralisation osseuse	Langer et al., 2008 ; Gijsbers et al. 2003 ; Bjelobaba et al., 2006
NPP2	ATP	ATP→AMP +PPi	Cervelet, plexus choroïde, vaisseaux sanguins	Oligodendrocytes, cellules endothéliales	Migration, différenciation, prolifération et survie, régule les concentrations en ATP/AMP	Savaskan et al., 2007 ; Gijsbers et al. 2003
NPP3	ATP	ATP→AMP +PPi	Couche germinale de la zone ventriculaire, plexus choroïde, vaisseaux sanguins	Astrocites, cellules endothéliales	Régule les concentrations en AMP/adénosine ; migration et prolifération gliale	Gijsbers et al. 2003 ; Blass-Kampmann et al., 1997
NT5E	AMP	AMP→Adénosine +Pi	Hippocampe, bulbe olfactif caudé putamen, cervelet, striatum	Astrocites, microglie, oligodendrocytes, neurones	Régule les concentrations extracellulaires en AMP/adénosine ; synaptogenèse	Kulesskaya et al., 2013 ; Langer et al., 2008 ; Bjelobaba et al., 2007
TNAP	AMP>> ADP, ATP	ATP→ADP→AMP →Adénosine + Pi	Cortex cérébral, vaisseaux sanguins, bulbe olfactif, thalamus, hypothalamus, cervelet (faible)	Neurones, cellules endothéliales	Migration, différenciation axonale, régule les concentrations extracellulaires en ATP/ADP/AMP/adénosine	Langer et al., 2008, Brun-Heath et al., 2012

Tableau 3 : Caractéristiques principales des ectonucléotidases impliquées dans la production d'adénosine extracellulaire dans le système nerveux central.

C. Le transport de l'adénosine

Hormis la production intracellulaire et extracellulaire d'adénosine via la dégradation de diverses molécules (nucléotides intra- ou extracellulaires et SAH), il existe un transfert d'adénosine entre les deux compartiments. En effet, l'adénosine extracellulaire peut provenir du transport de l'adénosine intracellulaire vers le milieu extracellulaire via les transporteurs de nucléosides dits équilibratifs (ENT). L'adénosine intracellulaire provient également du transport de l'adénosine extracellulaire via les ENT mais aussi via un autre type de transporteurs dits concentratifs : les CNT (Cass et al., 1998) (*Figure 5*).

1. Les transporteurs de nucléosides équilibratifs (ENT)

Les ENT sont des transporteurs bidirectionnels passifs car le flux de nucléosides à travers la membrane est uniquement dépendant du gradient de concentration.

Les ENT sont divisés en deux catégories selon leur sensibilité à l'inhibition par le nucléoside analogue, S-6-(4-nitrobenzyl)mercaptopurine riboside (NBMPR) : les transporteurs équilibratifs dits sensibles (ENT1) et les transporteurs équilibratifs dits insensibles (ENT2). En fait, les ENT1 sont inhibés par le NBMPR avec des concentrations de l'ordre du nanomolaire tandis que les ENT2 sont également inhibés mais uniquement avec des concentrations en NBMPR de l'ordre du micromolaire (Belt et al., 1993).

Les ENT sont très présents dans tous les tissus et certaines cellules expriment les deux types de transporteurs à la fois (ENT1 et ENT2) (Noji et al., 2004). Une étude d'hybridation *in situ* a permis de révéler la large distribution des ARN messagers codant pour l'ENT1 chez le rat. Les ARNm ont été détectés dans environ 50 % des neurones de l'hippocampe, du cervelet, du cortex cérébral et du striatum (Anderson et al., 1999). Il apparaît également que les ARNm codant pour l'ENT1 sont exprimés au niveau des astrocytes, des cellules du plexus choroïde, et des cellules musculaires lisses des vaisseaux sanguins (Anderson et al., 1999).

Le transporteur ENT2 chez le rat présente le même pattern d'expression que l'ENT1. En effet, par RT-PCR, Northern Blot et hybridation *in situ*, il a été montré que les ARNm ENT2 sont

présents dans diverses régions du cerveau telles que l'hippocampe, le striatum, le thalamus et le cortex cérébral. Au sein de ces structures, l'ENT2 est exprimé par les neurones, les astrocytes, les cellules du plexus choroïde, et des cellules musculaires lisses des vaisseaux sanguins (Anderson et al., 1999). De plus, l'hybridation *in situ* indique que près de 90% des cellules expriment l'ARNm ENT2 suggérant que l'ENT2 est le transporteur prédominant chez le rat.

2. Les transporteurs de nucléosides concentratifs (CNT)

Les CNT assurent le transport unidirectionnel (du milieu extracellulaire vers le milieu intracellulaire) des nucléosides grâce à un symport avec des ions Na^+ et/ou des ions H^+ . L'énergie fournie par le gradient des ions sodium, qui se met en place au niveau des membranes plasmiques, permet le transport des nucléosides contre leur gradient de concentration : c'est un transport actif. Les CNT sont localisés dans divers tissus et organes tels que le foie, les reins, les macrophages, l'épithélium intestinal, le plexus choroïde et le cerveau (Griffith and Jarvis, 1996 ; Cass et al., 1998). Ces transporteurs sont subdivisés en six sous-types sur la base de leur sélectivité à un substrat donné et de leur sensibilité à l'inhibiteur NBMPR : le CNT1 transporte les nucléosides pyrimidiques et l'adénosine, le CNT2 transporte les nucléosides puriques et l'uridine, le CNT3 a une spécificité plus large puisqu'il transporte les nucléosides puriques et pyrimidiques, le CNT4 transporte les mêmes nucléosides que CNT1 ainsi que la guanosine, le CNT5 est sélectif des analogues de l'adénosine et enfin le CNT6 qui lui est sélectif de la guanosine (Revue de Cass et al., 2002).

Les transporteurs CNT1 et CNT2 présentent la même distribution au sein du système nerveux central chez le rat. Ils sont tous deux exprimés dans le cortex cérébral, l'hippocampe, le cervelet, le striatum, le colliculus supérieur (Anderson et al., 1996).

D. Le métabolisme de l'adénosine

L'adénosine peut être dégradée en inosine, que ce soit dans le milieu intracellulaire ou dans le milieu extracellulaire, par l'adénosine déaminase (ADA) (Yegutkin, 2008). L'inosine est ensuite métabolisée en hypoxanthine par des purines nucléosides phosphorylases (PNP), puis en xanthine et enfin en acide urique par des xanthines oxydases (XO) (Yegutkin, 2008) (*Figure 5*). Dans le milieu intracellulaire, l'adénosine peut être rephosphorylée en AMP par l'adénosine kinase (AdK) (Latini et Pedata, 2001).

L'adénosine kinase a une affinité plus forte pour l'adénosine ($K_m = 0.2\text{-}2 \mu\text{M}$) que l'adénosine déaminase ($K_m = 20\text{-}100 \mu\text{M}$) (Lloyd et Fredholm, 1995). Du fait de l'absence d'adénosine kinase dans le milieu extracellulaire, il existe une régulation cyclique du métabolisme des purines entre le milieu extracellulaire et le milieu intracellulaire. En effet, l'adénosine peut être capturée du milieu extracellulaire vers le milieu intracellulaire où elle sera phosphorylée en AMP par l'adénosine kinase (Lloyd et Fredholm, 1995). Dans le milieu intracellulaire, l'AMP pourra par la suite être phosphorylée en ADP par une adénylate kinase (ADK). L'ADP est ensuite phosphorylé en ATP par une nucléoside diphosphate kinase (NDK) (Yegutkin, 2008). Par la suite, l'ATP est éventuellement libérée dans le milieu extracellulaire puis dégradée par les ectonucléotidases en adénosine.

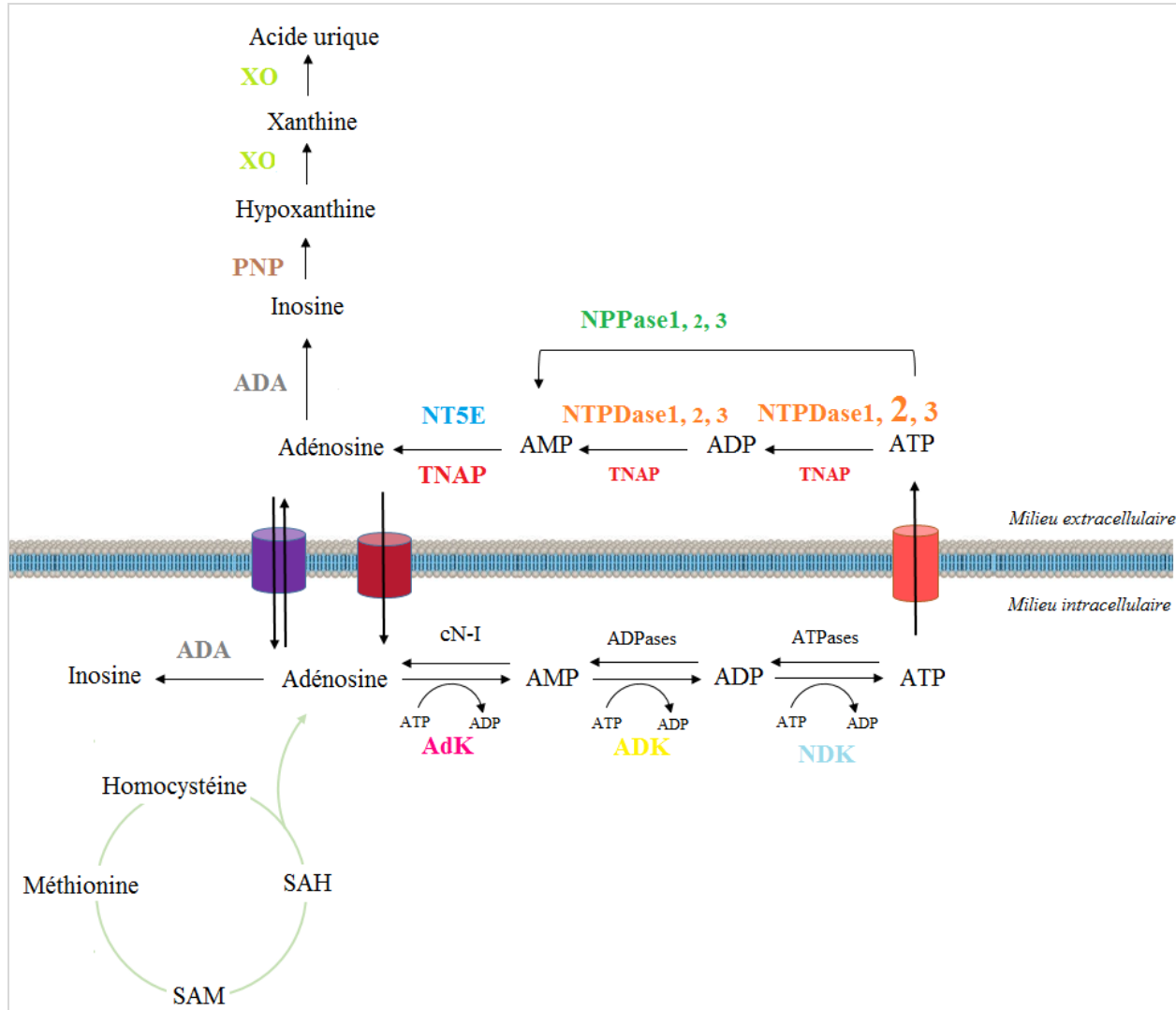


Figure 5 : Transport et métabolisme de l'adénosine extracellulaire et intracellulaire dans le système nerveux central. L'ENT (en violet) est un transporteur bidirectionnel tandis que le CNT (en rouge) est un transporteur unidirectionnel chargé du transport de l'adénosine du milieu extracellulaire vers le milieu intracellulaire. **ADA** : adénosine déaminase ; **AdK** : adénosine kinase ; **ADK** : adénylate kinase ; **cN-I** : nucléotidase cytosolique I ; **NDK** : nucléoside diphosphate kinase ; **PNP** : purine nucléoside phosphate ; **SAH** : S-adénosylhomocystéine ; **SAM** : S-adénosylméthionine ; **XO** : xanthine oxydase.

E. Les récepteurs à l'adénosine

De manière générale, les récepteurs à l'adénosine sont des récepteurs à 7 domaines transmembranaires couplés aux protéines G (RCPG) avec la partie N-terminale de la protéine

qui se trouve du côté extracellulaire et la partie C-terminale qui se trouve sur le côté cytoplasmique de la membrane. Les différentes caractéristiques des récepteurs à l'adénosine sont récapitulées dans le tableau 4.

En 1979, Van Calker et ses collaborateurs ont rapporté deux effets opposés de l'adénosine sur des cellules de cerveaux de souris en culture : l'inhibition de l'accumulation de l'AMP cyclique et la stimulation de l'accumulation de l'AMP cyclique. Ils ont alors proposé le terme de récepteur A1 pour celui qui induit une inhibition de l'accumulation d'AMP cyclique ; et le nom de récepteur A2 pour celui qui stimule l'accumulation d'AMP cyclique. Ces deux effets opposés sont dus au couplage de chaque récepteur à une protéine G distincte. Le récepteur A1 est couplé à une protéine G inhibitrice (Gi) tandis que les récepteurs A2 sont couplés à une protéine G stimulatrice (Gs ou Gq). Par ailleurs, la protéine Gi du récepteur A1 peut se lier directement aux canaux calciques dépendants du voltage. Les récepteurs A2 ont été subdivisés en 2 types : A2a et A2b. Cette distinction réside dans le fait que la stimulation de l'adénylate cyclase par l'adénosine s'effectue via des sites de liaison distincts de haute affinité (A2a) et de faible affinité (A2b) (Daly et al., 1983 ; Bruns et al., 1986). Un quatrième sous-type de récepteurs à l'adénosine, le récepteur A3 a été mis en évidence chez le rat par Zhou et ses collaborateurs (1992). Dans le cerveau, il semblerait que le récepteur A3 soit couplé à une protéine Gi et également à une protéine Gq (Zhou et al., 1992 ; Abbracchio et al., 1995). Les mécanismes de transduction associés à chaque sous-type de récepteur à l'adénosine, identiques à ceux décrits dans la partie I.B.2.b, sont schématisés dans la figure 6.

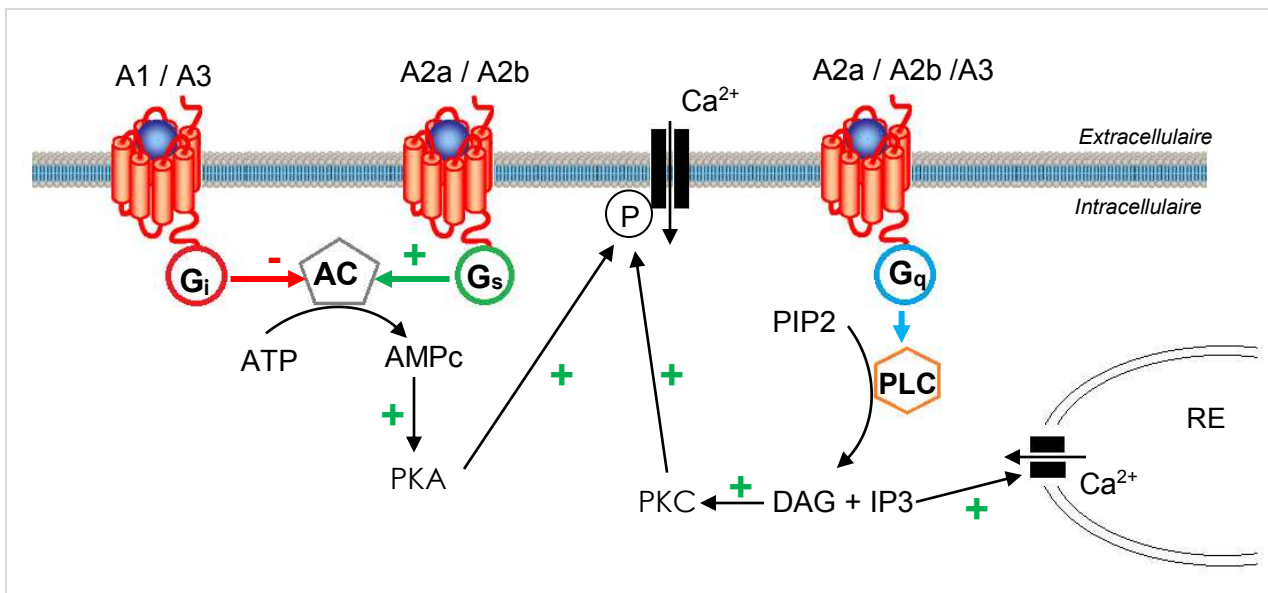


Figure 6 : Représentation schématique des mécanismes de transduction associés aux récepteurs à l'adénosine. A gauche, la voie de signalisation dépendante de l'AMP cyclique (AMPc). L'activation de la protéine Gi inhibe l'adénylate cyclase (AC) limitant la production de second messager AMPc, ce qui empêche l'activation de la protéine kinase A (PKA). L'activation de la protéine Gs stimule l'adénylate cyclase qui induit la production d'AMPc. L'AMPc active des protéines kinases, notamment la protéine kinase A (PKA) qui, via la phosphorylation des canaux calciques, permet leur ouverture. A droite, la voie de signalisation dépendante de l'inositol phosphate. L'activation de la protéine G_q stimule la phospholipase C (PLC) induisant l'hydrolyse phosphatidyl-inositol-4-5-diphosphate (PIP2) en diacylglycérol (DAG) et inositol-3-phosphate (IP3). L'IP3 permet la libération des stocks de calcium intracellulaires via l'ouverture des canaux calciques du réticulum endoplasmique (RE). Le DAG active la protéine kinase C (PKC) qui phosphoryle les canaux calciques présents au niveau de la membrane plasmique et provoque ainsi leur ouverture.

1. Le récepteur A1

Dans le système nerveux central, ce récepteur est le plus abondant dans plusieurs régions du cerveau. Il est exprimé à la fois par les neurones et les cellules gliales. On le trouve dans le cortex cérébral, le cervelet, le bulbe olfactif, l'hippocampe, le thalamus, la moelle épinière (Dixon et al., 1996). Dans les neurones, le récepteur A1 est localisé au niveau présynaptique (Fredholm et al., 2005) et également au niveau postsynaptique (Rebola et al., 2003). Le récepteur A1 est exprimé par les astrocytes, par les oligodendrocytes et par la microglie

(Ciccarelli et al., 2001) où son activation par l'adénosine conduit à la production de substances neuroprotectrices (TGF-beta, NGF) (Dare et al., 2007).

La plupart des antagonistes sélectifs des récepteurs A1 sont des composés contenant des dérivés de xanthine. Le 8-cyclopentyl-1,3-dimethylxanthine (CPT) et le 8-cyclopentyl-1,3-dipropylxanthine (DPCPX) sont les antagonistes les plus couramment utilisés du fait de leur grande affinité et sélectivité pour le sous type A1 (Bruns et al 1987).

L'un des effets le plus connu de l'adénosine sur l'activité nerveuse est l'inhibition de la libération de neurotransmetteurs et l'inhibition de l'excitation neuronale via l'activation des récepteurs A1.

Dans les neurones, le récepteur A1 localisé au niveau présynaptique est responsable d'une inhibition de la transmission synaptique excitatrice (Fredholm et al., 2005). La liaison de la protéine Gi aux canaux calciques dépendants du voltage dans la terminaison présynaptique a pour effet d'inhiber l'entrée de calcium qui est requise pour la libération des neurotransmetteurs.

Par conséquent, cela diminue la libération de glutamate (Ribeiro, 1995).

De plus, l'activation du récepteur A1 localisé au niveau postsynaptique active des canaux potassiques. L'augmentation de la conductance potassique induit une hyperpolarisation de la membrane provoquant une diminution de l'excitabilité neuronale (Greene et Haas, 1991).

Cependant, cet effet postsynaptique ne contribue pas de manière importante au contrôle de la transmission synaptique. En revanche, il semblerait que ce mécanisme postsynaptique soit plutôt impliqué lors d'activité intense des neurones (Fredholm et al., 2005). L'adénosine ou les agonistes du récepteur A1 présentent des propriétés anticonvulsives résultant de l'inhibition de la libération de glutamate et d'une action hyperpolarisante médiee par l'activation des canaux potassiques (Khan et al. 2001) ainsi que des propriétés analgésiques.

L'inosine peut se lier au récepteur A1 avec une affinité équivalente à celle de l'adénosine (Nascimento et al., 2015) et possède des propriétés anticonvulsives puisque lorsqu'elle est administrée par voie intraventriculaire, l'inosine s'oppose aux convulsions induites par de fortes doses de caféine (Marangos et al., 1981). De plus, il a été montré que l'inosine a un effet antidouleur et antidépresseur chez la souris (Nascimento et al., 2010 ; Muto et al., 2014) .

2. Le récepteur A2a

Le récepteur A2a est très abondant au niveau du striatum, du noyau accumbens et du tubercule olfactif. Ce récepteur est également présent, mais plus faiblement exprimé, dans l'hippocampe, le cortex cérébral et la substance noire (Dixon et al., 1996). Au niveau du striatum, ce récepteur est localisé au niveau postsynaptique dans les neurones GABAergiques de la voie indirecte projetant sur le globus pallidum où ces neurones GABAergiques expriment fortement les récepteurs à la dopamine D2. Le récepteur A2a est exprimé au niveau présynaptique dans le striatum où il est localisé dans les terminaisons glutamatergiques qui entrent en contact avec les neurones de la voie nigro-striée GABAergique directe (Quiroz et al., 2009). Dans l'hippocampe, le récepteur A2a est exprimé par les neurones pyramidaux et est localisé au niveau des terminaisons nerveuses glutamatergiques (Rebola et al., 2005). Le récepteur A2a est localisé dans les astrocytes où il stimule leur prolifération (Hindley et al., 1994), dans la microglie et les vaisseaux sanguins (Revue de Fredholm et al., 2005) et dans les neurones du néocortex (Rebola et al., 2002).

Contrairement au récepteur A1, le récepteur A2a est impliqué dans la facilitation de la libération des neurotransmetteurs. Au niveau présynaptique dans le striatum, le récepteur A2a contrôle la libération de glutamate. En effet, en s'hétéromérisant avec le récepteur A1, le récepteur A2a contrecarre l'inhibition de la transmission synaptique médiée par le récepteur A1 (Ciruela et al., 2006). Par ailleurs, il a été montré que les récepteurs A1 et A2a sont colocalisés au niveau des terminaisons nerveuses glutamatergiques dans l'hippocampe chez le rat ce qui leur conférerait un rôle dans le contrôle de la libération du glutamate (Rebola et al., 2005). De plus, les récepteurs A2a peuvent moduler l'activité d'autres récepteurs tels que le récepteur à la dopamine, à l'acétylcholine et au glutamate (Revue de Cunha, 2001).

Les récepteurs A1 et A2a sont tous deux impliqués dans le cycle sommeil/éveil. En effet, l'administration d'adénosine ou d'agoniste du récepteur A1 induit une somnolence et altère la vigilance (Dunwiddie et Worth, 1982). Les récepteurs A2a sont impliqués dans la médiation des

effets somnogènes de l'adénosine via l'excitation des neurones actifs du sommeil. De plus, les antagonistes des récepteurs A1 et A2a, tels que la caféine et la théophylline, contrecarrent les effets somnogènes de l'adénosine (Strecker et al., 1999).

3. Le récepteur A2b

Grâce à la RT-PCR, Dixon et ses collaborateurs (1996) ont pu détecter les ARNm codant pour le récepteur A2b dans le cerveau de rat. Bien que les niveaux d'expression soient faibles, les ARNm ont été détectés dans le cervelet, l'hypothalamus, le thalamus et l'hippocampe. Au niveau cellulaire, ce récepteur est exprimé au niveau des neurones et des astrocytes (Feoktistov et Biaggioni, 1997). Gonçalves et al. (2015) ont mis en évidence la présence du récepteur A2b au niveau des terminaisons nerveuses glutamatergiques de l'hippocampe chez la souris. La principale fonction de ce récepteur serait de contrôler l'inhibition médiée par le récepteur A1. En effet, l'activation du récepteur A2b par un agoniste atténue la libération du glutamate ainsi que la transmission glutamatergique médiée par le récepteur A1 (Gonçalves et al., 2015).

Comparée au récepteur A2a, ce récepteur a une affinité plus faible pour l'adénosine. Il serait ainsi activé seulement en condition d'hypoxie ou d'ischémie, où l'adénosine est libérée en fortes concentrations (de l'ordre du micromolaire) comme c'est le cas au niveau des astrocytes (Trincavelli et al., 2004). Sous ces conditions, la stimulation du récepteur A2b par l'adénosine ou des agonistes provoque la libération d'interleukine-6 (IL-6) par les astrocytes (Fiebich et al., 1996). Étant donné que l'IL-6 est une cytokine neuroprotective contre l'hypoxie et la neurotoxicité due au glutamate, l'activation du récepteur A2b permet de réguler les dommages lors de lésions du système nerveux central (Hasko et al., 2005).

4. Le récepteur A3

Bien que les niveaux d'expression de ce récepteur détectés dans le cerveau soient plus faibles comparés aux autres récepteurs, le récepteur A3 est exprimé dans les neurones de l'hippocampe au niveau présynaptique (Lopes et al., 2003), dans le striatum et le cervelet (Jacobson et al, 1993), dans l'hypothalamus et le thalamus (Yaar et al., 2005) et dans le cortex cérébral (Fredholm et al., 2011). Le récepteur A3 est également exprimé par les astrocytes (Abbracchio et al., 1997 ; Wittendrop et al., 2004) et les cellules microgliales (Hammarberg et al., 2003).

Il a été montré que l'agoniste Cl-IBMECA du récepteur A3, désigné comme étant sélectif, peut également activer le récepteur A1 (Costenla et al., 2001). Ainsi, les rôles fonctionnels de ce récepteur attribués au récepteur A3 pourraient être en réalité le reflet de l'activation du récepteur A1 qui est présent dans le cerveau de manière beaucoup abondante que le récepteur A3. En 2012, Tosh et collaborateurs ont mis au point un agoniste de haute affinité et sélectivité pour le récepteur A3 dérivé du Cl-IBMECA, le MRS5698, ce qui a permis de mettre en évidence par la suite que l'activation du récepteur A3 par l'adénosine endogène a un effet antidiouleur (Little et al., 2015).

Récepteurs	Couplage	Localisation dans le système nerveux	Localisation cellulaire	Localisation subcellulaire (neurones)	Rôles	Références
A1	Gi	Cortex cérébral, cervelet, bulbe olfactif, hippocampe, thalamus, moelle épinière	Neurones, astrocytes, oligodendrocytes, microglie	Pré- et postsynaptique	Inhibition présynaptique, neuroprotecteur, anticonvulsif, régulation cycle éveil/sommeil (hypnogène), analgésique	Fredholm et Dunwiddie, 1988 ; Dixon et al., 1996 ; Rebola et al., 2003 ; Dare et al., 2007 ; Khan et al., 2001.
A2a	Gs/Gq	Striatum, ganglions de la base, substance noire, hippocampe, néocortex, vaisseaux sanguins	Dendrites, astrocytes, microglie, neurones, cellules endothéliales	Pré- et postsynaptique	Facilite la transmission synaptique prolifération astrocytes, excitotoxicité, régulation cycle éveil/sommeil (somnogène).	Dixon et al., 1996 ; Rebola et al., 2005 ; Quiroz et al., 2009; Strecker et al., 1999, Hindley et al., 1994.
A2b	Gs/Gq	Hippocampe, thalamus, hypothalamus, cervelet	Neurones, astrocytes, microglie	Postsynaptique	Neuroprotecteur, contrôle de l'inhibition présynaptique médiée par A1	Dixon et al., 1996 ; Feoktistov et Biaggioni, 1997 ; Gonçalves et al., 2015 ; Hasko et al., 2005.
A3	Gi/Gq	Hippocampe, striatum, cervelet, hypothalamus, thalamus, cortex cérébral	Neurones, astrocytes, microglie	Présynaptique	Modulation de la douleur : antidouleur	Fredholm et al., 2011 ; Lopes et al., 2003, Jacobson et al., 1993 ; Abbracchio et al., 1997 ; Hammarberg et al., 2003, Little et al., 2015.

Tableau 4 : Caractéristiques principales des récepteurs P1 à l'adénosine.

II. ADENOSINE ET PLASTICITE SYNAPTIQUE A COURT TERME

Dans la synapse chimique, un potentiel d'action généré à proximité du corps cellulaire se propage le long de l'axone jusqu'à atteindre la terminaison synaptique. La dépolarisation créée par le potentiel d'action active les canaux calciques voltages-dépendants entraînant une entrée de calcium. Cette augmentation de calcium dans la terminaison présynaptique stimule la fusion des vésicules synaptiques avec la membrane plasmique. En effet, le calcium entrant dans la terminaison présynaptique se lie à un senseur calcique, la synaptotagmine. Cette protéine de la membrane des vésicules synaptiques est requise pour la fusion des membranes des vésicules afin de libérer les neurotransmetteurs dans la fente synaptique. Cette libération de neurotransmetteurs se fait en deux phases : une phase rapide synchrone résultant des courants calciques présynaptiques, et une phase lente asynchrone résultant du calcium résiduel restant dans la terminaison après le potentiel d'action (Atluri et Regehr, 1998). Les neurotransmetteurs peuvent alors activer les récepteurs post-synaptiques et transmettre le signal au neurone post-synaptique (*Figure 7*). La libération des neurotransmetteurs étant proportionnelle à l'entrée de calcium, la régulation des canaux calciques présynaptiques serait une façon de réguler la libération des neurotransmetteurs.

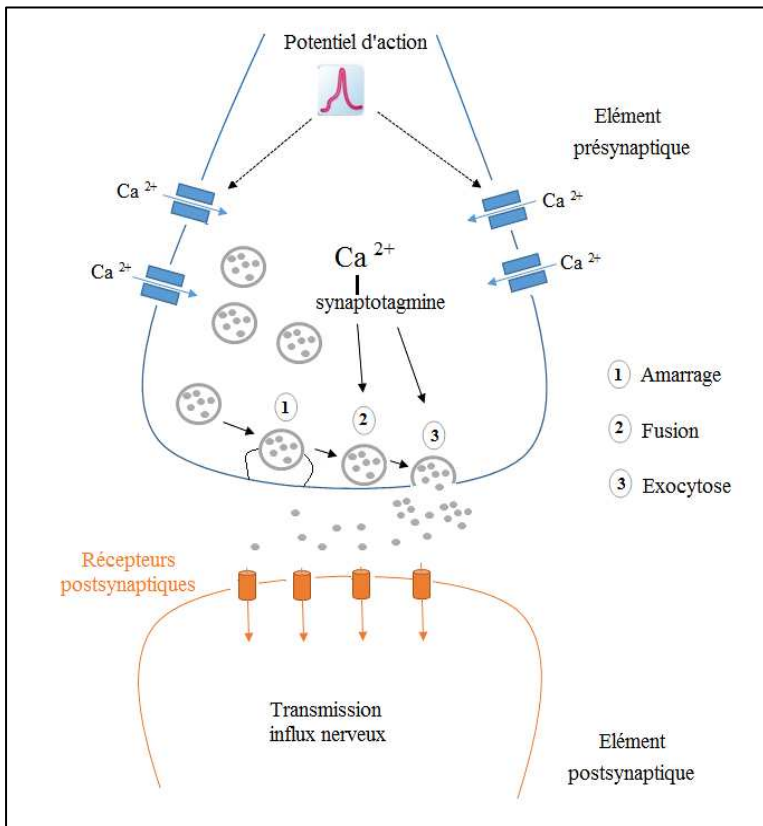


Figure 7 : Représentation schématique du mécanisme de la neurotransmission. La libération de neurotransmetteurs se fait en 3 étapes : l'amarrage des vésicules à la membrane présynaptique, la fusion des vésicules à la membrane synaptique puis l'exocytose des vésicules synaptiques. La fusion et l'exocytose des vésicules synaptiques requièrent le complexe Calcium-synaptotagmine. Les neurotransmetteurs libérés dans la fente synaptique activent ensuite des récepteurs postsynaptiques et transmettre le signal au neurone

La plasticité synaptique correspond aux modifications morphologiques (croissance neuronale, modifications du cytosquelette), fonctionnelles (modifications à court terme et à long terme de l'efficacité synaptique) et moléculaires (synthèse de protéines) qui interviennent au cours du temps au niveau des synapses. On parle de plasticité à court terme lorsque les modifications de l'efficacité synaptique ne perdurent pas plus de quelques minutes. A l'inverse, on parle de plasticité à long terme allant de quelques minutes jusqu'à plusieurs jours et induisant des changements structurels des synapses (Citri et Malenka, 2008).

Comme exposé dans la première partie de cette thèse, l'adénosine est une purine endogène qui joue un rôle important dans l'excitabilité neuronale et dans la transmission synaptique. C'est pourquoi l'hypothèse que l'adénosine pourrait également moduler la plasticité synaptique a été avancée (Dunwiddie and Hoffer, 1980).

Dans cette deuxième partie, je détaillerai les différents mécanismes de la plasticité à court terme ainsi que l'intérêt fonctionnel d'une telle plasticité. Ensuite, je détaillerai les effets de l'adénosine sur ce type de plasticité.

A. La plasticité synaptique à court terme

La plasticité à court terme s'exprime par une augmentation ou une diminution transitoire de l'amplitude de la réponse postsynaptique. La plupart des études sur la plasticité synaptique à court terme ont été réalisées en appliquant des paires de pulses qui sont deux stimulations séparées par un intervalle de temps très court, de l'ordre de quelques dizaines de millisecondes (Moore et al., 2003). Les caractéristiques de la deuxième réponse, suite à la deuxième stimulation, sont comparées avec celles la première réponse, c'est le paired-pulse ratio. Lorsque le ratio de l'amplitude de la deuxième stimulation comparée à la première stimulation est supérieur à 1, on parle de facilitation ou paired-pulse facilitation (PPF). Le mécanisme qui soutient la PPF résiderait dans l'augmentation transitoire de calcium intracellulaire au niveau de la terminaison présynaptique suite à la première stimulation conduisant à une augmentation de libération de neurotransmetteurs lors de la deuxième stimulation. De plus, deux autres formes de renforcement de la plasticité synaptique peuvent être observées : l'augmentation et la potentialisation post-tétanique (PTP). Ces trois formes de plasticité sont caractérisées par des décours temporels différents (Zucker et Regehr, 2002).

A l'inverse, si le paired-pulse ratio est inférieur à 1, on parle de dépression ou paired-pulse depression (PPD). La dépression repose sur le fait que la première réponse induit une plus grande libération de neurotransmetteurs et diminue ainsi la probabilité de libération de neurotransmetteurs lors de la seconde stimulation. Par ailleurs, la plasticité à court terme peut aussi être induite, expérimentalement, par des stimulations répétées et espacées d'intervalles très courts.

La plasticité au sein des synapses reflète l'interaction entre différentes formes de plasticité (Fioravante et Regehr, 2011). Il est admis que la plasticité à court terme est le reflet d'une modification présynaptique dans la libération des neurotransmetteurs et est dépendante du calcium dans la terminaison présynaptique (Zucker et Regehr, 2002). Cependant d'autres mécanismes, y compris des mécanismes postsynaptiques, ont été proposés pour expliquer les phénomènes de facilitation et de dépression.

1. La facilitation synaptique à court terme

La facilitation à court terme est une augmentation transitoire, de l'ordre de quelques centaines de millisecondes, de la réponse synaptique provoquée par des trains de potentiels d'action (*Figure 8*).

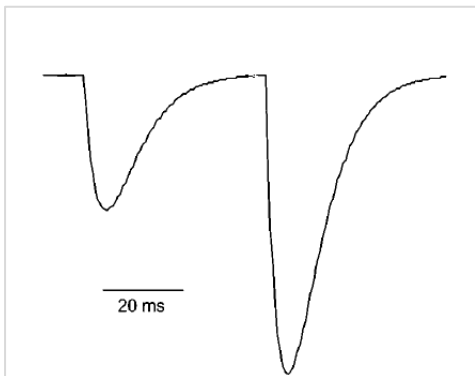


Figure 8 : Exemple de tracés électrophysiologiques obtenus suite à une stimulation par paire de pulses. La réponse synaptique à la deuxième stimulation est augmentée par rapport à celle obtenue lors de la première stimulation.

Expérimentalement, on peut induire ce type de plasticité par des stimulations répétées à haute fréquence. La facilitation provient d'une augmentation des concentrations de calcium présynaptique lors de stimulations répétées et à l'augmentation de la probabilité de fusion des vésicules de neurotransmetteurs. Trois mécanismes ont été proposés dans la littérature afin de rendre compte de la facilitation.

a. Les mécanismes de la facilitation à court terme.

- *Hypothèse du calcium résiduel*

Premièrement, les travaux de Katz et Miledi en 1968 ont permis d'avancer l'hypothèse du « calcium résiduel » selon laquelle un potentiel d'action présynaptique provoque un influx calcique et le calcium qui persiste au niveau de la terminaison présynaptique est appelé calcium résiduel.

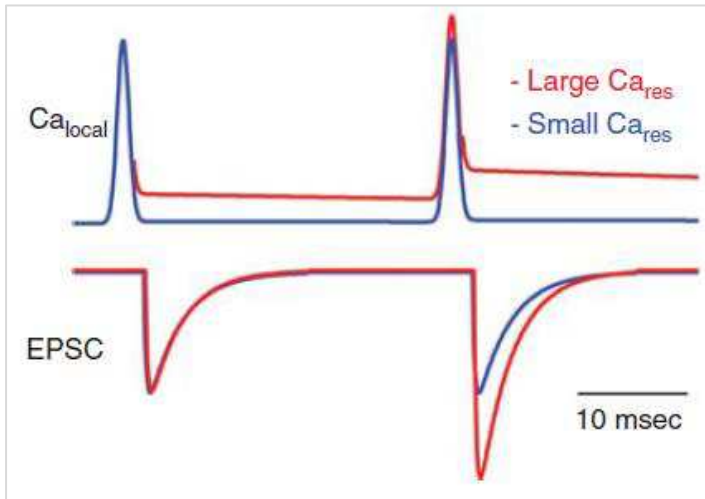


Figure 9 : Hypothèse du calcium résiduel. Lorsque l'entrée de calcium induite par une seconde stimulation s'ajoute au calcium présent dans la terminaison à la première stimulation, cela provoque une augmentation de la réponse synaptique.

Ainsi, l'entrée de calcium provoquée par une deuxième stimulation s'ajoute au calcium résiduel et augmente la probabilité de libération des neurotransmetteurs (*Figure 13A*). Par conséquent, on observe une facilitation de la réponse synaptique (*Figure 9*). Cependant, la mesure des concentrations de calcium résiduel durant les phases de facilitation sont de l'ordre du micromolaire (voire moins) tandis que le pic de concentration de calcium intracellulaire qui déclenche la libération des vésicules est de l'ordre de 100 μM (Helmchen et al., 1997). La simple sommation du calcium résiduel induit par un potentiel d'action ne serait donc pas suffisante pour induire la facilitation et ainsi expliquer les fortes variations d'amplitude que l'on peut observer dans certains systèmes (Felmy et al., 2003).

Plusieurs modes d'action du « calcium résiduel » ont donc été envisagés. Il pourrait agir en se liant à des sites à haute affinité de la machinerie d'exocytose, en se liant à des sites spéciaux responsables de la facilitation ou en modulant le degré de saturation des tampons de calcium à haute affinité.

- *Saturation des tampons calciques endogènes*

Un premier mécanisme serait la saturation des protéines de liaison du calcium présynaptique dont la calbindine D-28k et la parvalbumine. Ces protéines interceptent le calcium entre le site d'entrée du calcium, c'est-à-dire les canaux calciques, et les sites de fusion des vésicules, réduisant ainsi la probabilité initiale de libération des neurotransmetteurs (Matveev et al., 2004). A la première stimulation, le calcium entrant est en partie capté au niveau de ces protéines de liaison et en sature une grande partie (*Figure 13A*). Par conséquent, lors de la stimulation suivante, une plus grande fraction de calcium entrant libre peut se lier aux senseurs responsables de la libération des neurotransmetteurs comme la synaptotagmine, et ainsi augmenter la probabilité de libération des neurotransmetteurs. Cela provoque donc une facilitation de la réponse synaptique (Catterall et Few, 2008 ; Fioravante et Regehr, 2011) (*Figure 10*).

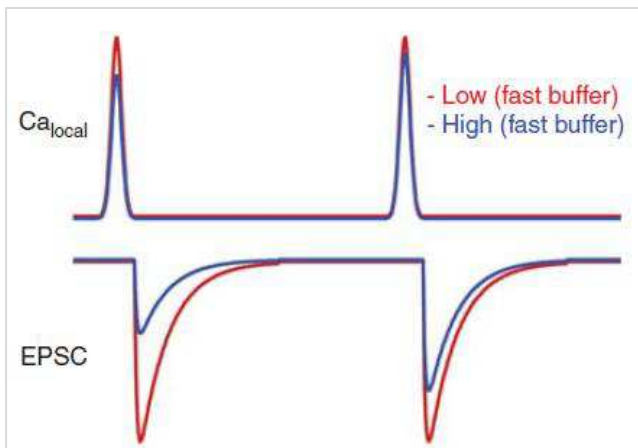


Figure 10 : Mécanisme de saturation des tampons calciques. Si la concentration de senseur calcique dans la terminaison synaptique est élevée (courbe bleue), alors une plus grande fraction de calcium pourra se lier à la stimulation suivante et ainsi augmenter la réponse synaptique. (Issu de Regehr, 2012).

- *Senseurs calciques*

Un deuxième mécanisme ferait intervenir un type de protéine, des senseurs calciques, autre que la synaptotagmine, tels que le senseur calcique neuronal 1 (NCS-1) (Catterall et Few, 2008). Le calcium résiduel se lie aux senseurs calciques et les active afin d'augmenter la libération des neurotransmetteurs (*Figure 13A*). Dans des cultures de neurones hippocampiques de rat, Sippy et al. (2003) ont montré que NCS-1 favorise la libération des neurotransmetteurs suite à des paires de stimulations et des trains de stimulations à haute fréquence sans pour autant modifier

la probabilité initiale de libération. Les canaux calciques peuvent également être modulés par les senseurs calciques. En effet, NCS-1 peut se lier directement aux canaux dépendants du voltage de type P/Q (Lian et al., 2014). Cette interaction permet le passage d'un influx calcique plus important et participe donc à la facilitation.

b. Augmentation et potentialisation post-tétanique (PTP)

Il existe deux autres formes de facilitation synaptique à court terme : l'augmentation et la potentialisation post tétanique (PTP). Ces deux formes de renforcement de la plasticité peuvent être observées lorsque le nombre de stimuli dans un train de stimulation augmente (*Figure 11*) (Regehr, 2012).

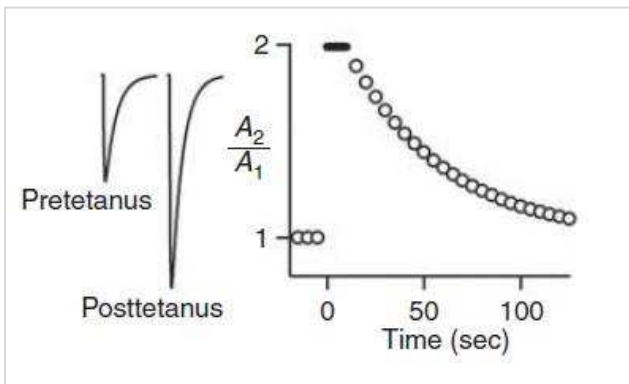


Figure 11 : Exemple de tracés électrophysiologiques obtenus suite à une stimulation tétanique. La réponse synaptique à la deuxième stimulation comparée à la première (A_2/A_1) est représentée en fonction du temps. (Issu de Regehr, 2012).

L'augmentation et la PTP se distinguent par leur décours temporels différents. En effet, l'augmentation dure une dizaine de secondes tandis que la PTP dure de 30 secondes à quelques minutes (Zucker et Regehr, 2002). Tout comme la facilitation, l'augmentation et la potentialisation post tétanique dépendent de l'accumulation de calcium dans les terminaisons synaptiques suite à des trains de stimulation, qui peut être due à une augmentation de l'influx calcique ou bien à l'augmentation de l'exocytose des vésicules (Delaney et Tank, 1994). En effet, l'augmentation accroît la disponibilité des vésicules en vue d'être exocytées alors que la facilitation augmente la probabilité de libérer une vésicule disponible (*Figure 13B*).

Concernant les mécanismes de la potentialisation post tétanique, l'étude *in vitro* de Tang et Zucker (1997) montre l'implication du calcium mitochondrial (*Figure 13B*). En effet, pendant une stimulation tétanique, le calcium mitochondrial serait séquestré puis libéré lentement dans le cytoplasme après la stimulation post tétanique via des pompes d'extrusion au niveau de la membrane mitochondriale. Le calcium agirait ensuite au niveau des sites distincts de ceux impliqués dans la facilitation pour induire la PTP. D'autre part, la stimulation tétanique provoque une accumulation en Na⁺ au niveau des terminaisons présynaptiques ce qui réduit le gradient transmembranaire de sodium et par conséquent ralentit l'efflux de calcium cytoplasmique via la pompe Na⁺/Ca²⁺ (Mulkey et Zucker, 1992).

2. Dépression synaptique à court terme

A l'inverse de la facilitation, la dépression à court terme est une diminution transitoire de la réponse synaptique provoquée par des trains de potentiels d'action (*Figure 12*).

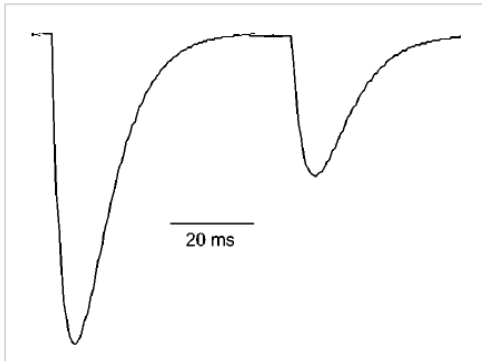


Figure 12 : Exemple de tracés électrophysiologiques obtenus suite à une stimulation par paire de pulses. La réponse synaptique à la deuxième stimulation est diminuée par rapport à celle obtenue lors de la première stimulation.

Plusieurs mécanismes ont été proposées afin d'expliquer ce phénomène de dépression à court terme (*Figure 13C*). Parmi ces mécanismes, la plupart sont présynaptiques bien que certains mécanismes postsynaptiques aient été décrits. Tous ces mécanismes ont des constantes de temps différentes dont certaines peuvent être très rapides (de l'ordre de la dizaine de millisecondes) ou plus lentes (l'ordre de la seconde à quelques minutes).

a. Mécanismes présynaptiques de la dépression synaptique

- *Diminution du stock de vésicules*

La dépression synaptique serait principalement due à une diminution des stocks de vésicules disponibles suite à un premier potentiel d'action (Fioravante et Regehr, 2011). Lors des stimulations suivantes, il y a moins de vésicules mobilisables pour libérer les neurotransmetteurs. Par conséquent, une quantité plus faible de neurotransmetteurs sera libérée et donc la réponse synaptique sera réduite. Ainsi, plus la probabilité de libération initiale de la synapse sera élevée, plus le stock de vésicules sera utilisé lors de la première stimulation et moins il restera de vésicules disponibles pour la stimulation suivante. Ce type de dépression est un mécanisme plutôt lent puisque la constante de temps de récupération associée est de l'ordre de la dizaine de secondes (Stevens et Tsujimoto, 1995).

- *Inactivation des sites de libération*

Un autre mécanisme beaucoup plus rapide, de l'ordre de la milliseconde (Dobrunz et al., 1997) propose que la fusion d'une vésicule au niveau d'un site de libération entraînerait une inhibition de la fusion de vésicules au niveau de ce même site, même si le stock de vésicule n'est pas affecté (von Gersdorff et Borst, 2002 ; Neher et Sakaba, 2008).

- *Diminution de l'influx calcique*

Une réduction de l'activité des canaux calciques responsables de l'influx de calcium dans la terminaison synaptique pourrait également être responsable des phénomènes de dépression à court terme (Fioravante et Regehr, 2011). En effet, il a été montré que le calcium entrant lors d'une première stimulation inactive les canaux calciques et entraîne une réponse post-synaptique de plus faible amplitude à la deuxième stimulation (Xu and Wu, 2005). Cette inactivation des canaux calciques passerait en partie par la calmoduline, protéine activée par le calcium (Catterall and Few, 2008). En effet, il a été montré que la délétion du domaine de fixation à la calmoduline

des canaux calciques de type P impliqués dans l'entrée de calcium dans la terminaison synaptique, permettait de réduire la dépression synaptique à court terme (Mochida et al., 2008). De plus, plusieurs études ont montré que l'inactivation des canaux calciques présynaptiques est responsable d'une dépression synaptique rapide pour des stimuli allant de 2 Hz à 30 Hz (Xu et Wu, 2005) alors que des stimulations à 100 Hz induisant une dépression synaptique robuste sont causées par la diminution des vésicules (Xu et Wu, 2005).

b. Mécanismes postsynaptiques de la STD

Bien qu'ils semblent avoir une part moins importante que les mécanismes présynaptiques (Zucker and Regehr, 2002), les mécanismes postsynaptiques responsables de la dépression à court terme apparaissent comme plus importants pour des fréquences supérieures à 100 Hz (Von Gersdorff et Borst 2002).

- *Désensibilisation des récepteurs postsynaptiques*

Les réponses postsynaptiques peuvent être diminuées par un phénomène appelé désensibilisation dans lequel les récepteurs postsynaptiques activés par un neurotransmetteur, suite à un premier potentiel d'action, entrent dans un état inactif. La désensibilisation des récepteurs AMPA joue un rôle dans la transmission synaptique au niveau de nombreuses synapses (Zucker and Regehr, 2002). Il a été montré que l'inhibition de la désensibilisation des récepteurs AMPA réduisait partiellement la dépression à court terme lors de trains de stimulation (Brenowitz and Trussell, 2001). Cependant, l'implication de la désensibilisation des récepteurs dans les mécanismes de plasticité à court terme varie fortement en fonction de la synapse étudiée (Xu-Friedman and Regehr, 2004). Par exemple, ce phénomène n'est retrouvé ni pour les synapses cortico-striatales, ni pour les synapses thalamo-striatales chez la souris (Ding et al., 2008). Hormis les récepteurs AMPA, la désensibilisation d'autres types de récepteurs postsynaptiques, tels que les récepteurs GABA et NMDA, est également possible (Zucker et Regehr, 2002). De plus, la désensibilisation des récepteurs AMPA est un mécanisme très rapide (10 à 20 msec) (Trussell et al., 1993).

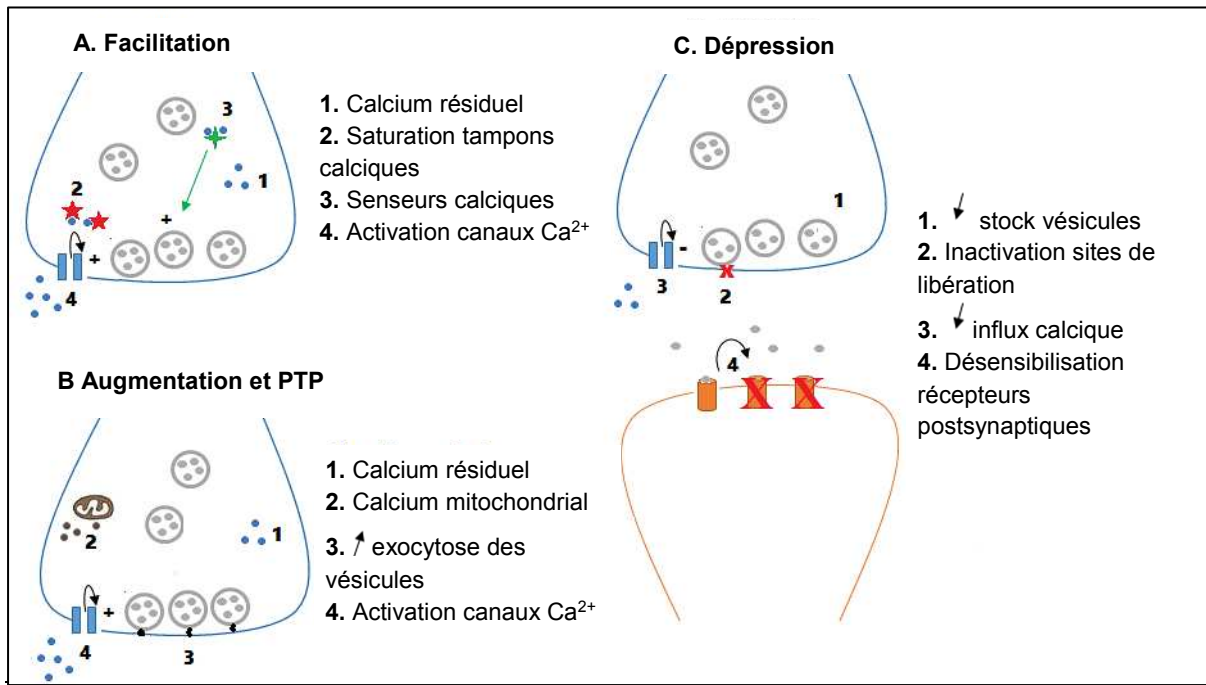


Figure 13 : Schéma récapitulatif des différents mécanismes impliqués dans la plasticité synaptique à court terme. **A.** Mécanismes présynaptiques de la facilitation à court terme. (1) Le calcium résiduel suite à une première stimulation augmente la probabilité de libération des neurotransmetteurs lors de la stimulation suivante. (2) Les tampons calciques piégent le calcium entrant à la première stimulation, saturant ainsi une grande partie des sites de liaison de ces tampons. A la deuxième stimulation, une plus grande quantité de calcium pourra se lier à la synaptotagmine responsable de la libération des neurotransmetteurs. (3) Le calcium résiduel peut se lier à des senseurs calciques qui vont favoriser la libération des neurotransmetteurs. (4) Les canaux calciques et les senseurs calciques peuvent interagir directement et augmenter l'influx calcique dans la terminaison présynaptique **B.** Mécanismes présynaptiques de l'augmentation et de la potentiation post-tétanique (PTP). (1) voir A. (2) Le calcium mitochondrial est libéré lentement dans la terminaison suite à la stimulation tétanique. Il agit ensuite sur des protéines autres que la synaptotagmine pour induire la PTP. (3) L'augmentation accroît la disponibilité des vésicules prêtes à être exocytées ce qui entraîne une augmentation de la libération des neurotransmetteurs. (4) voir A. **C.** Mécanismes pré- et postsynaptiques de la dépression à court terme. (1) Suite à une première stimulation, une grande partie des vésicules sont exocytées. A la stimulation suivante, moins de vésicules sont disponibles pour libérer des neurotransmetteurs. (2) La fusion d'une vésicule en un site de libération inhibe la fusion de vésicule au niveau de ce même site. (3) Le calcium entrant à la première stimulation inactive les canaux calciques, réduisant ainsi la concentration de calcium entrant dans la terminaison présynaptique à la seconde stimulation. (4) Les neurotransmetteurs libérés dans la fente synaptique, suite à la première stimulation, vont activer des récepteurs postsynaptiques qui entrent dans un état inactif (Inspiré de Fioravante et Regehr, 2011).

3. Les rôles de la plasticité synaptique à court terme.

La plasticité synaptique à court terme régule l'activité des réseaux neuronaux et est impliquée dans le traitement de l'information sensorielle dans le système nerveux (Fioravante et Regehr, 2011). Par exemple, la dépression synaptique joue un rôle important dans la localisation des sons (Kuba et al., 2002).

La plasticité à court terme peut altérer la façon dont les neurones présynaptiques activent les cibles postsynaptiques. Les synapses qui présentent une dépression dans leur plasticité synaptique ont une probabilité de libération initiale de neurotransmetteurs élevée tandis que les synapses facilitatrices ont une probabilité de libération faible (Abbott et Regehr, 2004). Dans les synapses qui présentent une dépression, l'activation répétée de la synapse provoque une diminution de la libération des neurotransmetteurs et/ou de la réponse postsynaptique. Par conséquent, les synapses avec dépression ont tendance à diminuer la force de la transmission synaptique suite à un train de potentiels d'action à haute fréquence. Du point de vue de la cellule postsynaptique, cela signifie que les informations à haute fréquence sont supprimées par rapport aux informations à basse fréquence. Ainsi les synapses qui dépriment peuvent être vues comme un filtre passe-bas et contribuer à l'adaptation des réponses neuronales suite à une activation soutenue (Wang et al., 2012). A l'inverse, certaines synapses montrent une facilitation pour certaines fréquences d'activation présynaptique. Dans ce cas, à mesure que la fréquence de stimulation augmente jusqu'à atteindre un certain point, la probabilité de libération augmente. Ces synapses peuvent améliorer les réponses à une activité présynaptique à plus haute fréquence, et donc agir comme des filtres passe-haut. D'autres synapses ont une probabilité de libération dite intermédiaire et auront tendance à faciliter à haute fréquence, mais si la fréquence de stimulation est trop élevée, on observera une dépression. Ainsi, ces synapses sont considérées comme des filtres passe-bande, puisqu'elles favorisent le passage de l'information pour une gamme de fréquence spécifique.

Cependant, les caractéristiques de filtres de chaque synapse, elles ne sont pas fixes et peuvent être ajustées en fonction de la modulation de la probabilité initiale de libération ou d'autres

aspects de la neurotransmission. Les neuromodulateurs activent des récepteurs présynaptiques qui, dans la plupart des cas, diminuent la libération des neurotransmetteurs. Il en résulte une modification des caractéristiques de filtre de la synapse de telle sorte que la facilitation devient dominante par rapport à la dépression. De cette façon, l'inhibition présynaptique peut convertir une synapse qui était un filtre passe-bas en un filtre passe-bande ou alors d'une filtre passe-bande en un filtre passe-haut.

4. Les modèles phénoménologiques de la plasticité à court terme

Afin d'étudier les mécanismes de la plasticité à court terme d'un point de vue quantitatif, plusieurs modèles de plasticité synaptique ont été adaptés de celui de Tsodyks et ses collaborateurs (1998). Ce modèle permet de fournir une description phénoménologique des dynamiques à court terme des réponses synaptiques en termes de modification de la probabilité de libération des neurotransmetteurs, représentatif de l'utilisation des ressources, et de l'utilisation et du renouvellement des vésicules synaptiques qui représentent les ressources.

Il permet donc de faire le lien entre les diverses dynamiques synaptiques observées et les différences dans les paramètres du modèle qui sont : l'utilisation, la récupération des ressources ainsi que leurs constantes de temps. Le modèle permet de prédire les réponses postsynaptiques en fonction d'une séquence arbitraire de stimuli présynaptiques.

Le premier modèle phénoménologique de Tsodyks et Markram (1997) fut formulé avec trois paramètres : le paramètre A, qui représente l'efficacité synaptique absolue ; le paramètre U qui correspond à la fraction de l'efficacité synaptique utilisée et une constante de temps de récupération de la dépression, T_{rec} . Le modèle de dépression synaptique est basé sur le fait que la fraction de l'efficacité synaptique utilisée par un potentiel d'action devient instantanément indisponible pour une utilisation ultérieure et récupère selon une constante de temps de dépression T_{rec} . U et T_{rec} sont des paramètres cinétiques qui déterminent la dynamique de la transmission synaptique, en particulier, le taux de dépression. Plus U est grand, plus les ressources synaptiques sont utilisées.

Cependant, ce modèle rendait uniquement compte du phénomène de dépression et ne tenait pas compte du phénomène de facilitation. Afin de modéliser la facilitation à court terme, Tsodyks et ses collaborateurs (1998) ont introduit un facteur de facilitation dans ce modèle. Les auteurs partent du principe que la valeur de l'utilisation de l'efficacité synaptique (U) n'est pas fixe mais est augmentée d'une certaine valeur à chaque potentiel d'action. Cette valeur de U augmentée est appelée « u » et récupère selon une constante de temps de facilitation, T_{fac} jusqu'à atteindre la valeur basale U . Par exemple, une augmentation de la valeur U pourrait être le reflet d'une accumulation de calcium, causée par des potentiels d'action au niveau de la terminaison présynaptique, responsable de la libération des neurotransmetteurs (Bertram et al., 1996).

Lorsque la synapse est dans un état de repos, l'efficacité synaptique disponible, appelée R , est totale et la fraction restante juste après le premier potentiel d'action d'un train de stimulation peut être définie selon l'équation suivante :

$$R_1 = 1 - U$$

Pendant le train de potentiels d'action, chaque potentiel d'action utilise une fraction supplémentaire de « R ». Par conséquent, la valeur de R change constamment en fonction des potentiels d'action, en fonction de la récupération de l'efficacité synaptique selon la constante de temps T_{rec} et de l'augmentation de « u » causée par chaque potentiel d'action. La valeur de R lors de potentiels d'action consécutifs dans un train de stimulation s'écrit donc comme suit :

$$R_{n+1} = R_n (1 - u_{n+1}) \exp ((-\Delta t)/T_{rec}) + 1 - \exp ((-\Delta t)/T_{rec})$$

$$\text{où } u_{n+1} = u_n \exp ((-\Delta t)/T_{fac}) + U(1 - u_n \exp ((-\Delta t)/T_{fac}))$$

Δt est l'intervalle de temps entre un potentiel d'action n et le potentiel d'action suivant $n+1$.

Les synapses qui présentent uniquement de la dépression sont caractérisées par des constantes de temps de facilitation négligeables et u_n est égal à U .

B. Les effets de l'adénosine sur la plasticité synaptique à court terme.

Étant donné que l'adénosine, via l'activation des récepteurs présynaptiques, régule la transmission synaptique excitatrice, il a été proposé que l'adénosine puisse être impliquée dans la modulation de la plasticité synaptique (de Mendonça et Ribeiro, 1996).

En 1985, Dunwiddie et Haas ont étudié, *in vitro*, l'effet de l'adénosine au niveau de la région CA1 de l'hippocampe chez le rat. Ils ont montré que bien que 50 µM d'adénosine diminuent la transmission synaptique, elle augmente la facilitation (Dunwiddie et Haas, 1985). L'interprétation qui a été faite concernant l'augmentation de la facilitation en présence d'adénosine est que l'adénosine en inhibant la libération de neurotransmetteurs à la première stimulation, augmenterait la probabilité de libération de neurotransmetteurs à la seconde stimulation.

Des résultats similaires ont été obtenus dans l'étude de Kerr et collaborateurs (2013). Dans cette étude, ils ont observé que l'adénosine (100 µM) augmente la facilitation suite à une stimulation à 30 Hz dans le néocortex somatosensoriel de rat. De plus, le blocage des récepteurs A1 à l'adénosine par un antagoniste sélectif (8-CPT) induit une diminution du paired-pulse ratio dans les mêmes conditions expérimentales. L'inhibition des récepteurs A1 provoque une augmentation du signal dû à l'apport plus important de calcium à l'intérieur de la synapse. Ceci induirait par voie de conséquence, une libération accrue de vésicules de neurotransmetteurs.

Par ailleurs, Moore et collaborateurs (2003) ont étudié l'effet de l'adénosine sur la plasticité synaptique au niveau des synapses des fibres moussues. De la même façon qu'avec l'utilisation d'un antagoniste des récepteurs A1, Moore et coll. ont observé une diminution de la facilitation en éliminant l'adénosine extracellulaire par l'adénosine déaminase, enzyme qui dégrade l'adénosine en inosine. Ainsi, la dégradation de l'adénosine extracellulaire ainsi que le blocage pharmacologique des récepteurs A1 causerait une augmentation de la libération des neurotransmetteurs au niveau des fibres moussues. Or les synapses qui ont une forte probabilité de libération de neurotransmetteurs ont plutôt tendance à montrer des propriétés de dépression. Ainsi l'adénosine, en modulant la probabilité de libération des neurotransmetteurs, joue un rôle dans le contrôle de la plasticité synaptique.

III. OBJECTIFS DE LA THESE ET APPROCHES

EXPERIMENTALES

A. Les objectifs de la thèse

Les fonctions de la TNAP dans le système nerveux central est un des sujets d'étude de l'équipe depuis plusieurs années. Bien que cette enzyme soit exprimée dans le cerveau, son rôle fonctionnel au sein de ce tissu n'est, à ce jour, pas entièrement connu. Des mutations du gène codant pour la TNAP (gène ALPL chez l'Homme et Akp2 chez la souris) conduisent à une pathologie : l'hypophosphatasie. Cette maladie génétique rare a pour principale conséquence des défauts de minéralisation osseuse et dentaire. De plus dans certaines formes sévères de cette maladie (périnatale et infantiles), on observe de graves crises d'épilepsie suggérant un possible rôle de la TNAP dans le tissu cérébral (Whyte et al., 1988). Un modèle murin de l'hypophosphatasie, où le gène de la TNAP a été invalidé chez des souris, développent des crises d'épilepsies qui sont létales (Waymire et al., 1995 ; Narisawa et al., 1997). De plus, dans le cerveau de la souris, il a été montré qu'un défaut de l'expression de la TNAP perturbe, entre autres, la myélinisation des fibres et la synaptogenèse dans le cortex (Hanics et al., 2012). Ainsi l'absence d'activité TNAP pourrait altérer la propagation et la transmission du signal nerveux dans le cortex. Plusieurs mécanismes pourraient être à l'origine de ces altérations. En effet, il a été montré que la TNAP participe à la biosynthèse du GABA via le pyridoxal-5'-phosphate (PLP), forme active de la vitamine B6 (Waymire et al., 1995). La TNAP hydrolyse le PLP extracellulaire en pyridoxal (PL) qui peut diffuser de façon passive au travers de la membrane de la cellule (Coburn, 2015). Une fois dans la cellule, le PL est rephosphorylé en PLP par des kinases intracellulaires (Narisawa et al., 1997). Le PLP agit, entre autres, en tant que cofacteur dans la synthèse des neurotransmetteurs comme le gamma-aminobutyrate (GABA), la sérotonine, la dopamine et la noradrénaline. Le GABA, neurotransmetteur inhibiteur, est formé à partir d'acide glutamique par des glutamates décarboxylases (GAD65 et GAD67) qui utilisent le PLP comme

cofacteur. Les dosages réalisés dans le cerveau de souris KO pour la TNAP ont révélé non seulement que la concentration de GABA est diminuée d'environ 50 % mais la concentration intracellulaire de PLP est aussi réduite comparée aux souris sauvages (Waymire et al., 1995). Etant donné que le PLP n'est plus déphosphorylé par la TNAP chez les souris déficientes, il ne peut plus entrer dans la cellule et servir de cofacteur à la synthèse de GABA. Cela pourrait expliquer, en partie, pourquoi les souris KO pour la TNAP développent des crises d'épilepsies qui sont létales (Waymire et al., 1995 ; Narisawa et al., 1997).

L'administration de pyridoxal (PL), chez des souris KO pour la TNAP permet seulement de retarder l'apparition des crises d'épilepsies sans les supprimer définitivement (Narisawa, 2001). Cela suggère donc qu'un autre mécanisme, indépendant du PLP, pourrait être impliqué dans la pathologie. La TNAP, qui a aussi une fonction d'ectonucléotidase, pourrait réguler la concentration extracellulaire de nucléotides et nucléosides impliqués dans la signalisation purinergique. Cette signalisation joue un rôle important dans le développement neuronal puisqu'il a été mis en évidence, entre autres, que les nucléotides et nucléosides stimulent la migration et la prolifération des oligodendrocytes et stimulent la myélinisation dans le système nerveux central (Fields et Burnstock, 2006).

En 2012, une étude a également révélé que la concentration en adénosine chez souris KO pour la TNAP est diminuée comparé aux souris sauvages (Fonta et al., 2012b). Ainsi la TNAP pourrait être impliquée dans la synthèse d'adénosine dans le cerveau. Les travaux de Street et ses collaborateurs (2013) ont montré que la TNAP hydrolyse l'AMP en adénosine dans la moelle épinière chez la souris ; et Zhang et al. (2012), ont réalisé une étude dans laquelle ils suggèrent que la TNAP contribuerait à la synthèse d'adénosine dans l'hippocampe chez la souris. Outre ces rares études, peu de travaux se sont attachés à étudier le rôle direct de la TNAP dans la synthèse d'adénosine dans le cerveau.

Par conséquent, la TNAP pourrait intervenir, par différents processus, dans l'équilibre entre les systèmes excitateurs et les systèmes inhibiteurs et l'inactivité de cette enzyme pourrait sous-

tendre diverses neuropathologies observées chez les patients hypophosphatasiques et les souris KO telles que l'épilepsie.

Les objectifs de la thèse sont les suivants. Premièrement, une étude en collaboration avec l'équipe de chimistes de Myriam Malet- Martino de l'université Paul Sabatier et à laquelle j'ai contribué, avait pour objectif d'**identifier les métabolites régulés par la TNAP dans le cerveau (1^{er} article)** à l'aide d'une approche métabolomique sur des cerveaux entiers de souris. En parallèle, une deuxième étude a été réalisée afin de **vérifier, d'un point de vue fonctionnel, si la TNAP est impliquée dans la synthèse d'adénosine (2^{ème} article)** à l'aide d'une approche électrophysiologique combinée à une approche pharmacologique dans le cortex piriforme chez la souris. Le dernier objectif de cette thèse a été d'étudier, en électrophysiologie, **l'influence de l'adénosine sur les mécanismes de la plasticité synaptique (4^{ème} article)**, en collaboration avec Simon Perrier. L'effet de différentes concentrations en adénosine a été testé sur une large gamme de fréquences de stimulations (de 3.125 Hz à 100 Hz) dans le but de déterminer si l'inhibition produite par l'adénosine dépend de la fréquence de stimulation. Ce travail a été précédé par une étude préliminaire concernant **l'influence du calcium sur la transmission synaptique et sur les mécanismes de la plasticité synaptique à court terme (3^{ème} article)** dont on sait qu'ils dépendent grandement des concentrations de calcium extracellulaire.

B. Les approches expérimentales

1. Approche métabolomique sur des souris KO pour la TNAP

Afin d'identifier les métabolites régulés par la TNAP, nous avons travaillé en collaboration avec une équipe de chimistes (Thomas Cruz, Myriam Malet-Martino, Véronique Gilard et Stéphane Balayssac) du laboratoire de Synthèse et Physico-Chimie des Molécules d'Intérêt Biologique (Université Paul Sabatier). Les chimistes ont examiné le métabolome de cerveaux entiers de souris grâce à la spectrométrie à résonance magnétique nucléaire (RMN). Ces souris présentent trois génotypes : des souris KO pour la TNAP, Akp2-/ ; des souris hétérozygotes, Akp2+/- et des

souris sauvages, Akp2^{+/+}. Grâce à l'analyse des spectres RMN, ils ont pu quantifier les différents métabolites présents dans nos échantillons de cerveaux de souris.

2. Approche électrophysiologique et pharmacologique dans le cortex piriforme de souris wild-type *in vitro*.

Nous avons réalisé des enregistrements électrophysiologiques extracellulaires sur des tranches de cerveaux de souris. Ces enregistrements électrophysiologiques ont été faits dans le cortex piriforme, plus précisément dans la couche la du cortex piriforme.

a. Le cortex piriforme

- Pourquoi avoir choisi cette structure d'étude ?***

Tout d'abord, c'est une structure qui est très riche en activité phosphatase alcaline (Langer et al., 2008). De plus, le cortex piriforme contient en grande partie la machinerie de la signalisation purinergique : les ectonucléotidases responsables de la dégradation des nucléotides et nucléosides et les récepteurs à l'adénosine. En effet, l'expression de la NT5E a été rapportée dans le cortex piriforme au niveau de la couche la alors que la couche Ib n'en contient pas (Trieu et al., 2015). La NPP1 est également présente dans cette structure (Bjelobaba et al., 2006) tout comme les NTPDases1, 2 et 3 dont l'inhibition provoque une augmentation de la transmission synaptique dans le tractus olfactif latéral (TOL) (Trieu et al., 2015 ; Langer et al., 2008). On trouve le récepteur à l'adénosine A1 dans le cortex piriforme (Namvar et al., 2008). Cependant, aucune étude n'a spécifié la localisation des récepteurs A2a, A2b et A3 dans le cortex piriforme chez la souris. En ce qui concerne la distribution des récepteurs P2 dans le cortex piriforme, les récepteurs P2X2, P2X4, P2X6 sont localisés dans le cortex piriforme (Collo et al., 1996 ; Guo et al., 2008 ; Kahk et al., 2003). Le récepteur P2X1 est absent du cortex piriforme (Florenzano et al., 2002) ainsi que le récepteur P2X3 qui est absent du système nerveux central (Collo et al.,

1996). Les récepteurs P2Y2, P2Y4 ont été retrouvés dans le cortex piriforme (Namba et al., 2010 ; Song et al., 2011). En revanche aucune information n'est disponible concernant la localisation des récepteurs P2Y1, P2Y6, P2Y12, P2Y13 et P2Y14 dans le cortex piriforme.

La dernière raison expliquant l'utilisation du cortex piriforme dans cette thèse réside dans la facilité expérimentale que nous offre cette structure. En effet, l'organisation anatomique de ce cortex nous permet de stimuler, lors des enregistrements électrophysiologiques, de manière isolée un seul type d'afférence (tractus olfactif latéral). De plus, les potentiels évoqués monosynaptiques sont simples à interpréter puisque la couche Ia est quasiment dépourvue de corps cellulaires de neurones. Par conséquent, les potentiels évoqués ne sont ni affectés par la présence de potentiels d'action ni par la présence d'activité récurrente.

- *Structure du cortex piriforme*

Le cortex piriforme fait partie du cortex olfactif et est la structure la plus étendue de ce cortex. Il est impliqué dans le traitement olfactif (discrimination, association et apprentissage des odeurs) et dans le codage de la mémoire olfactive (Neville et Haberly, 2003).

Le bulbe olfactif et le cortex piriforme présentent une activité oscillatoire spontanée et également induite lors de « l'échantillonnage » des odeurs. Ceci est lié à l'activité rythmique imposée par la respiration de l'animal (respiration et flairage à 2-8 Hz). Les oscillations à hautes fréquences (bêta : 12-30 Hz et gamma : 40-80 Hz) sont induites lors de la présentation des odeurs.

La principale voie d'entrée des informations olfactives dans le cortex piriforme se fait via les cellules mitrales et les cellules touffues du bulbe olfactif. Ces informations olfactives encodées par ces cellules peuvent être influencées par les propriétés des synapses entre le bulbe olfactif et le cortex qui produisent une facilitation à court terme et une dépression à court terme.

Le cortex piriforme est divisé en deux régions (*Figure 14*) : le cortex piriforme antérieur (aPC) et postérieur (pPC) (Haberly et Price, 1978). Le cortex antérieur reçoit principalement les afférences du bulbe olfactif, ce qui lui conférerait la propriété d'encoder des odeurs. A l'inverse, le cortex

postérieur reçoit plutôt des afférences associatives et peu d'afférences du bulbe olfactif lui conférant plutôt la propriété d'encoder la qualité des odeurs (Gottfried 2010).

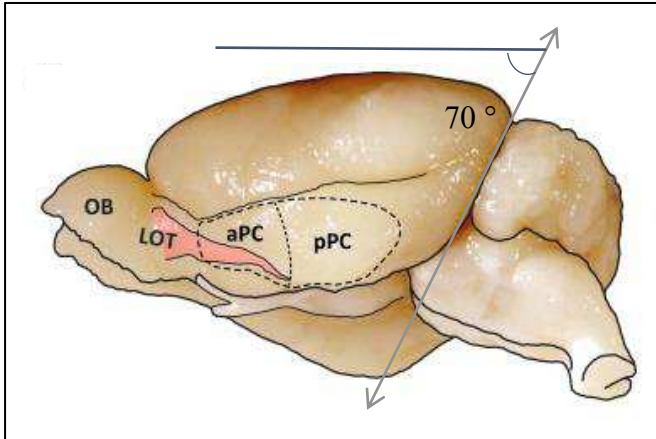


Figure 14 : Vue latérale de cerveau de souris (Bekkers & Suzuki, 2013). OB, bulbe olfactif ; LOT, tractus olfactif lateral ; aPC, cortex piriforme antérieur ; pPC, cortex piriforme postérieur. L'angle de coupe lors de la préparation des tranches de cerveau est représenté en gris.

D'un point de vue phylogénétique, le cortex piriforme est un cortex dit ancien ou paléocortex (au même titre que l'hippocampe) constitué de trois couches contrairement au néocortex qui est constitué de six couches (*Figure 15*).

- La couche I du cortex piriforme, aussi appelée couche plexiforme, contient des axones et des dendrites. Cette couche est subdivisée en deux parties : la partie la plus superficielle de cette couche (couche Ia) reçoit les axones myélinisés du tractus olfactif latéral (TOL) alors que la partie la plus profonde (couche Ib) reçoit les fibres d'association des cellules pyramidales depuis l'intérieur du cortex piriforme.
- La couche II, ou couche cellulaire compacte, est peuplée de corps cellulaires de neurones glutamatergiques. Cette couche est également divisée en une couche superficielle (couche IIa) et couche profonde (couche IIb). La couche IIa contient des cellules semi-lunaires, tandis que la couche IIb est densément peuplée de cellules pyramidales.
- La couche III contient une densité modérée de cellules pyramidales et de cellules multipolaires principalement dans la partie superficielle de cette couche et de cellules non pyramidales dans

la partie la plus profonde de cette couche. Tout comme la couche Ib, elle contient également une forte densité de fibres d'association.

Les cellules pyramidales et les cellules semi-lunaires sont les principaux types de neurones excitateurs du cortex piriforme : les cellules pyramidales, similaires à celles que l'on retrouve dans le néocortex et l'hippocampe, et les cellules semi-lunaires constituent les cellules de projection du cortex olfactif (Haberly et Price, 1978). Dans le cortex piriforme, on trouve également des interneurones, dont la plupart sont GABAergiques, localisés dans toutes les couches du cortex piriforme. Ces interneurones exercent à la fois une proaction inhibitrice et une rétro inhibition sur les cellules pyramidales (Suzuki et Bekkers, 2012).

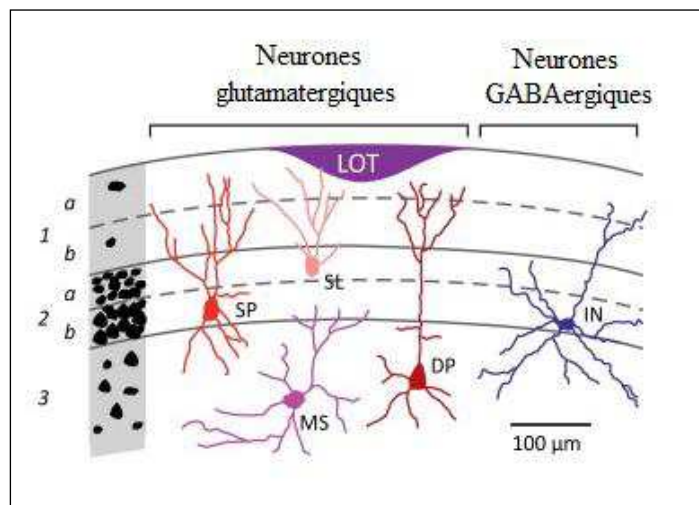


Figure 15 : Représentation schématique de la cytoarchitecture du cortex piriforme. La densité relative en corps cellulaires de chaque couche est schématisée à gauche. Les cellules semi-lunaires (SL) ont leurs corps cellulaires dans la couche IIa tandis que les cellules pyramidales (SP) ont leurs corps cellulaires concentrés dans la couche IIb. La couche III contient des cellules pyramidales profondes (DP) et des cellules multipolaires (MS). Les interneurones inhibiteurs (IN) sont localisés dans toutes les couches du cortex piriforme. (Adapté de Bekkers et Suzuki, 2013).

- *Plasticité dans le cortex piriforme*

Le phénomène de plasticité synaptique dans le cortex piriforme a été rapporté pour la première fois en 1957 par MacLean et collaborateurs qui ont mis en évidence une facilitation de la réponse synaptique avec des paires de stimulations. De même, Bower et Haberly (1986) ont mis en évidence que, suite à des stimulations par paire, les réponses postsynaptiques des synapses de la couche Ia du cortex piriforme sont facilitées contrairement aux réponses des synapses de la couche Ib qui ne facilitent pas. En 2006, Suzuki et Bekkers ont également rapporté que les fibres afférentes présentaient une facilitation suite à des stimulations en paire alors que les fibres d'association (couche Ib) ne présentent que très peu de facilitation. Ils ont également mis en évidence que cette facilitation a une origine présynaptique et est liée au calcium résiduel et à la faible probabilité de libération des neurotransmetteurs au niveau des synapses afférentes.

b. Pharmacologie

Afin d'étudier la contribution de la TNAP dans la synthèse d'adénosine dans le cerveau, nous avons cherché à modifier la signalisation purinergique en inhibant les ectonucléotidases responsables de la dégradation des nucléosides extracellulaires (TNAP et NT5E), en bloquant le transport de l'adénosine entre les compartiments extra- et intracellulaires et en bloquant l'action de l'adénosine sur les récepteurs P1. Des contrôles histologiques et des tests de toxicité (en collaboration avec David Magne et Anne Briolay de l'Institut de Chimie et Biochimie Moléculaires et Supramoléculaires à Lyon) sur des cultures de cellules ont été réalisés afin de s'assurer du bon fonctionnement des inhibiteurs utilisés et de la présence des ectonucléotidases dans le cortex piriforme.

c. Plasticité synaptique à court terme *in vitro*

Pour l'étude de la plasticité à court terme dans le cortex piriforme, de trains de stimulation dans une gamme de fréquence qui couvre la gamme des oscillations cérébrales (de 3,125 Hz à 100

Hz) ont été appliqués. Les trains de stimulation étaient composés de 5 pulses consécutifs, ce qui nous a permis de révéler la chronologie du phénomène de plasticité, ce que n'aurait pas forcément permis une stimulation par paire de pulses. Par ailleurs, la comparaison du paired-pulse ratio (PPR) à 25 Hz avant et après ajout de molécules pharmacologiques nous permet de déterminer si la molécule agit au niveau présynaptiques ou postsynaptiques. Si le PPR n'est pas modifié par l'ajout de la molécule, alors on conclut que la molécule agit au niveau postsynaptique. En revanche si le PPR après ajout de la molécule est augmenté ou diminué, cela signifie que la probabilité de libération des neurotransmetteurs a été modifiée, et par conséquent que la molécule a agi au niveau présynaptique.

L'étude de l'effet du calcium sur la plasticité synaptique était une étude préliminaire nous permettant de valider nos conditions expérimentales. L'étude de l'influence de l'adénosine est une manière d'examiner les effets en miroir d'un défaut d'expression de la TNAP.

Dans le chapitre suivant, chacun des articles énoncés dans la partie objectifs de la thèse sera constitué d'un résumé et du manuscrit associé. Les résultats de ces différentes études seront ensuite discutés plus amplement dans la discussion générale et les perspectives de la thèse.

CHAPITRE III : LES TRAVAUX DE LA THESE

A. *Identification of altered brain metabolites associated with TNAP activity in a mouse model of hypophosphatasia using untargeted NMR-based metabolomics analysis.*
Thomas Cruz, Marie Gleizes, Stéphane Bayassac, Etienne Mornet, Grégory Marsal, José Luis Millán, Myriam Malet-Martino, Lionel G Nowak, Véronique Gilard, and Caroline Fonta. Journal of neurochemistry. 2017;140(6):919-940.

1. Résumé

L'objectif de ce travail a été d'identifier les métabolites régulés par la TNAP dans le tissu nerveux. La TNAP joue un rôle majeur dans la minéralisation osseuse et des mutations du gène de la TNAP (ALPL chez l'homme) conduisent à une pathologie : l'hypophosphatasie (HPP). Cette maladie génétique rare est principalement caractérisée par des défauts de minéralisation osseuse et dentaire ; et les formes sévères de cette maladie sont associées à des crises d'épilepsie et des anomalies morphologiques du cerveau. Par ailleurs, les souris dont le gène de la TNAP a été invalidé présentent un retard de myélinisation dans le cortex et la moelle épinière, ainsi qu'une perturbation de la maturation des synapses au niveau du cortex. Tout ceci suggère que la TNAP joue un rôle important dans le système nerveux notamment dans les crises d'épilepsie chez la souris KO TNAP.

À ce jour, trois substrats de la TNAP ont été identifiés : la phosphoéthanolamine (PE), le pyrophosphate (PPi) et la pyridoxal-5-phosphate (PLP). Il a été montré que la phosphoéthanolamine s'accumule dans le plasma et les urines de patients atteints d'hypophosphatasie et chez les souris KO pour la TNAP. Le pyrophosphate, qui est hydrolysé par la TNAP en phosphate inorganique (Pi), joue un rôle important dans les mécanismes de la minéralisation osseuse puisqu'il empêche le Pi de se lier au calcium pour former des cristaux d'hydroxyapatite essentiels dans la minéralisation. Enfin, le PLP via sa déphosphorylation par la

TNAP est impliqué dans la synthèse de GABA et d'autres neurotransmetteurs (sérotonine, noradrénaline, dopamine).

La TNAP, via son activité ectonucléotidase, pourrait contrôler les concentrations extracellulaires en nucléotides et nucléosides qui sont impliqués, notamment, dans la neurogenèse durant le développement embryonnaire et adulte chez la souris.

Afin d'identifier d'autres substrats et produits de la TNAP qui pourraient révéler d'autres fonctions de cette enzyme, nous avons travaillé en collaboration avec une équipe de chimistes (Thomas Cruz, Myriam Malet-Martino, Véronique Gilard et Stéphane Balayssac) du laboratoire de Synthèse et Physico-Chimie des Molécules d'Intérêt Biologique (Université Paul Sabatier). L'analyse du métabolome de cerveaux de souris (sauvages, Akp2^{+/+} ; hétérozygotes, Akp2⁺⁻ et KO pour la TNAP, Akp2^{-/-}) a été réalisée par les chimistes grâce à la spectrométrie par résonance magnétique nucléaire du proton et du phosphore (1H-RMN et 31P-RMN). Cela a permis de confirmer une diminution de la concentration de GABA chez les souris KO pour la TNAP et d'identifier des altérations pour 7 autres métabolites, chez ces mêmes souris, qui n'avaient jamais été décrites dans la littérature : l'adénosine, la cystathionine, la méthionine, l'histidine, la 3-méthylhistidine, le N-acétylaspartate (NAA) et le N-acétyl-aspartylglutamate (NAAG). Certains de ces métabolites sont impliqués dans la neurotransmission (GABA et adénosine), dans la synthèse de myéline (NAA et NAAG) et dans le cycle de la méthionine et la voie de la trans-sulfuration (cystathionine et méthionine). Du fait que la TNAP est impliquée, entre autre, dans la maturation des synapses, la transmission et la conduction axonale, une défaillance de cette enzyme pourrait expliquer l'aggravation des crises d'épilepsies observées chez les souris KO pour la TNAP.

2. Article

**ORIGINAL
ARTICLE**

Identification of altered brain metabolites associated with TNAP activity in a mouse model of hypophosphatasia using untargeted NMR-based metabolomics analysis

Thomas Cruz,* Marie Gleizes,† Stéphane Balayssac,* Etienne Mornet,‡ Grégory Marsal,† José Luis Millán,§ Myriam Malet-Martino,* Lionel G Nowak,† Véronique Gilard* and Caroline Fonta† 

*Groupe de RMN Biomédicale, Laboratoire SPCMIB (CNRS UMR 5068), Université Paul Sabatier, Université de Toulouse, Toulouse Cedex, France

†Centre de Recherche Cerveau et Cognition (CerCo), Université de Toulouse UPS; CNRS UMR 5549, Toulouse, France

‡Unité de Génétique Constitutionnelle Prénatale et Postnatale, Service de Biologie, Centre Hospitalier de Versailles, Le Chesnay, France

§Sanford Children's Health Research Center, Sanford Burnham Prebys Medical Discovery Institute, La Jolla, California, USA

Abstract

Tissue non-specific alkaline phosphatase (TNAP) is a key player of bone mineralization and TNAP gene (*ALPL*) mutations in human are responsible for hypophosphatasia (HPP), a rare heritable disease affecting the mineralization of bones and teeth. Moreover, TNAP is also expressed by brain cells and the severe forms of HPP are associated with neurological disorders, including epilepsy and brain morphological anomalies. However, TNAP's role in the nervous system remains poorly understood. To investigate its neuronal functions, we aimed to identify without any *a priori* the metabolites regulated by TNAP in the nervous tissue. For this purpose we used ¹H- and

³¹P NMR to analyze the brain metabolome of *Alpl* (*Akp2*) mice null for TNAP function, a well-described model of infantile HPP. Among 39 metabolites identified in brain extracts of 1-week-old animals, eight displayed significantly different concentration in *Akp2*^{-/-} compared to *Akp2*^{+/-} and *Akp2*^{+/+} mice: cystathione, adenosine, GABA, methionine, histidine, 3-methylhistidine, N-acetylaspartate (NAA), and N-acetyl-aspartyl-glutamate, with cystathione and adenosine levels displaying the strongest alteration. These metabolites identify several biochemical processes that directly or indirectly involve TNAP function, in particular through the regulation of ecto-nucleotide levels and of pyridoxal phosphate-dependent enzymes. Some

Received October 11, 2016; revised manuscript received December 18, 2016; accepted January 4, 2017.

Address correspondence and reprint requests to Caroline Fonta, Centre de Recherche Cerveau et Cognition (CerCo), Université de Toulouse UPS; CNRS UMR 5549, Pavillon Baudot, CHU Purpan, BP 25202, 31052 Toulouse cedex 3, France. E-mail: caroline.fonta@cnrs.fr

Abbreviations usage: 3-MHis, 3-methylhistidine; Ace, acetate; Ade, adenine; Ala, alanine; AP, alkaline phosphatase; Asn, asparagine; Asp, aspartate; AXP, adenosine mono-, di-, and triphosphate; Bet, betaine; CBS, cystathione β -synthase; CGL, cystathione γ -lyase; Cho, choline; CI, confidence interval; Cit, citrate; Cr, creatine; CXP, cytidine mono-, di- and triphosphate; FID, free induction decay; Fum, fumarate; GAD, glutamate decarboxylase; GDP, guanosine diphosphate; Gln, glutamine; Glu, glutamate; Gly, glycine; GMP, guanosine monophosphate; GPC, glycerophosphocholine; GTP, guanosine triphosphate; GXP,

guanosine mono-, di-, and triphosphate; His, histidine; HPP, hypophosphatasia; Ile, isoleucine; Lac, lactate; Leu, leucine; Mal, malate; MeOH, methanol; MS, mass spectrometry; NAAG, N-acetyl-aspartyl-glutamate; NAA, N-acetylaspartate; Nico, nicotinamide; Oxo, oxoproline; PCA, principal component analysis; PC, phosphocholine; PCr, phosphocreatine; PE, phosphoethanolamine; Phe, phenylalanine; PLP, pyridoxal phosphate; PL, pyridoxal; PLS-DA, partial least squares discriminant analysis; PND, postnatal day; ppm, parts per million; S/N, signal-to-noise ratio; SAH, S-adenosylhomocysteine; SRM, selected reaction monitoring; Suc, succinate; Tau, taurine; TNAP, tissue non-specific alkaline phosphatase; Trp, tryptophan; TSP, Sodium 2,2,3,3-tetradeutero-3-trimethylsilylpropionate; Tyr, tyrosine; UDP, uridine diphosphate; UHPLC, ultra-high performance liquid chromatography; UMP, uridine monophosphate; UTP, uridine triphosphate; UXP, uridine mono-, di-, and triphosphate; Val, valine; VIP, variable importance in the projection.

of these metabolites are involved in neurotransmission (GABA, adenosine), in myelin synthesis (NAA, NAAG), and in the methionine cycle and transsulfuration pathway (cystathione, methionine). Their disturbances may contribute to the neurodevelopmental and neurological phenotype of HPP.

Keywords: cystathione, MSCA-1, neuron, nucleotide, pyridoxal phosphate, tissue non-specific alkaline phosphatase.

J. Neurochem. (2017) **140**, 919–940.

The ubiquitous expression of alkaline phosphatase (AP, EC 3.1.3.1) has been largely demonstrated among the vertebrate and invertebrate phyla (Yang *et al.* 2012; Zimmermann *et al.* 2012). Tissue non-specific alkaline phosphatase (TNAP) is one of the AP isozymes found in vertebrates. In mammals, it is expressed as isoforms in tissues such as bone, cartilage, kidney, liver, lung, as well as in the brain (e.g., Weiss *et al.* 1988; Hoshi *et al.* 1997; Brun-Heath *et al.* 2011; Buchet *et al.* 2013). In adult brains, blood vessels are nicely delineated by the AP activity of endothelial cells, (e.g., Newman *et al.* 1950; Bell and Ball 1985; Anstrom *et al.* 2002; Fonta and Imbert 2002). AP activity has also been demonstrated in adult brain parenchyma (Shimizu 1950), where its spatial distribution displays species-specific patterns (e.g., Friede 1966; Fonta *et al.* 2004; Langer *et al.* 2008; Negyessy *et al.* 2011; Kantor *et al.* 2015). Electron microscopy studies further showed dense AP activity at sites of synaptic connections and on nodes of Ranvier (Pinner *et al.* 1964; Sugimura and Mizutani 1979; Mori and Nagano 1985; Fonta *et al.* 2004, 2005). This activity is displayed on the extracellular side of the cell membrane, giving TNAP its status of ectoenzyme (e.g., Mayahara *et al.* 1967; Fedde and Whyte 1990; Fonta *et al.* 2004).

TNAP activity is also strongly associated with brain development. Strong TNAP activity is observed in cerebral regions of increased proliferative activity such as the ventricular zones (Narisawa *et al.* 1994; Langer *et al.* 2007). Studies also suggested that TNAP participates to neuronal differentiation and axonal growth (Ermonval *et al.* 2009; Kermér *et al.* 2010; Diez-Zaera *et al.* 2011) and that it is involved in myelination and synaptogenesis (Narisawa *et al.* 1997; Fonta *et al.* 2005; Hanics *et al.* 2012).

These results suggest that TNAP plays an important role in brain development and functioning. This hypothesis is corroborated by observations collected from humans with TNAP mutations leading to the severe forms of hypophosphatasia (HPP) (Rathbun 1948; Weiss *et al.* 1988; Greenberg *et al.* 1993; Taillandier *et al.* 2005; Taketani 2015) and from mice in which TNAP gene function has been ablated (Waymire *et al.* 1995; Narisawa *et al.* 1997): a neurological phenotype, mainly characterized by epileptic seizures, is observed in both cases. In patients with the severe perinatal form of HPP, cerebral imaging revealed, among others, hypodensity of the white matter and dilated ventricles, thereby adding convincing evidence that TNAP malfunction directly impacts brain structure (Nunes *et al.*

2002; Demirbilek *et al.* 2012; Hofmann *et al.* 2013; de Roo *et al.* 2014).

Although clinical and experimental studies support the hypothesis that TNAP contributes to the development and functioning of the nervous system, a more complete understanding of the roles of this enzyme requires examining its functions at the molecular level. Studies in other tissues have revealed several TNAP substrates, whose levels are increased in HPP patients and TNAP-knockout mice. Historically, phosphoethanolamine (PE) was the first compound associated with HPP as its plasmatic and urinary concentrations were found to be considerably increased in HPP patients (Fraser *et al.* 1955; McCance *et al.* 1955). Likewise, urinary PE levels are also elevated in TNAP-knockout mice (Fedde *et al.* 1999). Inorganic pyrophosphate (PPi), a key player in bone mineralization (Harmey *et al.* 2004), is also a substrate of TNAP as it is found in higher concentrations in HPP patients (Russell 1965) as well as in TNAP-knockout mice (Fedde *et al.* 1999). Finally, pyridoxal phosphate (PLP), the major form of vitamin B6, accumulates in the serum of both HPP patients (Whyte *et al.* 1985, 1988) and TNAP-knockout mice (Waymire *et al.* 1995). TNAP hydrolyzes extracellular PLP into pyridoxal (PL), which can passively diffuse through the cell membrane (reviewed in Coburn 2015). Within the cells, PL is rephosphorylated to PLP, which is used as co-factor of numerous enzymatic reactions (> 60 in mammals, Percudani and Peracchi 2009). Among these so-called B6-enzymes, some are involved in the metabolism of neurotransmitters, biogenic amines and sphingolipids. Thus in the brain, TNAP dysfunction has consequences on GABA, serotonin and dopamine synthesis (Waymire *et al.* 1995; Balasubramanian *et al.* 2010; Fonta *et al.* 2012).

In addition to the aforementioned PE, PPi, and PLP, studies showed that TNAP is also capable of hydrolyzing extracellular adenine nucleotides in several tissues such as airways, bone, or liver (e.g., van Belle 1976; Say *et al.* 1991; Picher *et al.* 2003; Ciancaglini *et al.* 2010). TNAP may also act as an ectonucleotidase in the nervous system (Dorai and Bachhawat 1977; Ohkubo *et al.* 2000; Diez-Zaera *et al.* 2011; Street *et al.* 2013). It may thus modulate the extracellular ATP/adenosine ratio and affect cellular processes of brain development, neurotransmission and neuroinflammation, via purinergic signaling regulation (Zimmermann 2006; Langer *et al.* 2008; Pike *et al.* 2015; Street and Sowa 2015).

The results published thus far point toward the manifold molecular functions exerted by TNAP in the brain, but the picture remains fragmentary given the targeted experimental approaches used in the previous studies. To provide a more global insight, a metabolomics approach was carried out. In the last decade metabolomic studies of brain tissue or biofluids from animal models and patients have led to the identification of metabolic signatures of various neurodegenerative diseases and mental disorders (Dumas and Davidovic 2015; Gonzalez-Riano *et al.* 2016; and references therein). Our project aimed to identify without any *a priori* the metabolites specifically altered by the lack of TNAP activity in the brain. These metabolites could be the substrates and products of TNAP itself, or substrates and products of other biochemical processes indirectly involving TNAP such as those implicating PLP-dependent enzymes. For this purpose, we compared the metabolomes of wild-type mice (*Akp2*^{+/+}, *Akp2* being the murine TNAP gene) to that of mice partially or totally deficient in TNAP activity (heterozygous *Akp2*⁺⁻ and homozygous *Akp2*^{-/-}, respectively). We used *in vitro* proton nuclear magnetic resonance (¹H NMR) spectroscopy as the main tool. Complementary analyses were performed using phosphorus-31 nuclear magnetic resonance (³¹P NMR) and mass spectrometry (MS). Of 39 well-identified metabolites, we found eight (7 for the first time) that showed significantly altered concentration in the brain of TNAP-knockout mice.

Materials and methods

Animals and sample collection

Inactivation of the TNAP gene in the mouse phenocopies severe lethal infantile HPP (Waymire *et al.* 1995; Narisawa *et al.* 1997; Fedde *et al.* 1999). *Akp2* mice (Narisawa *et al.* 1997) were bred in the CerCo animal facilities in accordance with the Guide for the Care and Use of Laboratory Animals (National Research Council 1996, European Directive 86/609) and the guidelines of the local institutional animal care and use committee. The study was approved by the Regional (Midi-Pyrénées) Ethics Committee (ref. No. MP/06/79/11/12).

In our rearing conditions, *Akp2*^{-/-} mice do not survive beyond 8–10 days. Previous experiments have shown modifications in the growth of the cerebral white matter from 4 days of age and delayed myelination and synaptic maturation in 7–8 day-old *Akp2*^{-/-} mice (Hanics *et al.* 2012). On the other hand, neuronal circuits and, more specifically, GABA inhibitory transmission in the cortex, are not functional before 7–8 postnatal days (PND) in mice (Daw *et al.* 2007). Therefore, the experiments were performed with 7-day-old animals.

Young animals, both males and females, were obtained from *Akp2*⁺⁻ couples that had free access to tap water and commercial solid food [(E) expended, Special Diet Service] containing vitamin B6 (Pyridoxine, 18.25 mg/kg). No additional vitamin B6 was given to the adult or young mice.

All brain samples were collected in the late morning. Mice were weighed, anesthetized by hypothermia to slow down brain metabolism, and then decapitated. Brains, including olfactory bulbs,

cerebral hemispheres, brainstem and cerebellum, were quickly removed, weighed, immediately frozen in liquid nitrogen and stored at –80°C.

Mice genotypes were specified *a posteriori* using tail samples. Genotyping was performed by PCR analysis of the *Akp2* region containing the 1100 bp insert in exon 6 used to inactivate the *Akp2* gene. The wild-type PCR product is expected to have a size of 187 bp, whereas the mutant PCR product with an insert has a size of 1287 bp. Briefly, 10–50 ng of genomic DNA in a total volume of 20 µL was subjected to 36 cycles of PCR (94°C 30 s, 55°C 40 s, 72°C 5 min 30 s) using the Promega PCR Master Mix. The sequences of oligonucleotides used to amplify the target were 5'TGCTGCTCCACTCACGTCGAT (forward) and 5'AGTCGGT GGGCATTGTGACTA (reverse). The expected sizes were 187 bp for *+/+* mice, 187 bp and 1287 bp for *+/-* mice, and 1287 bp for *-/-* mice.

A total of 32 mice were studied, including 11 wild-type *Akp2*^{+/+}, 12 heterozygous *Akp2*⁺⁻, and 9 homozygous knockout *Akp2*^{-/-} mice. Except for one *Akp2*^{-/-} mouse, the TNAP-deficient animals were all from the same litters as the control mice.

Chemicals

Sodium 2,2,3,3-tetradeutero-3-trimethylsilylpropionate (TSP) and all reference compounds for NMR signal assignments (cystathione, GABA, adenosine, serine, cysteine, homocysteine, alpha ketobutyrate, methionine, PLP, PPi) were purchased from Sigma-Aldrich (St Louis, MO, USA). Methanol and chloroform were supplied by Carlo Erba (Val de Reuil, France).

Tissue extraction

The frozen tissues were weighed (260 ± 23 mg, mean ± SD) and the brain extracts prepared according to the procedure described by Beckonert *et al.* (2007) using a chloroform:methanol:water mixture [2:2:1.425 (v/v/v)]. The whole brain was transferred into an ice-cold glass vial maintained on ice. Ultra-pure cold water (0.425 mL) and cold methanol (2 mL) were added. The suspension was pulverized with an Ultra-Turrax (IKA-Werke, Staufen, Germany) for 3 × 10 s and then sonicated with a sonicator probe (Vibra cell™, Sonic, Newtown, USA) for 3 × 10 s. Two mL of cold chloroform and 1 mL of ultra-pure cold water were then added and the mixture was vortexed for 15 s and kept on ice for 15 min. After centrifugation (15 min, 1100 g, 5000 rpm, 4°C), the upper methanol/water phase was collected. This solution was lyophilized overnight, then suspended in 2 mL of water. 1.5 mL was collected for NMR analysis and 0.5 mL withdrawn for MS investigations. After analysis, all samples were dried anew by speed vacuum centrifugation for 8 h, lyophilized overnight and stored at –80°C.

¹H NMR spectroscopy

550 µL of borate buffer in D₂O at pH 10 was added to the lyophilized sample (final concentration 62.5 mM) and 5 µL of a 5 mM solution (25 nmol) of TSP was added as an internal chemical shift and quantification reference. Using a pH of 10 allowed resolving several resonances that overlap at pH 7, taking advantage of chemical shift variations of NMR signals from metabolites with ionisable groups such as aminoacids, amines, or organic acids with pH (Robert *et al.* 2011). The quality of the extraction protocol in the

chosen conditions and the stability of brain metabolites at pH 10 have previously been demonstrated (Lalande *et al.* 2014).

The solution was then transferred into a 5 mm diameter NMR tube and ¹H NMR spectra were recorded on a Bruker Avance spectrometer (Bruker Biospin AG, Fallanden, Switzerland) operating at 400.13 MHz and equipped with a 5 mm broadband inverse probe. ¹H NMR experiments were acquired at 298 K using a classical 1D pulse sequence (relaxation delay-pulse-acquisition), a 2.0 s pre-saturation pulse for water (HOD) signal suppression, and a repetition time of 5.7 s. A flip angle of 30° was used with 32K data points for acquisition over a spectral width of 11 ppm (4400 Hz) and 768 scans were collected.

Data were processed using the Bruker TopSpin 3.2 software with one level of zero-filling and Fourier transformation after multiplying the FIDs by an exponential line-broadening function of 0.3 Hz. Phase adjustment of NMR signals and baseline correction using the sine function tool included in the TopSpin software were done manually on each spectrum. Under these recording conditions, all ¹H resonances were fully relaxed as previously reported (Lalande *et al.* 2014).

Metabolite identities were assigned with an in-house metabolite database at pH 10 and with a public database (Wishart *et al.* 2013). Pure standard compounds (cystathionine, homocysteine, serine, alpha ketobutyrate, cysteine, adenosine, GABA, methionine, PLP) were added to the analyzed extracts for confirming assignments for regions presenting strong overlap between signals or for checking suitability of signal detection for metabolites that were not detected in the brain extracts. Signals used for quantification were chosen after their assignments based on previous studies (Robert *et al.* 2011) and/or comparison with in-house metabolite database.

The selective ¹H 1D COSY experiments (selcogp) were performed on cystathionine NMR signals with an off-resonance 180° pulse of 118.5 ms (GausCascadeG3, 256 points). The parameters were as follows: relaxation delay 1 s, acquisition time 1.64 s (32K data points), spectral width of 20 ppm (8000 Hz), and 1024 or 2048 scans. The transmitter frequency offset (o1p) was adjusted at 3.9 or 4.7 ppm depending on the selective excitation.

³¹P NMR spectroscopy

¹H-decoupled ³¹P NMR spectra were recorded without nuclear Overhauser effect using the same Bruker Avance spectrometer operating at 161.99 MHz and equipped with a Triple resonance Broadband Observe (TBO) probe. Spectra were acquired by re-analyzing the solutions used for ¹H NMR except that 5 mg of the paramagnetic agent chromium(III) acetylacetone were added to shorten the T1 relaxation times of the phosphorylated compounds as well as 20 μL of a 5 mM solution of an internal reference (methylene diphosphonic acid) which was used as chemical shift reference and calibrated at 16.30 ppm. Spectra were recorded under the following instrumental conditions: sweep width, 270 ppm; flip angle, 30°; repetition time, 6.54 s; 7680 scans (14 h recording). Spectra were processed by exponential multiplication with a line broadening of 3 Hz. In these experimental conditions, the detection limit is 25 μmol/L with an S/N of 3, the S/N being 2.5 × (peak height/noise height measured peak-to-peak) for a molecule containing one phosphorus atom, and 12.5 μmol/L for PPi that contains two equivalent nuclei.

Targeted UHPLC-MS/MS analysis of cystathionine

Nine samples coming from *Akp2*^{+/+} (*n* = 2), *Akp2*^{+/-} (*n* = 3), and *Akp2*^{-/-} (*n* = 4) mice previously analyzed by ¹H NMR were investigated. Samples withdrawn for MS analysis were suspended in 1 mL acetonitrile:water (50 : 50) under vortex agitation during 1 min and then sonicated for 5 min. The suspension was then centrifuged (5 min, 4000 rpm) and the supernatant analyzed after filtration using 3 kDa Amicon Ultra-0.5 mL filters (Merck Millipore, Darmstadt, Germany) with a ultra-high performance liquid chromatography (UHPLC) Thermo Scientific Dionex UltiMate 3000 system coupled to a Q-TRAP 4500 AB Sciex (AB SCIEX, Warrington, UK) mass spectrometer. The chromatographic conditions for analysis were as follows: C8 Symmetry[®] column (75 × 4.6 mm i.d.; 3.5 μm particle size); mobile phase: (A) demineralized water with 0.1% (v/v) formic acid and (B) methanol (HPLC grade); flow rate: 0.3 mL/min. The elution conditions were a 60:40 A:B mixture from 0 to 6 min, then a linear gradient up to 0:100 A:B from 6 to 8 min, followed by an isocratic elution during 1 min, and finally a reequilibration to 60:40 A:B mixture in 1 min. Cystathionine eluted at 2.67 min. For MS detection, the instrument parameters were as follows: for MS analysis, declustering potential (DP) 50 V and scan range m/z 160–1000; for MS/MS analysis: DP 50 V, collision energy 20 V, and scan range m/z 50–230. Detection of cystathionine was achieved by selected reaction monitoring (SRM) in positive mode using a QTrap mass spectrometer with a Turbo ion spray source at 400°C. The ion spray voltage was set at 5500 V, DP was 30 V, collision energy was 20 V. The monitored transition was m/z 223 ([M+H]⁺) → 134.

Chemometric data analysis

¹H NMR spectra were transferred to the KnowItAll[®] software (Bio-Rad, Cambridge, MA, USA). The bin area method was used to segment the spectra between 0.8 and 9.3 ppm using the intelligent variable size bucketing tool included in the KnowItAll[®] package. Close to 600 variables were generated with one signal (or noise) per bucket. The bins of water (HOD) (4.7–5.2 ppm) and residual methanol (3.34–3.36 ppm) resonances were excluded.

A manual filtering procedure was applied to the whole spectrum to exclude buckets that contained only noise. Buckets corresponding to one metabolite were grouped when possible, according to NMR signal assignment. A total of 223 variables (buckets) were thus retained for the subsequent statistical analyses. Bin areas were integrated and transferred to the Pirouette software (Infometrics, Inc., Woodinville, WA, USA), which generated a matrix consisting of rows representing the 32 samples and columns representing the 223 variables. Integrated regions were normalized by dividing their areas by that of the internal standard TSP and by brain weight.

The statistical approach followed for metabolomics analysis has already been described (Lalande *et al.* 2014). Multivariate statistical analyses were carried out using an in-house package developed in the R environment (Balayssac *et al.* 2013) and the SIMCA-P + 12.0 software (Umetrics, Umeå, Sweden). First, an unsupervised approach by principal component analysis (PCA) was applied to the ¹H NMR dataset. PCA was primarily used for outlier detection and for determining trends for grouping determined by mouse genotypes. Then, after Unit Variance scaling of the data in which the standard deviation of each column was used as the scaling factor, three groups corresponding to three genotypes (*Akp2*^{+/+}, *Akp2*^{+/-}, and *Akp2*^{-/-})

were considered for supervised statistical analysis by partial least squares discriminant analysis (PLS-DA) and were pairwise compared. The predictive ability of the PLS-DA models was validated by the goodness-of-fit (R^2_Y , R^2_X) and the goodness of prediction (Q^2) parameters, the response permutation test (based on 999 permutations) and the analysis of variance of the cross-validated residuals (CV-ANOVA). Loading plot, coefficient plot, and variable importance in the projection (VIP) from PLS-DA models were used to identify the variables driving the separation between classes, i.e., the metabolites which can be potential biomarkers. Correlation coefficients were mainly used for the attribution of the NMR signals of cystathionine. Indeed, the Pearson's linear correlation coefficient captures linear dependency between two variables, providing, for a threshold > 0.9 , a statistical indicator on the structural correlations of a metabolite. Metabolites concentrations were obtained from their targeted NMR signals (Table 1) using the general equation: $C_x = (A_x/A_{TSP}) \times (9/N_x) \times (n/m)$, where A_x and A_{TSP} represent the areas of the signals of the metabolite X and of TSP, respectively, 9 and N_x the number of protons of TSP and of the metabolite X, respectively, n the number of nmol of TSP in the solution, and m the brain weight (g). This quantification method has been validated in a previous publication (Robert *et al.* 2011). Metabolite concentrations were compared with non-parametric tests. For each metabolite, comparisons between the three genotypes were performed using the Kruskal–Wallis test (p -values corrected for multiple comparisons using the Holm–Šídák procedure). Paired comparisons between groups of mice were done with the Mann–Whitney test (p -values corrected for multiple comparisons). To provide a quantitative estimate of the difference between groups, we calculated the ratio of the means, and the associated 95% confidence intervals using Fieller's method (Franz 2007).

Results

¹H NMR spectra and metabolite signal assignments

1D ¹H NMR spectra were collected from aqueous extracts of whole brains of control wild-type *Akp2^{+/+}* ($n = 11$), heterozygous *Akp2^{+/−}* ($n = 12$), and homozygous *Akp2^{−/−}* ($n = 9$) mice. A typical ¹H NMR spectrum of an aqueous extract of an *Akp2^{+/+}* mouse brain is presented in Fig. 1. Classical brain metabolites of mammals were detected, with N-acetylaspartate (NAA), creatine (Cr), lactate (Lac), taurine (Tau), and phosphocholine (PC) generating the most prominent signals.

On visual inspection, all spectra appeared qualitatively similar, the same signals being detected for all genotypes. However, a careful inspection of some regions of the spectra revealed differences in signal intensities between wild-type, heterozygous, and knockout samples. Although most differences could be attributed to resonances of assigned metabolites (see below, statistical analysis), there were nevertheless three regions of the spectra (around δ (ppm) 3.50, 2.88, and 2.65) where *Akp2^{−/−}* brain extracts demonstrated additional or stronger signals in comparison to *Akp2^{+/+}* and *Akp2^{+/−}* (Fig. 2a). These additional signals did not fit with those of any metabolite in our database. Statistical analyses revealed strong Pearson correlation coefficients [> 0.9 ($p < 10^{-8}$)]

between these signals, suggesting that they belonged to the same metabolite. This finding was confirmed with COSY selective NMR experiments that showed correlations (i) between the multiplet centered at 2.88 ppm and the signal at 3.50 ppm, (ii) between the signal at 3.50 ppm and the multiplet at 2.88 ppm and a signal centered around 2.00 ppm that overlapped with signals for glutamate and glutamine. A selective irradiation of the region centered at 2.00 ppm highlighted correlations with the triplet (t) at 2.65 ppm and the multiplet (m) at 3.50 ppm. These experiments led us to hypothesize that these unassigned NMR resonances came from cystathionine, a dipeptide formed from serine and homocysteine. This was confirmed by spiking with the authentic standard. Chemical shifts for this metabolite are δ (ppm) 3.50 (m, 2H, CH 1 and 5); 2.88 (ABd, $J_{AB} = 13.7$ Hz, $J_{AH5} = 5.0$ Hz, $J_{BH5} = 7.0$ Hz, 2H, CH₂ 4); 2.65 (t, 2H, $J = 7.5$ Hz, CH₂ 3 and 2.00 (m, 2H, CH₂ 2) (see Fig. 2 for numbering).

To confirm the presence of cystathionine with a complementary method, a targeted analysis using MS was performed by UHPLC-MS/MS with the SRM mode to enhance sensitivity. Conditions were first optimized using a standard solution of cystathionine. Chromatographic conditions carried out in our study were close to those from literature data for cystathionine (Bartl *et al.* 2014). The selected fragmentation for SRM was that of the pseudo-molecular ion [M+H]⁺ at m/z 223 to the main fragment at m/z 134 as shown in Fig. 2b. The superimposition of representative chromatograms of brain extracts from *Akp2^{+/+}*, *Akp2^{+/−}*, and *Akp2^{−/−}* mice clearly shows that the cystathionine peak, although detected in all extracts, was much higher in the brain extracts of *Akp2^{−/−}* mice (Fig. 2c). Cystathionine is thus a first discriminating metabolite for knockout mice. Statistical analyses were next performed to identify other potential biomarkers distinguishing between groups.

Statistical analyses

A non-supervised PCA analysis was first carried out to analyze the NMR data (Fig. 3a). The PCA score plot did not show dominant trends by visualization on the first and second components, which accounted for 61% and 16%, respectively, of the variance of the data. Yet a trend for a clustering of *Akp2^{−/−}* mice versus other mice was observed on the third component of the PCA, although it explained only 7% of the variation. The PCA analysis indicated that the metabolome of *Akp2^{−/−}* mice was distinct from that of *Akp2^{+/−}* and *Akp2^{+/+}* mice. A supervised analysis with PLS-DA was next performed to identify discriminating metabolites.

The results of the supervised PLS-DA analyses of pairwise comparisons on the 223 variables are reported in Fig. 3b. Comparison between *Akp2^{+/+}* and *Akp2^{+/−}* resulted in a non-predictive model with two principal PLS components ($Q^2_{cum} = 0.008$ and $R^2_{Ycum} = 0.57$). In contrast,

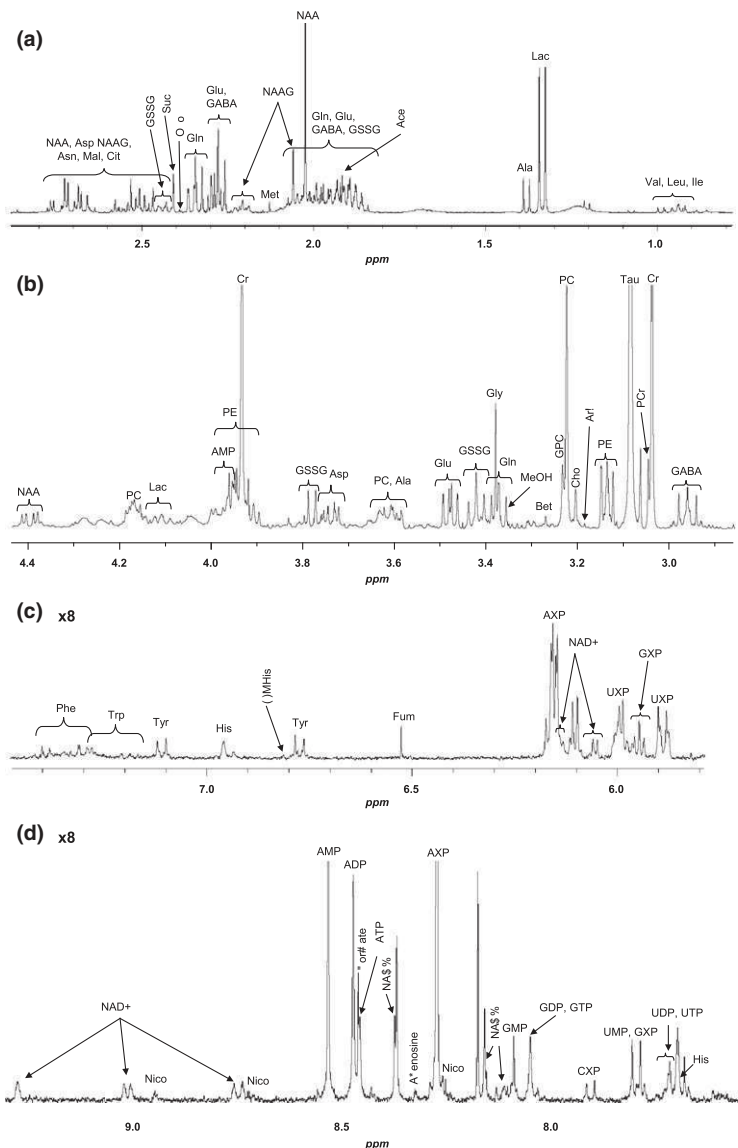


Fig. 1 ^1H NMR spectrum of an aqueous extract of the brain from an $\text{Akp}2^{+/+}$ mouse. (a) 2.9–0.8 ppm region, (b) 4.4–2.9 ppm region, (c) 7.5–5.65 ppm region, (d) 9.3–7.5 ppm region. (a) and (b) regions of the spectrum: valine (Val), isoleucine (Ile), leucine (Leu), lactate (Lac), alanine (Ala), glutamate (Glu), glutamine (Gln), oxoproline (Oxo), γ -aminobutyric acid (GABA), acetate (Aco), glutathione disulfide (GSSG), N-acetyl-aspartyl-glutamate (NAA), N-acetyl-aspartyl-glutamate (NAAG), succinate (Suc), aspartate (Asp), citrate (Cit), asparagine (Asn), malate (Mal), creatine (Cr), phosphocreatine (PCr), taurine (Tau), phosphoethanolamine (PE), choline (Cho), phosphocholine (PC), glycerocephosphocholine (GPC), betaine (Bet), and glycine (Gly). Methanol (MeOH) is a residual solvent. (c) and (d) regions of the spectrum: nicotinamide adenine dinucleotide (NAD^+), adenosine diphosphate (ADP), nicotinamide (Nico), adenosine monophosphate (AMP), adenine (Ade), adenosine mono-, di-, and triphosphate (AXP), guanosine triphosphate (GTP), guanosine diphosphate (GDP), guanosine monophosphate (GMP), guanosine mono-, di-, and triphosphate (GXP), uridine triphosphate (UTP), uridine diphosphate (UDP), uridine monophosphate (UMP), uridine mono-, di-, and triphosphate (UXP), cytidine mono-, di-, and triphosphate (CXP), phenylalanine (Phe), tryptophan (Trp), tyrosine (Tyr), histidine (His), 3-methylhistidine (3-MHis), fumarate (Fum). Peaks for the most abundant compounds (Tau and Cr) have been truncated.

comparison of $\text{Akp}2^{+/+}$ with $\text{Akp}2^{-/-}$ led to a model with three principal PLS components with good predictive values ($Q^2_{\text{cum}} = 0.92$ and $R^2_{\text{Y,cum}} = 0.97$). Likewise, a comparison of $\text{Akp}2^{+/+}$ versus $\text{Akp}2^{-/-}$ led to a model with two principal PLS components with good predictive values ($Q^2_{\text{cum}} = 0.79$ and $R^2_{\text{Y,cum}} = 0.92$). For the two comparisons with knockout mice, the p-values of the CV-ANOVA were 2.6×10^{-4} and 2.5×10^{-5} , respectively. All Q^2 and R^2 values were lower in the permutation tests than in the model, revealing great predictability and goodness of the PLS-DA models. In both comparisons, the same three most discriminating metabolites were highlighted: adenosine, GABA, and cystathionine. Boxplots of each metabolite are presented in Fig. 3C, showing that adenosine and GABA levels were lower in $\text{Akp}2^{-/-}$ than in $\text{Akp}2^{+/+}$ and $\text{Akp}2^{+/+}$ brain extracts, whereas cystathionine was more concentrated in the brain of knockout mice. Other

metabolites that ranked lower in the VIP plot (not shown) are considered below. Therefore, the complete loss of TNAP activity in the cerebral tissue has significant metabolic consequences on three metabolites that objectively discriminate $\text{Akp}2^{-/-}$ mice from their littermates $\text{Akp}2^{+/+}$ and $\text{Akp}2^{+/+}$: adenosine, GABA, and cystathionine.

^1H NMR absolute quantification of metabolites

In addition to cystathionine, GABA and adenosine, 36 metabolites have been unambiguously identified in the ^1H NMR spectra. The levels of metabolites measured in our $\text{Akp}2^{+/+}$ control mice are consistent with those that have been quantified in previous studies in similarly aged rodents (Huguet *et al.* 1998; Kulak *et al.* 2010; Schmitt *et al.* 2013).

The mean concentrations of the 39 metabolites are gathered in Table 1 along with their variations between the

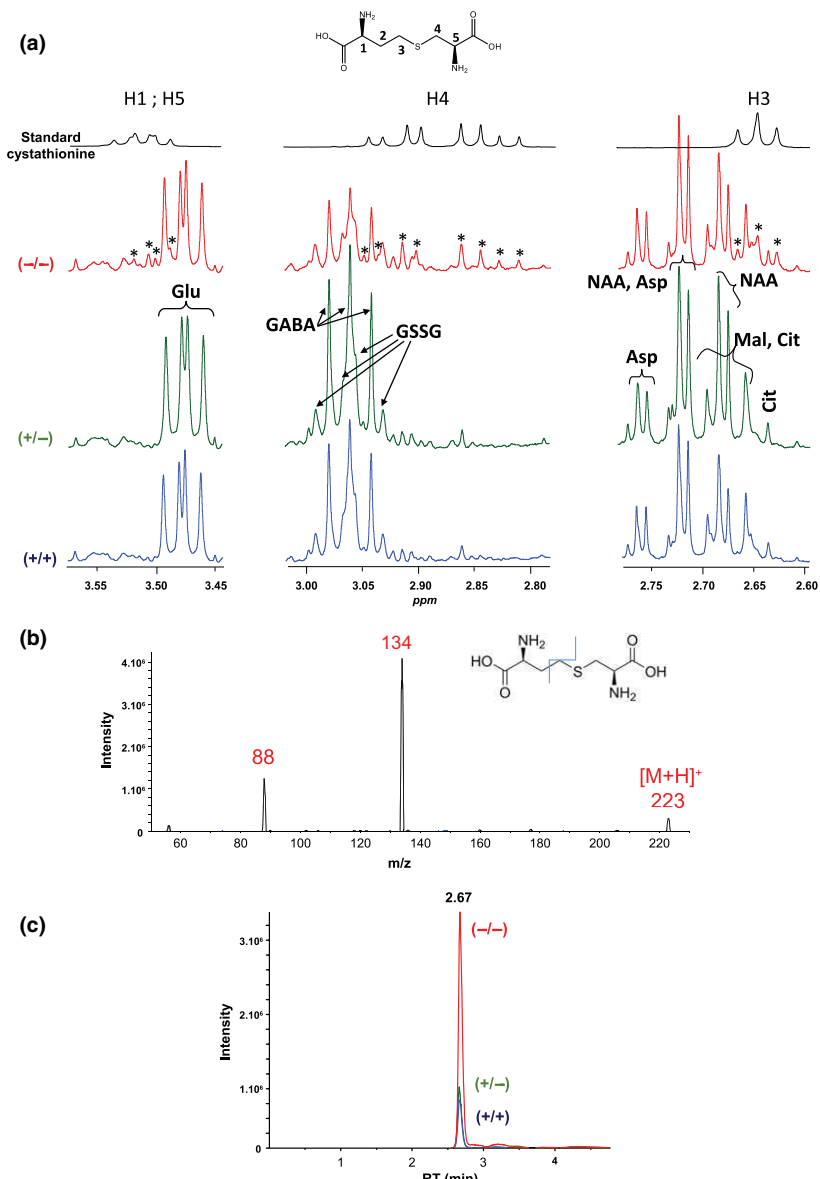


Fig. 2 (a) Comparison of ¹H NMR spectra (zooms around 2.7, 2.9 and 3.5 ppm) of a solution of standard cystathionine and of aqueous brain extracts from *Akp2^{+/+}* (blue), *Akp2^{+/-}* (green), and *Akp2^{-/-}* (red) mice. *signals fitting with those of cystathionine standard. Abbreviations of metabolites: see caption of Fig. 1. (b) Full scan mass spectrometry (MS) spectrum of standard cystathionine. (c) Ultra-high performance liquid chromatography (UHPLC)-MS/MS chromatograms by selected reaction monitoring (SRM) (223 → 134 transition).

three groups of mice. The *p*-values of the comparisons between groups are reported in Table 2. Cumulative distributions of the concentrations of the 39 metabolites in the three groups of mice are presented in Fig. 4; they are largely non-overlapping whenever differences between groups are significant. Differences between groups are summarized in Fig. 5 that presents ratios of the mean concentrations and their 95% confidence intervals. Significant differences are highlighted by colored symbols. These data show that *Akp2^{+/+}* and *Akp2^{+/-}* mice have very similar metabolomes except for cystathionine (*p* = 0.04). In contrast, very large changes are observed for GABA, adenosine, and cystathionine in knockout mice compared to *Akp2^{+/+}* and *Akp2^{+/-}* mice. The amplitude of the concentration variation between the TNAP-knockout mice and the other genotypes grouped together reaches

≈–40% for GABA, ≈–80% for adenosine and is much higher for cystathionine (≈+450%) (Table 1, Fig. 5).

Beyond these highly discriminating metabolites, significant differences were observed for five additional metabolites: methionine, 3-methylhistidine, histidine, NAA and the dipeptide N-acetyl-aspartyl-glutamate (NAAG). Although the NMR variables for these five metabolites were observed in the top 30 variables ranked in the VIP plots (score > 1.3), other converging criteria (% variations and non-parametric tests) were taken into account for confirming the influence of TNAP in their metabolisms. The concentrations of these five metabolites were significantly higher in *Akp2^{-/-}* than in *Akp2^{+/+}* or *Akp2^{+/-}* mice (Tables 1 and 2, Figs 4 and 5). Methionine and 3-methylhistidine levels were around 50% higher in

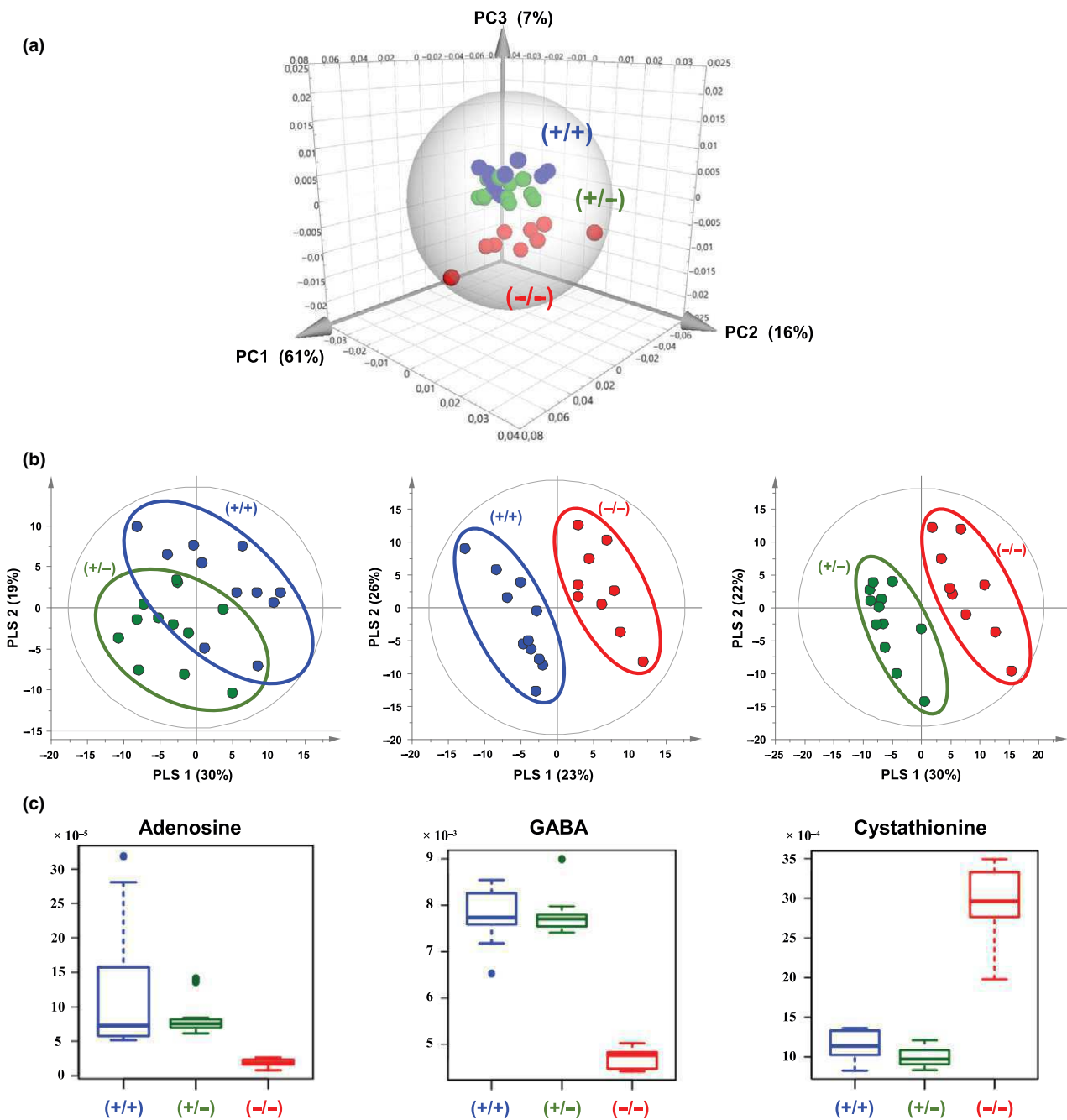


Fig. 3 (a) Three-dimensional score plot of principal component analysis (PCA) on the NMR data collected from all brain extracts. The confidence ellipse (Hotelling's T₂) defines the region that contains 99% of the data. (b) Score plots of the partial least squares discriminant analysis (PLS-DA) on NMR data of *Akp2*^{+/+} versus *Akp2*^{-/-} mice. (c) Boxplots for adenosine (singlet at 8.33 ppm), GABA (triplet at 2.29 ppm) and cystathionine (triplet at 2.65 ppm). The ordinates of the boxplots represent normalized areas of NMR signals. *Akp2*^{+/+} are shown in blue, *Akp2*^{+/-} in green, and *Akp2*^{-/-} in red.

Akp2^{+/+} versus *Akp2*^{-/-} mice and *Akp2*^{+/-} versus *Akp2*^{-/-} mice. (c) Boxplots for adenosine (singlet at 8.33 ppm), GABA (triplet at 2.29 ppm) and cystathionine (triplet at 2.65 ppm). The ordinates of the boxplots represent normalized areas of NMR signals. *Akp2*^{+/+} are shown in blue, *Akp2*^{+/-} in green, and *Akp2*^{-/-} in red.

TNAP-knockout mice. More modest variations (between +10 and +20%) were observed for histidine, NAA, and NAAG.

Non-parametric statistical tests did not reveal any significant variations between the genotypes for the 31

other metabolites (Table 1). Although their metabolisms are associated to PLP-dependent enzymes, metabolites such as taurine, glycine, phenylalanine, pyruvate, aspartate and alanine did not show significant variations between the three groups of mice.

Table 1 Concentrations, along with the considered NMR signals, of the 39 metabolites identified in aqueous brain extracts of $Akp2^{+/+}$ (+/+), $Akp2^{+-}$ (+/-), and $Akp2^{-/-}$ (-/-) mice brains (s: singlet; d: doublet; dd: doublet of doublet; t: triplet; m: multiplet)

Metabolites	NMR signals considered for quantification δ (multiplicity)	Mean concentration nmol/g (SD)			Variation Ratio of the means [CI low-CI high]		
		+/+	+/-	-/-	-/-	+/-	+/-
					vs. +/+	vs. +/-	vs. +/+
Adenosine	8.327 (s)	37 (29)	25 (8)	5 (2)	0.14 [0.08–0.29]	0.20 [0.14–0.28]	0.69 [0.43–1.40]
Cystathione	2.884	94 (31)	67 (23)	366 (62)	3.89 [3.10–5.05]	5.49 [4.36–7.14]	0.71 [0.52–0.96]
	(ABd system) ^a						
GABA	2.288 (t)	1169 (87)	1 165 (64)	702 (33)	0.60 [0.57–0.64]	0.60 [0.58–0.63]	1.00 [0.94–1.06]
Methionine	2.127 (s)	94 (19)	83 (16)	141 (48)	1.50 [1.11–1.93]	1.69 [1.27–2.16]	0.89 [0.75–1.05]
3-methylhistidine	6.810 (s)	27 (11)	34 (9)	47 (11)	1.75 [1.31–2.43]	1.39 [1.10–1.75]	1.26 [0.95–1.74]
Histidine	6.955 (s)	156 (31)	138 (16)	187 (37)	1.20 [0.99–1.44]	1.36 [1.15–1.57]	0.88 [0.77–1.02]
NAA	2.024 (s)	1 719 (199)	1 680 (173)	2 010 (192)	1.17 [1.06–1.29]	1.20 [1.09–1.31]	0.98 [0.89–1.08]
NAAG	2.058 (s)	702 (63)	691 (43)	794 (54)	1.13 [1.05–1.22]	1.15 [1.08–1.22]	0.99 [0.92–1.06]
AMP	8.532 (s)	925 (152)	913 (103)	1 023 (194)	1.11 [0.93–1.31]	1.12 [0.96–1.29]	0.99 [0.88–1.12]
ADP	8.473 (s)	479 (137)	605 (190)	465 (152)	0.97 [0.71–1.30]	0.77 [0.56–1.03]	1.26 [0.97–1.64]
ATP	8.458 (s)	179 (85)	185 (76)	132 (74)	0.74 [0.42–1.20]	0.71 [0.42–1.11]	1.03 [0.70–1.57]
Alanine	1.379 (d)	662 (150)	633 (75)	662 (143)	1.00 [0.81–1.23]	1.05 [0.88–1.23]	0.96 [0.82–1.13]
Arginine	3.186 (t) ^a	715 (102)	641 (112)	688 (150)	0.96 [0.80–1.14]	1.07 [0.89–1.29]	0.90 [0.78–1.03]
Aspartate	3.740 (dd) ^a	1 370 (311)	1 055 (174)	1 432 (462)	1.05 [0.78–1.35]	1.36 [1.04–1.71]	0.77 [0.65–0.92]
Betaine	3.271 (s)	35 (5)	35 (3)	43 (7)	1.22 [1.05–1.42]	1.23 [1.07–1.40]	0.99 [0.90–1.10]
Choline	3.205 (s)	77 (29)	68 (9)	64 (7)	0.83 [0.66–1.10]	0.94 [0.84–1.05]	0.89 [0.71–1.17]
Creatine	3.039 (s)	4 813 (467)	4 485 (321)	4 355 (255)	0.91 [0.84–0.98]	0.97 [0.92–1.03]	0.93 [0.87–1.01]
Fumarate	6.524 (s)	33 (8)	30 (5)	35 (6)	1.05 [0.86–1.29]	1.15 [0.98–1.34]	0.91 [0.76–1.11]
Glutamate	2.277 (t)	3 477 (461)	3 279 (331)	3 531 (325)	1.02 [0.92–1.13]	1.08 [0.99–1.18]	0.94 [0.85–1.05]
Glutamine	2.344 (m)	2 805 (453)	2 859 (333)	2 703 (434)	0.96 [0.83–1.12]	0.95 [0.83–1.08]	1.02 [0.90–1.16]
Glutathione disulfide	3.783	676 (88)	645 (45)	667 (97)	0.99 [0.86–1.12]	1.04 [0.92–1.15]	0.95 [0.87–1.05]
	(AB system) ^a						
Glycerophosphocholine	3.23.4 (s)	289 (47)	299 (30)	308 (32)	1.06 [0.94–1.21]	1.03 [0.94–1.13]	1.03 [0.92–1.17]
Glycine	3.380 (s)	1 321 (149)	1 237 (149)	1 256 (197)	0.95 [0.83–1.08]	1.02 [0.89–1.16]	0.94 [0.85–1.04]
GMP	8.091 (s)	157 (40)	127 (38)	177 (40)	1.13 [0.90–1.42]	1.40 [1.10–1.79]	0.81 [0.63–1.03]
Isoleucine	0.975 (d) ^a	70 (19)	74 (10)	73 (15)	1.04 [0.83–1.30]	0.99 [0.83–1.16]	1.05 [0.88–1.28]
Lactate	1.333 (d)	2 823 (707)	2 740 (499)	3 315 (682)	1.17 [0.95–1.46]	1.21 [1.00–1.46]	0.97 [0.81–1.19]
Leucine	0.925 (d) ^a	234 (52)	234 (020)	254 (52)	1.09 [0.89–1.33]	1.09 [0.92–1.26]	1.00 [0.87–1.17]
NAD⁺	8.748 (d), 9.013 (d) and 9.273 (s)	160 (24)	146 (15)	157 (25)	0.99 [0.85–1.14]	1.08 [0.95–1.22]	0.91 [0.82–1.02]
Nicotinamide	8.716 (dd) and 8.946 (d)	35 (10)	32 (9)	46 (12)	1.30 [1.00–1.70]	1.43 [1.11–1.84]	0.91 [0.70–1.18]
Oxoproline	2.387 (m)	323 (67)	311 (53)	374 (117)	1.16 [0.88–1.48]	1.21 [0.93–1.51]	0.96 [0.82–1.14]
Phenylalanine	7.348 (m)	108 (16)	106 (12)	123 (18)	1.14 [1.01–1.30]	1.16 [1.06–1.28]	0.98 [0.87–1.10]
Phosphocholine	3.225 (s)	879 (88)	907 (98)	1 072 (171)	1.22 [1.07–1.38]	1.18 [1.03–1.34]	1.03 [0.94–1.13]
Phosphocreatine	3.046 (s)	506 (78)	596 (216)	504 (112)	1.00 [0.82–1.19]	0.85 [0.65–1.13]	1.18 [0.91–1.47]
Phosphoethanolamine	3.136 (m)	3 129 (371)	3 056 (192)	3 003 (230)	0.96 [0.88–1.05]	0.98 [0.92–1.05]	0.98 [0.90–1.06]
Succinate	2.407 (s)	201 (34)	195 (18)	228 (34)	1.13 [0.98–1.32]	1.17 [1.04–1.31]	0.97 [0.86–1.10]
Taurine	3.085 (s)	14 153 (1 206)	13 996 (666)	14 312 (1 401)	1.01 [0.93–1.10]	1.02 [0.95–1.10]	0.99 [0.93–1.05]
Tryptophane	7.183 (m) and 7.530 (m)	41 (15)	43 (6)	54 (19)	1.31 [0.92–1.84]	1.26 [0.94–1.59]	1.04 [0.83–1.36]
Tyrosine	6.771 and 7.107 (AA'XX' system)	141 (38)	138 (15)	150 (31)	1.07 [0.86–1.34]	1.09 [0.93–1.27]	0.98 [0.82–1.19]
Valine	0.989 (d)	118 (27)	126 (18)	122 (21)	1.03 [0.86–1.25]	0.97 [0.83–1.12]	1.07 [0.91–1.27]

^aOnly a part of the signal was considered for quantification.

The eight discriminating metabolites are shown at the top of the table (bold), followed by the 31 other metabolites alphabetically listed. The mean concentrations and standard deviations (SD) are expressed in nmol/g of wet brain tissue. Variations were calculated with the mean concentration values (CI: 95% confidence interval).

Table 2 Statistical comparisons of the mean concentrations of the eight discriminating metabolites between *Akp2^{+/+}*, *Akp2^{-/-}*, and *Akp2^{+/-}* genotypes (non-parametric tests, with correction for multiple comparisons)

Metabolites	Kruskal–Wallis	p-values			
		Mann–Whitney			
		−/– vs. +/+	−/– vs. +/–	+/– vs. +/+	
Adenosine	2.4×10^{-3}	4.0×10^{-4}	3.0×10^{-4}		
Cystathionine	3.0×10^{-5}	4.0×10^{-4}	3.0×10^{-4}	4.2×10^{-2}	
GABA	1.4×10^{-4}	4.0×10^{-4}	3.0×10^{-4}		
Methionine	2.1×10^{-3}	6.8×10^{-3}	1.2×10^{-3}		
3-methylhistidine	1.4×10^{-2}	8.1×10^{-3}	2.1×10^{-2}		
Histidine	2.9×10^{-2}	4.9×10^{-2}	8.4×10^{-3}		
NAA	4.6×10^{-2}	2.2×10^{-2}	8.4×10^{-3}		
NAAG	4.7×10^{-3}	4.2×10^{-3}	2.4×10^{-3}		

³¹P NMR analysis

PPi and PLP are well-established substrates of TNAP. As PLP was not detected and PPi could not be observed with our ¹H NMR methodology, and in an attempt to complement the analysis of phosphorylated metabolites, we performed ³¹P NMR experiments on the same samples of brain extracts. A proton decoupled ³¹P NMR spectrum of the aqueous extract of a wild-type (*Akp2^{+/+}*) mouse whole brain is presented in Fig. 6. Signals were assigned by addition of authentic compounds and/or with literature data on ³¹P NMR analysis of tissue extracts (Iles *et al.* 1985; Gribbestad *et al.* 1994). The analysis allowed the detection of PE (3.98 ppm), PC (3.46 ppm), Pi (2.74 ppm), glycerophosphocholine (−0.07 ppm), phosphocreatine (−3.08 ppm) and of the adenine nucleotides AMP (3.96 ppm, singlet), ADP (−5.75 ppm, doublet (d), ²J_{PP} = 21.4 Hz; −10.27 ppm, d, ²J_{PP} = 21.4 Hz), and ATP (−5.30 ppm, d, ²J_{PP} = 17.8 Hz). The two other signals of ATP at ≈−10.5 ppm (d) and −21.4 ppm (t) were difficult to detect because of their low intensity and partial overlap with unknown signals for the doublet. Neither PPi nor PLP could be detected in the brain extracts, although addition of standard PPi and PLP revealed signals for both compounds at −5.35 ppm and 3.81 ppm, respectively (not illustrated). Thus, if PPi and PLP were present, their concentrations must have been under the detection limits, which are 25 µmol/L for PLP and 12.5 µmol/L for PPi in our experimental conditions. Therefore, it appears from all these experiments that ³¹P NMR did not add much in comparison to ¹H NMR.

Discussion

The aim of this study was to specify, without any *a priori*, the products and substrates whose synthesis or use are linked, directly or indirectly, to TNAP function in the nervous tissue. As such our study was the first to use

metabolomics for analyzing the brain metabolism in an animal model of HPP. We found that the levels of eight metabolites differed when comparing TNAP-knockout mice to wild-type and heterozygous mice. Thus, non-supervised PCA analysis indicated that the metabolome of *Akp2^{-/-}* mice was distinct from those of *Akp2^{+/+}* and *Akp2^{+/-}* mice, whereas supervised PLS-DA revealed that GABA, adenosine, and cystathionine were the metabolites that most strongly distinguished *Akp2^{-/-}* mice from the other genotypes (Fig. 3). Further analyses showed that five other metabolites (methionine, 3-methylhistidine, histidine, NAA and NAAG) were found in significantly higher concentrations in *Akp2^{-/-}* mice brain (Tables 1 and 2, Figs 4 and 5).

¹H NMR power

Untargeted ¹H NMR requires minimal sample preparation prior to analysis, offers relatively short analytical run times and produces highly reproducible results. It is particularly well suited to the analysis of metabolites available in limited amounts from samples of small sizes, as often occurs with brain tissue. The number of metabolites detected and quantified in our study – 39 – is in the upper range of that described in previous studies using ¹H NMR from brain extracts. Indeed, although Liu *et al.* (2013) have been able to quantify 36 metabolites in the brain of neonatal mice using a 900 MHz spectrometer, recent studies on mice brain extracts typically described < 30 metabolites (Salek *et al.* 2010; Botosoa *et al.* 2012; Lalande *et al.* 2014). NMR analysis on human CSF is more powerful and allows the detection of > 50 metabolites (Wishart *et al.* 2008; Sinclair *et al.* 2010; Stoop *et al.* 2010; Mandal *et al.* 2012; Smolinska *et al.* 2012). However, for specific diseases, it remains necessary to work in exploratory studies with animal models in which the collection of CSF is difficult to achieve. Interestingly, among the eight metabolites highlighted in this study, only 3 – methionine and histidine (Wishart *et al.* 2008), 3-methylhistidine (Stoop *et al.* 2010) – have been detected using untargeted ¹H NMR in human CSF, whereas the detection of the other five in the CSF required alternative targeted methods – cystathionine (Strauss *et al.* 2007), adenosine (Traut 1994), GABA (Nisijima and Ishiguro 1995), NAA and NAAG (Do *et al.* 1995).

Limitations of this study

As the ¹H NMR analysis was conducted on the whole brain, it is not possible to state as to whether the metabolites measured were located in the intra- or extracellular compartment and to compare metabolites levels between whole brain and CSF.

In addition, the whole brain homogenates mixed the diverse cell types that express TNAP. However, TNAP vascular activity appears around 10–12 PND in the mouse

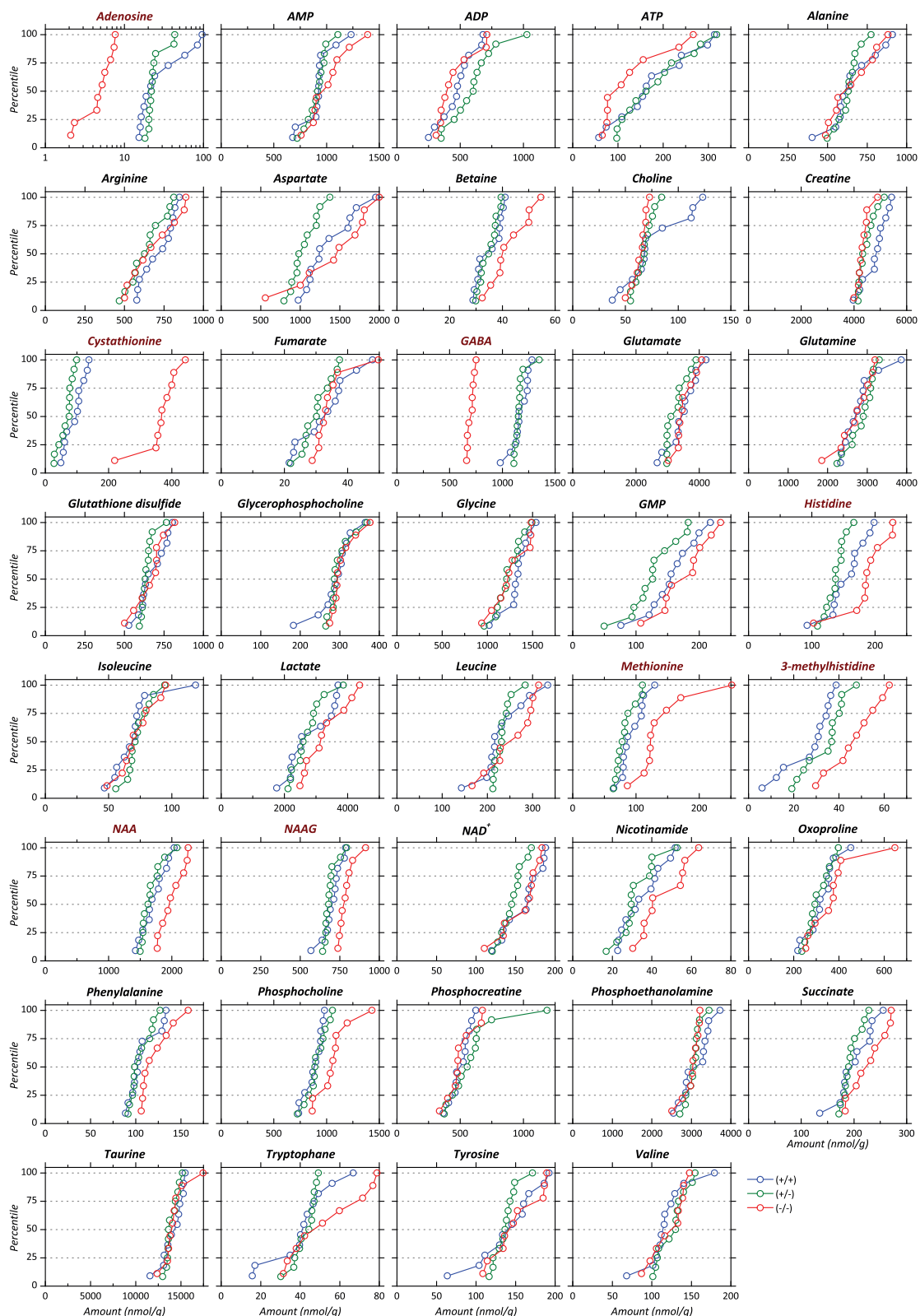


Fig. 4 Cumulative distributions of the concentrations of the 39 metabolites identified for the three groups of mice: *Akp2*^{+/+} (blue), *Akp2*^{+/-} (green), and *Akp2*^{-/-} (red). Metabolites have been ordered

alphabetically. Names in red correspond to metabolites whose concentration differed significantly between *Akp2*^{-/-} and *Akp2*^{+/+} and ^{+/-} mice. Note log scale for adenosine.

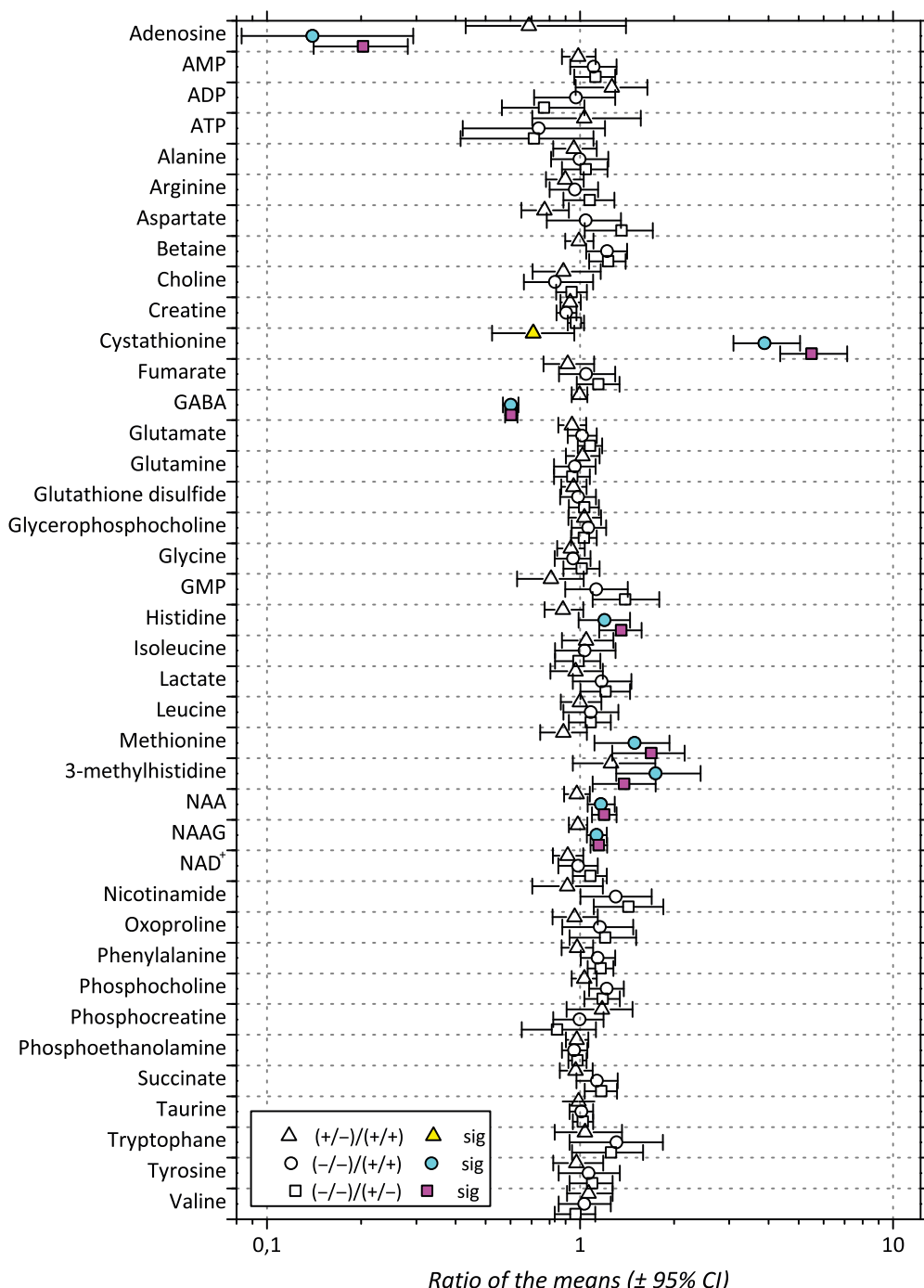


Fig. 5 Ratios of the mean concentrations for the 39 metabolites identified in aqueous extracts of *Akp2^{+/+}* (+/+), *Akp2^{+/-}* (+/-), and *Akp2^{-/-}* (-/-) mice brains. Symbols correspond to the actual ratio and bars encompass the 95% confidence interval of the ratio. Triangles represent the *Akp2^{+/-}/Akp2^{+/+}* ratios, squares the *Akp2^{-/-}/Akp2^{+/+}*

ratios and circles the *Akp2^{-/-}/Akp2^{+/+}* ratios. Colored symbols indicate significant differences ($p < 0.05$) between *Akp2^{-/-}* and *Akp2^{+/+}* (cyan), *Akp2^{+/-}* and *Akp2^{+/+}* (yellow), and *Akp2^{-/-}* and *Akp2^{+/-}* (magenta) mice. Significant differences are typically associated to 95% confidence intervals that do not straddle the unity ratio value.

brain (Vorbrodt *et al.* 1986; Langer *et al.* 2007; Fonta *et al.* 2015). Thus the metabolites affected by TNAP deficiency most likely originated from neurons and glial cells in our 7-day-old mice.

Furthermore, our ^1H NMR approach was limited to revealing small hydrosoluble molecules, such that there remain putative phosphoproteins and lipophilic molecules of interest that still need to be assayed for consequences of TNAP dysfunction.

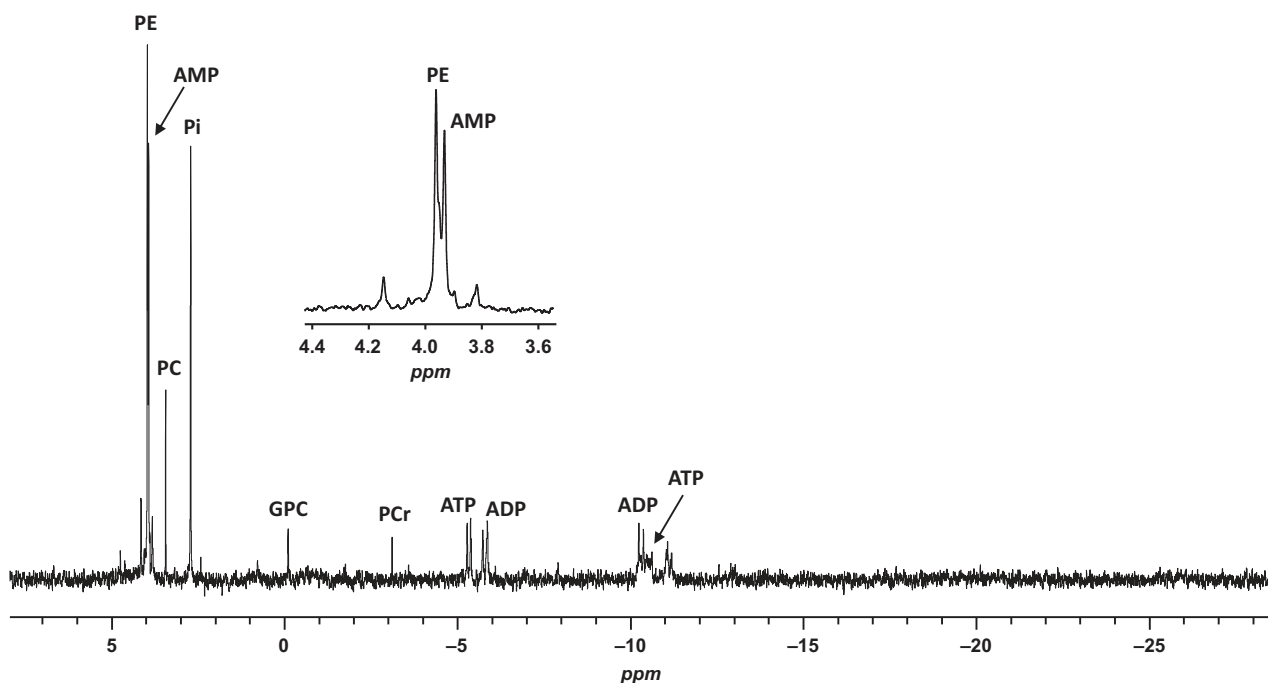


Fig. 6 ^{31}P NMR spectrum of an aqueous extract of a mouse brain with an $\text{Akp}2^{+/+}$ phenotype. PE: phosphoethanolamine; PC: phosphocholine; AMP: adenosine monophosphate; Pi: inorganic phosphate;

GPC: glycerophosphocholine; PCr: phosphocreatine; ATP: adenosine triphosphate; ADP: adenosine diphosphate (ADP).

Finally, we could not conclude definitely on the effect of deficient TNAP activity for a number of metabolites. Some metabolites displayed large inter-subject variability (especially nucleotides), which may have hindered detecting subtle differences between phenotypes. Furthermore, by applying a correction for multiple comparisons, our statistical analyses were quite conservative. We noticed that the cumulative distributions for some metabolites overlapped only weakly when comparing $\text{Akp}2^{-/-}$ mice to $\text{Akp}2^{+/+}$ and $\text{Akp}2^{+-}$ mice, although the differences did not show up as significant (phosphocholine and betaine for example). Some of these differences might become significant in future studies on more numerous animals. Other metabolites that have been shown to be directly or indirectly related to TNAP, such as PLP, PPi, and aminergic neurotransmitters, were not detected as a consequence of the relatively high detection limit of the NMR technique. Some potentially interesting metabolites such as serine, cysteine, homocysteine, alpha ketobutyrate, which could be related to cystathione metabolism as well as to PLP-dependent enzymes, were not detected either because of their low concentrations or because of possible overlap with other metabolites.

Nevertheless, we have been able to confirm reduced levels for one metabolite (GABA) (Waymire *et al.* 1995; Fonta *et al.* 2012) and to reveal, for the first time, alterations for seven other metabolites in the brain of TNAP-knockout mice.

Wild-type versus heterozygous mice

Literature data reported that TNAP activity in the serum and different organs (bone, liver, and kidney) of heterozygous transgenic mice is about 50% of that observed in wild-type mice (Waymire *et al.* 1995; Narisawa *et al.* 1997; Fedde *et al.* 1999). Despite this difference, the brain metabolomes of $\text{Akp}2^{+/+}$ and $\text{Akp}2^{+-}$ mice appeared essentially similar, at least in 7-day-old $\text{Akp}2$ mice. HPLC analyses showed that the whole-brain level of PLP is very similar for the wild-type and heterozygous mice (Waymire *et al.* 1995), implying that the functioning of PLP-dependent enzymes is similar in both genotypes. This is paralleled by lack of gross behavioral or phenotypic anomalies in heterozygous mice (Waymire *et al.* 1995; Narisawa *et al.* 1997).

Akp2-knockout versus wild-type mice

Comments on the known markers of TNAP dysfunction

PE accumulates in the urine and plasma of HPP patients and of TNAP-knockout mice (McCance *et al.* 1955; Fraser 1957; Fedde *et al.* 1999). One study also reported a drastic increase in PE concentration in the CSF of young HPP patients (Balasubramaniam *et al.* 2010). Yet we did not detect any change in the whole brain of TNAP transgenic mice. The most likely reason for this discrepancy is that extracellular PE, which is amenable to dephosphorylation by TNAP, represents a tiny fraction ($\leq 0.3\%$) of total PE (Hamberger

and Nystrom 1984; Hamberger *et al.* 1991), such that changes in this fraction would have gone unnoticed in our whole-brain-based measurements.

PPi is another classical marker of HPP. Yet, to our knowledge, no study has thus far reported PPi concentration in the normal brain and TNAP gene inactivation does not seem to be able to raise this concentration above 12.5 µM in the brain of TNAP-knockout mice.

PLP, whose concentration in whole brain extracts in rodents is of the order of 5–15 nmol/g (Spector 1978; Waymire *et al.* 1995; Masisi *et al.* 2012), was not detected with the methods we used (detection limit 25 µmol/L), such that we cannot absolutely ascertain its variation in the brain of our mouse model. Nevertheless, it is well established that extracellular PLP is primarily dephosphorylated by TNAP: studies reported markedly elevated PLP concentration in the serum of HPP patients (Whyte *et al.* 1985, 1988). Likewise, PLP concentration appears to be elevated in the CSF of children with HPP (Belachew *et al.* 2013; Hofmann *et al.* 2013). On the other hand, Waymire *et al.* (1995) reported a two to three times decrease in PLP level in whole-brain measurement in their TNAP-knockout mouse model. Since the whole-brain concentration of vitamin B6 is more than 10 times larger than that of the CSF (Spector 1978), the decreased PLP content reported by Waymire *et al.* (1995) must chiefly reflect a reduction in intracellular PLP content. We assume that TNAP gene ablation led to a reduction in intracellular PLP content in the *Akp2* model as well, consequently affecting the functioning of PLP-dependent enzymes. This is largely supported by the fact that most metabolites alterations reported here are also observed in vitamin B6 deficiency, as detailed below.

Metabolites related to PLP-dependent enzymes

GABA. In Waymire *et al.* (1995) mouse strain, TNAP inactivation resulted in a 50% decrease in GABA contents in 10–14 PND mice. We report here a similar decrease (\approx –40%) in the *Akp2* model, confirming previous results obtained by HPLC with the same mouse strain (Fonta *et al.* 2012). This decrease can be explained by the dependence for GABA synthesis on PLP. GABA concentration is reduced in the brain of rats deprived of vitamin B6 (Stephens *et al.* 1971; Kurtz *et al.* 1972; Guilarte 1989) and is low in the brain of infants and children with vitamin B6-dependent seizures (Lott *et al.* 1978; Kurlemann *et al.* 1987).

In the mammalian brain, GABA is produced from glutamic acid by two forms of glutamate decarboxylase, GAD65 and GAD67 (Martin and Rimvall 1993), that both require PLP as cofactor. Yet GAD65 and GAD67 differ with respect to their affinities for PLP: PLP is more loosely bound to GAD65 in comparison to GAD67 (Battaglioli *et al.* 2003). This would predict that the decreased GABA level observed in vitamin B6-deprived animals and in TNAP-knockout mice was mostly because of a reduction in GAD65 activity. On the

other hand, in normal brain GAD65 is mostly present in its apoenzyme form (Kaufman *et al.* 1991; Martin *et al.* 1991), such that the bulk of GABA synthesis may be ascribed to GAD67 (Mason *et al.* 2001; Patel *et al.* 2006). This is strengthened by the observation that GABA concentration is minimally altered in GAD65-knockout mice (Asada *et al.* 1996; Kash *et al.* 1997), whereas it is drastically reduced in GAD67-knockout mice (Asada *et al.* 1997). This would imply that the decreased GABA level observed in vitamin B6-deprived animals and in TNAP-knockout mice was mostly because of a reduction in GAD67 activity. It is to be noticed, however, that GAD65 does contribute to GABA synthesis in pathological conditions, in particular epileptic seizures (Asada *et al.* 1996; Kash *et al.* 1997; Patel *et al.* 2006) that may also be observed in vitamin B6-deprived animals and in TNAP-knockout mice.

Cystathionine. Cystathionine is the intermediate compound in the two steps transsulfuration pathway that generates cysteine from homocysteine and serine. Cystathionine concentration was increased several fold in the brain of TNAP-knockout mice. Studies showed that cystathionine is the most sensitive marker of PLP deficiency in amino acid and nucleotides metabolism [discussed in (Nijhout *et al.* 2009)]. Vitamin B6 restriction in rats results in a several-fold increase in cystathionine level in the brain (Hope 1964; Kurtz *et al.* 1972; Wasynczuk *et al.* 1983). In humans with dietary vitamin B6 restriction, cystathionine level increases in blood and urine (Park and Linkswiler 1970; Davis *et al.* 2006; Lamers *et al.* 2009; Gregory *et al.* 2013). It has also been shown to accumulate in the brain of a patient with vitamin B6-dependent seizures (Lott *et al.* 1978).

Both cystathionine synthesis – by cystathionine β -synthase (CBS) – and catabolism – by cystathionine γ -lyase (CGL, also known as CSE or as cystathionase) – require PLP (e.g., Kery *et al.* 1999; Oh and Churchich 1973; Taoka *et al.* 1999). Yet CBS activity is less impacted than CGL by PLP deficiency (Finkelstein and Chalmers 1970; Sato *et al.* 1996; Martinez *et al.* 2000; Davis *et al.* 2006; Lima *et al.* 2006). Accumulation of cystathionine in our experimental model therefore likely resulted from the stronger dependency of CGL activity on PLP.

Expression of CGL and CBS are widely distributed in the brain (Heinonen 1973; Diwakar and Ravindranath 2007; Linden *et al.* 2008) and their developmental regulation suggests that cystathionine level is linked to brain development from the early embryonic to the postnatal stages (Heinonen 1973; Robert *et al.* 2003; Enokido *et al.* 2005).

To our knowledge cystathionine has not been associated to HPP or TNAP dysfunction. In other contexts, studies showed that altered tissue level of cystathionine, brain included, is reflected by increased urinary excretion of cystathionine (Hope 1957, 1964; Harris *et al.* 1959; Kraus *et al.* 2009;

Espinosa *et al.* 2010). This opens the possibility of using cystathionine as an additional marker for diagnostic purposes in HPP.

Methionine. Methionine is metabolically linked to cystathionine through the methionine cycle and the transsulfuration pathway. In normal conditions, the two pathways share a common substrate, which is homocysteine: homocysteine can either be transformed in cystathionine through the action of CBS (first step of the transsulfuration pathway), or can be used to synthesize methionine through methylation. Methionine is then converted back to homocysteine through a two-step-process (methionine cycle). Accumulation of methionine (+50%) in the TNAP-knockout mouse brain may be the consequence of the increased amount of cystathionine that may result in an accumulation of homocysteine that would in turn be diverted to form additional methionine. In support of this possibility, studies showed that not only cystathionine, but also homocysteine and methionine are present in higher concentrations in the blood of CGL-knockout than in wild-type mice (Yang *et al.* 2008; Ishii *et al.* 2010; Jiang *et al.* 2015). Methionine accumulation would therefore be an indirect consequence of PLP deficiency.

Histidine. Histidine accumulated in the brains of our TNAP deficient mice (+20%). Histidine is a precursor for histamine through PLP-dependent histidine decarboxylase (Kahlson and Rosengren 1968; Watanabe *et al.* 1991). Thus accumulation of histidine may be readily explained by reduced availability of intracellular PLP. We hypothesize that increased levels of histidine in TNAP-knockout mice could lead to lower level of histamine, a multipotent compound that is devoted to homeostatic (biological rhythms, thermoregulation, stress) and higher (mood, cognition, learning, and memory) brain functions and that may also regulate brain development (Kinnunen *et al.* 1998; Karlstedt *et al.* 2001, 2003). Alteration of histamine level in TNAP-knockout mice could precipitate the effects produced by the dysregulation of other metabolites. Further HPLC analyses would help to establish a link between histidine accumulation and altered histaminergic system in hypophosphatasia, which has not been reported till now.

3-methylhistidine. Schwartz and colleagues (Schwartz *et al.* 1973) suggested that methylhistidine could be another substrate of the histidine decarboxylase. Thus, as for histidine, 3-methylhistidine accumulation in the brain of TNAP-knockout mice might result from reduction in intracellular PLP. Although it is mostly known as a constituent of the myofibrillar proteins actin and myosin (Young *et al.* 1972; Elzinga *et al.* 1973; Long *et al.* 1975, 1988), 3-methylhistidine has also been detected in the CSF (Ferraro and Hare 1985; Gerrits *et al.* 1998; Stoop *et al.* 2010). The

functions of 3-methylhistidine in the brain and the consequences of its accumulation are not, to our knowledge, established.

Adenosine

We found that the adenosine level was dramatically reduced ($\approx -80\%$) in the brain of TNAP-knockout mice. There are several possible explanations for this reduction. One first possibility is related to the ectonucleotidase activity of TNAP, and in particular its ability to dephosphorylate AMP to adenosine, that has been documented for various tissues (e.g., Ciancaglini *et al.* 2010; Picher *et al.* 2003; Say *et al.* 1991; van Belle 1976). This activity has also been reported in brain homogenates (Dorai and Bachhawat 1977), in brain cell cultures (Ohkubo *et al.* 2000; Diez-Zaera *et al.* 2011) and in the spinal cord *in vitro* (Street *et al.* 2013). If the decreased adenosine concentration we observed resulted from a compromised ectonucleotidase activity, it should have been associated with an increase in adenine nucleotide levels, which we did not detect (Fig. 5). It is to be noticed, however, that adenosine level represents a minute fraction of the sum of adenosine and adenine nucleotide levels: 2.3% in *Akp2^{+/+}* and 0.3% in *Akp2^{-/-}* mice. This implies that the total adenine nucleotide level should increase by $\approx 2\%$ in *Akp2*-knockout mice. Yet such a small increase would go unnoticed given the large intersubject variability (for purpose of comparison the 95% confidence intervals for ATP, ADP, and AMP in *Akp2* mice represented between 7% and 36% of the means).

TNAP is not the sole nucleotidase that can generate adenosine. Extracellular adenosine results from the successive dephosphorylation of ATP released in the extracellular space in ADP and AMP by several ectonucleotidases (e.g., Zimmermann *et al.* 2012) among which TNAP is the only one capable to ensure all the dephosphorylation steps of the adenosine nucleotides. Apart from TNAP, ecto-5'-nucleotidase ensures extracellular AMP to adenosine conversion in the brain. In the cytoplasm adenosine is also produced from AMP by cytosolic-5'-nucleotidase I (Sala-Newby *et al.* 1999; Le *et al.* 2014).

The effect of TNAP dysfunction on adenosine level in our 7-day-old mice is much larger than what could be anticipated from studies performed in older rodents (e.g., Kulesskaya *et al.* 2013; Lovatt *et al.* 2012; Street *et al.* 2013; Wall and Dale 2013; Zhang *et al.* 2012). In those studies, the contribution of TNAP to extracellular adenosine synthesis appears to be minor in comparison to that of ecto-5'-nucleotidase. A possible explanation for this discrepancy resides in opposite developmental changes for TNAP and 5'-nucleotidase activities: TNAP is most strongly expressed in embryos and in early postnatal ages, and its expression thereafter declines during postnatal development (Goldstein and Harris 1981; Narisawa *et al.* 1994; Langer *et al.* 2007); on the contrary both cytosolic- and ecto-5'-nucleotidase

expression/activity progressively increase during postnatal development (Mackiewicz *et al.* 2006; Grkovic *et al.* 2014).

Another possibility for explaining reduced adenosine level in TNAP-knockout mice, quite relevant in the context of this study, pertains to the methionine cycle and the transsulfuration pathway. In the methionine cycle, homocysteine is methylated to yield methionine. The methionine cycle continues with the production of S-adenosylmethionine, which in turn can be demethylated to produce S-adenosylhomocysteine (SAH). SAH hydrolase completes the loop by regenerating homocysteine and by generating adenosine. Therefore, under normal conditions the methionine cycle is another source of adenosine. Interestingly, in liver and thymus of vitamin B6-deprived animals, accumulation of cystathione is reverberated by an increase in homocysteine, which results in an increase in SAH (Nguyen *et al.* 2001; Isa *et al.* 2006). This was explained by a reversal of SAH hydrolase activity (Isa *et al.* 2006); in vitamin B6 deficiency therefore, SAH hydrolase should not produce, but should instead consume adenosine. Likewise, the reduction in intracellular PLP in TNAP-knockout mice could lead to a decrease in intracellular adenosine. Unfortunately the only study we are aware of (Nguyen *et al.* 2001), that examined the consequence of vitamin B6 deficiency on SAH concentration in the brain, found no difference in comparison to normally fed controls, although it reported strong increase in SAH level in liver and thymus. However, this result was obtained in 9-week-old rats and may not be transposed to our 7-day-old mice.

N-Acetylaspartate/N-acetyl-aspartyl-glutamate

NAA and NAAG, whose biosynthesis is covered by enzymes that are *not* PLP-dependent, tended to accumulate (around +15–20%) in mice whose TNAP gene had been inactivated. NAAG is synthesized from NAA at constant rate and both metabolites are catabolized at the same rate, such that their concentrations are maintained at a constant ratio (Baslow *et al.* 2007). This may explain the higher level of NAAG that would simply follow NAA accumulation. NAA is produced in neurons and is taken up by oligodendrocytes, where it is split into aspartate and acetyl-CoA by aspartoacylase. Acetyl-CoA is involved in the metabolism of fatty acids and is incorporated in lipids required for myelin lipid synthesis (Chakraborty *et al.* 2001; Namboodiri *et al.* 2006). In TNAP-knockout mice, compromised myelination (Hanics *et al.* 2012) could result in less fatty acids demand for myelin formation. Therefore, NAA would not be converted and would accumulate instead.

This hypothesis is supported by results obtained in aspartoacylase-knockout mice (Matalon *et al.* 2000; Nordengen *et al.* 2015) and in Cavanav disease, which is caused by a deficiency of aspartoacylase activity (Hagenfeldt *et al.* 1987; Wolf *et al.* 2004; Hoshino and Kubota 2014): in both cases, hypomyelination and white matter degeneration are

associated with high levels of NAA in the urine, CSF, and brain tissue.

Phenotypic features of HPP in relation to brain metabolome changes

The severe forms of HPP often present with seizures, apnea, deafness, and encephalopathy (Hofmann *et al.* 2013; Takeuchi 2015). These disorders were initially considered to be consequences of deficient TNAP activity in other tissues, especially bone tissue in which TNAP plays an essential role in mineralization. For example, epilepsy and apnea were explained by cranial deformities and reduced thoracic volume by insufficient mineralization of the ribs. However, other clinical (Béthenod *et al.* 1967; Baumgartner-Sigl *et al.* 2007; Belachew *et al.* 2013; de Roo *et al.* 2014; Taketani *et al.* 2014) data evidenced that neurological consequences of TNAP gene deficits can be dissociated from bone defects. Moreover, experimental data (Foster *et al.* 2017) do not report any neurological disorders in mice in which TNAP deletion specifically targets bone and tooth cells, supporting the hypothesis that the neurological disorders observed in the severe form of hypophosphatasia are directly caused by TNAP dysfunction in the brain rather than indirectly in other tissues.

One of the main feature of perinatal and, to a lesser degree, infantile HPP, is the occurrence of epileptic seizures (e.g., (Béthenod *et al.* 1967; Fraser 1957; Rathbun 1948; Whyte *et al.* 1988), which are also observed in TNAP-knockout mice (Waymire *et al.* 1995; Narisawa *et al.* 1997, 2001). Seizures are classically attributed to defective GABAergic inhibition (reviewed in Cossart *et al.* 2005; Macdonald *et al.* 2010). Given that GABA is synthesized by PLP-dependent enzymes (see above) and since PLP metabolism appears defective in HPP, it quite logically follows that epileptic seizures in HPP patients and TNAP-knockout mice should result from defective GABAergic inhibition. Accordingly seizures observed in HPP patients may be controlled with vitamin B6 (Sia *et al.* 1975; Litmanovitz *et al.* 2002; Nunes *et al.* 2002; Yamamoto *et al.* 2004; Baumgartner-Sigl *et al.* 2007; Balasubramaniam *et al.* 2010; Nakamura-Utsunomiya *et al.* 2010; Demirbilek *et al.* 2012; Belachew *et al.* 2013; de Roo *et al.* 2014). Yet this treatment is not always successful (Béthenod *et al.* 1967; Posen *et al.* 1997; Hofmann *et al.* 2013) or the improvement may be only transitory (Whyte *et al.* 1988; Nakamura-Utsunomiya *et al.* 2010; de Roo *et al.* 2014). Despite vitamin B6 treatment, seizures also recur in *Akp2*-knockout mice (Narisawa *et al.* 2001). This suggests that in addition to GABA, TNAP dysfunction has consequences on other metabolites that may play a role in controlling epileptic seizures. One of these metabolites is adenosine.

Extracellular adenosine influences neuronal activity through two types of receptors, which reduce excitatory synaptic transmission (A1 receptors) or modulate inhibitory

synaptic transmission (A2 receptors) (for review: Cunha 2001; Rodrigues *et al.* 2015). Blocking adenosine receptors results in a worsening and a prolongation of seizures induced by other means, whereas adenosine and adenosine receptor agonists display anti-convulsive properties (Maitre *et al.* 1974; Dragunow *et al.* 1985; Pagonopoulou *et al.* 2006; Boison 2012). The dramatic reduction in adenosine level in TNAP-knockout mice implies that one natural means of controlling seizures is also deficient.

Among other alterations, myelination appears defective in TNAP-knockout mice (Narisawa *et al.* 1997; Hanics *et al.* 2012), whereas white matter appears abnormal in HPP patients (Nunes *et al.* 2002; Hofmann *et al.* 2013; de Roo *et al.* 2014). TNAP may intervene in myelination through both nucleotide and PLP metabolisms. First, the earliest stage of myelination is promoted by extracellular adenosine (Stevens *et al.* 2002). Later stages depend on the extracellular concentration of ATP (Ishibashi *et al.* 2006). Thus TNAP gene inactivation and subsequent decrease in adenosine level may compromise myelination. We recently speculated that levamisole-induced multifocal leukoencephalopathy is based on the same mechanisms (Nowak *et al.* 2015). Secondly, myelination is altered in vitamin B6 deficiency (Lott *et al.* 1978; Morre *et al.* 1978; Jardim *et al.* 1994). This is paralleled by decreases in the amount of sphingolipids in the brain of rats deprived of vitamin B6 (Kurtz *et al.* 1972; Stephens and Dakshinamurti 1975). Sphingomyelin synthesis involves two PLP-dependent enzymes (Bourquin *et al.* 2011). Although lipophilic metabolites were not examined in our study, accumulation of NAA and NAAG suggests that the metabolism of fatty acids was indeed altered in our TNAP-knockout mice.

Our study revealed dysregulation of the methionine cycle and transsulfuration pathway in the brain of TNAP-knockout mice, evidenced by a significant increase in methionine level and by a several fold increase in cystathione concentration. The roles of cystathione in neuronal development have not been examined and studies exploring its neural functions were not conclusive (Werman *et al.* 1966; Key and White 1970; Regnier *et al.* 2012). It is worth mentioning that patients with CGL mutations may express neurologic symptoms such as seizures and mental retardation (Frimpter 1965; Kraus *et al.* 2009; Espinos *et al.* 2010). This suggests that alteration of cystathione level or, more generally, of the transsulfuration pathway from methionine to cysteine, glutathione and hydrogen sulfide, may also contribute to the neurologic defects observed in HPP. This possibility warrants further study.

Acknowledgments and conflict of interest disclosure

The authors wish to acknowledge Hypophosphatasie Europe for financial support (ref CNRS n° 088461). They thank Fabrice Collin

and Catherine Claparols for mass spectrometry experiments and Camille Grange for his contribution to the animal care and breeding. The authors report no conflict of interest.

All experiments were conducted in compliance with the ARRIVE guidelines.

References

- Anstrom J. A., Brown W. R., Moody D. M., Thore C. R., Challa V. R. and Block S. M. (2002) Anatomical analysis of the developing cerebral vasculature in premature neonates: absence of precapillary arteriole-to-venous shunts. *Pediatr. Res.* **52**, 554–560.
- Asada H., Kawamura Y., Maruyama K. *et al.* (1996) Mice lacking the 65 kDa isoform of glutamic acid decarboxylase (GAD65) maintain normal levels of GAD67 and GABA in their brains but are susceptible to seizures. *Biochem. Biophys. Res. Commun.* **229**, 891–895.
- Asada H., Kawamura Y., Maruyama K. *et al.* (1997) Cleft palate and decreased brain gamma-aminobutyric acid in mice lacking the 67-kDa isoform of glutamic acid decarboxylase. *Proc. Natl Acad. Sci. USA* **94**, 6496–6499.
- Balasubramaniam S., Bowling F., Carpenter K., Earl J., Chaitow J., Pitt J., Mornet E., Sillence D. and Ellaway C. (2010) Perinatal hypophosphatasia presenting as neonatal epileptic encephalopathy with abnormal neurotransmitter metabolism secondary to reduced co-factor pyridoxal-5'-phosphate availability. *J. Inherit. Metab. Dis. Suppl.* **3**, S25–S33.
- Balayssac S., Déjean S., Lalande J., Gilard V. and Malet-Martino M. (2013) A toolbox to explore NMR metabolomic data sets using the R environment. *Chemometrics and Intelligent Laboratory Systems* **126**, 50–59.
- Bartl J., Chrastina P., Krijt J., Hodik J., Peskova K. and Kozich V. (2014) Simultaneous determination of cystathione, total homocysteine, and methionine in dried blood spots by liquid chromatography/tandem mass spectrometry and its utility for the management of patients with homocystinuria. *Clin. Chim. Acta* **437**, 211–217.
- Baslow M. H., Hrabe J. and Guilfoyle D. N. (2007) Dynamic relationship between neurostimulation and N-acetylaspartate metabolism in the human visual cortex: evidence that NAA functions as a molecular water pump during visual stimulation. *J. Mol. Neurosci.* **32**, 235–245.
- Battaglioli G., Liu H. and Martin D. L. (2003) Kinetic differences between the isoforms of glutamate decarboxylase: implications for the regulation of GABA synthesis. *J. Neurochem.* **86**, 879–887.
- Baumgartner-Sigl S., Haberlandt E., Mumm S., Scholl-Burgi S., Sergi C., Ryan L., Ericson K. L., Whyte M. P. and Hogler W. (2007) Pyridoxine-responsive seizures as the first symptom of infantile hypophosphatasia caused by two novel missense mutations (c.677T>C, p. M226T; c.1112C>T, p.T371I) of the tissue-nonspecific alkaline phosphatase gene. *Bone* **40**, 1655–1661.
- Beckonert O., Keun H. C., Ebbels T. M., Bundy J., Holmes E., Lindon J. C. and Nicholson J. K. (2007) Metabolic profiling, metabolomic and metabonomic procedures for NMR spectroscopy of urine, plasma, serum and tissue extracts. *Nat. Protoc.* **2**, 2692–2703.
- Belachew D., Kazmerski T., Libman I., Goldstein A. C., Stevens S. T., Deward S., Vockley J., Sperling M. A. and Balest A. L. (2013) Infantile hypophosphatasia secondary to a novel compound heterozygous mutation presenting with pyridoxine-responsive seizures. *JMD Reports* **11**, 17–24.
- Bell M. A. and Ball M. J. (1985) Laminar variation in the microvascular architecture of normal human visual cortex (area 17). *Brain Res.* **335**, 139–143.

- van Belle H. (1976) Kinetics and inhibition of rat and avian alkaline phosphatases. *Gen. Pharmacol.* **7**, 53–58.
- Bethenod M., Cotte M. F., Collombel C., Frederich A. and Cotte J. (1967) Neonatal discovery of hypophosphatasia. Bone improvement. Fatal convulsant encephalopathy. *Ann. Pediatr. (Paris)* **14**, 835–841.
- Boison D. (2012) Adenosine dysfunction in epilepsy. *Glia* **60**, 1234–1243.
- Botosoa E. P., Zhu M., Marbeuf-Gueye C., Triba M. N., Dutheil F., Duyckaerts C., Beaune P., Loriot M. A. and Le Moyec L. (2012) NMR metabolomic of frontal cortex extracts: first study comparing two neurodegenerative diseases, Alzheimer disease and amyotrophic lateral sclerosis. *Irbm* **33**, 281–286.
- Bourquin F., Capitani G. and Grutter M. G. (2011) PLP-dependent enzymes as entry and exit gates of sphingolipid metabolism. *Protein Sci.* **20**, 1492–1508.
- Brun-Heath I., Ermonval M., Chabrol E. et al. (2011) Differential expression of the bone and the liver tissue non-specific alkaline phosphatase isoforms in brain tissues. *Cell Tissue Res.* **343**, 521–536.
- Buchet R., Millan J. L. and Magne D. (2013) Multisystemic functions of alkaline phosphatases. *Methods Mol. Biol.* **1053**, 27–51.
- Chakraborty G., Mekala P., Yahya D., Wu G. and Ledeen R. W. (2001) Intraneuronal N-acetylaspartate supplies acetyl groups for myelin lipid synthesis: evidence for myelin-associated aspartoacylase. *J. Neurochem.* **78**, 736–745.
- Ciancaglini P., Yadav M. C., Simao A. M., Narisawa S., Pizauro J. M., Farquharson C., Hoylaerts M. F. and Millan J. L. (2010) Kinetic analysis of substrate utilization by native and TNAP-, NPP1-, or PHOSPHO1-deficient matrix vesicles. *J. Bone Miner. Res.* **25**, 716–723.
- Coburn S. P. (2015) Vitamin B-6 metabolism and interactions with TNAP. *Subcell. Biochem.* **76**, 207–238.
- Cossart R., Bernard C. and Ben-Ari Y. (2005) Multiple facets of GABAergic neurons and synapses: multiple fates of GABA signalling in epilepsies. *Trends Neurosci.* **28**, 108–115.
- Cunha R. A. (2001) Adenosine as a neuromodulator and as a homeostatic regulator in the nervous system: different roles, different sources and different receptors. *Neurochem. Int.* **38**, 107–125.
- Davis S. R., Quinlivan E. P., Stacpoole P. W. and Gregory J. F., 3rd (2006) Plasma glutathione and cystathionine concentrations are elevated but cysteine flux is unchanged by dietary vitamin B-6 restriction in young men and women. *J. Nutr.* **136**, 373–378.
- Daw M. I., Ashby M. C. and Isaac J. T. (2007) Coordinated developmental recruitment of latent fast spiking interneurons in layer IV barrel cortex. *Nat. Neurosci.* **10**, 453–461.
- Demirbilek H., Alanay Y., Alikasifoglu A., Topcu M., Mornet E., Gonc N., Ozon A. and Kandemir N. (2012) Hypophosphatasia presenting with pyridoxine-responsive seizures, hypercalcemia, and pseudotumor cerebri: case report. *J. Clin. Res. Ped. Endocrinol.* **4**, 34–38.
- Diez-Zaera M., Diaz-Hernandez J. I., Hernandez-Alvarez E., Zimmermann H., Diaz-Hernandez M. and Miras-Portugal M. T. (2011) Tissue-nonspecific alkaline phosphatase promotes axonal growth of hippocampal neurons. *Mol. Biol. Cell* **22**, 1014–1024.
- Diwakar L. and Ravindranath V. (2007) Inhibition of cystathionine-gamma-lyase leads to loss of glutathione and aggravation of mitochondrial dysfunction mediated by excitatory amino acid in the CNS. *Neurochem. Int.* **50**, 418–426.
- Do K. Q., Lauer C. J., Schreiber W., Zollinger M., Gutteckamsler U., Cuenod M. and Holsboer F. (1995) Gamma-glutamylglutamine and taurine concentrations are decreased in the cerebrospinal-fluid of drug-naive patients with schizophrenic disorders. *J. Neurochem.* **65**, 2652–2662.
- Dorai D. T. and Bachhawat B. K. (1977) Purification and properties of brain alkaline phosphatase. *J. Neurochem.* **29**, 503–512.
- Dragunow M., Goddard G. V. and Laverty R. (1985) Is adenosine an endogenous anticonvulsant? *Epilepsia* **26**, 480–487.
- Dumas M. E. and Davidovic L. (2015) Metabolic profiling and phenotyping of central nervous system diseases: metabolites bring insights into brain dysfunctions. *J. Neuroimmune Pharmacol.* **10**, 402–424.
- Elzinga M., Collins J. H., Kuehl W. M. and Adelstein R. S. (1973) Complete amino-acid sequence of actin of rabbit skeletal muscle. *Proc. Natl Acad. Sci. USA* **70**, 2687–2691.
- Enokido Y., Suzuki E., Iwasawa K., Namekata K., Okazawa H. and Kimura H. (2005) Cystathionine beta-synthase, a key enzyme for homocysteine metabolism, is preferentially expressed in the radial glia/astrocyte lineage of developing mouse CNS. *FASEB J.* **19**, 1854–1856.
- Ermonval M., Baudry A., Baychelier F. et al. (2009) The cellular prion protein interacts with the tissue non-specific alkaline phosphatase in membrane microdomains of bioaminergic neuronal cells. *PLoS ONE* **4**, e6497.
- Espinosa C., Garcia-Cazorla A., Martinez-Rubio D., Martinez-Martinez E., Vilaseca M. A., Perez-Duenas B., Kozich V., Palau F. and Artuch R. (2010) Ancient origin of the CTH allele carrying the c.200C>T (p. T67I) variant in patients with cystathioninuria. *Clin. Genet.* **78**, 554–559.
- Fedde K. N. and Whyte M. P. (1990) Alkaline phosphatase (tissue-nonspecific isoenzyme) is a phosphoethanolamine and pyridoxal-5'-phosphate ectophosphatase: normal and hypophosphatasia fibroblast study. *Am. J. Hum. Genet.* **47**, 767–775.
- Fedde K. N., Blair L., Silverstein J. et al. (1999) Alkaline phosphatase knock-out mice recapitulate the metabolic and skeletal defects of infantile hypophosphatasia. *J. Bone Miner. Res.* **14**, 2015–2026.
- Ferraro T. N. and Hare T. A. (1985) Free and conjugated amino acids in human CSF: influence of age and sex. *Brain Res.* **338**, 53–60.
- Finkelstein J. D. and Chalmers F. T. (1970) Pyridoxine effects on cystathionine synthase in rat liver. *J. Nutr.* **100**, 467–469.
- Fonta C. and Imbert M. (2002) Vascularization in the primate visual cortex during development. *Cereb. Cortex* **12**, 199–211.
- Fonta C., Negyessy L., Renaud L. and Barone P. (2004) Areal and subcellular localization of the ubiquitous alkaline phosphatase in the primate cerebral cortex: evidence for a role in neurotransmission. *Cereb. Cortex* **14**, 595–609.
- Fonta C., Negyessy L., Renaud L. and Barone P. (2005) Postnatal development of alkaline phosphatase activity correlates with the maturation of neurotransmission in the cerebral cortex. *J. Comp. Neurol.* **486**, 179–196.
- Fonta C., Negyessy L., Brun Heath I., Ermonval M., Czege D., Nowak L., Frances B., Xiao J. and Millan J. (2012) TNAP in the brain: functions in neurotransmission. *Bull. Group. Int. Rech. Sci. Stomatol. Odontol.* **51**, e27.
- Fonta C., Barone P., Rodriguez Martinez L. and Negyessy L. (2015) Rediscovering TNAP in the brain: a major role in regulating the function and development of the cerebral cortex. *Subcell. Biochem.* **76**, 85–106.
- Foster B. L., Kuss P., Yadav M. C. et al. (2017) Conditional alp ablation phenocopies dental defects of hypophosphatasia. *J. Dent. Res.* **96**, 81–91.
- Franz V. H. (2007) Ratios: a short guide to confidence limits and proper use. <https://arxiv.org/pdf/0710.2024v1.pdf>.
- Fraser D. (1957) Hypophosphatasia. *Am. J. Med.* **22**, 730–746.
- Fraser D., Yendt E. R. and Christie F. H. (1955) Metabolic abnormalities in hypophosphatasia. *Lancet* **268**, 286.

- Friede R. L. (1966) A quantitative mapping of alkaline phosphatase in the brain of the rhesus monkey. *J. Neurochem.* **13**, 197–203.
- Frimpter G. W. (1965) Cystathioninuria: nature of the defect. *Science* **149**, 1095–1096.
- Gerrits G. P., Kamphuis S., Monnens L. A., Trijbels J. M., Schroder C. H., Koster A. and Gabreels F. J. (1998) Cerebrospinal fluid levels of amino acids in infants and young children with chronic renal failure. *Neuropediatrics* **29**, 35–39.
- Goldstein D. J. and Harris H. (1981) Mammalian brain alkaline phosphatase: expression of liver/bone/kidney locus. Comparison of fetal and adult activities. *J. Neurochem.* **36**, 53–57.
- Gonzalez-Riano C., Garcia A. and Barbas C. (2016) Metabolomics studies in brain tissue: a review. *J. Pharm. Biomed. Anal.* **130**, 141–168.
- Greenberg C. R., Taylor C. L., Haworth J. C., Seargent L. E., Phillips S., Triggs-Raine B. and Chodirkar B. N. (1993) A homoallelic Gly317→Asp mutation in ALPL causes the perinatal (lethal) form of hypophosphatasia in Canadian Mennonites. *Genomics* **17**, 215–217.
- Gregory J. F. 3rd., Park Y., Lamers Y. et al. (2013) Metabolomic analysis reveals extended metabolic consequences of marginal vitamin B-6 deficiency in healthy human subjects. *PLoS ONE* **8**, e63544.
- Gribbestad I. S., Petersen S. B., Fjosne H. E., Kvinnslund S. and Krane J. (1994) 1H NMR spectroscopic characterization of perchloric acid extracts from breast carcinomas and non-involved breast tissue. *NMR Biomed.* **7**, 181–194.
- Grkovic I., Bjelobaba I., Nedeljkovic N., Mitrovic N., Drakulic D., Stanojlovic M. and Horvat A. (2014) Developmental increase in ecto-5'-nucleotidase activity overlaps with appearance of two immunologically distinct enzyme isoforms in rat hippocampal synaptic plasma membranes. *J. Mol. Neurosci.* **54**, 109–118.
- Guilarte T. R. (1989) Regional changes in the concentrations of glutamate, glycine, taurine, and GABA in the vitamin B-6 deficient developing rat brain: association with neonatal seizures. *Neurochem. Res.* **14**, 889–897.
- Hagenfeldt L., Bollgren I. and Venizelos N. (1987) N-acetylaspartic aciduria due to aspartoacylase deficiency—a new aetiology of childhood leukodystrophy. *J. Inherit. Metab. Dis.* **10**, 135–141.
- Hamberger A. and Nystrom B. (1984) Extra- and intracellular amino acids in the hippocampus during development of hepatic encephalopathy. *Neurochem. Res.* **9**, 1181–1192.
- Hamberger A., Nystrom B., Larsson S., Silfvenius H. and Nordborg C. (1991) Amino acids in the neuronal microenvironment of focal human epileptic lesions. *Epilepsy Res.* **9**, 32–43.
- Hanics J., Barna J., Xiao J., Millan J. L., Fonta C. and Negyessy L. (2012) Ablation of TNAP function compromises myelination and synaptogenesis in the mouse brain. *Cell Tissue Res.* **349**, 459–471.
- Harmey D., Hessle L., Narisawa S., Johnson K. A., Terkeltaub R. and Millan J. L. (2004) Concerted regulation of inorganic pyrophosphate and osteopontin by akp2, enpp1, and ank: an integrated model of the pathogenesis of mineralization disorders. *Am. J. Pathol.* **164**, 1199–1209.
- Harris H., Penrose L. S. and Thomas D. H. (1959) Cystathionuria. *Ann. Hum. Genet.* **23**, 442–453.
- Heinonen K. (1973) Studies on cystathionase activity in rat liver and brain during development. Effects of hormones and amino acids in vivo. *Biochem. J.* **136**, 1011–1015.
- Hofmann C., Liese J., Schwarz T. et al. (2013) Compound heterozygosity of two functional null mutations in the ALPL gene associated with deleterious neurological outcome in an infant with hypophosphatasia. *Bone* **55**, 150–157.
- Hope D. B. (1957) L-cystathione in the urine of pyridoxine-deficient rats. *Biochem. J.* **66**, 486–489.
- Hope D. B. (1964) Cystathione Accumulation in the Brains of Pyridoxine-Deficient Rats. *J. Neurochem.* **11**, 327–332.
- Hoshi K., Amizuka N., Oda K., Ikebara Y. and Ozawa H. (1997) Immunolocalization of tissue non-specific alkaline phosphatase in mice. *Histochem. Cell Biol.* **107**, 183–191.
- Hoshino H. and Kubota M. (2014) Canavan disease: clinical features and recent advances in research. *Pediatr. Int.* **56**, 477–483.
- Huguet F., Guerraoui A., Barrier L., Guilloteau D., Tallineau C. and Chalon S. (1998) Changes in excitatory amino acid levels and tissue energy metabolites of neonate rat brain after hypoxia and hypoxia-ischemia. *Neurosci. Lett.* **240**, 102–106.
- Iles R. A., Stevens A. N., Griffiths J. R. and Morris P. G. (1985) Phosphorylation status of liver by 31P-n.m.r. spectroscopy, and its implications for metabolic control. A comparison of 31P-n.m.r. spectroscopy (in vivo and in vitro) with chemical and enzymic determinations of ATP, ADP and Pi. *Biochem. J.* **229**, 141–151.
- Isa Y., Tsuge H. and Hayakawa T. (2006) Effect of vitamin B6 deficiency on S-adenosylhomocysteine hydrolase activity as a target point for methionine metabolic regulation. *J. Nutr. Sci. Vitaminol. (Tokyo)* **52**, 302–306.
- Ishibashi T., Dakin K. A., Stevens B., Lee P. R., Kozlov S. V., Stewart C. L. and Fields R. D. (2006) Astrocytes promote myelination in response to electrical impulses. *Neuron* **49**, 823–832.
- Ishii I., Akahoshi N., Yamada H., Nakano S., Izumi T. and Suematsu M. (2010) Cystathione gamma-Lyase-deficient mice require dietary cysteine to protect against acute lethal myopathy and oxidative injury. *J. Biol. Chem.* **285**, 26358–26368.
- Jardim L. B., Pires R. F., Martins C. E., Vargas C. R., Vizioli J., Kliemann F. A. and Giugliani R. (1994) Pyridoxine-dependent seizures associated with white matter abnormalities. *Neuropediatrics* **25**, 259–261.
- Jiang H., Hurt K. J., Breen K., Stabler S. P., Allen R. H., Orlicky D. J. and Maclean K. N. (2015) Sex-specific dysregulation of cysteine oxidation and the methionine and folate cycles in female cystathione gamma-lyase null mice: a serendipitous model of the methylfolate trap. *Biol. Open* **4**, 1154–1162.
- Kahlson G. and Rosengren E. (1968) New approaches to the physiology of histamine. *Physiol. Rev.* **48**, 155–196.
- Kantor O., Cserpan D., Volgyi B., Lukats A. and Somogyvari Z. (2015) The retinal TNAP. *Subcell. Biochem.* **76**, 107–123.
- Karlstedt K., Nissinen M., Michelsen K. A. and Panula P. (2001) Multiple sites of L-histidine decarboxylase expression in mouse suggest novel developmental functions for histamine. *Dev. Dyn.* **221**, 81–91.
- Karlstedt K., Ahman M. J., Anichtchik O. V., Soinila S. and Panula P. (2003) Expression of the H3 receptor in the developing CNS and brown fat suggests novel roles for histamine. *Mol. Cell Neurosci.* **24**, 614–622.
- Kash S. F., Johnson R. S., Tecott L. H., Noebels J. L., Mayfield R. D., Hanahan D. and Baekkeskov S. (1997) Epilepsy in mice deficient in the 65-kDa isoform of glutamic acid decarboxylase. *Proc. Natl Acad. Sci. USA* **94**, 14060–14065.
- Kaufman D. L., Houser C. R. and Tobin A. J. (1991) Two forms of the gamma-aminobutyric acid synthetic enzyme glutamate decarboxylase have distinct intraneuronal distributions and cofactor interactions. *J. Neurochem.* **56**, 720–723.
- Kermer V., Ritter M., Albuquerque B., Leib C., Stanke M. and Zimmermann H. (2010) Knockdown of tissue nonspecific alkaline phosphatase impairs neural stem cell proliferation and differentiation. *Neurosci. Lett.* **485**, 208–211.

- Kery V., Poneleit L., Meyer J. D., Manning M. C. and Kraus J. P. (1999) Binding of pyridoxal 5'-phosphate to the heme protein human cystathione beta-synthase. *Biochemistry* **38**, 2716–2724.
- Key B. J. and White R. P. (1970) Neuropharmacological comparison of cystathione, cysteine, homoserine and alpha-ketobutyric acid in cats. *Neuropharmacology* **9**, 349–357.
- Kinnunen A., Lintunen M., Karlstedt K., Fukui H. and Panula P. (1998) In situ detection of H1-receptor mRNA and absence of apoptosis in the transient histamine system of the embryonic rat brain. *J. Comp. Neurol.* **394**, 127–137.
- Kraus J. P., Hasek J., Kozich V. *et al.* (2009) Cystathione gamma-lyase: clinical, metabolic, genetic, and structural studies. *Mol. Genet. Metab.* **97**, 250–259.
- Kulak A., Duarte J. M., Do K. Q. and Gruetter R. (2010) Neurochemical profile of the developing mouse cortex determined by in vivo 1H NMR spectroscopy at 14.1 T and the effect of recurrent anaesthesia. *J. Neurochem.* **115**, 1466–1477.
- Kulesskaya N., Voikar V., Peltola M., Yegutkin G. G., Salmi M., Jalkanen S. and Rauvala H. (2013) CD73 is a major regulator of adenosinergic signalling in mouse brain. *PLoS ONE* **8**, e66896.
- Kurlemann G., Loscher W., Dominick H. C. and Palm G. D. (1987) Disappearance of neonatal seizures and low CSF GABA levels after treatment with vitamin B6. *Epilepsy Res.* **1**, 152–154.
- Kurtz D. J., Levy H. and Kanfer J. N. (1972) Cerebral lipids and amino acids in the vitamin B 6 -deficient suckling rat. *J. Nutr.* **102**, 291–298.
- Lalande J., Halley H., Balayssac S., Gilard V., Dejean S., Martino R., Frances B., Lassalle J. M. and Malet-Martino M. (2014) 1H NMR metabolomic signatures in five brain regions of the AbetaPPswe Tg2576 mouse model of Alzheimer's disease at four ages. *J. Alzheimers Dis.* **39**, 121–143.
- Lamers Y., Williamson J., Ralat M. *et al.* (2009) Moderate dietary vitamin B-6 restriction raises plasma glycine and cystathione concentrations while minimally affecting the rates of glycine turnover and glycine cleavage in healthy men and women. *J. Nutr.* **139**, 452–460.
- Langer D., Ikebara Y., Takebayashi H., Hawkes R. and Zimmermann H. (2007) The ectonucleotidases alkaline phosphatase and nucleoside triphosphate diphosphohydrolase 2 are associated with subsets of progenitor cell populations in the mouse embryonic, postnatal and adult neurogenic zones. *Neuroscience* **150**, 863–879.
- Langer D., Hammer K., Koszalka P., Schrader J., Robson S. and Zimmermann H. (2008) Distribution of ectonucleotidases in the rodent brain revisited. *Cell Tissue Res.* **334**, 199–217.
- Le G. Y., Essackjee H. C. and Ballard H. J. (2014) Intracellular adenosine formation and release by freshly-isolated vascular endothelial cells from rat skeletal muscle: effects of hypoxia and/or acidosis. *Biochem. Biophys. Res. Commun.* **450**, 93–98.
- Lima C. P., Davis S. R., Mackey A. D., Scheer J. B., Williamson J. and Gregory J. F. 3rd. (2006) Vitamin B-6 deficiency suppresses the hepatic transsulfuration pathway but increases glutathione concentration in rats fed AIN-76A or AIN-93G diets. *J. Nutr.* **136**, 2141–2147.
- Linden D. R., Sha L., Mazzone A., Stoltz G. J., Bernard C. E., Furne J. K., Levitt M. D., Farrugia G. and Szurszewski J. H. (2008) Production of the gaseous signal molecule hydrogen sulfide in mouse tissues. *J. Neurochem.* **106**, 1577–1585.
- Litmanovitz, Reish O., Dolfin T., Arnon S., Regev R., Grinshpan G., Yamazaki M. and Ozono K. (2002) Glu274Lys/Gly309Arg mutation of the tissue-nonspecific alkaline phosphatase gene in neonatal hypophosphatasia associated with convulsions. *J. Inher. Metab. Dis.* **25**, 35–40.
- Liu J., Sheldon R. A., Segal M. R., Kelly M. J. S., Pelton J. G., Ferriero D. M., James T. L. and Litt L. (2013) 1H nuclear magnetic resonance brain metabolomics in neonatal mice after hypoxia-ischemia distinguished normothermic recovery from mild hypothermia recoveries. *Pediatr. Res.* **74**, 170–179.
- Long C. L., Haverberg L. N., Young V. R., Kinney J. M., Munro H. N. and Geiger J. W. (1975) Metabolism of 3-methylhistidine in man. *Metabolism* **24**, 929–935.
- Long C. L., Dillard D. R., Bodzin J. H., Geiger J. W. and Blakemore W. S. (1988) Validity of 3-methylhistidine excretion as an indicator of skeletal muscle protein breakdown in humans. *Metabolism* **37**, 844–849.
- Lott I. T., Coulombe T., Di Paolo R. V., Richardson E. P. Jr. and Levy H. L. (1978) Vitamin B6-dependent seizures: pathology and chemical findings in brain. *Neurology* **28**, 47–54.
- Lovatt D., Xu Q., Liu W., Takano T., Smith N. A., Schnermann J., Tieu K. and Nedergaard M. (2012) Neuronal adenosine release, and not astrocytic ATP release, mediates feedback inhibition of excitatory activity. *Proc. Natl Acad. Sci. USA* **109**, 6265–6270.
- Macdonald R. L., Kang J. Q. and Gallagher M. J. (2010) Mutations in GABA_A receptor subunits associated with genetic epilepsies. *J. Physiol.* **588**, 1861–1869.
- Mackiewicz M., Nikanova E. V., Zimmermann J. E., Romer M. A., Cater J., Galante R. J. and Pack A. I. (2006) Age-related changes in adenosine metabolic enzymes in sleep/wake regulatory areas of the brain. *Neurobiol. Aging* **27**, 351–360.
- Maitre M., Chesielski L., Lehmann A., Kempf E. and Mandel P. (1974) Protective effect of adenosine and nicotinamide against audiogenic seizure. *Biochem. Pharmacol.* **23**, 2807–2816.
- Mandal R., Guo A. C., Chaudhary K. K., Liu P., Yallou F. S., Dong E., Azzat F. and Wishart D. S. (2012) Multi-platform characterization of the human cerebrospinal fluid metabolome: a comprehensive and quantitative update. *Genome Med.* **4**, 38.
- Martin D. L. and Rimvall K. (1993) Regulation of gamma-aminobutyric acid synthesis in the brain. *J. Neurochem.* **60**, 395–407.
- Martin D. L., Martin S. B., Wu S. J. and Espina N. (1991) Regulatory properties of brain glutamate decarboxylase (GAD): the apoenzyme of GAD is present principally as the smaller of two molecular forms of GAD in brain. *J. Neurosci.* **11**, 2725–2731.
- Martinez M., Cuskelly G. J., Williamson J., Toth J. P. and Gregory J. F. 3rd (2000) Vitamin B-6 deficiency in rats reduces hepatic serine hydroxymethyltransferase and cystathione beta-synthase activities and rates of in vivo protein turnover, homocysteine remethylation and transsulfuration. *J. Nutr.* **130**, 1115–1123.
- Masisi K., Suidasari S., Zhang P., Okazaki Y., Yanaka N. and Kato N. (2012) Comparative study on the responses of concentrations of B (6)-vitamers in several tissues of mice to the dietary level of pyridoxine. *J. Nutr. Sci. Vitaminol. (Tokyo)* **58**, 446–451.
- Mason G. F., Martin D. L., Martin S. B., Manor D., Sibson N. R., Patel A., Rothman D. L. and Behar K. L. (2001) Decrease in GABA synthesis rate in rat cortex following GABA-transaminase inhibition correlates with the decrease in GAD(67) protein. *Brain Res.* **914**, 81–91.
- Matalon R., Rady P. L., Platt K. A. *et al.* (2000) Knock-out mouse for Canavan disease: a model for gene transfer to the central nervous system. *J. Gene Med.* **2**, 165–175.
- Mayahara H., Hirano H., Saito T. and Ogawa K. (1967) The new lead citrate method for the ultracytochemical demonstration of activity of non-specific alkaline phosphatase (orthophosphoric monoester phosphohydrolase). *Histochemistry* **11**, 88–96.
- McCance R. A., Morrison A. B. and Dent C. E. (1955) The excretion of phosphoethanolamine and hypophosphatasia. *Lancet* **268**, 131.
- Mori S. and Nagano M. (1985) Electron microscopic cytochemistry of alkaline phosphatase in neurons of rats. *Arch. Histol. Jpn.* **48**, 389–397.

- Morre D. M., Kirksey A. and Das G. D. (1978) Effects of vitamin B-6 deficiency on the developing central nervous system of the rat. *Myelination. J. Nutr.* **108**, 1260–1265.
- Nakamura-Utsunomiya A., Okada S., Hara K. et al. (2010) Clinical characteristics of perinatal lethal hypophosphatasia: a report of 6 cases. *Clin. Pediatr. Endocrinol.* **19**, 7–13.
- Namboodiri A. M., Moffett J. R., Arun P. et al. (2006) Defective myelin lipid synthesis as a pathogenic mechanism of Canavan disease. *Adv. Exp. Med. Biol.* **576**, 145–163; discussion 361–143.
- Narisawa S., Hasegawa H., Watanabe K. and Millan J. L. (1994) Stage-specific expression of alkaline phosphatase during neural development in the mouse. *Dev. Dyn.* **201**, 227–235.
- Narisawa S., Frohlander N. and Millan J. L. (1997) Inactivation of two mouse alkaline phosphatase genes and establishment of a model of infantile hypophosphatasia. *Dev. Dyn.* **208**, 432–446.
- Narisawa S., Wennberg C. and Millan J. L. (2001) Abnormal vitamin B6 metabolism in alkaline phosphatase knock-out mice causes multiple abnormalities, but not the impaired bone mineralization. *J. Pathol.* **193**, 125–133.
- Nagyessy L., Xiao J., Kantor O. et al. (2011) Layer-specific activity of tissue non-specific alkaline phosphatase in the human neocortex. *Neuroscience* **172**, 406–418.
- Newman W., Feigin I., Wolf A. and Kabat E.A. (1950) Histochemical studies on tissue enzymes; distribution of some enzyme systems which liberate phosphate at pH 9.2 as determined with various substrates and inhibitors; demonstration of three groups of enzymes. *Am. J. Pathol.* **26**, 257–305.
- Nguyen T. T., Hayakawa T. and Tsuge H. (2001) Effect of vitamin B6 deficiency on the synthesis and accumulation of S-adenosylhomocysteine and S-adenosylmethionine in rat tissues. *J. Nutr. Sci. Vitaminol. (Tokyo)* **47**, 188–194.
- Nijhout H. F., Gregory J. F., Fitzpatrick C., Cho E., Lamers K. Y., Ulrich C. M. and Reed M. C. (2009) A mathematical model gives insights into the effects of vitamin B-6 deficiency on 1-carbon and glutathione metabolism. *J. Nutr.* **139**, 784–791.
- Nisijima K. and Ishiguro T. (1995) Cerebrospinal-fluid levels of monoamine metabolites and gamma-aminobutyric-acid in neuroleptic malignant syndrome. *J. Psychiatr. Res.* **29**, 233–244.
- Nordengen K., Heuser C., Rinholm J. E., Matalon R. and Gundersen V. (2015) Localisation of N-acetylaspartate in oligodendrocytes/myelin. *Brain Struct Funct* **220**, 899–917.
- Nowak L. G., Rosay B., Czege D. and Fonta C. (2015) Tetramisole and levamisole suppress neuronal activity independently from their inhibitory action on tissue non-specific alkaline phosphatase in mouse cortex. *Subcell. Biochem.* **76**, 239–281.
- Nunes M. L., Mugnol F., Bica I. and Fiori R. M. (2002) Pyridoxine-dependent seizures associated with hypophosphatasia in a newborn. *J. Child Neurol.* **17**, 222–224.
- Oh K. J. and Churchich J. E. (1973) Binding of pyridoxal 5-phosphate to cystathionase. *J. Biol. Chem.* **248**, 7370–7375.
- Ohkubo S., Kimura J. and Matsuoka I. (2000) Ecto-alkaline phosphatase in NG108-15 cells: a key enzyme mediating P1 antagonist-sensitive ATP response. *Br. J. Pharmacol.* **131**, 1667–1672.
- Pagonopoulou O., Efthimiadou A., Asimakopoulos B. and Nikolettos N. K. (2006) Modulatory role of adenosine and its receptors in epilepsy: possible therapeutic approaches. *Neurosci. Res.* **56**, 14–20.
- Park Y. K. and Linkswiler H. (1970) Effect of vitamin B6 depletion in adult man on the excretion of cystathione and other methionine metabolites. *J. Nutr.* **100**, 110–116.
- Patel A. B., de Graaf R. A., Martin D. L., Battaglioli G. and Behar K. L. (2006) Evidence that GAD65 mediates increased GABA synthesis during intense neuronal activity in vivo. *J. Neurochem.* **97**, 385–396.
- Percudani R. and Peracchi A. (2009) The B6 database: a tool for the description and classification of vitamin B6-dependent enzymatic activities and of the corresponding protein families. *BMC Bioinformatics* **10**, 273.
- Picher M., Burch L. H., Hirsh A. J., Spychala J. and Boucher R. C. (2003) Ecto 5'-nucleotidase and nonspecific alkaline phosphatase. Two AMP-hydrolyzing ectoenzymes with distinct roles in human airways. *J. Biol. Chem.* **278**, 13468–13479.
- Pike A. F., Kramer N. I., Blaabooer B. J., Seinen W. and Brands R. (2015) An alkaline phosphatase transport mechanism in the pathogenesis of Alzheimer's disease and neurodegeneration. *Chem. Biol. Interact.* **226**, 30–39.
- Pinner B., Davison J. F. and Campbell J. B. (1964) Alkaline phosphatase in peripheral nerves. *Science* **145**, 936–938.
- Posen S., Whyte M. P., Coburn S. P., Freeman R., Collins F., Fedde K. N. and Bye A. (1997) Infantile hypophosphatasia with fatal status epilepticus. *J. Bone Miner. Res.* **12**, S528.
- Rathbun J. C. (1948) Hypophosphatasia; a new developmental anomaly. *Am. J. Dis. Child.* **75**, 822–831.
- Regnier V., Billard J. M., Gupta S. et al. (2012) Brain phenotype of transgenic mice overexpressing cystathionine beta-synthase. *PLoS ONE* **7**, e29056.
- Robert K., Vialard F., Thiery E., Toyama K., Sinet P. M., Janel N. and London J. (2003) Expression of the cystathionine beta synthase (CBS) gene during mouse development and immunolocalization in adult brain. *J. Histochem. Cytochem.* **51**, 363–371.
- Robert O., Sabatier J., Desoubzanne D., Lalande J., Balayssac S., Gilard V., Martino R. and Malet-Martino M. (2011) pH optimization for a reliable quantification of brain tumor cell and tissue extracts with ¹H NMR: focus on choline-containing compounds and taurine. *Anal. Bioanal. Chem.* **399**, 987–999.
- Rodrigues R. J., Tome A. R. and Cunha R. A. (2015) ATP as a multi-target danger signal in the brain. *Front Neurosci* **9**, 148.
- de Roo M. G., Abeling N. G., Majoe C. B., Bosch A. M., Koelman J. H., Cobben J. M., Duran M. and Poll-The B. T. (2014) Infantile hypophosphatasia without bone deformities presenting with severe pyridoxine-resistant seizures. *Mol. Genet. Metab.* **111**, 404–407.
- Russell R. G. (1965) Excretion of Inorganic Pyrophosphate in Hypophosphatasia. *Lancet* **2**, 461–464.
- Sala-Newby G. B., Skladanowski A. C. and Newby A. C. (1999) The mechanism of adenosine formation in cells. Cloning of cytosolic 5'-nucleotidase-I. *J. Biol. Chem.* **274**, 17789–17793.
- Salek R. M., Xia J., Innes A., Sweatman B. C., Adalbert R., Randle S., McGowan E., Emson P. C. and Griffin J. L. (2010) A metabolomic study of the CRND8 transgenic mouse model of Alzheimer's disease. *Neurochem. Int.* **56**, 937–947.
- Sato A., Nishioka M., Awata S. et al. (1996) Vitamin B6 deficiency accelerates metabolic turnover of cystathionase in rat liver. *Arch. Biochem. Biophys.* **330**, 409–413.
- Say J. C., Ciuffi K., Furriel R. P., Ciancaglini P. and Leone F. A. (1991) Alkaline phosphatase from rat osseous plates: purification and biochemical characterization of a soluble form. *Biochim. Biophys. Acta* **1074**, 256–262.
- Schmitt B., von Both I., Amara C. E. and Schulze A. (2013) Quantitative assessment of metabolic changes in the developing brain of C57BL/6 mice by In vivo proton magnetic resonance spectroscopy. *J. Alzheimers Dis. Parkinsonism* **3** • Issue 4 • 1000129 3, 129.
- Schwartz J. C., Rose C. and Caillens H. (1973) Metabolism of methylhistamine formed through a new pathway: decarboxylation of L-3-methylhistidine. *J. Pharmacol. Exp. Ther.* **184**, 766–779.
- Shimizu N. (1950) Histochemical studies on the phosphatase of the nervous system. *J. Comp. Neurol.* **93**, 201–217.

- Sia C., Wapnir R., Sokal M., Harper R. G., Intizar S. and Manhasset F. (1975) Effects of pyridoxine on neonatal hypophosphatasia. *Pediatr. Res.* **9**, 355.
- Sinclair A. J., Viant M. R., Ball A. K., Burdon M. A., Walker E. A., Stewart P. M., Rauz S. and Young S. P. (2010) NMR-based metabolomic analysis of cerebrospinal fluid and serum in neurological diseases—a diagnostic tool? *NMR Biomed.* **23**, 123–132.
- Smolinska A., Blanchet L., Buydens L. M. and Wijmenga S. S. (2012) NMR and pattern recognition methods in metabolomics: from data acquisition to biomarker discovery: a review. *Anal. Chim. Acta* **750**, 82–97.
- Spector R. (1978) Vitamin B6 transport in the central nervous system: in vivo studies. *J. Neurochem.* **30**, 881–887.
- Stephens M. C. and Dakshinamurti K. (1975) Brain lipids in pyridoxine-deficient young rats. *Neurobiology* **5**, 262–269.
- Stephens M. C., Havlicek V. and Dakshinamurti K. (1971) Pyridoxine deficiency and development of the central nervous system in the rat. *J. Neurochem.* **18**, 2407–2416.
- Stevens B., Porta S., Haak L. L., Gallo V. and Fields R. D. (2002) Adenosine: a neuron-glial transmitter promoting myelination in the CNS in response to action potentials. *Neuron* **36**, 855–868.
- Stoop M. P., Coulier L., Rosenling T. et al. (2010) Quantitative Proteomics and Metabolomics Analysis of Normal Human Cerebrospinal Fluid Samples. *Mol. Cell Proteomics* **9**, 2063–2075.
- Strauss K. A., Morton D. H., Puffenberger E. G. et al. (2007) Prevention of brain disease from severe 5,10-methylenetetrahydrofolate reductase deficiency. *Mol. Genet. Metab.* **91**, 165–175.
- Street S. E. and Sowa N. A. (2015) TNAP and pain control. *Subcell. Biochem.* **76**, 283–305.
- Street S. E., Kramer N. J., Walsh P. L. et al. (2013) Tissue-nonspecific alkaline phosphatase acts redundantly with PAP and NT5E to generate adenosine in the dorsal spinal cord. *J. Neurosci.* **33**, 11314–11322.
- Sugimura K. and Mizutani A. (1979) Histochemical and cytochemical studies of alkaline phosphatase activity in the synapses of rat brain. *Histochemistry* **61**, 123–129.
- Taillandier A., Sallinen S. L., Brun-Heath I., De Mazancourt P., Serre J. L. and Mornet E. (2005) Childhood hypophosphatasia due to a de novo missense mutation in the tissue-nonspecific alkaline phosphatase gene. *J. Clin. Endocrinol. Metab.* **90**, 2436–2439.
- Taketani T. (2015) Neurological symptoms of hypophosphatasia. *Subcell. Biochem.* **76**, 309–322.
- Taketani T., Onigata K., Kobayashi H., Mushimoto Y., Fukuda S. and Yamaguchi S. (2014) Clinical and genetic aspects of hypophosphatasia in Japanese patients. *Arch. Dis. Child.* **99**, 211–215.
- Taoka S., Widjaja L. and Banerjee R. (1999) Assignment of enzymatic functions to specific regions of the PLP-dependent heme protein cystathione beta-synthase. *Biochemistry* **38**, 13155–13161.
- Traut T. W. (1994) Physiological concentrations of purines and pyrimidines. *Mol. Cell. Biochem.* **140**, 1–22.
- Vorbrodt A. W., Lossinsky A. S. and Wisniewski H. M. (1986) Localization of alkaline phosphatase activity in endothelia of developing and mature mouse blood-brain barrier. *Dev. Neurosci.* **8**, 1–13.
- Wall M. J. and Dale N. (2013) Neuronal transporter and astrocytic ATP exocytosis underlie activity-dependent adenosine release in the hippocampus. *J. Physiol.* **591**, 3853–3871.
- Wasyniczuk A., Kirksey A. and Morre D. M. (1983) Effect of maternal vitamin B-6 deficiency on specific regions of developing rat brain: amino acid metabolism. *J. Nutr.* **113**, 735–745.
- Watanabe T., Taguchi Y., Maeyama K. and Wada H. (1991) Formation of histamine: histidine decarboxylase, in *Handbook of experimental pharmacology* (Uvnäs B. ed), Vol. 97, pp. 145–163. Springer Verlag, Berlin.
- Waymire K. G., Mahuren J. D., Jaje J. M., Guilarte T. R., Coburn S. P. and MacGregor G. R. (1995) Mice lacking tissue non-specific alkaline phosphatase die from seizures due to defective metabolism of vitamin B-6. *Nat. Genet.* **11**, 45–51.
- Weiss M. J., Ray K., Henthorn P. S., Lamb B., Kadesch T. and Harris H. (1988) Structure of the human liver/bone/kidney alkaline phosphatase gene. *J. Biol. Chem.* **263**, 12002–12010.
- Werman R., Davidoff R. A. and Aprison M. H. (1966) The inhibitory action of cystathionine. *Life Sci.* **5**, 1431–1440.
- Whyte M. P., Mahuren J. D., Vrabel L. A. and Coburn S. P. (1985) Markedly increased circulating pyridoxal-5'-phosphate levels in hypophosphatasia. Alkaline phosphatase acts in vitamin B6 metabolism. *J. Clin. Investig.* **76**, 752–756.
- Whyte M. P., Mahuren J. D., Fedde K. N., Cole F. S., McCabe E. R. and Coburn S. P. (1988) Perinatal hypophosphatasia: tissue levels of vitamin B6 are unremarkable despite markedly increased circulating concentrations of pyridoxal-5'-phosphate. Evidence for an ectoenzyme role for tissue-nonspecific alkaline phosphatase. *J. Clin. Investig.* **81**, 1234–1239.
- Wishart D. S., Lewis M. J., Morrissey J. A. et al. (2008) The human cerebrospinal fluid metabolome. *Journal of chromatography. J. Chromatogr. B Analyt. Technol. Biomed. Life Sci.* **871**, 164–173.
- Wishart D. S., Jewison T., Guo A. C. et al. (2013) HMDB 3.0—the human metabolome database in 2013. *Nucleic Acids Res.* **41**, D801–D807.
- Wolf N. I., Willemse M. A., Engelke U. F. et al. (2004) Severe hypomyelination associated with increased levels of N-acetylaspartylglutamate in CSF. *Neurology* **62**, 1503–1508.
- Yamamoto H., Sasamoto Y., Miyamoto Y., Murakami H. and Kamiyama N. (2004) A successful treatment with pyridoxal phosphate for West syndrome in hypophosphatasia. *Pediatr. Neurol.* **30**, 216–218.
- Yang G., Wu L., Jiang B. et al. (2008) H2S as a physiologic vasorelaxant: hypertension in mice with deletion of cystathionine gamma-lyase. *Science* **322**, 587–590.
- Yang Y., Wandler A. M., Postlethwait J. H. and Guillemain K. (2012) Dynamic evolution of the LPS-detoxifying enzyme intestinal alkaline phosphatase in zebrafish and other vertebrates. *Front Immunol.* **3**, 314.
- Young V. R., Alexis S. D., Baliga B. S., Munro H. N. and Muecke W. (1972) Metabolism of administered 3-methylhistidine. Lack of muscle transfer ribonucleic acid charging and quantitative excretion as 3-methylhistidine and its N-acetyl derivative. *J. Biol. Chem.* **247**, 3592–3600.
- Zhang D., Xiong W., Chu S., Sun C., Albensi B. C. and Parkinson F. E. (2012) Inhibition of hippocampal synaptic activity by ATP, hypoxia or oxygen-glucose deprivation does not require CD73. *PLoS ONE* **7**, e39772.
- Zimmermann H. (2006) Nucleotide signaling in nervous system development. *Pflügers Arch.* **452**, 573–588.
- Zimmermann H., Zebisch M. and Strater N. (2012) Cellular function and molecular structure of ecto-nucleotidases. *Purinergic Signalling* **8**, 437–502.

B. Unexpected effect of TNAP and NT5E inhibition suggest that AMP acts as a A1 receptor agonist in the mouse piriform cortex. Marie Gleizes, Caroline Fonta et Lionel G. Nowak. En préparation.

1. Résumé

Ce travail s'appuie sur une étude antérieure (Cruz et al., 2017) destinée à identifier sans a priori les métabolites affectés par un défaut d'expression de la TNAP. Cela a été mené à l'aide d'une approche métabolomique et à partir d'extraits de cerveaux de souris jeunes (7 jours) pour lesquelles le gène de la TNAP a été invalidé. Dans l'étude présente, nous focalisons notre analyse sur la contribution de la TNAP dans la production d'adénosine, dont les niveaux ont été révélés altérés dans l'étude métabolomique. Nous avons donc examiné la transmission synaptique et l'inhibition présynaptique dans la couche la du cortex piriforme de la souris adulte qui est une couche riche en TNAP. A l'aide d'enregistrements électrophysiologiques extracellulaires, nous avons cherché à évaluer la contribution de la TNAP dans la signalisation purinergique. Au moyen d'une approche pharmacologique, nous avons perturbé cette signalisation en la potentialisant par l'ajout de nucléotides et nucléosides (ATP, AMP et adénosine) ; en inhibant les enzymes responsables de la production d'adénosine (TNAP et NT5E) à l'aide d'inhibiteurs spécifiques ; ainsi qu'en bloquant les récepteurs A1, A2Aet le transport de l'adénosine grâce à l'utilisation d'antagonistes sélectifs. Nous avons vérifié que l'adénosine exerçait une inhibition présynaptique par l'intermédiaire des récepteurs A1. Le blocage des enzymes responsables de l'hydrolyse de l'AMP en adénosine ne permet pas de supprimer l'inhibition présynaptique. Bien que ce travail ne nous permette pas de conclure formellement sur la contribution de la TNAP dans la production d'adénosine dans le cortex piriforme de la souris adulte, nos résultats suggèrent que l'AMP pourrait agir comme agoniste des récepteurs A1. Cela laisse donc supposer que la TNAP pourrait avoir d'autres rôles que la production d'adénosine dans le système nerveux.

2. Article

Unexpected effect of TNAP and NT5E inhibition suggests that AMP acts as an A1 receptor agonist in mouse piriform cortex.

Marie Gleizes¹, Caroline Fonta^{1*}, Lionel G. Nowak^{1*}

¹ CerCo, Université Toulouse 3, CNRS, Pavillon Baudot, CHU Purpan, BP 25202, 31052 Toulouse Cedex.

* Corresponding authors: lionel.nowak@cnrs.fr, caroline.fonta@cnrs.fr

ABSTRACT

Extracellular adenosine plays a prominent role in presynaptic inhibition through A1 receptors. Adenosine is partly produced by the degradation of released ATP by ectonucleotidases. Among these, tissue non-specific alkaline phosphatase (TNAP) and ecto-5'-nucleotidase (NT5E) are able to perform the last step – AMP to adenosine – of ATP degradation. Adenosine can also originate from the intracellular medium by methionine cycle and can be released through equilibrative transporters (ENT). Both TNAP and NT5E activities are located on the neuronal membrane (including synaptic cleft and nodes of Ranvier). Recently, we demonstrated that TNAP is involved in adenosine synthesis by using metabolomics approach. Here, we wanted to confirm this result by using an electrophysiological approach. We examined synaptic transmission and presynaptic inhibition in slices of mouse piriform cortex maintained *in vitro*. We recorded local field potentials (LFPs), evoked by stimulation of the lateral olfactory tract (LOT) in layer Ia. We first verified that AMP and adenosine inhibited postsynaptic responses and we confirmed that this effect was mediated through adenosine A1 receptors. We next tested whether the conversion AMP to adenosine depended on TNAP by using MLS-0038949, a selective TNAP inhibitor. We expected that AMP inhibitory effect would be suppressed in the presence of MLS-0038949. However, our results did not confirm this expectation. Yet our control histochemical experiments confirmed that MLS-0038949 was effective as a TNAP inhibitor. As NT5E could also be involved in the conversion of AMP to adenosine, we tested AOPCP, a NT5E inhibitor, either alone or in combination with MLS-0038949. Again, we did not see abolition of the presynaptic inhibitory effect of AMP. This led us to hypothesize that AMP could act as an agonist of A1 receptors. To test this possibility, we blocked A1 receptors with CPT while AMP degradation was blocked with TNAP and NT5E inhibitors. In these conditions, inhibition induced by exogenous AMP was largely counteracted. In addition, without exogenous AMP addition, we observed

that the putative endogenous AMP inhibitory effect was fully suppressed. These results suggest that AMP can act as an agonist of A1 receptors. Thus blockade of AMP conversion into adenosine cannot be considered a reliable, pharmacological strategy to prevent A1R activation.

Key-words: TNAP, ecto-5'-nucleotidase, NT5E, adenosine, AMP, A1 receptors, electrophysiology, piriform cortex.

INTRODUCTION

It is now well established that extracellular adenine nucleotides (ATP, ADP and AMP) and adenosine exert potent actions on physiological mechanisms throughout the body. A first description was made by Drury and Szent-Györgyi (1929), which showed that intravenous injection of AMP and adenosine decreases heart rate and causes arterial dilatation. Later, Gillespie (1934) showed that removal of phosphate groups from adenine nucleotides increases the ability of adenine compounds to induce vasodilatation and hypotension. He also showed that ATP causes an increase in blood pressure whereas this effect was never observed with AMP or adenosine.

Many studies have since demonstrated physiological effects of purines nucleotides in a variety of tissues and organs such as: smooth muscle contraction, blood flow modulation, inflammation and platelet aggregation (Burnstock and Kennedy, 1986). The different and often opposite actions of adenosine and ATP suggested the existence of several purine receptors. Two broad categories of purine receptors were proposed by Burnstock (1978): P1 receptors that are activated by adenosine, and P2 receptors that are activated by ATP, ADP and pyrimidine nucleotides (UTP, UDP, UDP-glucose). Two classes of P2 receptors have been distinguished depending on whether they are ligand-gated ion channels (P2X receptors) or coupled to G-protein (P2Y receptors) (Abbrachio and Burnstock, 1994), which have themselves been subdivided in 7 (P2X) or 14 (P2Y) receptor subtypes. P1 receptors have later been divided into 4 subtypes: A1, A2a, A2b and A3.

It has also been reported that adenine nucleotides and adenosine play a role in the regulation of central nervous function. Maitre and al. (1974) demonstrated that adenosine has sedative and antiepileptic actions. Phillis and al. (1975) found that adenosine decreases spontaneous firing rate in rat cortical neurons and a similar effect has been observed in other brain regions such as hippocampus, thalamus, superior colliculus, olfactory bulb and cerebellar cortex (Kostopoulos and Phillis, 1977). This depressant effect can be antagonized by the méthylxanthines, theophylline and caffeine (Sattin and

Rall 1970). Kuroda et al. (1976) and Scholfield (1978) showed that adenosine exerts a strong depressant effect on synaptic transmission in the olfactory cortex in guinea-pig and that this effect is antagonized by application of theophylline. In most brain regions, adenosine was found to exert this presynaptic inhibition through A1 receptor activation. A1 receptor activation induces a reduction of presynaptic calcium current, leading to a decrease in neurotransmitter release (Dolphin and Archer, 1983).

Several mechanisms can account for the presence of adenosine in the extracellular milieu. In the intracellular compartment, adenosine originates from the degradation of S-adenosylhomocysteine (methionine cycle) (Broch and Ueland, 1980) or from the intracellular degradation of ATP. Depending on concentration gradient, adenosine can be released in the extracellular milieu through bidirectional equilibrative nucleosides transporters (ENTs) (Cass et al., 2002).

Adenosine can be also produced by the degradation of released ATP by neurons and/or astrocytes. Extracellular ATP is then degraded through the ectonucleotidase pathway. Four major groups of ectonucleotidases are involved in ATP breakdown and in a general manner in adenine nucleotides breakdown. Cell surface located ectonucleoside triphosphate diphosphohydrolases (E-NTPDases 1, 2, 3 and 8) are involved in the first step of inactivating ATP as they hydrolyze ATP and ADP into AMP (Robson et al., 2006). In addition, extracellular ATP can be dephosphorylated by ectonucleotide pyrophosphatases/phosphodiesterases (E-NPP1, 2 and 3) (Stefan et al., 2005) resulting in the release of AMP and inorganic pyrophosphate (PPi). Alkaline phosphatases (APs) are also capable to degrade ATP in ADP and AMP. In addition, APs can hydrolyze AMP in adenosine. Finally, adenosine can also be produced from AMP by a last type of ectonucleotidase, ecto-5'-nucleotidase (NT5E) (Cusack, 1983; Ciancaglini et al., 2010).

Several types of AP have been identified, yet only one, Tissue NonSpecific Alkaline Phosphatase (TNAP), has been located in the brain. TNAP is an extracellular enzyme, which is anchored to the membrane by glycophosphatidylinositol. TNAP can hydrolyze ATP, ADP and AMP to generate adenosine (Zimmermann, 2006). TNAP is also able to hydrolyze other molecules including pyridoxal-5'-phosphate (the active form of vitamin B6), phosphoethanolamine and pyrophosphate. In the adult, TNAP is widely expressed in the central nervous system and its activity is located on the neuronal membrane (in particular synaptic cleft and nodes of Ranvier) (Fonta et al., 2004; Langer et al., 2008; Brun-Heath et al. 2011). TNAP activity has also been associated with cerebral developing regions (Narisawa et al. 1994; Fonta et al. 2005; Langer et al., 2007; Brun-Heath et al. 2011), and is involved in neuronal differentiation, myelination and synaptogenesis (Kermer et al. 2010; Hanics et al., 2012).

TNAP deficiency in humans leads to a rare disease called hypophosphatasia, which is characterized by bone mineralization impairments and epileptic seizures in its perinatal and infantile forms (reviewed in Millan and Whyte, 2016). Mice in which TNAP gene has been invalidated also develop seizures that are lethal within 2 weeks after birth (Waymire et al, 1995; Narisawa et al. 1997).

Although biochemical studies showed that TNAP purified from brain tissue is able to hydrolyze nucleotides (Dorai and Bachhawat 1977), extracellular adenosine synthesis in the brain is usually attributed to NT5E (Lovatt et al. 2012; Zhang et al. 2012; Kulesskaya et al., 2013; other references possible). Yet, we recently demonstrated that TNAP is strongly involved in adenosine synthesis by using a metabolomic approach in 7 day old mice (Cruz et al., 2017): indeed we found that adenosine level in TNAP knockout mice was reduced to less than 20% of that found in wildtype mice.

In the present study, we explored the contribution of TNAP to adenosine synthesis using alternative approaches: First, we used an electrophysiological approach on brain slices maintained in vitro: as adenosine plays a major role in presynaptic inhibition, the influence of TNAP in adenosine synthesis should be reflected by alteration of presynaptic inhibition. Second, we targeted one specific brain region, the piriform cortex that has, among other advantages, a high TNAP activity level (Brun-Heath et al. 2011). Third, we used adult brains and pharmacological means to inactivate ectonucleotidase

We first verified that ATP, AMP and adenosine inhibited postsynaptic responses and we confirmed that this effect was mediated through adenosine A1 receptors. We assumed that the inhibitory effect of ATP and AMP resulted from their degradation in adenosine by ectonucleotidases. Then, to determine the involvement of TNAP in adenosine synthesis, we used a TNAP inhibitor that should have reduced adenosine production, hence increased postsynaptic response amplitude. Contrary to our expectation, response amplitude actually decreased or remained unchanged. The same result was obtained after inhibition of NT5E or of both ectonucleotidases (TNAP and NT5E) together. Yet in these conditions, the inhibition induced by AMP was nevertheless alleviated by A1 receptor blockade. In line with a previous study performed in transfected cultured cells (Rittiner et al., 2012), our results can be interpreted as indicating that AMP is an A1 receptor agonist.

MATERIALS AND METHODS

Ethics statement

All procedures were conducted in accordance with the guidelines from the French Ministry of Agriculture (décret 87/848) and from the European Community (directive 86/609) and was approved

by the local ethical committee (comité d'éthique Midi-Pyrénées pour l'expérimentation animale, N° MP/06/79/11/12).

Slices preparation

Two- to 4-month-old C57BL/6 wildtype female mice were used for these experiments. The method used for brain slice preparation has been previously described (Gleizes et al., 2017). In brief, mice were deeply anesthetized with isoflurane and then rapidly decapitated. The brain was removed and prepared for slicing in ice-cold, oxygenated (95% O₂ / 5% CO₂) modified, Ca⁺⁺ free ACSF (mACSF) of the following composition (mM): NaCl 124, NaHCO₃ 26, KCl 3.2, 1 MgSO₄, NaH₂PO₄ 0.5, MgCl₂ 9, Glucose 10. Four hundred-micrometer-thick slices were then cut on a vibratome in the presence of cold, oxygenated mACSF. Slices were allowed to recover for at least 1 hour at room temperature in a holding chamber filled with oxygenated in vivo-like aCSF whose composition was based on ionic concentration measurements in vivo (refs in Gleizes et al., 2017). NaCl 124, NaHCO₃ 26, KCl 3.2, MgSO₄ 1, NaH₂PO₄ 0.5, CaCl₂ 1.1, and glucose 10. This ACSF was continuously bubbled with a 95% O₂ / 5% CO₂ mixture (pH 7.4).

Stimulation and recording

For recording, an individual slice was transferred in a submersion type chamber that was continuously gravity-fed with oxygenated in vivo-like aCSF at a flow rate of 3-3.5 ml/min. All recordings were performed at 34-35°C. Extracellular electrical stimulation (0.5 Hz) was applied through tungsten-in-epoxylite microelectrodes (FHC, 0.2-0.3 MΩ) implanted in the lateral olfactory tract (LOT) and consisted in monopolar cathodal square current pulses (6-35 μA, 200 μs duration) delivered by an isolated stimulator (A365 stimulus Isolator, WPI). Local field potentials were recorded in layer Ia of the piriform cortex through tungsten-in-epoxylite microelectrodes. The signal was amplified ($\times 1000$) and filtered (0.1 Hz-10 kHz) with a NeuroLog system (Digitimer, UK). Fifty Hz noise was eliminated with a Humbug system (Quest Scientific, Canada). All signals were digitized with a digitization rate of 20-50 kHz (1401plus or power1401, CED, UK). Real-time display of the signals was achieved with an oscilloscope and with Spike2 software (CED, UK).

In most experiments, short term plasticity (STP) was tested using stimulation trains consisting of five consecutive stimuli delivered at 6 different frequencies: 3.125, 6.25, 12.5, 25, 50 and 100 Hz as previously described (Gleizes et al., 2017).

The LFP recorded in layer Ia after stimulation of the LOT was composed of a fiber volley, which corresponds to the summation of synchronous action potentials traveling in axons, followed by a slow

negative wave (N-wave) (Yamamoto and McIlwain, 1966) reflecting the summation of monosynaptic excitatory postsynaptic potentials generated in the vicinity of the recording electrode. Response amplitude was measured as the maximal amplitude of the N-wave relative to prestimulus baseline. The amplitude of the fiber volley was measured similarly. The time course of the effect of reagents applied in the bath on field potential amplitude was monitored during the stimulation period.

Data analysis

Signal processing was performed using the Spike2 software with scripts written by the users. The control condition consisted of 15-20 minutes baseline recording and the recovery condition consisted of 15-20 minutes washing. In between, one or two different concentrations of adenine nucleotides, or different combination of antagonists/inhibitors, were bath applied for 15-20 minutes. For the analysis of the effect of various reagents applied in the bath on synaptic transmission at 0.5 Hz, signals were averaged over the last minute (thirty responses) of the 15-20 min-long series of stimuli. Amplitudes obtained in a given condition were normalized by that obtained in control condition. Paired-pulse ratios at 25 Hz was also examined to determine if changes induced by various manipulation were presynaptic or postsynaptic.

Enzyme histochemistry

Frontal and parasagittal sections (90 μ m thick) were cut on a vibratome from fresh tissue.

Alkaline phosphatase activity was detected as previously described (Fonta and Imbert 2002). In brief, frontal sections were fixed for 40 minutes in cold PFA 4%. Then fixed sections were incubated in a 0.1 M Tris solution containing 4-nitro blue tetrazolium chloride (NBT, 0.53 mM,) and 5-bromo-4-chloro-3-indolyl-phosphate-4-toluidine salt (BCIP, 0.38 mM; TNAP substrate). Detection of alkaline phosphatase activity was performed at pH 7.5 and pH 9.5. Incubation time was about 30 minutes at pH 7.5 and 10 minutes at pH 9.5. Reaction was stopped in 10 mM Tris pH 7.5 solution containing 1 mM EDTA and 10 mM levamisole. Enzymatic reaction product is visualized as a blue/violet deposit. Sections were then rinsed in Tris, mounted, dehydrated in graded alcohol and embedded in DPX.

For localization of ecto-5'-nucleotidase activity, a modification of lead phosphate method was used (Schoen et Kreutzberg, 1997) and is briefly summarized here. Parasagittal sections were fixed in cold 4% PFA-cacodylate buffer for 40 minutes. Then, sections were incubated for 90 minutes at room temperature in Tris maleate buffer solution containing 2% Pb(NO₃)₂ and NT5E substrate: AMP (1 mM). After incubation, sections were rinsed in Tris maleate sucrose buffer. Sections were processed for 5 minutes at room temperature in 1% aqueous (NH₄)₂S. Enzymatic reaction product is visualized

as a brown deposit. Sections were rinsed in Tris maleate sucrose buffer, then mounted on slides, dehydrated and embedded in DPX.

Reagents

ATP, 5'-AMP, adenosine, NT5E inhibitor (Adenosine 5'-(alpha, bêta-methylene) diphosphate, 10 µM), 8-cyclopentyltheophylline (A1 receptors selective antagonist, 0.2 µM), S-(4-Nitrobenzyl)-6-thioinosine (ENT inhibitor, 10 µM), NBT, BCIP, Cibacron Blue 3GA (non-selective P2Y antagonist, 30 µM) and suramine (non-selective P2 receptors, 50 and 100 µM) were purchased from Sigma-Aldrich France. TNAP inhibitor, MLS-0038949 was purchased from Merck. ATP, adenosine, AMP and Cibacron Blue were prepared and diluted to different concentrations in in vivo-like ACSF. CPT was prepared and diluted to 0.2 µM in our in vivo-like ACSF. MLS-003849 and AOPCP were dissolved in DMSO then diluted in in vivo-like ASCF to obtain a final DMSO concentrations of 1/1000.

Statistical analysis

ANOVA and Tukey's HSD post hoc tests were used to examine effect of various conditions with multiple comparisons. Population data are shown as means ± SEM.

RESULTS

Adenine nucleotides act as presynaptic inhibitors by activating adenosine A1 receptors in mouse piriform cortex.

We first examined the effect of extracellular ATP, AMP and adenosine on the amplitude of the synaptic responses at the LOT-layer Ia synapse in piriform cortex. LFPs were thus evoked by stimuli delivered in the LOT at 0.5 Hz. Effect of 100 µM ATP (n=13) and of varying extracellular adenosine and AMP concentrations has been examined in 51 experiments. Six extracellular adenosine concentrations were tested: 1 µM (n=2); 10 µM (n=7); 30 µM (n=10); 100 µM (n=14); 300 µM (n=8); 1000 µM (n=7). Four extracellular AMP concentrations were tested: 1 µM (n=3); 10 µM (n=4); 100 µM (n=18); 1000 µM (n=4). One to four different concentrations were tested in the same experiment.

Fig 1 shows examples of LFPs recorded in layer Ia with various adenosine and AMP concentrations. Extracellular electrical stimulation was applied in the LOT at 0.5 Hz. Fig 1A illustrates the effects of 3 different extracellular adenosine concentrations. In the presence of 100 µM adenosine, the amplitude

of the N-wave was 46% smaller than in the control condition, while it was largely suppressed with 300 μ M adenosine and 1 mM adenosine. Control and recovery displayed the same amplitudes.

Fig 1B shows the effects of 1 AMP concentration. When 100 μ M AMP was bath applied, the amplitude of the N-wave was approximatively decreased by 48 %. Control and recovery displayed similar amplitudes. The amplitude of the fiber volley did not change, indicating that changes in N-wave amplitude were of synaptic origin and did not result from changes in axonal excitability. The paired-pulse ratio increased in the presence of AMP or adenosine (not illustrated), indicating that their inhibitory actions were presynaptic.

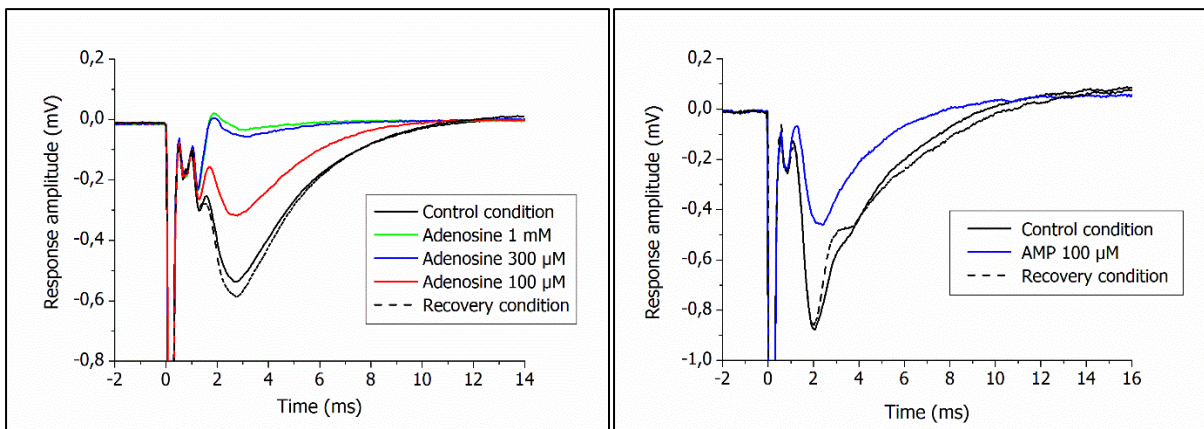


Figure 1: Effect of extracellular adenosine and AMP concentrations on the amplitude of the response evoked at 0.5 Hz at the LOT-layer Ia synapse of the piriform cortex. Each trace is the average of 30 responses (1 min recording) recorded at the end of each condition. A: LFP recorded with 3 different extracellular adenosine concentrations (100, 300 and 1000 μ M). B: LFP recorded with 1 extracellular AMP concentrations (100 μ M).

Population data are presented in Fig 2. Before averaging, data were normalized: the normalized response amplitudes correspond to the peak amplitudes of the N-wave in a given adenine nucleotides concentration expressed as a percentage of the response amplitude in the control condition, which represents 100 % of response amplitude. Fiber volley amplitude was not significantly affected by various adenine nucleotides application (ANOVA, $p=0.93$, data not shown). In contrast, we observed a dose-dependent decrease of response amplitudes with increasing concentrations from 30 μ M adenine nucleotides (ANOVA, $P<0.001$). No significant change in response amplitude was observed when 1 μ M AMP or adenosine was applied in the medium (Tukey's HSD, $p = 0.9756$). Response amplitudes were decreased by 23 % and 8% relative to the control with 10 μ M AMP or 10 μ M adenosine, respectively. 30 μ M of adenosine significantly decreased response amplitudes by 24% compared to the control condition (Tukey's HSD, $p = 0.001$). 100 μ M of ATP, AMP and adenosine produced the same

decrease of response amplitude (Tukey's HSD, $p = 0.991$ for AMP 100 μM vs Adenosine 100 μM , $p = 0.882$ for AMP 100 μM vs ATP 100 μM and $p = 0.161$ for adenosine 100 μM vs ATP 100 μM). 100 μM of ATP decreased response amplitudes by 44%, AMP decreased response amplitudes by 53% and adenosine decreased response amplitudes by 60% relative to the control condition ($p < 0.001$). Adenosine at high concentrations (300 μM and 1 mM) exerted the same effect (Tukey's HSD, $p = 0.999$); these concentrations led to a decrease in response amplitudes by 90% relative to the control condition (Tukey's HSD, $p < 0.001$). These results suggest that the effect of extracellular adenosine on response amplitude saturates when its concentration is larger than 300 μM . No significant difference was observed between 1mM AMP and 100 μM adenosine ($p=0.59$). Control (100%) and recovery displayed similar amplitudes (Tukey's HSD, $p=0.08$)

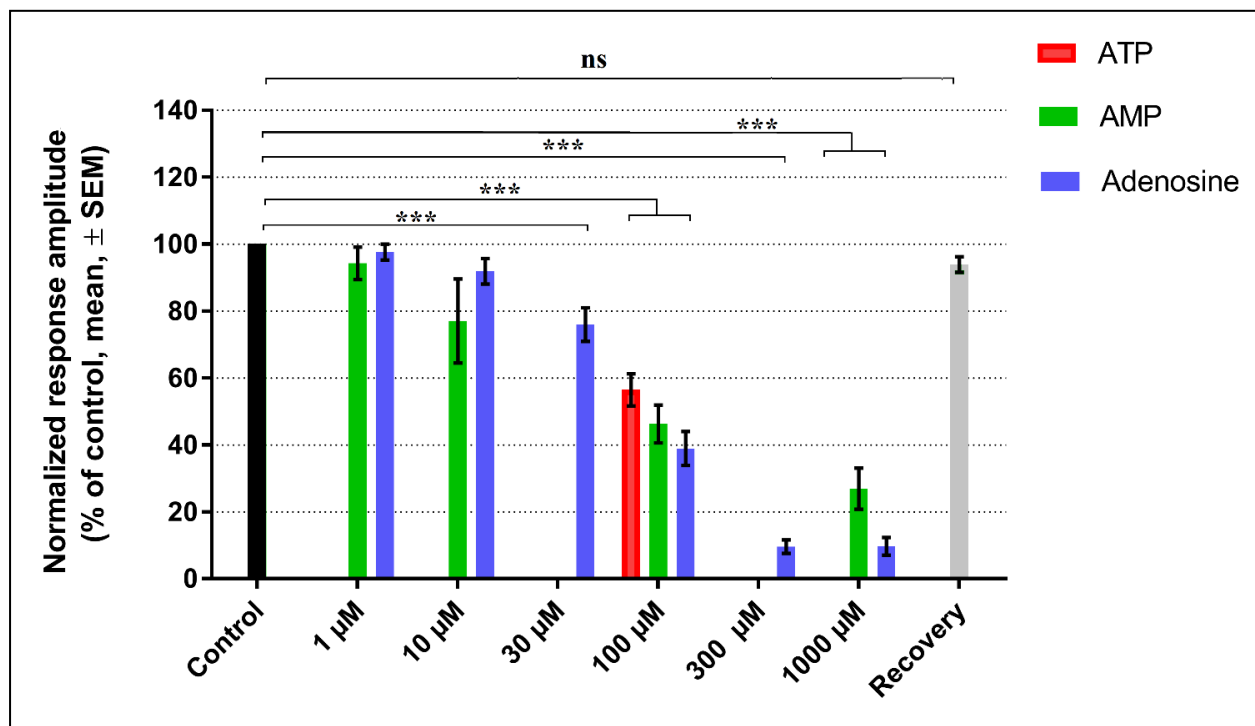


Figure 2: Effect of varying extracellular adenine nucleotides concentrations, population data ($n=51$ experiments). Bars correspond to the mean of response amplitudes and error bars to $\pm \text{SEM}$. The recovery condition refers to normalized response amplitude upon return to the control medium. There was a significant decrease in response amplitude regarding increasing adenosine and adenine nucleotides concentrations ($***p \leq 0.001$, ANOVA followed by Tukey's post hoc tests)

To confirm that adenosine and adenine nucleotides exerted their inhibitory effects on synaptic transmission through adenosine A1 receptors, we used 8-cyclopentyl-1,3-dimethylxanthine (CPT; 0.2 μ M), which is a competitive antagonist at adenosine A1 receptors.

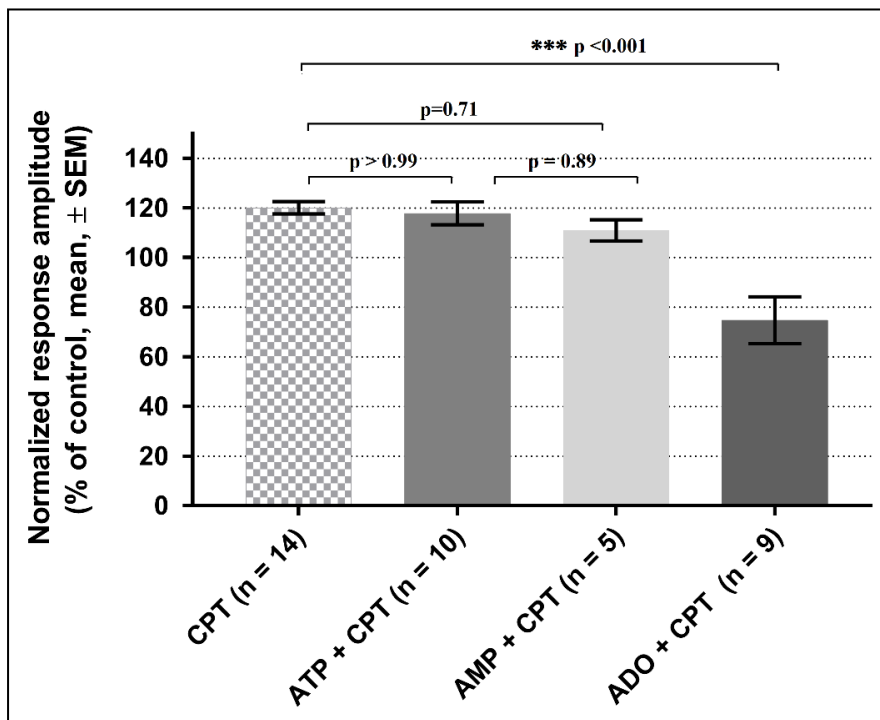


Figure 3: Adenine nucleotides (100 μ M) inhibitory effect was blocked by CPT 0,2 μ M except for 100 μ M adenosine. Normalized response amplitudes are represented for each condition relative to the control condition which corresponds to 100 % of response amplitudes (n corresponds to the number of experiments for each condition).

As presented in figure 3, addition of 0.2 μ M CPT *alone* significantly increased response amplitudes by +20% relative to the control condition (Tukey's HSD, P = 0,002). This increase in response amplitude can be explained by the presence of endogenous adenosine in the brain slice.

The inhibitory effect elicited by 100 μ M ATP or 100 μ M AMP was fully canceled by 0.2 μ M CPT. Indeed, relative to control condition, response amplitudes were increased by +17.8 % and +11 % with 100 μ M of ATP or 100 μ M of AMP respectively. However, adenosine inhibitory effect was not fully blocked by CPT 0.2 μ M (Tukey's HSD, P < 0.001). We attributed this partial block to the competitive nature of the antagonism exerted by CPT, which may be partially displaced given the large amount of adenosine present in the bath (see supplemental data). CPT antagonism was more complete against AMP or ATP, suggesting that the degradation of these compounds leaves a time window where adenosine concentration is not as high as to be able to strongly compete with CPT.

This first set of experiments confirmed that ATP, AMP and adenosine acts as a presynaptic inhibitor through the activation of adenosine A1 receptors. We hypothesized that the inhibitory effect seen with

ATP and AMP can be attributed to the effect of the degradation of these compound into adenosine, as ATP and AMP should be sequentially degraded into adenosine by various ectonucleotidases. We next examined whether TNAP could be one of these ectonucleotidases.

TNAP contribution in adenosine synthesis in layer Ia of piriform cortex.

Although our metabolomics experiments demonstrated that TNAP is involved in adenosine synthesis in 7-day-old mice (Cruz et al., 2017), we wanted to confirm this result in adult mice (2-4 months old) with regard to adenosine mediated presynaptic inhibition. To answer this question, we blocked TNAP activity with a specific TNAP inhibitor, MLS-0038949 (50 μ M) (Sergienko et al., 2009). We first examined the contribution of TNAP to *endogenous* adenosine production. The results are illustrated in figure 4A. Our expectation was that addition of TNAP inhibitor in the bath would block endogenous ADP, AMP and adenosine production. In these condition, response amplitudes should reach a value similar to that observed with 0.2 μ M CPT in the bath. On the opposite, we observed a significant decrease in response amplitude when MLS-0038949 was added alone in the bath (Fig 4A). Relative to control response amplitude (100%), the relative response amplitude was decreased by 12 % (Tukey's HSD, $p = 0.4$). In comparison to CPT, the response decrease averaged 32 % (Tukey's HSD, $p < 0,001$).

In contrast to other manipulation, there was no recovery after MLS application. Response amplitudes remained 20 % below control (Tukey's HSD, $p = 0.01$) even after more up to 45 minutes washout. In contrast, CPT recovery was not different from control condition (Tukey's HSD, $p = 0.95$; data not shown).

We also expected that the inhibitory effect of exogenous AMP would be suppressed by TNAP inhibitor. Indeed, added AMP would not be degraded into adenosine in the presence of MLS-0038949. However, as illustrated in Fig 4B, AMP (100 μ M) inhibitory effect was not suppressed MLS-0038949 (50 μ M). Response amplitudes in the presence of 100 μ M AMP alone and with the addition of MLS-0038949 were similar: 47% and 43% of control response amplitudes, respectively (Tukey's HSD, $p = 0.97$).

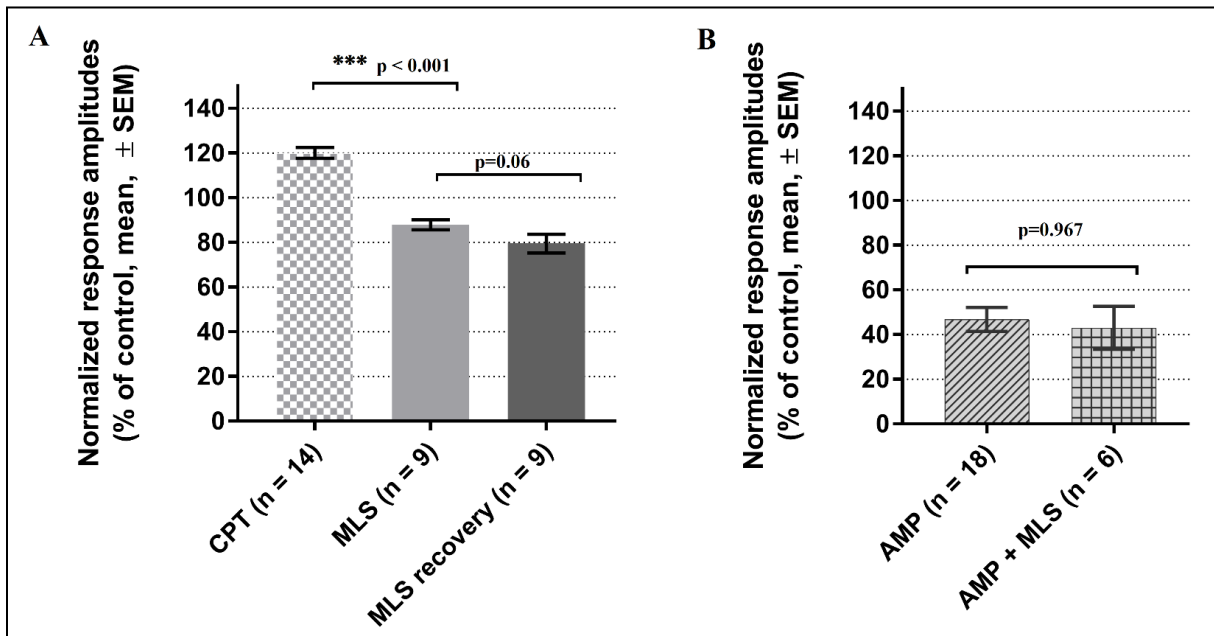


Figure 4: Effect of TNAP inhibition (MLS-0038949, 50 μ M) on response amplitudes in mouse piriform cortex, on population data (15 experiments). A. MLS-0038949 alone significantly decreased response amplitudes compared to 0,2 μ M CPT. Response amplitude during recovery of MLS condition was significantly different from the control (Tukey's HSD, $p < 0.001$). B. Effect of MLS-0038949 in combination with 100 μ M of AMP in the medium. Addition of TNAP inhibitor to AMP 100 μ M did not change response amplitudes compared to 100 μ M AMP alone. ***: $p < 0.001$. Recovery of AMP + MLS condition was not different from the control (Tukey's HSD, $p = 0.06$, data not shown).

The decrease in response during and after MLS-0038949 application (Fig 4A) led us to hypothesize that it exerted some toxic action in brain slices. MLS-0038949 toxicity assays were therefore performed on neuronal cell cultures (David Magne and Anne Briolay, Institut de Chimie et de Biochimie Moléculaires et Supramoléculaires), using analysis of lactate dehydrogenase (LDH) activity, which is commonly used to evaluate cell death. No LDH activity could be revealed, indicating that MLS-0038949 was not toxic on the time scale of our experimental conditions.

MLS does inhibit TNAP activity in layer Ia of mouse piriform cortex.

Given our unexpected results, we next hypothesized that TNAP inhibitor was not effective at inhibiting TNAP activity in piriform cortex. To determine whether MLS-0038949 was effective at inhibiting TNAP activity in layer Ia of piriform cortex, we performed NBT/BCIP histochemistry on mouse brain slices at pH 9.5 (replicated on ten slices times) and at pH 7.5 (replicated on nine slices).

Alkaline phosphatase activity was assessed in the absence and in the presence of 50 μ M MLS-0038949. In the absence of TNAP inhibitor, a strong alkaline phosphatase activity was detected throughout the brain (Fig 5, 6). We observed that layer Ia of piriform cortex was heavily stained by NBT/BCIP complex (fig 5C). 50 μ M MLS-0038949 abolished staining in the whole section. These results demonstrate that MLS-0038949 (50 μ M) was highly efficient at inhibiting TNAP activity in mouse brain.

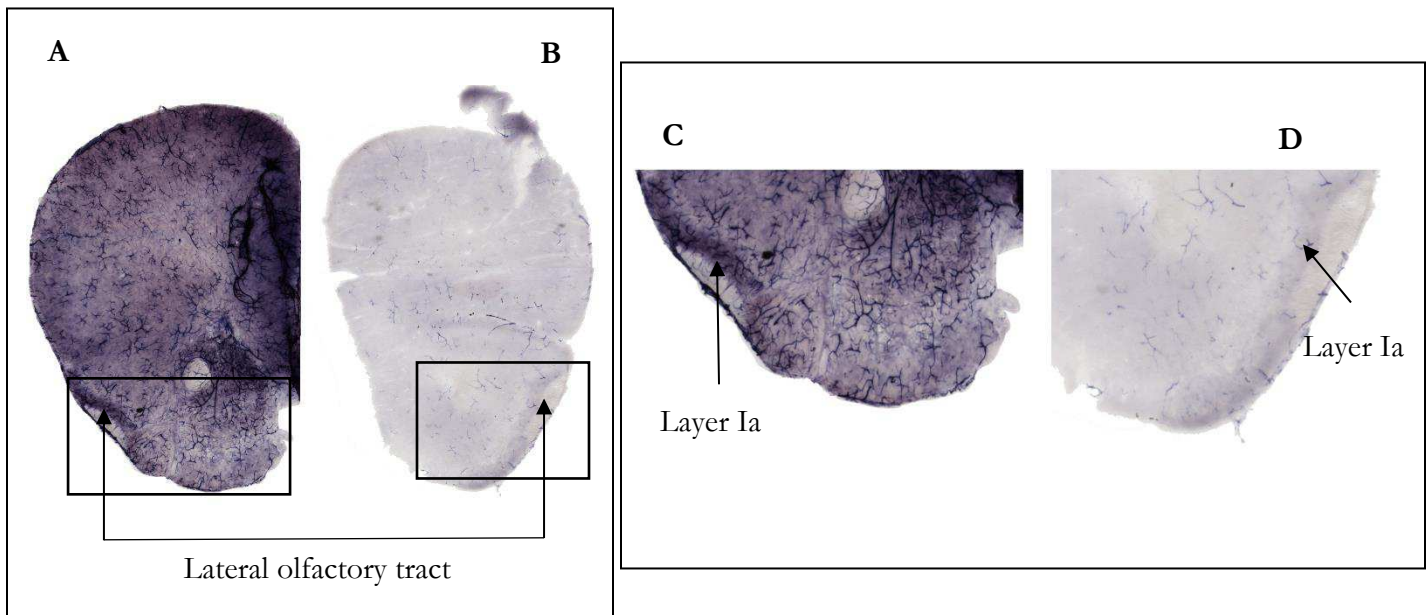


Figure 5: Alkaline phosphatase activity is detected throughout the mouse brain at pH 9.5. Frontal brain slices from WT mice were stained using NBT/BCIP histochemistry at pH 9.5 in the absence (A) or presence (B) of 50 μ M MLS-0038949. Scale bar, 200 μ m (C & D) Enlargement of the areas framed in Figure A & B. (C) Strong staining is observed in layer Ia of the piriform cortex. (D) Staining was abolished in layer Ia of the piriform cortex by MLS-0038949.

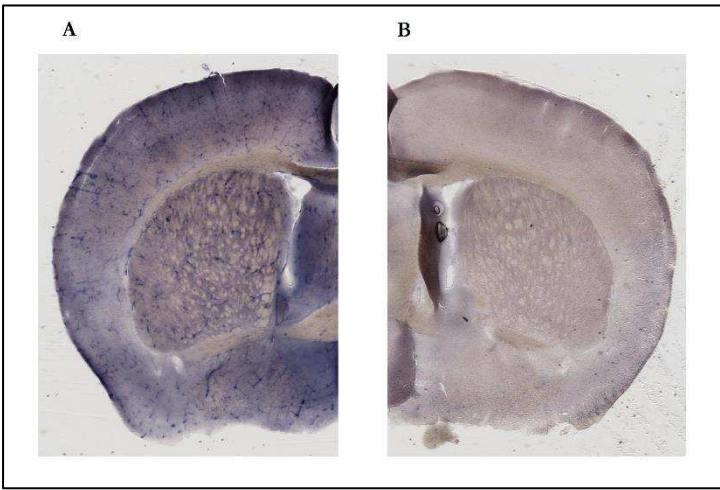


Figure 6: Alkaline phosphatase activity is detected throughout the mouse brain at pH 7.5. Frontal brain slices from WT mice were stained using NBT/BCIP histochemistry at pH 7.5 in the absence (A) or presence (B) of 50 μ M MLS-0038949. Staining background observed in the presence of MLS-0038949 was also present in no substrate condition (NBT only). This confirmed that MLS-0038949 was effective at pH 7.5.

Ecto-5'-nucleotidase (NT5E) contribution to adenosine synthesis in mouse cortex piriform.

We showed that MLS-0038949 is effective at inhibiting TNAP activity throughout the brain, yet MLS-0038949 did not suppress presynaptic inhibition in endogenous condition and did not suppress presynaptic inhibition induced by AMP. NT5E, another ectonucleotidase that is also able to generate adenosine from AMP (Cusack, 1983), has been localized in the layer Ia of the piriform cortex (Trieu et al., 2015). We therefore tested whether this ectonucleotidase could be responsible for adenosine synthesis in layer Ia of the piriform cortex. For this purpose, we used AOPCP (10 μ M), a specific NT5E inhibitor (Burger and Lowenstein, 1975).

In the endogenous condition, as previously expected earlier with MLS-0038949, response amplitude should increase in the presence of AOPCP to reach a value similar to that obtained with 0.2 μ M CPT. Yet again, the results, illustrated in figure 7A, did not comply with this expectation. Instead, response amplitudes reached a value slightly lower than control response amplitude (7%, $p=0.55$) and remained 27% below the amplitude obtained in the presence of CPT (Tukey's HSD, $p < 0.001$).

Similarly, in the exogenous condition we expected that the inhibitory effect of added AMP would be suppressed in the presence of AOPCP. However, as shown in figure 7B, the inhibitory effect of AMP (100 μ M) was not at all suppressed when AOPCP was added to the bath (Tukey's HSD, $p=0.71$).

There still remained the possibility that NT5E and TNAP act redundantly, the activity of one enzyme palliating for the inhibition of the other, as previously reported in the spinal cord (Street et al. 2013). To test this hypothesis, we decided to integrally block the degradation of AMP into adenosine by

combining the two ectonucleotidases inhibitors: MLS-0038949 (50 μ M) and AOPCP (10 μ M). Yet, in the endogenous condition, response amplitude remained below that observed in the CPT condition by 23.4% (Tukey's HSD, $p < 0.001$). In addition, response amplitude in the presence of AOPCP + MLS did not differ significantly from that obtained in the presence of AOPCP alone ($p = 0.98$), or in the presence of MLS-0038949 alone ($p=0.76$).

Similarly, in exogenous condition, the AMP inhibitory effect was not at all suppressed when the two ectonucleotidases inhibitors were added in the bath (Tukey's HSD, $p = 0.66$). Instead, whether with one inhibitor or both, response amplitudes were equivalent to those obtained with 100 μ M AMP: AMP + AOPCP = 32.3 % of control response amplitudes, AMP + AOPCP + MLS = 29.3 % and AMP alone = 46.8 % (ANOVA, $p=0.244$). Recovery condition with AOPCP alone and with AOPCP + MLS were not different from the control condition (Tukey's HSD, $p > 0.99$ and $p = 0.8$ respectively; data not shown).

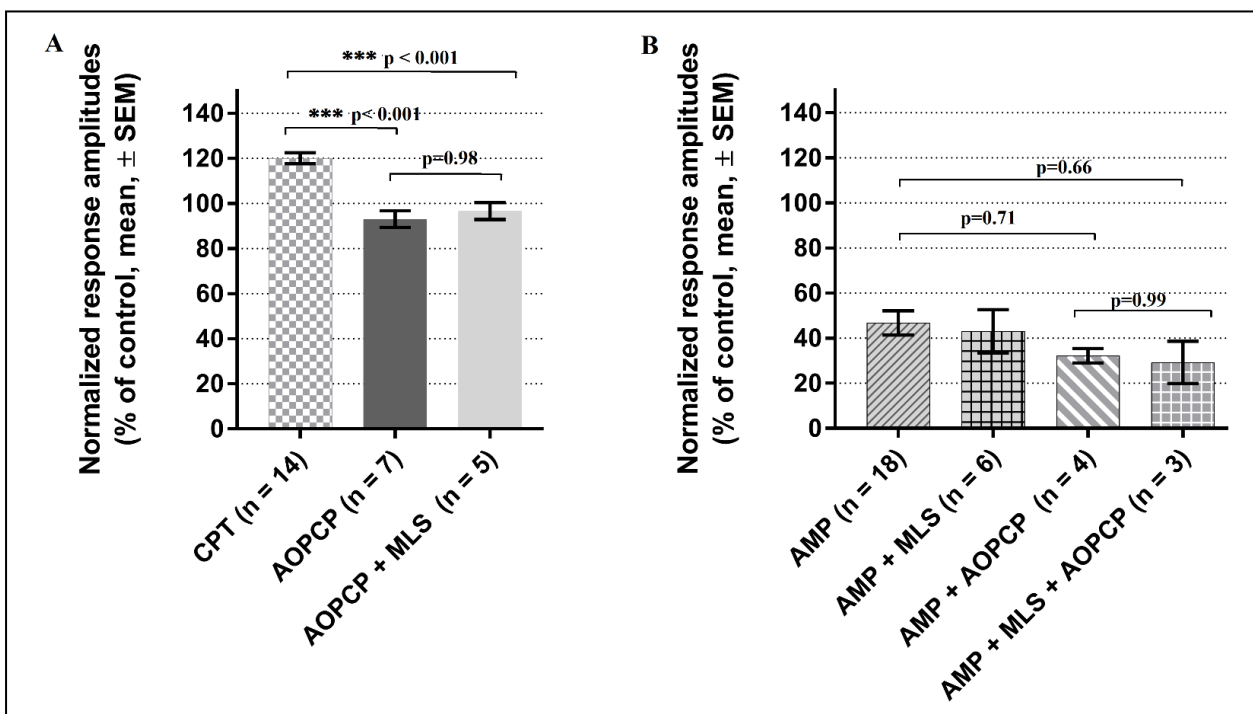


Figure 7: Contribution of ectonucleotidases in adenosine synthesis in layer Ia of mouse piriform cortex. A. Endogenous condition. B. Exogenous condition.

As response amplitude in the presence of MLS or AOPCP appeared to be slightly below control response amplitude (Fig 4A and 7A), short-term plasticity (5 pulses at 25 Hz) was examined to determine the presence of changes in presynaptic inhibition. However, as illustrated in Fig 8,

normalized response amplitude as a function of stimulus rank appeared identical in control condition and in presence of the ectonucleotidase inhibitors. This suggests that the decrease in response amplitude was not due to a decrease in neurotransmitter release.

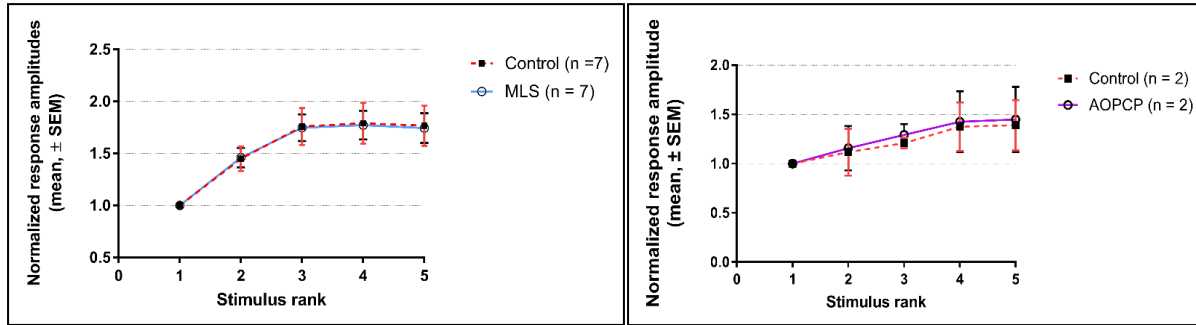


Figure 8: No indicated that presynaptic mechanisms are involved.

As for TNAP, histochemical experiments were performed in order to ensure that AOPCP was effective at inhibiting NT5E activity (replicated on 12 slices). AMP (1 mM) was used as a substrate. As documented in previous studies (Langer et al., 2008), enzyme histochemical staining was the strongest in the caudoputamen and the olfactory tubercle (Fig 9A). In comparison, most brain regions displayed only faint AMPase staining (Fig 9A). The outskirt of the piriform cortex, presumably corresponding to the LOT and/or layer 1a, showed relatively dense label. 10 μ M AOPCP reduced enzyme histochemistry staining in the whole brain but did not abolish it (Fig 9B). The residual staining could be attributed to the endogenous activity of other ectonucleotidases that could also release phosphate and/or to an AOPCP concentration too low to completely inhibit all NT5E activity. However, although not completely suppressed, staining in the piriform cortex was quite strongly reduced.

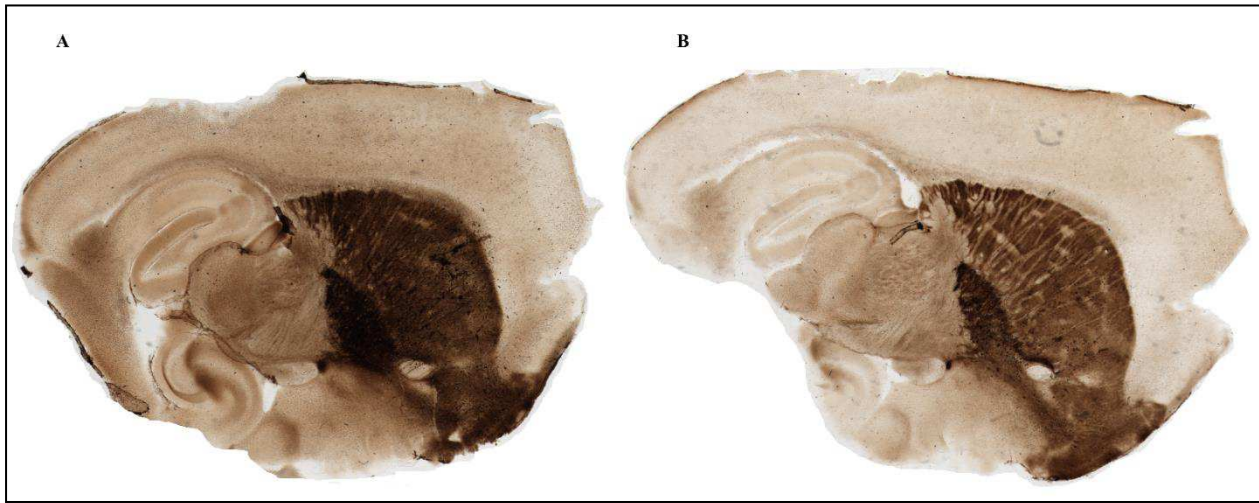


Figure 9: NT5E phosphatase activity is detected throughout the mouse brain at pH 6.8. Sagittal brain slices from WT mice were stained the lead phosphate method in absence (A) or presence (B) of 10 μ M AOPCP. CP: caudoptamen; OT; olfactory tubercle; PC: piriform cortex.

Is adenosine released from intracellular compartment responsible for the residual inhibition?

Given the results presented above, extracellular adenosine production in the piriform cortex should have been largely reduced by the ectonucleotidase inhibitors. Nevertheless, the inhibitory tone evidenced with CPT (Fig 3) remained in the presence of NT5E and/or TNAP inhibitor (Figs 4A and 7A). Yet another source of adenosine could be responsible for this inhibitory tone. Indeed, adenosine may be produced in the intracellular compartment. From the intracellular compartment, and depending on the concentration gradient, adenosine may reach the extracellular milieu through equilibrative nucleoside transporters (ENTs) (Cass et al., 1998). One possibility worse exploring was that NT5E and/or TNAP inhibition, by reducing extracellular adenosine production, created a sink for intracellular adenosine that in turn, would have maintained the inhibitory tone. In order to determine whether the release of intracellular adenosine was the source of the residual inhibition, we blocked adenosine transporters (ENT1 and ENT2) using S-(4-Nitrobenzyl)-6-thioinosine (NBFI). We used a concentrations of 10 μ M as it would block both ENT1 and ENT2 (Ward et al., 2000). The results are presented in figure 10.

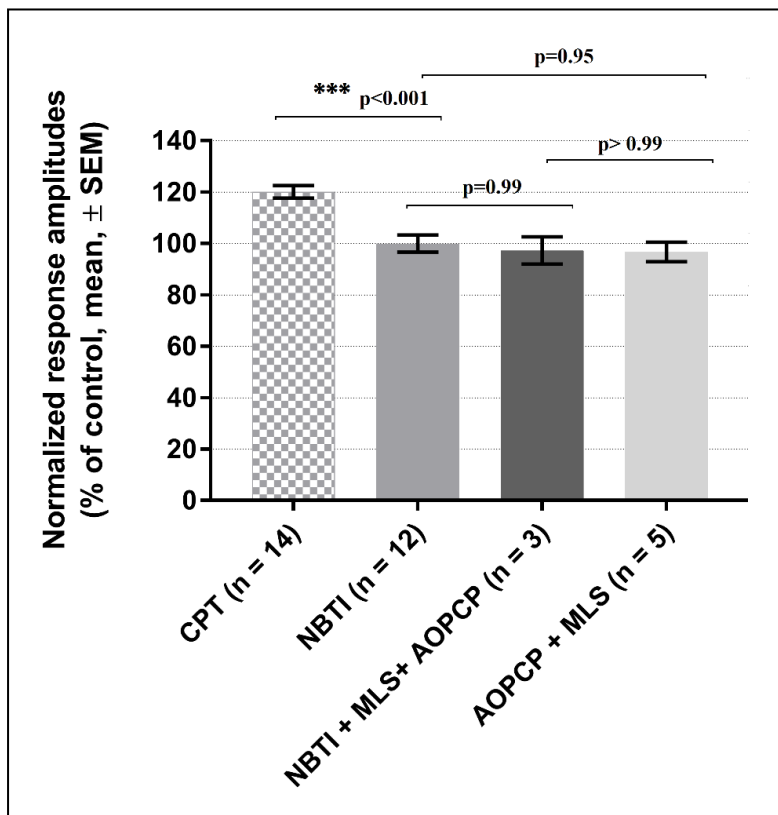


Figure 10: Intracellular adenosine release does not contribute to the residual inhibition. NBTI (10 μ M) applied alone or in combination with MLS-0038949 (50 μ M) and AOPCP (10 μ M), does not restore response amplitudes to that obtained with 0.2 μ M CPT alone and the residual inhibition observed with MLS+AOPCP is still observed when NBTI is added to this combination. ***: $p < 0.001$.

Whether alone or in combination with NT5E and TNAP inhibition, blockade of ENTs by NBTI failed to increase response amplitude toward values comparable to those obtained with CPT. Application of 10 μ M NBTI in combination with MLS-0038949 and AOPCP did not change response amplitudes compared to the AOPCP+MLS condition (Tukey's HSD, $p = 0.999$). Response amplitude remained significantly lower (Tukey's HSD, $p < 0.001$), by more than 20%, than that observed with CPT (NBTI+AOPCP+MLS: 22.8%; AOPCP+MLS: 23.4%).

The inhibitory tone in the absence of adenosine is mediated through A1 receptors.

When TNAP and NT5E are inhibited and ENTs are blocked, adenosine can no longer leave the intracellular compartment and is no longer produced following extracellular AMP degradation. This should lead to the absence of adenosine in the extracellular medium. Yet in these conditions, a compound, which is not adenosine, is nevertheless capable to inhibit synaptic responses. The compound presumably accumulated due to TNAP and NT5E inhibition; it could thus be AMP, ADP or ATP. If such was the case, the inhibitory tone which is maintained in the presence of MLS-0038949 and AOPCP should remain in the presence of A1 receptor antagonists, as ADP and ATP acts through

P2 receptors and AMP is not supposed to be a purinergic receptor agonist. However, as shown in Fig 11, the residual inhibition was counteracted by CPT: blockade of A1 receptors in the presence of NT5E and TNAP inhibitors significantly increased response amplitude by 15.7 % compared to the condition where NT5E and TNAP only were inhibited (AOPCP + MLS = 96.7 % of control response amplitudes, Tukey's HSD, $p = 0.03$). Furthermore, response amplitude in the AOPCP + MLS + CPT condition was not significantly different from that in the CPT condition ($p = 0.28$). Up to that point, these results suggest that a compound, which is not adenosine, is nevertheless capable of inhibiting synaptic responses through A1 receptors. The results presented next indicate that this compound was AMP.

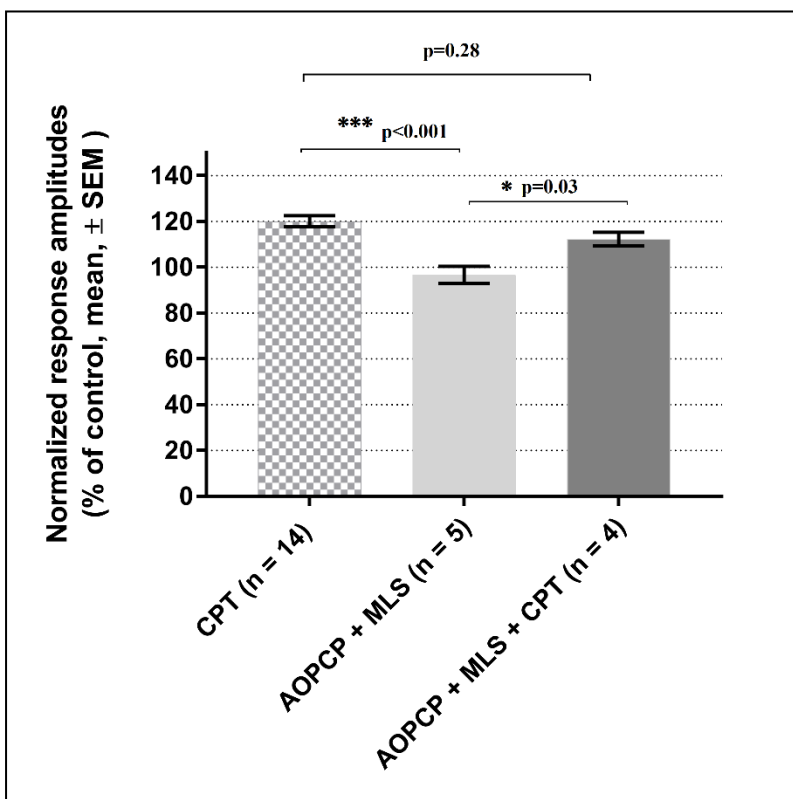


Figure 11: Blockade of A1 receptors by 0.2 μ M CPT counteracted the residual inhibition. n corresponds to the number of slices tested for each conditions.

AMP could act as an agonist of A1 receptors.

We tested the same conditions as above with the addition of 100 μ M AMP (fig 12). As shown above, AMP (100 μ M) inhibitory action was not counteracted by NT5E and/or TNAP inhibition. if AMP was able to act directly on A1 receptors, the inhibitory action of AMP in the presence of NT5E and TNAP inhibitor should be cancelled by CPT.

As shown earlier, 0.2 μ M CPT increased response amplitude by 20 % compared to control condition while response amplitude of 100 μ M AMP and 0.2 μ M CPT combination was not different from response amplitudes obtained with CPT alone (Tukey's HSD, $p= 0.99$). As with AMP alone, AMP and MLS combination decreased response amplitude by 76.3 % compared to the CPT condition (Tukey's HSD, $p < 0.001$). In figure 12, the addition of CPT to this combination increased response amplitude by 41.5 % compared to AMP + MLS combination. Although addition of CPT increased significantly response amplitude (Tukey's HSD, $p=0.004$), the latter did not reach the value obtained with 0.2 μ M CPT alone (Tukey's HSD, $p=0.04$).

The same observations can be made when NT5E only is inhibited in the presence of AMP (AMP + AOPCP). Response amplitude was decreased in the same way as found for AMP + MLS combination: 87 % decreased compared to CPT alone condition (Fig 12). Addition of CPT to this AMP and AOPCP combination led to a significant increase in response amplitude by 70 % (Tukey's HSD, $p < 0.001$). Moreover, response amplitude was no longer different from that obtained with CPT alone (Tukey's HSD, $p=0.74$).

When the two ectonucleotidases inhibitors were combined with 100 μ M AMP, response amplitude was decreased by 90% compared to 0.2 μ M CPT alone ($p < 0.001$). The addition of 0.2 μ M CPT to this combination led to an increased in response amplitude by 60% compared to CPT alone. However, response amplitude was significantly different from 0.2 μ M CPT condition (Tukey's HSD, $p = 0.012$) (Fig 12).

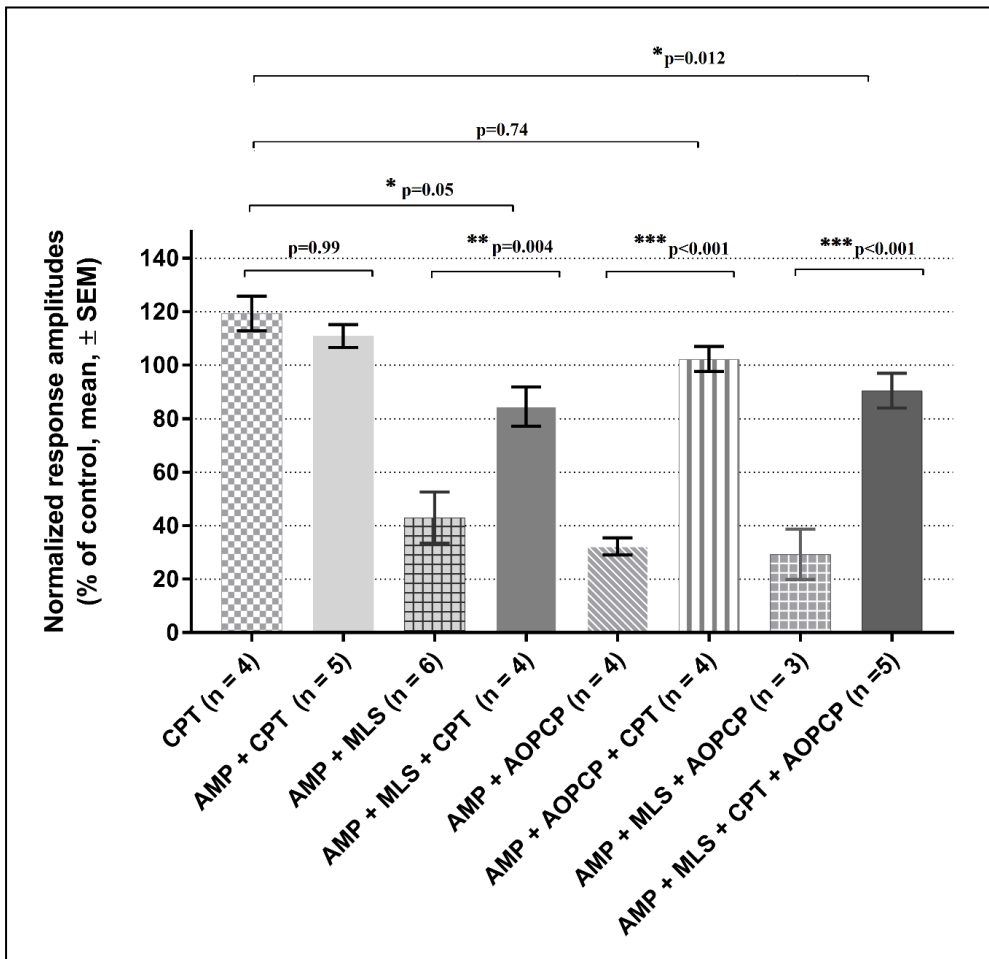


Figure 12: Blockade of A1 receptors partially suppressed exogenous AMP inhibitory effect in layer Ia of mouse piriform cortex. This graph represents population data on 35 experiments. n corresponds to the number of slices tested for each conditions.

Although not fully suppressed by CPT, we observed that most of AMP inhibitory effect – in the absence of adenosine – was counteracted in our experimental procedures. These results suggest that the compound, which is not adenosine, but that was capable of inhibiting synaptic responses through A1 receptors, is AMP. In other words, these results suggest that AMP can act as an agonist of A1 receptors.

DISCUSSION

We previously demonstrated that TNAP is involved in adenosine synthesis in the brain of the developing mouse using a metabolomic approach (Cruz et al., 2017). Indeed, adenosine concentrations were decreased by >80 % in knock-out mice for TNAP gene (*Akp2*^{-/-}) compared to WT and heterozygous mice. In the present study, we initially wanted to confirm the involvement of TNAP in adenosine synthesis using different models and approach: the present study was made using adult mice, we targeted a single cerebral region – the piriform cortex – and we used an electrophysiological and

pharmacological approaches. The main findings were that (1) the inhibition of TNAP and/or NT5E did not suppress endogenous presynaptic inhibition and exogenous AMP inhibitory effect although ectonucleotidase inhibitor were efficient; (2) the residual inhibition was not due to adenosine released from the intracellular milieu; (3) even when adenosine production was suppressed, the blockade of A1 receptors abolished the inhibition in the endogenous condition and suppressed most of the AMP inhibitory effect. The most likely explanation for these results is that AMP acts as an agonist of A1 receptors.

The first set of experiments confirmed that adenosine exert a depressant effect on synaptic transmission and that this depressant effect is mediated by A1 receptors. CPT, an A1 competitive receptor antagonist, produced per se a significant increase (+20 %) in response amplitude suggesting an action of endogenous adenosine in layer Ia of piriform cortex. Similar observations have been reported at corticostriatal synapses where application of 1 μ M CPT increase response amplitudes by 15 % (Calabresi et al., 1997). In piriform cortex, a +15% response increase was previously reported by McCabe and Scholfield (1985) after blocking endogenous adenosine intracellular signaling pathway. CPT also antagonized the inhibitory effect exerted by 100 μ M ATP and 100 μ M AMP. However, 100 μ M adenosine was not fully antagonized by 0.2 μ M CPT. We can hypothesize that A1 receptors binding sites were not fully blocked by 0.2 μ M CPT but this concentration was effective against AMP and ATP and is within the effective range reported in pharmacological studies (Dunwiddie et al., 1997 ; Nakata 1989).

Another explanation could be that of 100 μ M adenosine in the medium resulted in excessive adenosine concentration compared to CPT. Thus, adenosine could bind to the majority of A1 receptors binding sites and CPT could be less effective. The study of response kinetics when adenosine and CPT were simultaneously applied in the bath revealed that two types of responses can be observed over time. The first one is a fast decrease in response amplitude occurring within 2 minutes and the second one is a slow increase in response amplitude lasting 6 minutes before reaching a plateau. The fast decrease in response amplitude could be attributable to 100 μ M adenosine inhibitory effect. Indeed, response amplitude measured at 2 minutes is decreased by 44% which is comparable to the decrease observed when 100 μ M adenosine alone is applied in the bath (fig 13, supplementary data).

The second phase, where an increase in response amplitude was observed, could be due to the action of CPT. Indeed, in this phase, 35 % of response amplitude was restored (fig 13, supplementary data). This could be due to CPT that binds on available adenosine receptors binding sites or to CPT that

displaced some adenosine from its binding sites. Moreover, during the first 3 minutes of the recovery condition, we observed that response amplitude was increased by 24% compared to the control condition which is consistent with the effect observed in figure 2 when CPT is added alone in the medium. This phenomenon was also present with ATP and AMP but this time only a slight decrease was seen (occurring within a minute) compared to that observed with 100 μ M adenosine. This suggests that the degradation of ATP or AMP took more time than it takes for CPT to reach and bind A1 receptors.

Furthermore, in another experiment (fig 14, supplementary data), we decided to first add CPT instead of adding simultaneously CPT and adenosine in order to see if the fast adenosine effect observed above could be counteracted by CPT. Four minutes after the addition of 100 μ M adenosine in the medium, response amplitudes were decreased by 30% suggesting that adenosine was more competitive than CPT at binding A1 receptors.

We also tried using higher CPT concentration (0.5, 0.7 and 1 μ M) but at these concentration recovery often was not complete. With CPT 0.2 μ M, incomplete recovery occurred only once in 14 experiments. Next we wanted to determine whether TNAP was involved in the production of adenosine synthesis. Application of MLS-0038949, a specific TNAP inhibitor (Sergienko et al., 2009), failed to increase response amplitude in the endogenous condition and did not prevent AMP inhibition when exogenous AMP was added to the bath. Histochemical staining on brain slices revealed that MLS-0038949 was effective at inhibiting alkaline phosphatase activity. Moreover, we observed that response amplitude failed to recover in 8 out of 9 experiments (fig 4). The possibility that MLS-0038949 had a toxic effect was excluded by toxicity assays performed By David Magne and Anne Briolay on cells cultures.

To explain why synaptic inhibition remained with TNAP inhibitor alone or in combination of 100 μ M AMP, we formulated 5 hypothesis: (1) NT5E could be responsible for adenosine synthesis in piriform cortex; (2) another ectonucleotidase is responsible for adenosine synthesis in the brain; (3) adenosine could act on other adenosine receptors; (4) the residual inhibition observed was caused by the release of intracellular adenosine; (5) the residual inhibition observed is due to a compound which is not adenosine.

- (1) Neither the addition of AOPCP nor the combination of TNAP and AOPCP were able to counteract the inhibition in synaptic transmission although MLS-0038949 and AOPCP are effective at inhibiting TNAP and NT5E activities respectively.

(2) Street and collaborators (2013) showed that three ectonucleotidases act redundantly to generate adenosine in the spinal cord: TNAP, NT5E and prostatic acid phosphatase (PAP). Presence of PAP in piriform cortex has not been reported but a recent study in hippocampus showed that PAP is located in the compartment of interneurons (Nousiainen et al., 2014), ruling out the possibility that PAP is responsible for the hydrolysis of AMP to adenosine at the LOT-layer 1a synapse.

(3) Another explanation could be that adenosine act on adenosine receptor different from A1 (A2a, A2b or A3). However, currently, no study examined the distribution of other adenosine receptors (A2a, A2b and A3) in the mouse piriform cortex, we cannot exclude this hypothesis. However, the complete antagonism of AMP and ATP effects by CPT indicates that adenosine issued from their degradation acted solely through A1 receptors.

(4) Since adenosine could be released by specific transporters (ENTs; Lovatt et al. 2012; Wall and Dale), we next thought that the residual inhibition observed in the presence of NT5E and TNAP inhibitors could be due to the release of intracellular adenosine in response to an imbalance of adenosine concentrations between the intra- and the extracellular compartments. The blockade of adenosine transport by 10 µM NBTI, an inhibitor of ENT transporters, did not exert any effect on response amplitude. Thus residual inhibition was not due to intracellular adenosine released in extracellular medium.

(5) Finally we hypothesized that AMP could act as an agonist of A1 receptors. This was prompted by the work of Rittiner and collaborators (2012) who showed that AMP can activate A1 receptors in embryonic neurons culture and in transfected HEK cells. Interestingly, they showed that this AMP agonism was specific to A1 receptors and did not work for A2 receptors. In our conditions, the concurrent inhibition of AMP hydrolysis pathways and blockade of A1 receptors led to an increase in response amplitude equivalent to that observed when A1 receptors were blocked, although no adenosine should have been present. The inhibitory action of exogenous AMP, which persisted when the AMP hydrolysis pathways were blocked, was largely suppressed when A1 receptors were blocked, although no adenosine should have been present. These results are consistent with AMP acting directly on A1 receptors.

A concurrent hypothesis was that the compound that accumulated when TNAP and NT5E were inhibited is ATP. ATP could exert presynaptic inhibition through P2Y purinergic receptors (Guzman and Gerevich, 2016). Accumulation of ATP could thus be responsible for the inhibition (about 30%)

that remained in the last experiment presented above. Among four P2Y receptors that are activated by ATP (P2Y1, P2Y2, P2Y4 and P2Y6), only P2Y2 and P2Y4 have been localized in the piriform cortex (Namba et al., 2010; Song et al., 2011). To determine whether P2Y receptor activation could lead to the remaining inhibition in our experimental conditions, P2Y receptors were blocked by using broad-spectrum antagonists of P2 receptors: Cibacron-Blue 3GA, which is an isomer of Reactive blue 2 (30 μ M), and suramin (100 μ M).

As shown above in Figure 15, ATP reduced synaptic response amplitude by 45% compared to the control condition (100 %). CB did not suppress this inhibition, suggesting that ATP inhibitory effect was consecutive to its hydrolysis in adenosine by ectonucleotidases. The inhibition of TNAP and NT5E activity and the blockade of A1 receptors by CPT and PY2 receptors by CB in the presence of ATP 100 μ M should restore response amplitude observed with CPT 0.2 μ M alone. Although response amplitude was increased by 19% in this condition compared to the condition of ATP 100 μ M alone (ATP 100 μ M = 56.5 % vs ATP+AOPCP+MLS+CPT+CB = 75.5 %), response amplitude was still significantly different from that observed with CPT alone (Fig 15, supplementary data). This suggested that inhibitory effect of ATP was mediated by receptors insensitive to Cibacron Blue.

The addition of suramin, (100 μ M or 50 μ M) in addition to CB, should have block P2 receptors and a fortiori ATP inhibitory effect. Contrary to our expectations, response amplitude was even more decreased by suramine (fig 15, supplementary data). On the other hand, it has been shown that suramin inhibit glutamatergic synaptic transmission (Motin and Bennett, 1995; Nakasawa et al., 1995) at concentration that are effective for inhibiting P2 receptors. This could be a reason why the addition of 50 and 100 μ M suramin even more decreased response amplitude in our conditions.

In summary, although our study does not formally establish that TNAP and NT5E contribute to adenosine synthesis in adult mouse piriform cortex *in vitro*, our electrophysiological and pharmacological study revealed that inhibiting of adenosine synthesis does not prevent inhibition of AMP through A1 receptor, suggesting that AMP acts as an agonist of this receptor subtype.

SUPPLEMENTARY DATA

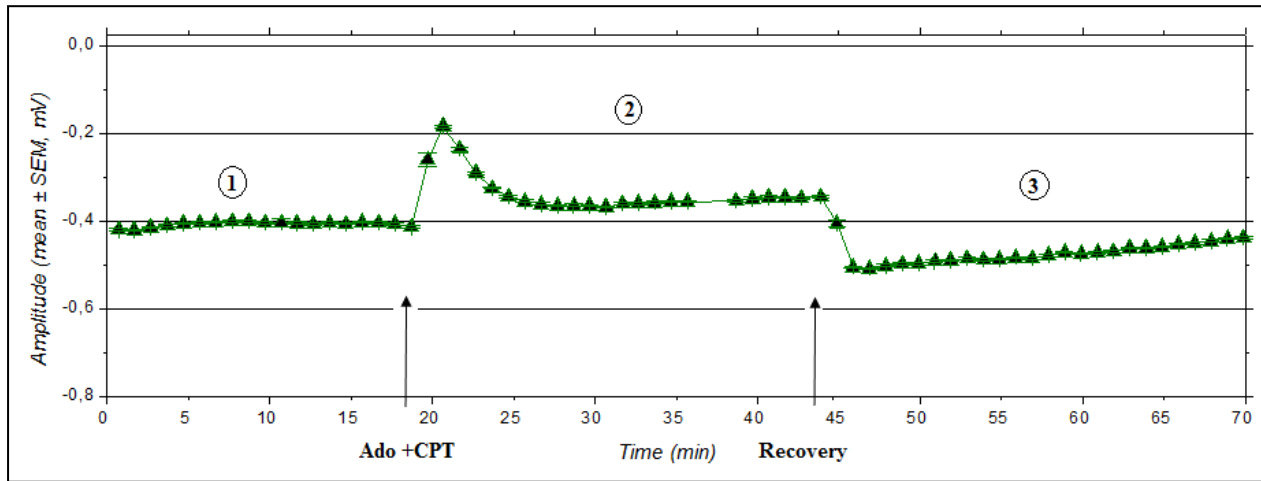


Figure 13: Response amplitude recorded over the stimulation time of 1) control condition, 2) Adenosine + CPT and 3) recovery condition in one mouse. The first arrow represents the time point of adding adenosine + CPT in the medium. The second arrow represents the time point of beginning the recovery condition. 25 minutes recording were tested for (2) and (3) is this experiment.

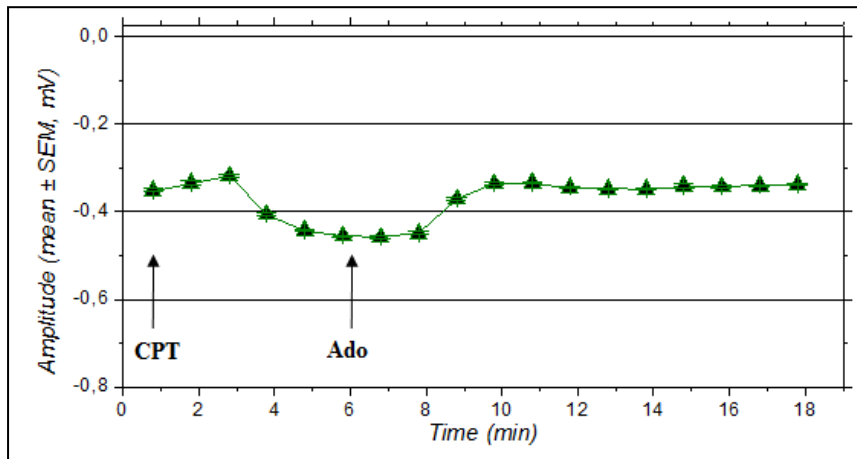


Figure 14: Response amplitude recorded over the stimulation time. The first arrow represents the time point of adding 0.2 μ M CPT alone in the medium. The second arrow represents the time point of 100 μ M adenosine addition still in presence of 0.2 μ M CPT.

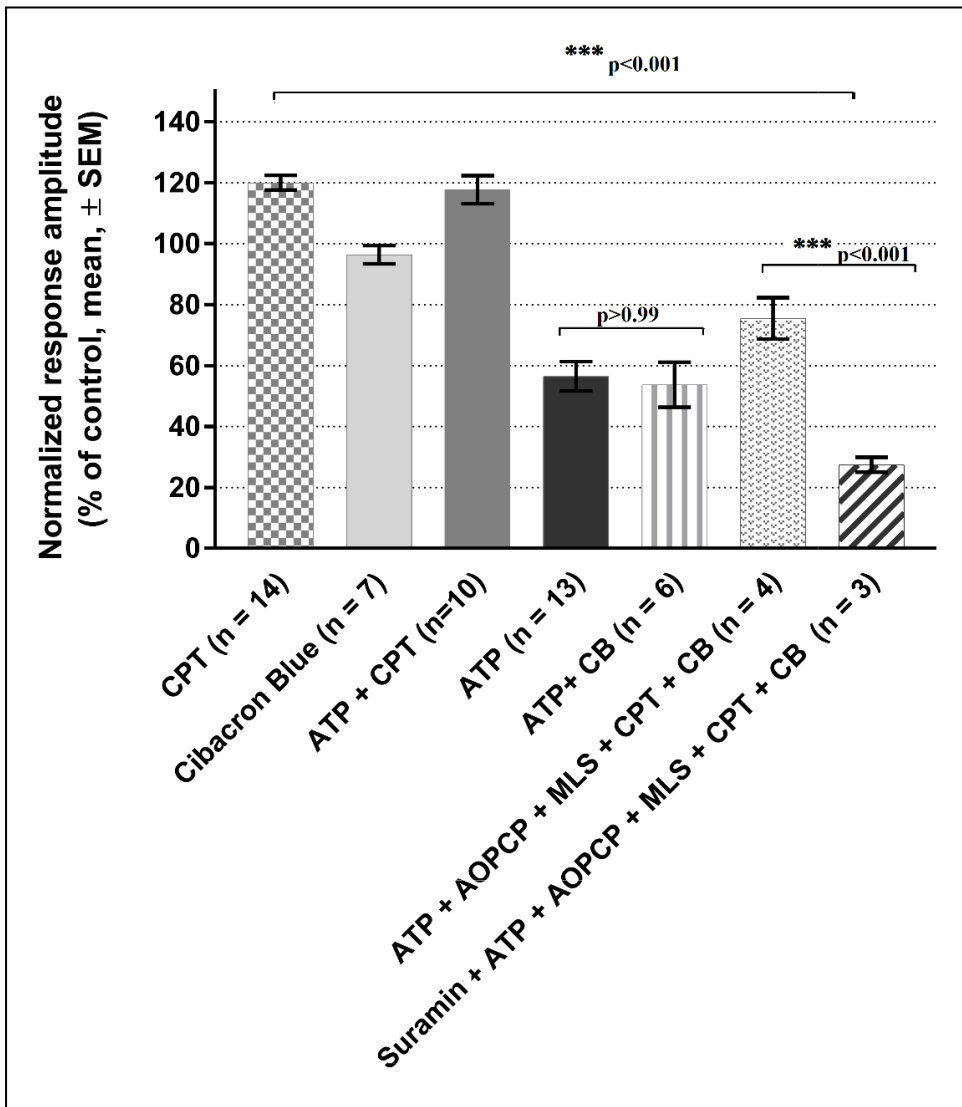


Figure 15: Effect of non-selective P2 receptors antagonists on response amplitudes. Addition of Cibacron Blue and suramine failed to restore response amplitudes.

As illustrated in figure 15, addition of 30 μ M Cibacron Blue did not change response amplitudes compared to the control condition (CB= 96.4%, Tukey's HSD, $p=0.98$). When added with 100 μ M ATP, ATP inhibitory effect was not suppressed by Cibacron Blue (ATP 100 μ M = 56.5 % of control response amplitudes, ATP 100 μ M + CB 30 μ M = 53.7 % of control response amplitudes; $p > 0.99$).

In order to determine if ATP could be responsible for the “remaining inhibition” observed in figure 13, activity of ectonucleotidases (TNAP and NT5E) was blocked, as well as adenosine A1 receptors to avoid possibly AMP inhibitory effect through A1R activation. In addition, P2Y receptors were also blocked by Cibacron Blue in combination with 100 μ M ATP. We also expected that response amplitudes elicited by the simultaneous blockade of P2Y receptors, A1 receptors and inhibition of ectonucleotidase activity would be equivalent to those observed with only 0.2 μ M CPT. In these conditions, response amplitudes were increased by 19 % compared to 100 μ M ATP alone (ATP 100

μM = 56.5 % vs ATP+AOPCP+MLS+CPT+CB = 75.5 %) but this increase was not significant (Tukey's HSD, p=0.12).

Then, when suramin (100 μM) was added to the combination ATP+AOPCP+MLS+CPT+CB, we observed 48 % reduction of response amplitude (ATP+AOPCP+MLS+CPT+CB = 75.5 % versus ATP+AOPCP+MLS+CPT+CB+suramin = 27.5%; Tukey's HSD, p < 0.001). The same decrease in response amplitude was observed with the addition of 50 μM suramin (data not shown).

REFERENCES

- Abbracchio, Maria P., Geoffrey Burnstock, Alexei Verkhratsky, and Herbert Zimmermann. 2009. "Purinergic Signalling in the Nervous System: An Overview." *Trends in Neurosciences* 32 (1): 19–29. doi:10.1016/j.tins.2008.10.001.
- Broch, Ole Jacob, and Per Magne Ueland. 1980. "Regional and Subcellular Distribution of S-Adenosylhomocysteine Hydrolase in the Adult Rat Brain." *Journal of Neurochemistry* 35 (2): 484–488.
- Brun-Heath, Isabelle, Myriam Ermonval, Elodie Chabrol, Jinsong Xiao, Miklós Palkovits, Ruth Lyck, Florence Miller, Pierre-Olivier Couraud, Etienne Mornet, and Caroline Fonta. 2011. "Differential Expression of the Bone and the Liver Tissue Non-Specific Alkaline Phosphatase Isoforms in Brain Tissues." *Cell and Tissue Research* 343 (3): 521–36. doi:10.1007/s00441-010-1111-4.
- Burger, Richard M., and John M. Lowenstein. 1975. "5'-Nucleotidase from Smooth Muscle of Small Intestine and from Brain. Inhibition by Nucleotides." *Biochemistry* 14 (11): 2362–2366.
- Burnstock, Geoffrey, and Charles Kennedy. 1986. "A Dual Function for Adenosine 5'-triphosphate in the Regulation of Vascular Tone. Excitatory Cotransmitter with Noradrenaline from Perivascular Nerves and Locally Released Inhibitory Intravascular Agent." *Circulation Research* 58 (3): 319–330.
- Calabresi, Paolo, Diego Centonze, Antonio Pisani, and Giorgio Bernardi. 1997. "Endogenous Adenosine Mediates the Presynaptic Inhibition Induced by Aglycemia at Corticostriatal Synapses." *Journal of Neuroscience* 17 (12): 4509–4516.
- Cass, Carol E., James D. Young, Stephen A. Baldwin, Miguel A. Cabrita, Kathryn A. Graham, Mark Griffiths, Lori L. Jennings, et al. 2002. "Nucleoside Transporters of Mammalian Cells."
- Ciancaglini, Pietro, Manisha C Yadav, Ana Maria Sper Simão, Sonoko Narisawa, João Martins Pizauro, Colin Farquharson, Marc F Hoylaerts, and José Luis Millán. 2009. "Kinetic Analysis of Substrate Utilization by Native and TNAP-, NPP1- or PHOSPHO1-Deficient Matrix Vesicles." *Journal of Bone and Mineral Research*, October, 091029140456050-37. doi:10.1359/jbm.091023.
- Cruz, Thomas, Marie Gleizes, Stéphane Balyssac, Etienne Mornet, Grégory Marsal, José Luis Millán, Myriam Malet-Martino, Lionel G Nowak, Véronique Gilard, and Caroline Fonta. 2017. "Identification of

Altered Brain Metabolites Associated with TNAP Activity in a Mouse Model of Hypophosphatasia Using Untargeted NMR-Based Metabolomics Analysis.” *Journal of Neurochemistry* 140 (6): 919–40. doi:10.1111/jnc.13950.

Cusack, N. J., J. D. Pearson, and J. L. Gordon. 1983. “Stereoselectivity of Ectonucleotidases on Vascular Endothelial Cells.” *Biochemical Journal* 214 (3): 975–981.

Díez-Zaera, María, Juan Ignacio Díaz-Hernández, Elena Hernández-Álvarez, H. Zimmermann, Miguel Díaz-Hernández, and María Teresa Miras-Portugal. 2011. “Tissue-Nonspecific Alkaline Phosphatase Promotes Axonal Growth of Hippocampal Neurons.” *Molecular Biology of the Cell* 22 (7): 1014–1024.

Dolphin, A.C., and E.R. Archer. 1983. “An Adenosine Agonist Inhibits and a Cyclic AMP Analogue Enhances the Release of Glutamate but Not GABA from Slices of Rat Dentate Gyrus.” *Neuroscience Letters* 43 (1): 49–54. doi:10.1016/0304-3940(83)90127-1.

Dorai, D. Thambi, and B. K. Bachhawat. 1977. “PURIFICATION AND PROPERTIES OF BRAIN ALKALINE PHOSPHATASE.” *Journal of Neurochemistry* 29 (3): 503–12. doi:10.1111/j.1471-4159.1977.tb10699.x.

Drury, A. N., and A. v Szent-Györgyi. 1929. “The Physiological Activity of Adenine Compounds with Especial Reference to Their Action upon the Mammalian Heart.” *The Journal of Physiology* 68 (3): 213–237.

Dunwiddie, Thomas V., Lihong Diao, and William R. Proctor. 1997. “Adenine Nucleotides Undergo Rapid, Quantitative Conversion to Adenosine in the Extracellular Space in Rat Hippocampus.” *The Journal of Neuroscience* 17 (20): 7673.

Fonta, C. 2004. “Areal and Subcellular Localization of the Ubiquitous Alkaline Phosphatase in the Primate Cerebral Cortex: Evidence for a Role in Neurotransmission.” *Cerebral Cortex* 14 (6): 595–609. doi:10.1093/cercor/bhh021.

Fonta, Caroline, and Michel Imbert. 2002. “Vascularization in the Primate Visual Cortex during Development.” *Cerebral Cortex* 12 (2): 199–211.

Fonta, Caroline, Laszlo Negyessy, Luc Renaud, and Pascal Barone. 2005. “Postnatal Development of Alkaline Phosphatase Activity Correlates with the Maturation of Neurotransmission in the Cerebral Cortex.” *The Journal of Comparative Neurology* 486 (2): 179–96. doi:10.1002/cne.20524.

Gillespie, J. H. 1934. “The Biological Significance of the Linkages in Adenosine Triphosphoric Acid.” *The Journal of Physiology* 80 (4): 345–359.

Gleizes, Marie, Simon P. Perrier, Caroline Fonta, and Lionel G. Nowak. 2017. “Prominent Facilitation at Beta and Gamma Frequency Range Revealed with Physiological Calcium Concentration in Adult Mouse Piriform Cortex in Vitro.” Edited by Giuseppe Gangarossa. *PLOS ONE* 12 (8): e0183246. doi:10.1371/journal.pone.0183246.

Guzman, Segundo J., and Zoltan Gerevich. 2016. “P2Y Receptors in Synaptic Transmission and Plasticity: Therapeutic Potential in Cognitive Dysfunction.” *Neural Plasticity* 2016: 1–12. doi:10.1155/2016/1207393.

Hanics, János, János Barna, Jinsong Xiao, José Luis Millán, Caroline Fonta, and László Négyessy. 2012. “Ablation of TNAP Function Compromises Myelination and Synaptogenesis in the Mouse Brain.” *Cell and Tissue Research* 349 (2): 459–71. doi:10.1007/s00441-012-1455-z.

Kermér, Vanessa, Mathias Ritter, Boris Albuquerque, Christoph Leib, Matthias Stanke, and Herbert Zimmermann. 2010. “Knockdown of Tissue Nonspecific Alkaline Phosphatase Impairs Neural Stem Cell Proliferation and Differentiation.” *Neuroscience Letters* 485 (3): 208–11. doi:10.1016/j.neulet.2010.09.013.

Kostopoulos, George K., and John W. Phillis. 1977. “Purinergic Depression of Neurons in Different Areas of the Rat Brain.” *Experimental Neurology* 55 (3): 719–724.

Kulesskaya, Natalia, Vootele V?ikar, Marjaana Peltola, Gennady G. Yegutkin, Marko Salmi, Sirpa Jalkanen, and Heikki Rauvala. 2013. “CD73 Is a Major Regulator of Adenosinergic Signalling in Mouse Brain.” Edited by Tobias Eckle. *PLoS ONE* 8 (6): e66896. doi:10.1371/journal.pone.0066896.

Kuroda, Yoichiro, Mitsuo Saito, and Kazuo Kobayashi. 1976. “Concomitant Changes in Cyclic AMP Level and Postsynaptic Potentials of Olfactory Cortex Slices Induced by Adenosine Derivatives.” *Brain Research* 109 (1): 196–201.

Langer, D., Y. Ikehara, H. Takebayashi, R. Hawkes, and H. Zimmermann. 2007. “The Ectonucleotidases Alkaline Phosphatase and Nucleoside Triphosphate Diphosphohydrolase 2 Are Associated with Subsets of Progenitor Cell Populations in the Mouse Embryonic, Postnatal and Adult Neurogenic Zones.” *Neuroscience* 150 (4): 863–79. doi:10.1016/j.neuroscience.2007.07.064.

Langer, David, Klaus Hammer, Patrycja Koszalka, Jürgen Schrader, Simon Robson, and Herbert Zimmermann. 2008. “Distribution of Ectonucleotidases in the Rodent Brain Revisited.” *Cell and Tissue Research* 334 (2): 199–217. doi:10.1007/s00441-008-0681-x.

Lovatt, D., Q. Xu, W. Liu, T. Takano, N. A. Smith, J. Schnermann, K. Tieu, and M. Nedergaard. 2012a. “Neuronal Adenosine Release, and Not Astrocytic ATP Release, Mediates Feedback Inhibition of Excitatory Activity.” *Proceedings of the National Academy of Sciences* 109 (16): 6265–70. doi:10.1073/pnas.1120997109.

Maitre, Michel, Lucien Ciesielski, Alice Lehmann, Eliane Kempf, and Paul Mandel. 1974. “Protective Effect of Adenosine and Nicotinamide against Audiogenic Seizure.” *Biochemical Pharmacology* 23 (20): 2807–2816.

McCabe, J., and C. N. Scholfield. 1985. “Adenosine-Induced Depression of Synaptic Transmission in the Isolated Olfactory Cortex: Receptor Identification.” *Pflügers Archiv European Journal of Physiology* 403 (2): 141–145

Motin, L., and M. R. Bennett. 1995. “Effect of P2-Purinoceptor Antagonists on Glutamatergic Transmission in the Rat Hippocampus.” *British Journal of Pharmacology* 115 (7): 1276–1280.

Nakata, H. 1989. “Purification of A1 Adenosine Receptor from Rat Brain Membranes.” *Journal of Biological Chemistry* 264 (28): 16545–16551.

- Nakazawa, K., K. Inoue, K. Ito, and S. Koizumi. 1995. "Inhibition by Suramin and Reactive Blue 2 of GABA and Glutamate Receptor Channels in Rat Hippocampal Neurons." *Naunyn-Schmiedeberg's Archives of Pharmacology* 351 (2): 202–208.
- Namba, Kazunori, Tokiko Suzuki, and Hiroyasu Nakata. 2010. "Immunogold Electron Microscopic Evidence of in Situ Formation of Homo- and Heteromeric Purinergic Adenosine A1 and P2Y2 Receptors in Rat Brain." *BMC Research Notes* 3 (1): 323. <https://doi.org/10.1186/1756-0500-3-323>.
- Narisawa, Sonoko, Nils Fröhlander, and José Luis Millán. 1997. "Inactivation of Two Mouse Alkaline Phosphatase Genes and Establishment of a Model of Infantile Hypophosphatasia." *Developmental Dynamics* 208 (3): 432–46. doi:10.1002/(SICI)1097-0177(199703)208:3<432::AID-AJA13>3.0.CO;2-1.
- Narisawa, Sonoko, Hideaki Hasegawa, Keiichi Watanabe, and José Luis Millán. 1994. "Stage-Specific Expression of Alkaline Phosphatase during Neural Development in the Mouse." *Developmental Dynamics* 201 (3): 227–235.
- Nousiainen, Heidi O., Ileana B. Quintero, Timo T. Myöhänen, Vootele Voikar, Jelena Mijatovic, Mikael Segerstråle, Annakaisa M. Herrala, et al. 2014. "Mice Deficient in Transmembrane Prostatic Acid Phosphatase Display Increased GABAergic Transmission and Neurological Alterations." Edited by Anna-Leena Sirén. *PLoS ONE* 9 (5): e97851. doi:10.1371/journal.pone.0097851.
- Phillis, John W., George K. Kostopoulos, and James J. Limacher. 1975. "A Potent Depressant Action of Adenine Derivatives on Cerebral Cortical Neurones." *European Journal of Pharmacology* 30 (1): 125–129.
- Ralevic, Vera, and Geoffrey Burnstock. 1998. "Receptors for Purines and Pyrimidines." *Pharmacological Reviews* 50 (3): 413.
- Rittiner, Joseph E., Ilia Korboukh, Emily A. Hull-Ryde, Jian Jin, William P. Janzen, Stephen V. Frye, and Mark J. Zylka. 2012. "AMP Is an Adenosine A₁ Receptor Agonist." *Journal of Biological Chemistry* 287 (8): 5301–9. doi:10.1074/jbc.M111.291666.
- Robson, Simon C., Jean Sévigny, and Herbert Zimmermann. 2006. "The E-NTPDase Family of Ectonucleotidases: Structure Function Relationships and Pathophysiological Significance." *Purinergic Signalling* 2 (2): 409–30. doi:10.1007/s11302-006-9003-5.
- Schoen, Siegfried W., and Georg W. Kreutzberg. 1997. "5'-Nucleotidase Enzyme Cytochemistry as a Tool for Revealing Activated Glial Cells and Malleable Synapses in CNS Development and Regeneration." *Brain Research Protocols* 1 (1): 33–43.
- Scholfield, C. N. 1978. "Depression of Evoked Potentials in Brain Slices by Adenosine Compounds." *British Journal of Pharmacology* 63 (2): 239–244.
- Sergienko, E., Y. Su, X. Chan, B. Brown, A. Hurder, S. Narisawa, and J. L. Millan. 2009. "Identification and Characterization of Novel Tissue-Nonspecific Alkaline Phosphatase Inhibitors with Diverse Modes of Action." *Journal of Biomolecular Screening* 14 (7): 824–37. doi:10.1177/1087057109338517.

Song, Xianmin, Wei Guo, Qiang Yu, Xiaofeng Liu, Zhenghua Xiang, Cheng He, and Geoffrey Burnstock. 2011. "Regional Expression of P2Y4 Receptors in the Rat Central Nervous System." *Purinergic Signalling* 7 (4): 469–88. <https://doi.org/10.1007/s11302-011-9246-7>.

Stefan, Cristiana, Silvia Jansen, and Mathieu Bollen. 2005. "NPP-Type Ectophosphodiesterases: Unity in Diversity." *Trends in Biochemical Sciences* 30 (10): 542–50. doi:10.1016/j.tibs.2005.08.005.

Street, S. E., N. J. Kramer, P. L. Walsh, B. Taylor-Blake, M. C. Yadav, I. F. King, P. Vihko, R. M. Wightman, J. L. Millan, and M. J. Zylka. 2013. "Tissue-Nonspecific Alkaline Phosphatase Acts Redundantly with PAP and NT5E to Generate Adenosine in the Dorsal Spinal Cord." *Journal of Neuroscience* 33 (27): 11314–22. doi:10.1523/JNEUROSCI.0133-13.2013.

Ward, Jeffrey L., Azeem Sherli, Zhi-Ping Mo, and Chung-Ming Tse. 2000. "Kinetic and Pharmacological Properties of Cloned Human Equilibrative Nucleoside Transporters, ENT1 and ENT2, Stably Expressed in Nucleoside Transporter-Deficient PK15 Cells: ENT2 EXHIBITS A LOW AFFINITY FOR GUANOSINE AND CYTIDINE BUT A HIGH AFFINITY FOR INOSINE." *Journal of Biological Chemistry* 275 (12): 8375–81. doi:10.1074/jbc.275.12.8375.

Waymire, Katrina G., J. Dennis Mahuren, J. Michael Jaje, Tomas R. Guilarte, Stephen P. Coburn, and Grant R. MacGregor. 1995. "Mice Lacking Tissue Non-Specific Alkaline Phosphatase Die from Seizures due to Defective Metabolism of Vitamin B-6." *Nat Genet* 11 (1): 45–51. doi:10.1038/ng0995-45.

Yamamoto, C., and H. McIlwain. 1966. "Electrical Activities in Thin Sections from the Mammalian Brain Maintained in Chemically-Defined Media in Vitro." *Journal of Neurochemistry* 13 (12): 1333–1343.

Yegutkin, Gennady G. 2008. "Nucleotide- and Nucleoside-Converting Ectoenzymes: Important Modulators of Purinergic Signalling Cascade." *Biochimica et Biophysica Acta (BBA) - Molecular Cell Research* 1783 (5): 673–94. doi:10.1016/j.bbamcr.2008.01.024.

Zhang, Dali, Wei Xiong, Stephanie Chu, Chao Sun, Benedict C. Albensi, and Fiona E. Parkinson. 2012. "Inhibition of Hippocampal Synaptic Activity by ATP, Hypoxia or Oxygen-Glucose Deprivation Does Not Require CD73." Edited by Steven Barnes. *PLoS ONE* 7 (6): e39772. doi:10.1371/journal.pone.0039772.

Zimmermann, Herbert. 1999. "Two Novel Families of Ectonucleotidases: Molecular Structures, Catalytic Properties and a Search for Function." *Trends in Pharmacological Sciences* 20 (6): 231–236.

Zimmermann, Herbert. 2006. "Nucleotide Signaling in Nervous System Development." *Pflügers Archiv - European Journal of Physiology* 452 (5): 573–88. doi:10.1007/s00424-006-0067-4.

C. Prominent facilitation at beta and gamma frequency range revealed with physiological calcium concentration in adult mouse piriform cortex in vitro. Marie Gleizes, Simon P. Perrier Caroline Fonta et Lionel G. Nowak. PLoS One. 2017;12(8):e0183246.

1. Résumé

Cette étude était une étape préliminaire nécessaire à la validation de nos conditions expérimentales des études électrophysiologiques que nous avons réalisées (article B et article D). En effet, nos enregistrements électrophysiologiques sont réalisés sur des tranches de cerveaux de souris qui sont maintenues dans un liquide céphalo-rachidien artificiel (LCRa) et dont la composition est proche de celle retrouvée *in vivo* chez le rongeur. Notamment la concentration de calcium dans le LCRa que nous utilisons est de 1, 1 mM alors que dans la plupart des études en électrophysiologie la concentration de calcium utilisée est comprise entre 2 et 2.5 mM. La transmission synaptique et la plasticité synaptique étant des phénomènes majoritairement dépendants du calcium, alors les mécanismes de facilitation et dépression synaptique pourraient être différents en fonction de la concentration de calcium.

Dans cette étude, nous avons examiné l'influence de deux concentrations de calcium (1, 1 mM et 2, 2 mM) sur le phénomène de plasticité synaptique à court terme (STP) dans la couche I du cortex piriforme de souris adultes. Nous avons réalisé des enregistrements électrophysiologiques extracellulaires et nous avons appliqué des stimulations électriques répétées avec une large gamme de fréquences qui couvre la gamme des oscillations cérébrales (fréquence entre 3.125 et 100 Hz) au niveau du tractus olfactif latéral. La plupart des études de la plasticité synaptique utilisent des stimulations par paire de pulses qui ne sont pas forcément informatives d'un point de vue du décours temporel de la plasticité. Afin de déterminer le ou les différents mécanismes (facilitation et dépression) impliqués dans la plasticité synaptique, notre protocole de stimulation était composé de trains de stimulation de 5 pulses, ce qui permet d'avoir une dynamique temporelle. De plus, un modèle phénoménologique de la plasticité à court terme adapté à nos données a permis de calculer les constantes de temps de récupération de facilitation et de

dépression et ainsi de déterminer la contribution de ces deux mécanismes en fonction de la concentration de calcium utilisée.

Nos résultats ont révélé que l'augmentation de la concentration de calcium augmente non seulement la transmission synaptique mais modifie également les caractéristiques de la STP. Le maximum de facilitation observé à 25 Hz à une concentration de 1,1 mM de calcium est déplacé vers des fréquences plus basses (12,5 Hz) lorsque l'on augmente la concentration de calcium à 2,2 mM. Par ailleurs, le modèle suggère que les résultats expérimentaux obtenus à 1,1 mM de calcium s'expliquent par l'interaction de trois mécanismes : une facilitation à court terme et deux dépressions à court terme (une dépression à court terme rapide (< à 20 ms) et une dépression lente (140 ms)). Lorsque la concentration de calcium est augmentée à 2.2 mM, la dépression lente est davantage sollicitée au détriment de la facilitation. Tous ces résultats montrent que, la contribution des mécanismes de facilitation et de dépression dans la plasticité à court terme est dépendante des conditions expérimentales : à 2.2 mM de calcium, la dépression à court terme est surestimée et la facilitation à court terme est sous-estimée relativement à une concentration de calcium physiologique d'environ 1 mM.

2. Article

RESEARCH ARTICLE

Prominent facilitation at beta and gamma frequency range revealed with physiological calcium concentration in adult mouse piriform cortex *in vitro*

Marie Gleizes^{1,2}, Simon P. Perrier^{1,2}, Caroline Fonta^{1,2*}, Lionel G. Nowak^{1,2*}

1 Centre de Recherche Cerveau et Cognition, Université de Toulouse, Toulouse, France, **2** Unité Mixte de Recherche 5549, Centre National de la Recherche Scientifique, Toulouse, France

* lionel.nowak@cnrs.fr (LGN); caroline.fonta@cnrs.fr (CF)



Abstract

Neuronal activity is characterized by a diversity of oscillatory phenomena that are associated with multiple behavioral and cognitive processes, yet the functional consequences of these oscillations are not fully understood. Our aim was to determine whether and how these different oscillatory activities affect short-term synaptic plasticity (STP), using the olfactory system as a model. In response to odorant stimuli, the olfactory bulb displays a slow breathing rhythm as well as beta and gamma oscillations. Since the firing of olfactory bulb projecting neurons is phase-locked with beta and gamma oscillations, structures downstream from the olfactory bulb should be driven preferentially at these frequencies. We examined STP exhibited by olfactory bulb inputs in slices of adult mouse piriform cortex maintained *in vitro* in an *in vivo*-like ACSF (calcium concentration: 1.1 mM). We replaced the presynaptic neuronal firing rate by repeated electrical stimulation (frequency between 3.125 and 100 Hz) applied to the lateral olfactory tract. Our results revealed a considerable enhancement of postsynaptic response amplitude for stimulation frequencies in the beta and gamma range. A phenomenological model of STP fitted to the data suggests that the experimental results can be explained by the interplay between three mechanisms: a short-term facilitation mechanism (time constant \approx 160 msec), and two short-term depression mechanisms (recovery time constants <20 msec and \approx 140 msec). Increasing calcium concentration (2.2 mM) resulted in an increase in the time constant of facilitation and in a strengthening of the slowest depression mechanism. As a result, response enhancement was reduced and its peak shifted toward the low beta and alpha ranges while depression became predominant in the gamma band. Using environmental conditions corresponding to those that prevail *in vivo*, our study shows that STP in the lateral olfactory tract to layer Ia synapse allows amplification of olfactory bulb inputs at beta and gamma frequencies.

OPEN ACCESS

Citation: Gleizes M, Perrier SP, Fonta C, Nowak LG (2017) Prominent facilitation at beta and gamma frequency range revealed with physiological calcium concentration in adult mouse piriform cortex *in vitro*. PLoS ONE 12(8): e0183246. <https://doi.org/10.1371/journal.pone.0183246>

Editor: Giuseppe Gangarossa, University Paris Diderot, FRANCE

Received: April 18, 2017

Accepted: August 1, 2017

Published: August 18, 2017

Copyright: © 2017 Gleizes et al. This is an open access article distributed under the terms of the [Creative Commons Attribution License](#), which permits unrestricted use, distribution, and reproduction in any medium, provided the original author and source are credited.

Data Availability Statement: All relevant data are within the paper and its Supporting Information files.

Funding: This research was supported by CNRS and by University of Toulouse 3 (IDEX transversalité 2015). The funder had no role in study design, data collection and analysis, decision to publish, or preparation of the manuscript.

Competing interests: The authors have declared that no competing interests exist.

Introduction

EEG and intracerebral LFP recordings have disclosed a variety of oscillatory phenomena in the brain. Although the precise ranges differ depending on the species and structure examined, several types of oscillations with characteristic frequencies and dynamic features have been associated with different sleep/waking states and with various perceptual and cognitive processes. For example, non-REM sleep is characterized by the presence of a slow sleep rhythm (< 1Hz), of delta oscillations (1–4 Hz) and short epochs of sleep spindles (11–15 Hz) [1–3]. Theta waves (typically 6–12 Hz in awake rodents) have been mostly studied in the hippocampus where they occur during a variety of behaviors as well as during REM sleep [4, 5]. Alpha waves (8–12 Hz), most prominent in visual cortex, are associated with rest [6] and may be involved in awareness and attention [7]. Beta waves (between 12 and 25–35 Hz) are most salient in sensorimotor cortex [8–10] and may also be involved in attentional processes [11, 12]. Gamma oscillations, with frequencies larger than 25–35 Hz, are typically observed during the processing of sensory stimuli in visual [13–16], somesthetic [17, 18] and auditory cortices [19, 20] as well as during various cognitive tasks involving awareness, attention and memory (reviewed in: [21, 22]).

Although they are clearly associated with a variety of perceptual and cognitive processes, the functional significance of oscillations, in particular beta and gamma oscillations, has remained elusive. At one extreme, it has been proposed that oscillations are merely an epiphenomenon of the functioning of cerebral networks (e. g., [23–25]) while at the other, it has been proposed that oscillations play prominent roles in feature binding, awareness and/or conscious perception (e. g., [22, 26–28]).

Here we adopted a “bottom-up” approach to try to learn more on the functional impacts of oscillations. More precisely, we examined the *consequences* of oscillatory activity on synaptic transmission. Indeed, synaptic transmission is not steady: on a short time range (e. g., less than a few minutes) postsynaptic responses usually display reversible dynamic changes, referred to as short-term plasticity (STP). Synaptic efficacy can thus be modulated by two broad types of STP: short-term facilitation (STF) and short-term depression (STD) (e. g., [29]). Several STF and STD mechanisms have been disclosed, each characterized by different time courses, which range from a few milliseconds up to hundreds of seconds, and may coexist in the same synapse. Thus, under the proviso that presynaptic action potentials are phase-locked with oscillations, we expected features of STP in postsynaptic neurons to change depending on the oscillatory frequency in the presynaptic structures and neurons.

We examined STP in the piriform cortex, one of the main relays of olfactory information after integration in the olfactory bulb (e. g., [30–32]). Three types of oscillations have been identified in the olfactory bulb. Breathing itself induces oscillations, which in rodents display frequencies between 1 and 5 Hz at rest and between 6 and 10 Hz during active sniffing (e. g., [33–35]). Presentation of odorant stimuli further induces both beta (between 15 and 35–40 Hz) [33, 36–43] and gamma (>35–40 Hz) fluctuations in the LFPs [33, 35, 36, 38–49]. Importantly, the firing of both mitral and tufted cells, the two projecting cell types of the olfactory bulb, appears to be phase-locked to both beta [40, 42] and gamma oscillations [40–42, 48–50]. Thus in physiological conditions, synapses in layer Ia of the piriform cortex, where terminals of olfactory bulb efferent neurons are concentrated (e. g., [30, 51, 52]), should be activated at frequencies corresponding to those observed in the olfactory bulb. Here we examined STP in layer Ia of the piriform cortex *in vitro*, while applying electrical stimulation in the lateral olfactory tract (LOT), which contains olfactory bulb efferent axons. The stimulation frequency range (0.1 to 100 Hz) encompasses that observed in natural brain rhythms.

Three conditions had to be met to obtain a relevant description of the effect of different stimulus frequencies on STP *in vitro*: 1) use of several stimuli in a train in order to be able to

observe the dynamics of STP, rather than the classical stimulus pair that limits the analysis to paired-pulse ratios; 2) model based, quantitative analysis of the data to obtain relevant parameter values for mechanisms of STD and STF, to be able to go beyond the mere phenomenological description of changes in response amplitude; 3) use of adult animals and of an extracellular medium that most closely mimics the one encountered in the adult brain *in vivo*; in particular, most *in vitro* experiments use an extracellular concentration of calcium of 2–2.5 mM while that measured *in vivo* is of the order of 1 mM; given the importance of calcium in synaptic transmission, this factor-two difference is likely to strongly affect STP and its dependence on stimulation frequency. Although 1 or 2 of these conditions have been met in the numerous studies devoted to STP in piriform cortex, our study would be the first where all 3 requirements were fulfilled: our experiments were performed using brain slices issued from adult mice and were maintained in an *in vivo*-like ACSF; we used stimulation trains of 5 stimuli and extracted the parameters of STP by fitting the data with a model derived from that initially developed by Tsodyks and Markram (1997) [53]. Results were compared with those obtained with a “classical” calcium concentration (2.2 mM).

Our experimental results and model parameters show that the interplay of STF and STD resulted either in an increase or a decrease of response amplitude that depended on stimulus frequency and calcium concentration. In the presence of high calcium concentration (2.2 mM), synaptic responses were enhanced, though weakly, at stimulation frequencies corresponding to the low beta and alpha bands while depression tended to occur at stimulation frequencies within the gamma band. On the other hand, in the presence of an *in vivo*-like calcium concentration (1.1 mM), response enhancement displayed a larger dynamic range. Additionally, response enhancement was maximal in the beta range and was also strong in the gamma range. These results suggest that short-term plasticity in layer Ia of the piriform cortex allows amplification of synaptic responses at frequencies corresponding to odor-induced beta and gamma oscillations in the olfactory bulb.

Material and methods

Ethics statement

All procedures were conducted in accordance with the guidelines from the French Ministry of Agriculture (décret 87/848) and from the European Community (directive 86/609) and was approved by the local ethical committee (comité d'éthique Midi-Pyrénées pour l'expérimentation animale, N° MP/06/79/11/12).

Slices preparation

The protocol for brain slice preparation was adapted from those previously described [54, 55] and is briefly summarized here. Two- to 4-month-old C57BL/6 female mice were used for these experiments. Mice were deeply anesthetized with isoflurane and then rapidly decapitated. The brain was removed and prepared for slicing in ice-cold, oxygenated (95% O₂ / 5% CO₂) modified artificial cerebrospinal fluid (mACSF) of the following composition (mM): NaCl 124, NaHCO₃ 26, KCl 3.2, MgSO₄ 1, NaH₂PO₄ 0.5, MgCl₂ 9, Glucose 10. Note that Ca⁺⁺ was omitted while the final Mg⁺⁺ concentration was 10 mM. Studies showed that axons innervating the piriform cortex leave the LOT at right angle [56], yet the lateral olfactory tract is not parallel to the long axis of the brain. Therefore, in order to preserve axons at best, a cut was made through the brain in the frontal plane with an angle of 70° at the level where cortex and cerebellum are adjacent. The brain was glued on a pedestal by the posterior side, the apex of the brain facing upward. Four hundred-micrometer-thick slices were then cut on a vibratome

in the presence of cold, oxygenated mACSF. Slices were allowed to recover for at least 1 hour at room temperature in a holding chamber filled with oxygenated *in vivo*-like ACSF.

In vivo-like ACSF composition

Synaptic transmission and STP are highly sensitive to extracellular ion concentrations, in particular that of calcium. We therefore used extracellular ionic concentrations close to those observed *in vivo*. Extracellular K⁺ and Ca⁺⁺ concentrations in the interstitial fluid have been reported in numerous studies using ion selective microelectrodes. Using the available literature for rodents [57–70], we calculated the median concentrations for K⁺ and Ca⁺⁺ and obtained values of 3.2 mM and 1.1 mM, respectively. Mg⁺⁺ concentration is of importance too as Mg⁺⁺ may partially antagonize voltage-dependent calcium channels. Mg⁺⁺ concentration is less documented than that of K⁺ and Ca⁺⁺ but values for concentration in the CSF of the mouse [71] and of other species (e.g., [72–76]) appear to be about to 1 mM. We also used a phosphate concentration of 0.5 mM, similar to that measured in the CSF [74, 77, 78]. Our *in vivo*-like ACSF was therefore composed of (in mM): NaCl 124, NaHCO₃ 26, KCl 3.2, MgSO₄ 1, NaH₂PO₄ 0.5, CaCl₂ 1.1, and glucose 10. This ACSF was continuously bubbled with a 95% O₂ / 5% CO₂ mixture (pH 7.4).

Stimulation and recording

For recording, an individual slice was transferred in a submersion type chamber that was continuously gravity fed with oxygenated *in vivo*-like ACSF at a flow rate of 3–3.5 ml/min. All recordings were performed at 34–35°C. Local field potentials were recorded in layer Ia of the piriform cortex either through tungsten-in-epoxylite microelectrodes (FHC, 0.2–0.3 MΩ) or through glass micropipettes filled with ACSF (3–7 MΩ). When recorded through microelectrodes, the signal was amplified (x1000) and filtered (0.1 Hz–10 kHz) with a NeuroLog system (Digitimer, UK). When recorded through micropipettes, the signal was first amplified on an AxoClamp 2B amplifier (Axon Instrument, Foster City, CA), further amplified with a Neurolog post-amplifier (final gain: ×1000) and low-pass filtered at 10 kHz.

Intracellular recording were performed in layer II of the piriform cortex using sharp micropipettes filled with 3 M K-Acetate (50–90 MΩ). Intracellular signal was amplified with the AxoClamp 2B amplifier (gain ×10). Criteria for accepting intracellular recording data were: stable membrane potential more negative than -60 mV, input resistance > 20 MΩ and ability of the cell to repetitively fire overshooting action potentials during depolarizing square current pulses lasting 120–300 msec.

Micropipettes for LFP or intracellular recordings were pulled on a P97 Flaming Brown micropipette puller from 1.2 mm OD medium walled capillaries with filament (GC120F, Harvard Apparatus).

Fifty Hz noise was eliminated with a Humbug system (Quest Scientific, Canada). All signals were digitized with a digitization rate of 20–50 kHz (1401plus or power1401, CED, UK). Real-time display of the signals was achieved with an oscilloscope and with Spike2 software (CED, UK).

Extracellular electrical stimulation was applied through tungsten-in-epoxylite microelectrodes (FHC, 0.2–0.3 MΩ) implanted in the LOT and consisted in monopolar cathodal square current pulses (6–35 μA, 200 μs duration) delivered by an isolated stimulator (A365 stimulus Isolator, WPI).

The LFP recorded in layer Ia was composed of a fiber volley followed by a slow negative wave (N-wave, [79]). The fiber volley corresponds to the summation of synchronous action potentials traveling in axons while the N-wave reflects the summation of excitatory postsynaptic potentials generated in the vicinity of the recording electrode [51]. Stimulation intensity

was kept in a range allowing reliable N-wave generation but low enough to avoid contamination by fast positive components that presumably resulted from postsynaptic action potential generation [80]. Low intensity also limited effective current spread to a few tens of μm [54], hence to within the LOT. Response amplitude was measured as the maximal amplitude of the N-wave relative to prestimulus baseline. The amplitude of the fiber volley was measured similarly.

In order to examine the effect of Ca^{++} on synaptic response amplitude, 6 concentrations of Ca^{++} have been used (0.3, 0.5, 0.7, 0.9, 2.2 and 3.3 mM) in addition to the 1.1 mM control concentration. The time course of the effect of modifying calcium concentration on field potential amplitude was monitored using electrical stimulation delivered at 0.5 Hz for 15–20 minutes. One or two calcium concentrations were tested between one control and one recovery test; data were included only if the value during recovery differed by less than 15% from that obtained in the control period.

STP has been examined in 1.1 and 2.2 mM Ca^{++} . When switching from one calcium concentration to another, ten minutes of stable baseline was required before proceeding to the STP protocol. In each experiment, STP was tested using stimulation trains consisting of five consecutive stimuli delivered at 6 different frequencies: 3.125, 6.25, 12.5, 25, 50 and 100 Hz. Each train was repeated 10 times to allow for averaging. The trains were spaced apart by ten seconds without stimulation. The number of stimuli was limited to 5 per train for two reasons: first because the number of successive oscillation cycles in the olfactory bulb is typically between 4 and 10 (e.g., [33, 38, 42, 48]), and second, because large number of pulses may recruit a slow adaptation (see [Discussion](#)) that would have hampered our model-based analysis.

Data analysis

Signal processing was performed using the Spike2 software with scripts written by the users. For the analysis of the effect of calcium on synaptic transmission at 0.5 Hz, signals were averaged over the last minute (thirty responses) of the 15–20 min-long series of stimuli. Amplitudes obtained in a given calcium concentration were normalized by that obtained in control (1.1 mM) calcium concentration (*normalized response amplitude*, NRA).

For STP analysis, the 10 traces obtained at a given frequency and with the same ordinal stimulus number were averaged. The individual-level data are represented as the mean \pm SEM. For population data analysis and for STP model fitting, we first calculated the *relative response amplitude* (RA_n) by dividing the amplitude of the N-wave obtained at the n^{th} stimulation (A_n) by that obtained at the first stimulation (A_1) in each stimulation train ($RA_n = A_n / A_1$, n between 1 and 5). Note that data obtained in 2.2 mM calcium were normalized by the first response amplitude in the *control* (1.1 mM) condition for each frequency.

Short-term plasticity model

We developed a phenomenological model to compute the parameters of short-term synaptic plasticity at the LOT-layer Ia synapse. The model, implemented in R (R-project v.3.3.1), is derived from models described in previous studies [53, 81, 82]. It included one term of facilitation and two terms of depression.

In response to the first stimulation of a train, the relative response amplitude is:

$$RA_1 = E \times U = 1$$

where E represents the maximal synaptic efficacy and U , the utilization of efficacy E , represents the fraction of E that is used at the first stimulation. U may be envisioned as the increase in

calcium concentration in the presynaptic terminals that leads to neurotransmitter release, while E would correspond to the theoretical maximal value obtained if the synapses released all their synaptic vesicles and/or if all postsynaptic receptors saturated.

The purpose of the model was then to approximate, for each stimulation rank $n > 1$, RA as the product of four terms:

$$RA_n = E \times r_{1,n}^- \times r_{2,n}^- \times u_n^+$$

where '*minus*' designates values just before the stimulation and '*plus*' designates the value at stimulation time. u , the utilization of efficacy, varies so as to implement facilitation: at each stimulation, u rises by a fraction of the parameter U ; then, during the interpulse interval (IPI), u decays to zero according to the time constant of facilitation (τ_F) as follows:

$$\text{at stimulation time : } u_{n+1}^+ = u_{n+1}^- + U \times (1 - u_{n+1}^-);$$

$$\text{during } IPI : u_{n+1}^- = u_n^+ \times e^{-\frac{IPI}{\tau_F}}.$$

r_1 and r_2 designate two available reserves of E , that can be assimilated to synaptic resources such as vesicles of neurotransmitters or availability of postsynaptic receptors. At rest, $r_1 = r_2 = 1$. At each stimulation, both reserves are decremented in proportion to the utilization of efficacy, u . Furthermore, u is assumed to be shared between both synaptic reserves by factors k and $(1-k)$, respectively. During the IPI , r_1 and r_2 recover with time constants that correspond to two time constants of recovery from depression (respectively, τ_{R1} and τ_{R2}), as follows:

$$\text{at stimulation time : } r_{1,n+1}^+ = r_{1,n}^- - r_{1,n}^- \times u_{n+1}^+ \times k, \quad r_{2,n+1}^+ = r_{2,n}^- - r_{2,n}^- \times u_{n+1}^+ \times (1 - k);$$

$$\text{during } IPI : r_{1,n+1}^- = (r_{1,n}^+ - 1) \times e^{-\frac{IPI}{\tau_{R1}}} + 1, \quad r_{2,n+1}^- = (r_{2,n}^+ - 1) \times e^{-\frac{IPI}{\tau_{R2}}} + 1.$$

For each sample, including either one or two calcium concentrations and five or six stimulation frequencies, the model was fit to the data using an iterative procedure that minimized the mean-squared error (MSE) between the recorded RA and the amplitudes predicted by the model. The method to determine MSE was an implementation of that of Nelder and Mead (1965) [83], that uses only function values and is robust although relatively slow. E was assumed to be independent of extracellular calcium concentration and therefore one single value of E was determined in the paired calcium manipulation experiments. One single set of parameters was determined for an experimental block containing one (6 parameters) or both (11 parameters) calcium concentration condition. During parameters optimization, E , U , τ_F , τ_{R1} , τ_{R2} and k were constrained as follows: E , U and k between 0 and, respectively, 10, 1 and 1; time constants between 0 and 3 seconds with the supplementary constraint that τ_{R1} had to be inferior to τ_{R2} . When optimal k was equal to 1, τ_{R2} had no more influence and was withheld from further analysis. Robustness of fitting was estimated using the root mean-squared error (RMSE). For the present data set, the RMSE ranged between 0.017 and 0.113.

Statistics

ANOVA and Fischer's PLSD posthoc tests were used to examine the effects of calcium concentration and stimulation frequency on response amplitude. Paired t-test was used to compare model parameter values in 1.1 and 2.2 mM Ca⁺⁺. Unless otherwise stated, population data are summarized by their means and 95% confidence intervals; values between brackets in text correspond to the 95% confidence interval. Unless otherwise stated, error bars in Figures delimit the 95% confidence interval.

Results

Effect of extracellular calcium concentration on response amplitude

We first examined the effect of varying the extracellular calcium concentration on the amplitude of the synaptic responses at the LOT-layer Ia synapse of piriform cortex using a stimulation frequency of 0.5 Hz. This frequency induced a very weak depression (-3% between first pulse response amplitude and steady state on average) but response amplitudes were measured only once the steady state was reached. Effect of varying extracellular calcium concentration has been examined in 16 experiments. Six extracellular calcium concentrations were tested in addition to the control concentration at 1.1 mM ($n = 18$): 0.3 ($n = 3$), 0.5 ($n = 5$), 0.7 ($n = 4$), 0.9 ($n = 4$), 2.2 ($n = 8$) and 3.3 mM ($n = 2$). One to four different concentrations were tested in one experiment.

[Fig 1A](#) shows an example of LFP recorded in layer Ia with 3 different extracellular calcium concentrations. In the presence of 0.5 mM calcium, the amplitude of the N-wave was about twice smaller than in the control condition, while it was approximately twice larger with 2.2 mM calcium. Control and recoveries displayed similar amplitudes. The amplitude of the fiber volley did not change, indicating that changes in N-wave amplitude were of synaptic origin and did not result from changes in axonal excitability. At the population level, fiber volley amplitude was not significantly affected by changes in calcium concentration (ANOVA, $P = 0.07$, not illustrated). In contrast, N-wave amplitude depended strongly on calcium concentration (ANOVA, $P < 0.0001$).

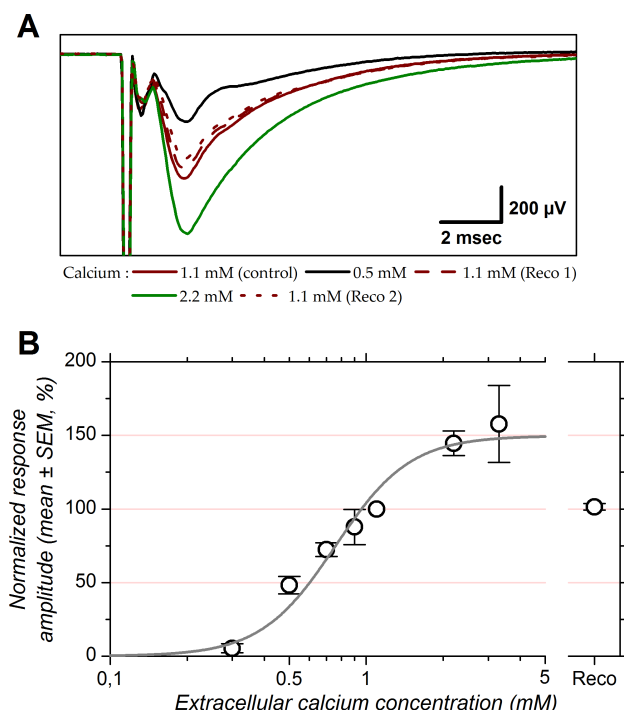


Fig 1. Effect of extracellular calcium concentration on the amplitude of the response evoked at 0.5 Hz at the LOT-layer Ia synapse. A: LFP recorded in layer Ia of the piriform cortex with 3 different extracellular calcium concentrations (0.5, 1.1 and 2.2 mM). Stimulation intensity was 15 μ A. B shows Hill equation fitted to population data. Data points correspond to the mean and error bars to ± 1 SEM computed after normalizing the individual amplitudes to their corresponding control values in 1.1 mM calcium (expressed as a percentage). Continuous line corresponds to Hill equation fitted to the data ($R^2 = 0.98$). “Reco”: recovery, mean normalized response amplitude upon return to 1.1 mM calcium.

<https://doi.org/10.1371/journal.pone.0183246.g001>

Population data for the N-wave are presented in Fig 1B. Before averaging, data were normalized: the normalized response amplitudes, NRA, correspond to the peak amplitudes of the N-wave in a given Ca^{++} concentration expressed as a percentage of the response amplitude in the control condition (1.1 mM calcium). The mean NRA as a function of extracellular calcium concentration, C, was fitted with Hill function:

$$\text{NRA} = A_{\max} \times \frac{C^h}{C^h + C_{0.5}^h}$$

with A_{\max} representing the maximal response amplitude, $C_{0.5}$ the extracellular calcium concentration eliciting half of A_{\max} and h the Hill coefficient. Synaptic responses were virtually suppressed (8% of control) with a calcium concentration of 0.3 mM. Reducing calcium concentration from 1.1 mM (control) to 0.5 mM reduced response amplitude to approximately half (48%), yet doubling calcium concentration from 1.1 mM to 2.2 mM did not double response amplitude. Instead, response amplitude was increased by +45% relative to control. This indicates the presence of a saturation level which is reflected by the A_{\max} of the fit at $+50 \pm 10$ (SE) %. Relative to A_{\max} , the $C_{0.5}$ has a value of 0.76 ± 0.05 (SE) mM. The Hill coefficient returned by the fit was 2.98 ± 0.33 (SE). The Hill coefficient suggests that the calcium sensor responsible for neurotransmitter release is activated by the binding of 3 calcium ions. These results suggest that the effect of extracellular calcium on response amplitude saturates when its bath concentration is larger than 3 mM and indicate that response amplitude in 2.2 mM calcium is already close to saturation.

Effect of calcium on short-term plasticity

STP was tested with trains of five stimulating pulses delivered at frequencies between 3.125 and 100 Hz. Effects of different stimulation frequencies on the postsynaptic responses are exemplified in Fig 2. Fig 2A displays the LFP traces for each of the 5 successive stimuli of the trains for each frequency tested in the presence of 1.1 mM extracellular calcium. Increasing stimulation frequency did not modify fiber volley amplitude (Fig 2A). This constancy implies that the changes in N-wave amplitude were determined by changes at the level of synaptic transmission. The amplitude of the N-wave as a function of stimulus time for the different frequencies tested is represented by the data points in Fig 2C. The successive responses evoked by the 3.125 Hz train displayed identical amplitudes. An enhancement of N-wave amplitude during the stimulation train became visible at 6.25 Hz. This enhancement was maximal at 25 Hz; at this frequency the amplitude of the N-wave induced by the fourth stimulus of the train was 1.5 time larger than that induced by the first. Amplitudes were only marginally smaller with the third and fifth stimulus of the same train. At 50 Hz, response amplitude reached a maximum with the third stimulus that was slightly smaller than that obtained at 25 Hz ($\times 1.45$ relative to first stimulus); response amplitude for the fourth and fifth stimulus plateaued at comparable levels. At 100 Hz response enhancement was barely visible ($\times 1.2$ for the third stimulus).

In addition to increasing N-wave amplitude, increasing extracellular calcium concentration to 2.2 mM also modified the features of STP (Fig 2B and 2C). Although less marked than with 1.1 mM calcium, response enhancement occurred with stimulation frequencies in the range 3.125–25 Hz. Yet at 12.5 and 25 Hz, maximal enhancement was visible with the second stimulus of the train and response amplitude obtained with the following stimuli declined back toward the amplitude obtained with the first stimulation. At 50 Hz and, more dramatically, at 100 Hz, response enhancement was no longer observed and was instead replaced by a progressive reduction of response amplitude that was not observed in 1.1 mM calcium. In the end,

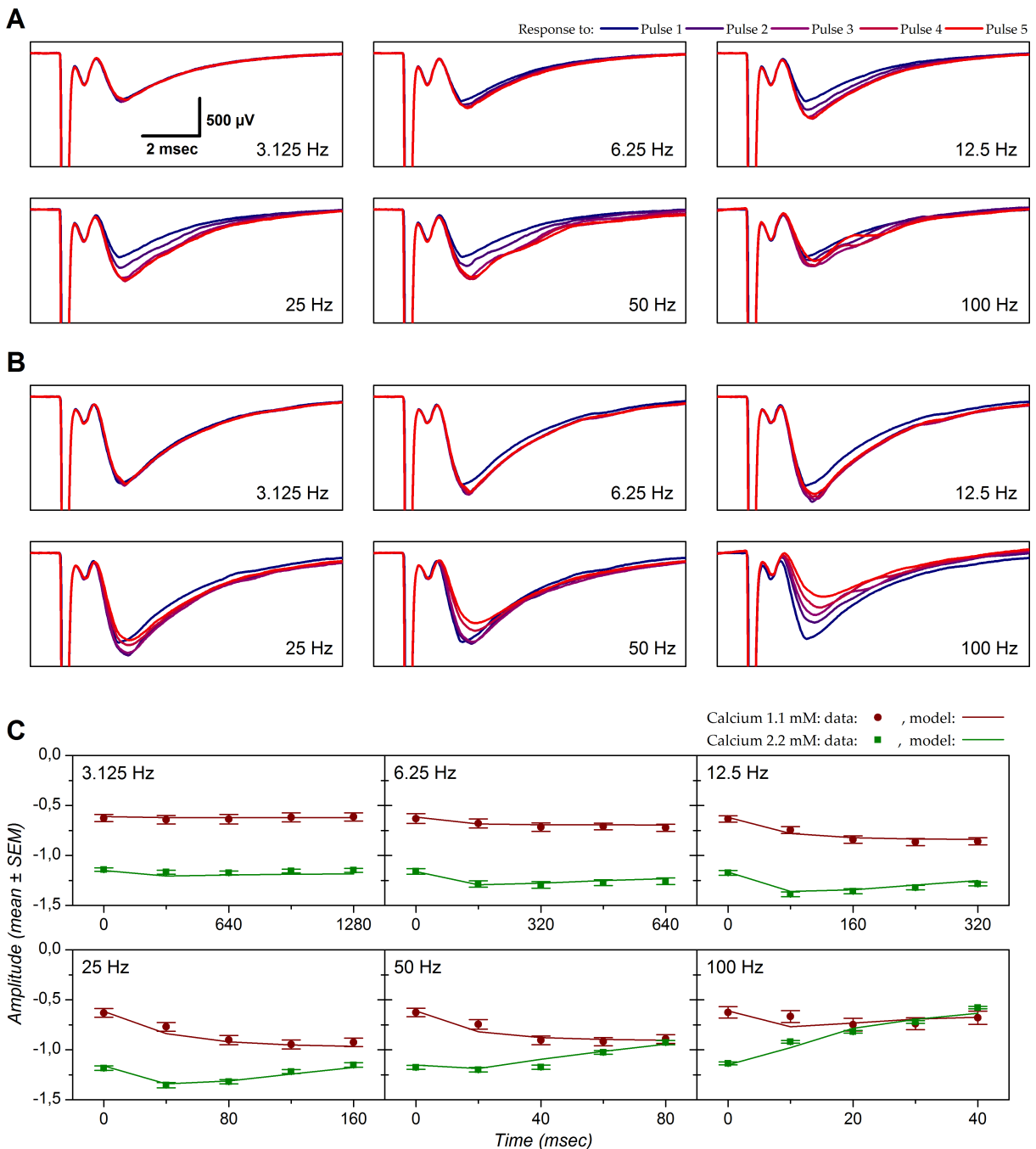


Fig 2. Short-term plasticity with 1.1 mM or 2.2 mM extracellular calcium in one experiment. LFPs evoked in layer Ia by stimuli applied in the LOT. Stimulation intensity was 20 μ A. A: Response obtained with an extracellular calcium concentration of 1.1 mM. Each panel corresponds to one stimulation frequency. Each panel shows five traces that correspond to the five stimuli of the train (rank color code on top of figure). Each trace corresponds to the average of 10 sweeps. B: Same as A but in 2.2 mM calcium. Scale presented in the 3.125 Hz panel in A applies to all the other panels in A and B. C: N-wave amplitude represented as a function of stimulus time. The data points correspond to the experimental values (mean \pm SEM) and the lines correspond to the result of the model fitted to the data. Model parameters were optimized for both conditions (1.1 mM and 2.2 mM) at once. Parameter E was shared for both conditions. Parameters values in 1.1 mM Ca^{++} : $U = 0.353$, $\tau_F = 92$ ms, $\tau_{R1} = 18$ ms, $\tau_{R2} = 87$ ms, $k = 0.980$. Parameters values in 2.2 mM Ca^{++} : $U = 0.666$, $\tau_F = 223$ ms, $\tau_{R1} = 15$ ms, $\tau_{R2} = 418$ ms, $k = 0.909$. Shared parameter $E = 2.761$. MSE value associated with this fit: 0.003. For illustration purpose the predicted RA has been de-normalized (RA multiplied by response amplitude obtained with first stimulus) to be presented on the same scale as the experimental data.

<https://doi.org/10.1371/journal.pone.0183246.g002>

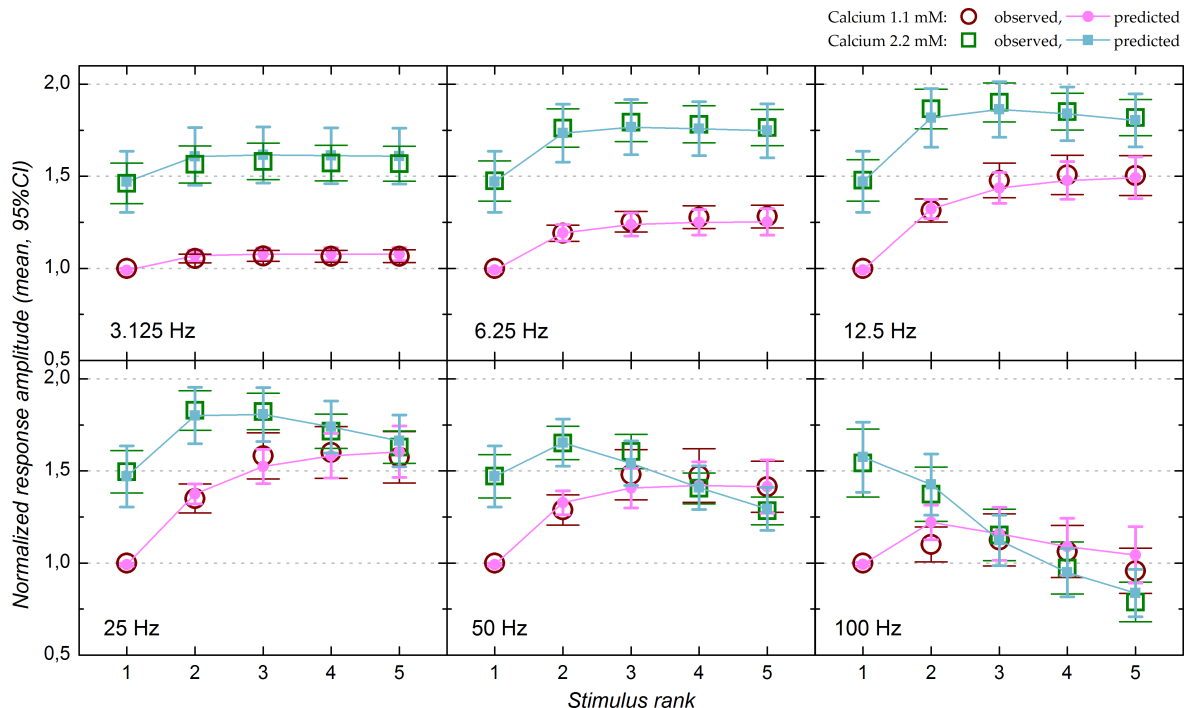


Fig 3. Short-term plasticity in 1.1 and 2.2 mM calcium: Population data (n = 17 experiments with 1.1 mM calcium and 8 experiments with 2.2 mM calcium). Before averaging, N-wave amplitudes in both 1.1 and 2.2 mM calcium were normalized by that obtained with the first stimulus of each trains in 1.1 mM calcium. Error bars correspond to the 95% CI. Stimulation ranks are presented on the x-axis. Hollow red circles and green squares represent the means of the experimental data in 1.1 and 2.2 mM calcium, respectively. Filled magenta circles and blue squares correspond to the means of the values predicted by the model in 1.1 and 2.2 mM calcium, respectively.

<https://doi.org/10.1371/journal.pone.0183246.g003>

response amplitude obtained with these frequencies declined toward the values observed with 1.1 mM calcium, with the 5th stimulation at 50 Hz and with the 3rd one at 100 Hz (Fig 2C).

The example in Fig 2 is representative of what we observed at the population level (Fig 3). Prior to averaging, response amplitudes in both 1.1 and 2.2 mM calcium were normalized by the amplitude obtained with the first stimulation of each stimulus trains in 1.1 mM calcium. Fiber volley amplitude was not modified by stimulus frequency (ANOVA, $P = 0.70$ in 1.1 mM calcium, $P = 0.99$ in 2.2 mM calcium). In contrast, N-wave response amplitude was strongly and significantly depended on stimulation frequency ($P < 0.0001$ in both 1.1 and 2.2 mM calcium) as well as on pulse ordinal number ($P < 0.0001$ in both 1.1 and 2.2 mM calcium).

Population data with 1.1 mM extracellular calcium ($n = 17$) are represented by open red circles in Fig 3. Response enhancement was weak at 3.125 Hz (+7% relative to first pulse response). Although weak, the increase in response amplitude was significant for pulses 2–5 in comparison to pulse 1 (Fisher's PLSD, $P < 0.0001$). Response enhancement was slightly stronger (+28%) at 6.25 Hz and quite important at 12.5 Hz (+50%). The maximal enhancement was achieved at 25 Hz (+60%). At 50 Hz the response enhancement (+48%) was less marked than at 25 Hz. For these four frequencies, the maximal enhancement was reached with the third pulse of the stimulus train (pulse 1 vs. pulse 3: $P < 0.0001$ at 6.25–50 Hz; pulse 2 vs. pulse 3: $P = 0.001$ at 6.25 Hz, $P < 0.0001$ at 12.5 and 25 Hz, $P = 0.0001$ at 50 Hz) while amplitude for the third, fourth and fifth pulses did not differ significantly, indicating that response amplitude reached a plateau level at the third pulse. Response enhancement (+12% max) was largely lost at 100 Hz: response amplitude with the second and third pulses were significantly larger than

with first pulse ($P = 0.03$ and 0.008 respectively) but those with the fourth and fifth pulse were not significantly different from that with the first pulse ($P = 0.2$ and 0.3 respectively).

In 2.2 mM calcium ($n = 8$; open green squares in Fig 3) the amplitude of the response evoked by the first stimulus in each train was 49% higher on average than in 1.1 mM calcium, as shown above (Fig 1). As in 1.1 mM calcium, a weak response enhancement was observed at 3.125 Hz (maximum +8% relative to first pulse response amplitude) as well as a slightly stronger enhancement at 6.25 Hz (maximum +22%). For both frequencies, response amplitude reached a plateau at the second stimulating pulse (pulse 1 vs. pulses 2–5: $P < 0.0001$ but no significant difference between pulses 2–5). For higher stimulation frequencies, the dynamics of STP diverged from that observed in 1.1 mM calcium: first, maximal response enhancement was obtained at 12.5 Hz (+29%) rather than at 25 Hz (+22%). Second, in 2.2 mM calcium responses at 12.5 Hz and 25 Hz were not followed by a plateau but by a decline in response amplitude: response amplitude was significantly less for the fifth pulse compared to the third one at 12.5 Hz ($P = 0.03$), and significantly less for the fourth and fifth pulse compared to the third one at 25 Hz ($P = 0.02$ and 0.0001 , respectively). Despite this decrement, response amplitudes with the fifth stimulus were still larger than in 1.1 mM calcium (12.5 Hz: $P < 0.0001$; 25 Hz: $P = 0.005$).

At 50 Hz the trends observed at 25 Hz were accentuated: response enhancement was weaker (maximum +12% with pulse 2), although still significant ($P = 0.001$ and 0.01 for second and third pulse responses compared to first pulse response), and was followed by a stronger response decline, such that response amplitude with the fifth pulse was actually less (-13%) than with the first ($P = 0.0007$). This decline brought response amplitude back to the values obtained in 1.1 mM calcium for the fourth and fifth stimulation pulse ($P = 0.4$ and 0.9 respectively). At 100 Hz there was no response enhancement in 2.2 mM calcium and response amplitude instead declined progressively throughout the stimulation train (-49% between the first and fifth pulse). All pulse comparisons were significant (P between 0.0004 and <0.0001). This strong decline brought response amplitude to values comparable to those obtained in 1.1 mM calcium at the third pulse and response amplitude for the third, fourth and fifth stimulation did not differ significantly in 1.1 and 2.2 mM calcium ($P = 0.2$, 0.9 and 0.3 respectively).

Altogether, although response amplitude for the first stimulation was higher in 2.2 mM calcium, weaker facilitation and/or stronger depression progressively attenuated this difference, or even suppressed it at high stimulation frequency.

We also performed intracellular recordings in order to more precisely identify the synaptic responses evoked by LOT stimulation and their STP. Intracellular recordings were performed in layer 2 of piriform cortex. We concentrated on 5 cells with monosynaptic excitatory postsynaptic potentials. The mean resting membrane potential was -79 mV [-79 – -85] and the mean input resistance was 38 M Ω [27–43]. In response to suprathreshold depolarizing current pulses, the cells emitted wide action potentials (half width at half-height: 0.64 msec [0.61 – 0.67]) and spike firing was regular with adaptation (not illustrated). These features suggest these cells were semi-lunar cells [84]. Effect of stimulation frequency on postsynaptic response is illustrated by one example in Fig 4A and 4B; the population data are presented in Fig 4C. Extracellular calcium concentration was 1.1 mM in all cases. Qualitatively, response amplitude as a function of stimulation frequency and of stimulus ordinal number showed the same features as observed with extracellularly recorded N-wave in 1.1 mM calcium: response amplitude showed little change when elicited at 3.125 Hz. Response enhancement was observed with higher stimulation frequencies and showed a maximum at 25 Hz. At 6.25–25 Hz, response amplitude reached a plateau at the third stimulation. Enhancement was only weak at 100 Hz and the response amplitude at this frequency returned to control response amplitude with the fifth pulse of the train. No synaptic summation was observed at 25 Hz; this suggest that

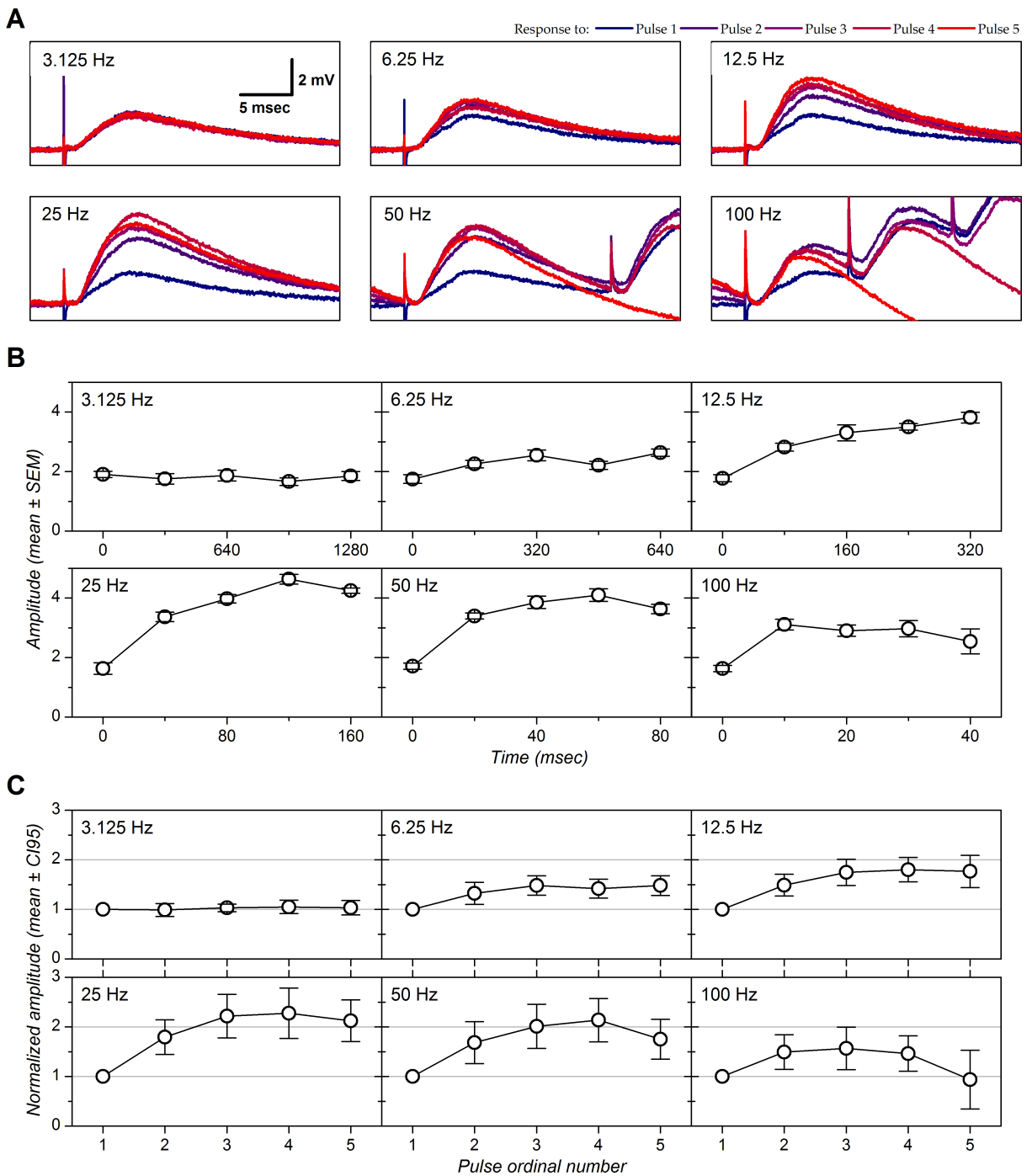


Fig 4. Short-term plasticity in intracellularly recorded cells with 1.1 mM extracellular calcium. A: Postsynaptic responses evoked by electrical stimulation applied in the LOT (stimulation intensity 6 μ A). Each panel corresponds to one stimulation frequency. Each panel shows five traces that correspond to the 5 stimulus ranks of the train (color code on top of figure). Each trace correspond to the average of 8 sweeps. B: EPSP amplitude as a function of stimulus time. Amplitudes were measured at a delay of 6 msec after stimulation and were calculated relative to baseline measured at the foot of each EPSP in order to cancel effect of temporal summation at high frequency. The data points correspond to the experimental values (mean \pm SEM). C: Population data ($n = 5$). EPSP amplitudes were normalized before averaging by the amplitude obtained with the first stimulus of each trains. Error bars correspond to the 95% CI.

<https://doi.org/10.1371/journal.pone.0183246.g004>

response enhancement, that was maximal at this frequency as for the N-wave, was not due to nonlinearities introduced by postsynaptic membrane potential changes, such as recruitment of NMDA receptors [85] or activation of persistent sodium conductance [86]. Maximal facilitation (+127%, Fig 4C) appears larger than in LFP recordings (Fig 3) but this does not necessarily imply a difference between intracellular and extracellular recording; as previously reported [84], STP differed widely between cells and the average based on our limited sample of intracellular recordings was unlikely to match the average based on hundreds or thousands of cells simultaneously recorded in the LFPs.

Short-term plasticity model

The experimental data suggested that STP at the LOT-layer Ia connection involves the interaction of facilitatory and depressant mechanisms with different temporal profiles, and moreover, that their relative contributions depended on extracellular calcium concentration. To achieve a quantitative description of these mechanisms, we used a model of STP adapted from models described in previous studies [53, 81, 82]. In order to satisfactorily fit the data, our model required 3 mechanisms: one facilitation and two depressions distinguished by their time constants of recovery. When experimental data were obtained with both 1.1 mM and 2.2 mM, the model was fitted on both datasets at once, with E as a shared parameter.

As highlighted in Fig 2C, the STP model reproduced the experimental data quite well (1.1 mM calcium: red line; 2.2 mM calcium: green line). The model suggests that, in this example, the dynamics of STP in 1.1 mM calcium can be accounted for by the presence of 3 phenomena: a facilitation mechanism with a recovery time constant of 92 msec, and two depression mechanisms that recovered with time constants of 18 and 87 msec. Yet the slowest depression impinged on only 2% of the available reserve ($k = 0.98$). Thus, response enhancement up to 25 Hz can be accounted for by the presence of short-term facilitation. Response enhancement was less marked at higher frequencies as a consequence of the recruitment of the short-term depression mechanism with a short time constant of recovery, which counteracted facilitation.

The model fitted to the data obtained in 2.2 mM calcium suggests the following changes to explain the differences observed between the two conditions: an 89% increase in resource utilization for the first response (U) accounts for the increased response amplitude in 2.2 mM calcium ($U = 0.666$ in 2.2 mM calcium vs. $U = 0.353$ in 1.1 mM calcium). The time constant of facilitation appears to be longer (223 msec). Yet, k decreased ($k = 0.909$), revealing a more important utilization of the slow depression mechanism than in control condition, that partially counteracted facilitation even at low frequency. Therefore the greater depression observed with the increase of calcium concentration can be explained by the increase of U —leading to stronger resource utilization—while appearance of depression for frequency lower than in 1.1 mM calcium results from the change in the value of k .

The population data for the relative amplitudes predicted by the model are represented by magenta circles (1.1 mM calcium) and blue squares (2.2 mM calcium) in Fig 3. Overall, the predicted values overlap well with the experimental data. Ability of the model to properly fit the data is further illustrated in Fig 5, which shows that the predicted response amplitudes are highly correlated with the amplitudes actually measured (correlation $r^2 = 0.962$ in 1.1 mM calcium and 0.986 in 2.2 mM calcium).

The overall quality of the model fit was estimated by the RMSE. At the population level the mean RMSE was 0.047 [0.036–0.058] ($n = 17$). We tested other variants of the model. The first variant was a model with only one depression mechanism (as in: [81, 82]). The RMSE values returned by this first variant were significantly higher ($P = 0.003$, paired t-test) by +45% [+11%—+79%] on average in comparison to the initial model. The second variant was one in

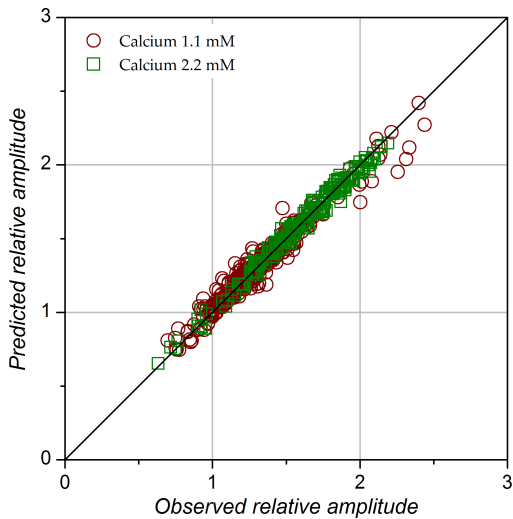


Fig 5. Scatterplot of RA values predicted by the model vs. observed RA values ($n = 715$ data points). Diagonal represents line of equality. The r^2 of the linear correlation between predicted and measured values was 0.962 in 1.1 mM calcium and 0.986 in 2.2 mM calcium.

<https://doi.org/10.1371/journal.pone.0183246.g005>

which parameter E was allowed to vary in the different calcium concentration conditions. For the 8 experiments in which the 2 calcium concentrations were tested, the mean RMSE was significantly ($P = 0.008$) lower (mean difference: -15% [-24%—-6%]), but this had the inconvenience of assuming that E , the total synaptic resource, varies with calcium concentration. The third variant was a model in which, in addition to E , the time constants of recovery from depression and facilitation were shared between the two calcium concentrations. This third variant performed less well on average: the RMSE was significantly ($P = 0.03$) increased by +32% [+11%—+53%] on average in comparison to the original model.

Distribution of model parameter values are presented in Fig 6 while Fig 7 presents scatter plots for each parameter in 1.1 vs. 2.2 mM Ca^{++} .

The parameter E corresponds to the maximum potential response, that is, a ceiling level for the response amplitude given the experimental conditions of the study. The mean value returned by the model was 2.825 [2.422–3.228] (Fig 6A). In other words, E represents, on average, 2.8 times the response amplitude at the first stimulation of a train in 1.1 mM calcium.

The parameter U allows defining the first level of u and corresponds to the fraction of E that is used at the first stimulation of a train. U increased with calcium concentration: U in 1.1 mM Ca^{++} was distributed from 0.198 to 0.571, with a mean of 0.377 [0.329–0.424] (Fig 6B). U was larger (+45%) in 2.2 mM Ca^{++} , with a mean at 0.548 [0.456–0.639]. Fig 7A shows the effect of increasing calcium concentration in a pairwise fashion. The increase of U was observed in all cases and was highly significant ($P = 0.001$, paired t-test).

Likewise, the time constant of facilitation was strongly affected by increasing Ca^{++} (Fig 6C). The mean value of τ_F in 1.1 mM Ca^{++} was 157 msec [0.139–0.176] and appeared to be shorter than the mean value obtained in 2.2 mM Ca^{++} , which was 236 msec [0.199–0.272]. When examined in a pairwise fashion we again notice a systematic and highly significant ($P = 0.0003$) increase of τ_F in 2.2 mM Ca^{++} (Fig 7B). The mean increase was +86% [+59%—+112%].

The parameter k determines the allocation of the synaptic resources into two subgroups, one that shows a fast and the other a slow recovery from depression. A value of 1 corresponds to cases where the slow depression mechanism was not required for fitting the data. This was the case in 6 of the 9 experiments where tests were made with 1.1 mM calcium only. On the

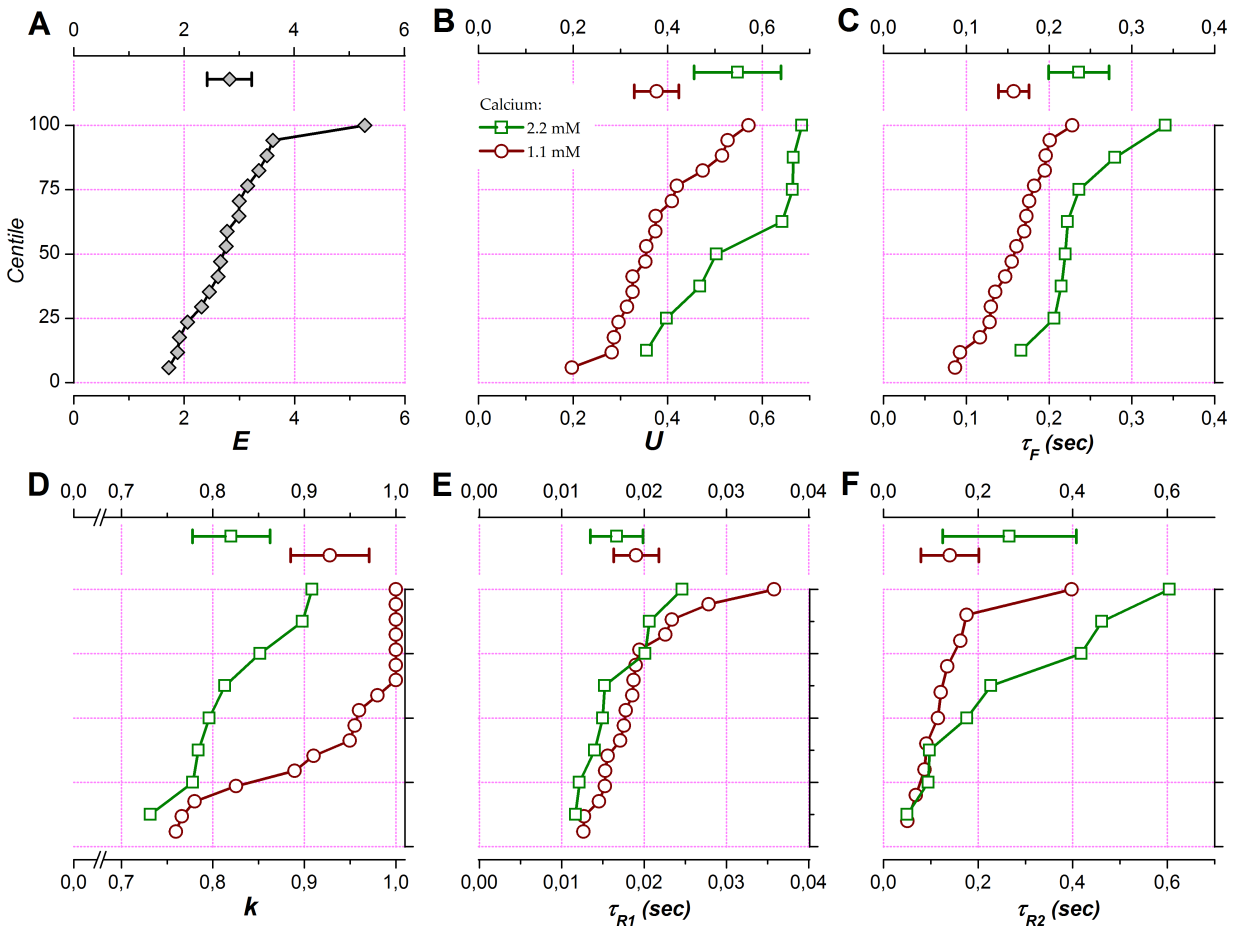


Fig 6. Short-term plasticity parameters at population levels with 1.1 and 2.2 mM calcium. Parameters optimized to fit the observed STP data are summarized as means and 95% confidence intervals (upper part in each panel) and as cumulative distributions (centile plots, lower part in each panel) for data obtained in 1.1 mM (red circles) and 2.2 mM calcium (green squares). The dashed line at 50% in the centile plots indicates the median of the distributions and lines at 25% and 75% delineate the interquartile range. A: E , efficacy. B: U , utilization of efficacy on a single stimulation at rest (fully recovered and non-facilitating). C: τ_F , time constant of facilitation. D: k , coefficient defining the partition of synaptic resources in two subgroups subjected to different time courses of recovery from depression. E: τ_{R1} , time constant of recovery for fast depression. F: τ_{R2} , recovery time constant of recovery for slow depression.

<https://doi.org/10.1371/journal.pone.0183246.g006>

other hand, $k < 1$ in most of the experiments (7/8) where both 1.1 and 2.2 mM calcium were tested (Figs 6D and 7C). Yet in these cases, k was on average higher in 1.1 mM calcium than in 2.2 mM calcium ($P = 0.038$, Fig 7C). On average, the value of k was 0.82 [0.78–0.86] in 2.2 mM Ca^{++} , meaning that about 20% of the synaptic resource underwent a process of slow recovery from depression. This proportion was less in 1.1 mM Ca^{++} : for the whole sample, the mean value of k was 0.93 [0.88–0.97] and it was 0.89 [0.83–0.96] for the subsample of experiments in which both 1.1 and 2.2 mM Ca^{++} were used.

Since $k \gg 0$ in all cases, the depression mechanism with fast recovery was systematically observed in both 1.1 and 2.2 mM Ca^{++} . The recovery time constant for this mechanism, τ_{R1} , was independent from calcium concentration ($P = 0.3$, Fig 7D). τ_{R1} averaged 19 msec [16–22 msec] in 1.1 mM Ca^{++} and 17 msec [13–20 msec] in 2.2 mM Ca^{++} (Fig 6E).

The depression mechanism with slow recovery displayed a recovery time constant, τ_{R2} , that averaged 140 msec [79–202 msec] in 1.1 mM Ca^{++} and 266 msec [125–407 msec] in 2.2 mM Ca^{++} (Fig 6F). Despite a trend for being slightly longer in 2.2 mM Ca^{++} , the τ_{R2} values did not

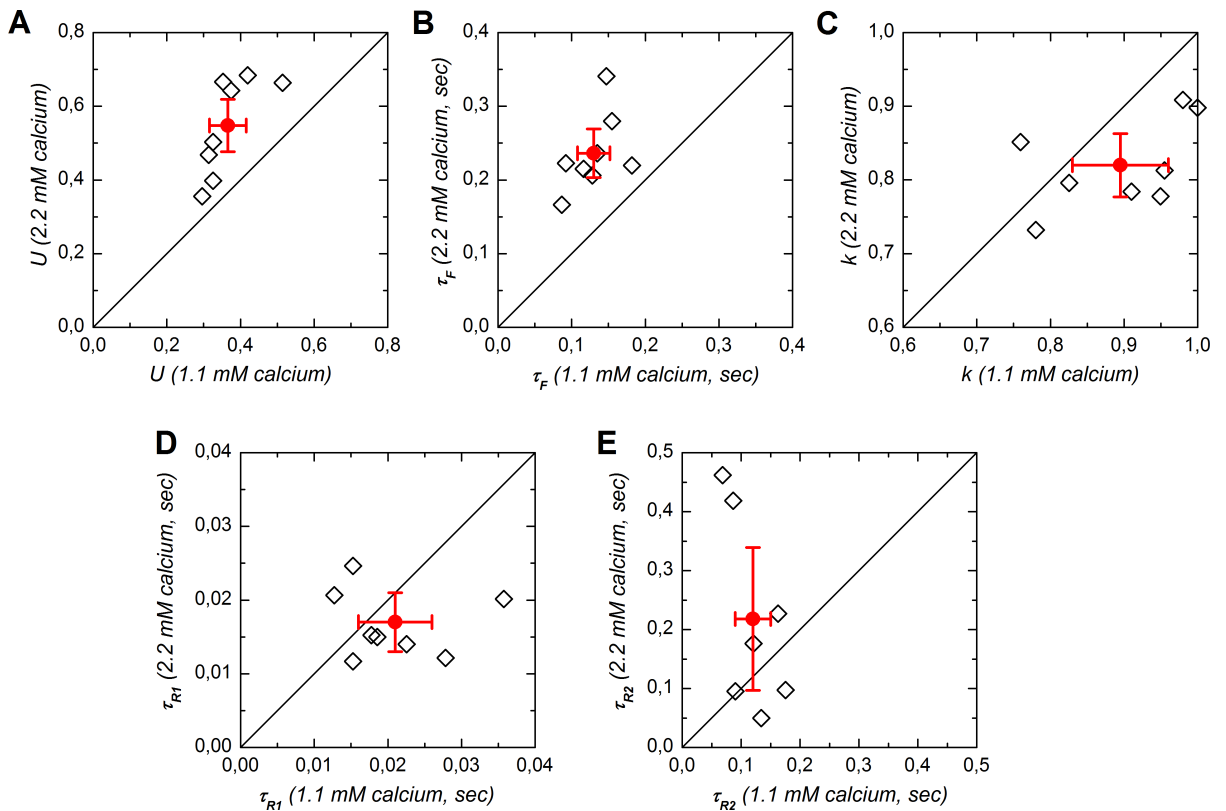


Fig 7. Scatter plot of short-term plasticity parameters for experiments performed with both 1.1 and 2.2 mM calcium (n = 8). A: U , utilization of efficacy on a single stimulation at rest (fully recovered and non-facilitating). B: τ_F , time constant of facilitation. C: k , partition of synaptic resources. D: τ_{R1} , time constant of recovery for fast depression. E: τ_{R2} , recovery time constant for slow depression. Diagonal lines represent equality lines. Open symbols correspond to individual experiments, plain symbols represent the mean for the subsample of experiments in which STP was tested in both 1.1 and 2.2 mM calcium, associated bars correspond to the 95% confidence intervals.

<https://doi.org/10.1371/journal.pone.0183246.g007>

differ significantly between the two calcium concentrations ($P = 0.2$, Fig 7E). The slow depression recovery time constant was of the same order of magnitude as the facilitation time constant but there was no correlation between τ_F and τ_{R2} ($r^2 = 0.26$ and $P = 0.5$ in 1.1 mM Ca^{++} , $r^2 = 0.45$ and $P = 0.3$ in 2.2 mM Ca^{++} , not illustrated).

The parameters returned by the model allowed reconstructing STP over a continuum of stimulation frequency. Fig 8 displays the predicted relative response amplitudes as a function of pulse ordinal number and stimulation frequency. In 1.1 mM calcium, the simulated RA reached a maximum that remained at 23 Hz with all stimulating pulses. The dynamic range increased from +41% with the second pulse to +65% with the fifth pulse, in close agreement with the experimental data (+35% and +58%, respectively, at 25 Hz). The range of frequencies over which response amplitude was more than half the maximal amplitude obtained for each pulse was quite broad with the second pulse (6–130 Hz) but narrowed with the following pulses to be restricted to the frequencies corresponding to active sniffing and to the beta and gamma band (7–76 Hz with the second pulse, 7–60 Hz with the fifth pulse).

In comparison to that observed in 1.1 mM, the dynamic range was reduced in 2.2 mM calcium, with a maximal enhancement at +22% with the second pulse and at +14% only with the fifth pulse. The frequency at which the maximum RA was reached was lower with the second pulse (17 Hz) and furthermore, it progressively drifted toward lower frequency with the

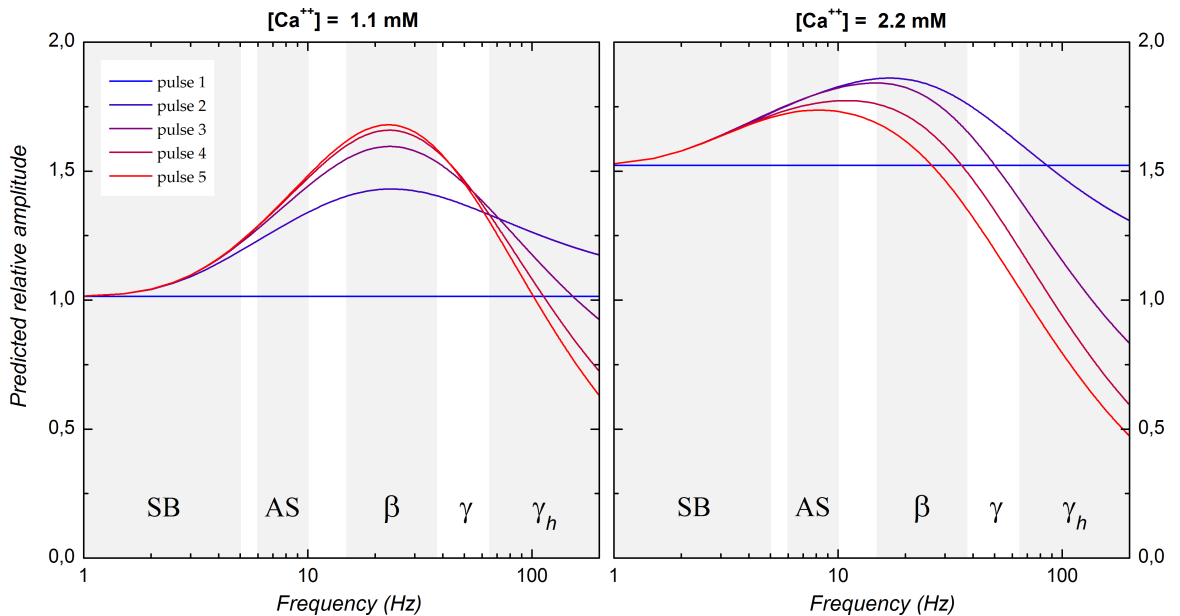


Fig 8. Relative response amplitude as a function of stimulation frequency reconstructed from short-term plasticity model parameters in 1.1 mM calcium (left) and 2.2 mM calcium (right). The simulation was computed using the mean of the parameter values after excluding one extreme value on each side of the distributions to limit possible influence of outliers. The frequency range has been subdivided into frequency bands typically observed in rodent olfactory bulb: SB, slow breathing (1–5 Hz); AS, active sniffing (6–10 Hz); β , beta band (15–37.5 Hz); γ , gamma band (37.5–65 Hz); γ_h , high gamma band (>65 Hz). The alpha band (8–12 Hz) is not represented as it partially overlaps with the AS band.

<https://doi.org/10.1371/journal.pone.0183246.g008>

following stimulation pulses (8 Hz with the fifth pulse). The half maximal amplitude frequency range drifted in parallel (5–50 Hz with the second pulse, 3–19 Hz with the fifth pulse). Finally, except for second pulse response, RA decreased below first pulse amplitude for frequencies within the gamma range (third pulse) and within the beta band (fifth pulse) whereas stimulation frequencies >100 Hz would be required to induce such reduction in 1.1 mM calcium.

Altogether these data show that the features of STP at the LOT-layer Ia synapse endows piriform cortex with the ability to amplify its afferent olfactory inputs. Yet using a “classical” extracellular calcium concentration (2.2 mM) resulted in underestimating both the amplification and the frequencies over which amplification took place. Using an *in vivo*-like ACSF revealed a larger amplification of synaptic responses especially when stimulation frequency straddled the range reported to be associated with odor-induced oscillations in the olfactory bulb.

Discussion

Our experimental data showed that, provided extracellular calcium concentration corresponds to that measured *in vivo*, response dynamics at the LOT-layer Ia synapse is characterized by a considerable response enhancement. This enhancement was maximal in the beta frequency range, although it also impinged on the gamma frequency range and on the range of frequencies associated with active sniffing. The STP model fitted to the data indicated that this enhancement was essentially achieved through the interaction of 3 mechanisms: a facilitation mechanism with a recovery time constant of 157 msec on average, that resulted in a progressive increase in response amplitude when stimulation frequency was $>$ about 2 Hz, a fast depression mechanism with a recovery time constant of 19 msec that curtailed facilitation

when stimulation frequency was > 23 Hz, and, in some cases, a depression mechanism with slower recovery. Increasing calcium concentration to 2.2 mM unsurprisingly increased the amplitude of responses evoked at low frequency but it also reduced the dynamic range of response enhancement. Furthermore, depending on pulse ordinal number, the frequency at which enhancement was maximal drifted from the low beta band to the alpha band. Finally, at stimulation frequency $> 30\text{--}50$ Hz, depression took over to the extent that response amplitude could be similar to that obtained in 1.1 mM calcium. The STP model provided three explanations for the changes induced by increasing calcium concentration: the longer time constant of facilitation accounted for part of the shift of enhancement toward lower frequencies; the slow depression mechanism, more prominent than in 1.1 mM calcium, also contributed to the shift of response enhancement toward lower frequencies; finally larger depletion of synaptic resources with the first pulse resulted in reduced reserve availability, in turn leading to stronger depression at high frequency.

Effect of calcium on response amplitude at low stimulation frequency

That postsynaptic response amplitude depends on extracellular calcium concentration is a well established fact that has been reported in numerous studies. Quantitative studies exploring this relationship initially examined the initial portion of the calcium concentration vs. response amplitude curve that can be linearized in logarithmic representation, while later studies relied on fitting the whole relationship with, among others, Hill equation as in the present study (Fig 1). These studies all demonstrated a nonlinear relationship between extracellular calcium concentration and response amplitude, with an exponent between 2 and 5 [87–95]. An exponent value of 2.5 has previously been reported in the piriform cortex [90], quite close to the Hill coefficient value of 3 reported here. A Hill coefficient of 3 suggests the cooperative action of three calcium ions in neurotransmitter release at the LOT-layer Ia synapse. Similar degree of cooperativity has been reported in other preparations [88, 93, 95]. The nonlinearity in the relationship between calcium concentration and response amplitude leads to the presence of a saturation level. This saturation level varies between synapse types, being ≈ 10 mM in the neuromuscular junction [88] and ≈ 5 mM in hippocampus [93]. Interestingly, in neocortex Rozov et al. (2001) [94] found that the saturation level depended on the identity of the postsynaptic neurons rather than that of the presynaptic neurons: ≈ 2 or ≈ 5 mM depending on whether the neurons postsynaptic to pyramidal cells were multipolar or bitufted interneurons. Our data also revealed the presence of a saturation of response amplitude with a calcium concentration of ≈ 5 mM in piriform cortex.

Comparison with previous short-term plasticity studies in piriform cortex

Short-term synaptic plasticity in piriform cortex has been examined in a number of studies, both *in vivo* and *in vitro*. Without exception all the studies relying on paired-pulse protocols revealed paired-pulse facilitation at the LOT-layer Ia synapse [84, 96–101]. The interpulse interval eliciting maximal facilitation varied from one study to another but most studies reported optimal intervals falling within the beta frequency range. Nevertheless, approaches based on paired-pulse protocols do not allow examining the whole dynamics of STP. For example, in our case the paired-pulse ratio indicated a maximal facilitation in the low beta range in 2.2 mM calcium, yet facilitation appeared to drift toward lower frequencies with additional stimuli (Fig 8). Fewer studies examined STP with trains of pulses [82, 97, 100, 102–104]. Qualitatively, our results conform with those obtained in these previous studies, although discrepancies can be noticed that may in part be attributed to differences in stimulation protocols, in animal's developmental stage, and, for *in vitro* studies, in ionic composition of the ACSF

(see below). In relation to these issues, it is noteworthy that our results (Figs 2 and 3) are very close to those obtained by Richards (1972) [97] under experimental conditions very similar to ours. Thus, typically, at the LOT-layer Ia synapse, response enhancement is observed over a range of frequencies that includes the alpha, the beta and, eventually, the gamma bands; at high stimulation frequency, recruitment of depression mechanisms tend to counteract response enhancement.

The phenomenology explained by the model

The phenomenology of STP at the LOT-layer Ia synapse is quite well established. We wanted to go further by unraveling the underlying mechanisms. For this purpose we fitted our experimental data with an STP model (adapted from: [53, 81, 82]). Optimal fit of the data required three distinct mechanisms: a facilitation mechanism and two depression mechanisms. The depression mechanisms operated on two time scales. Interestingly, the contribution of the slowest of the two depression mechanisms depended on extracellular calcium concentration. Extracellular calcium concentration also affected the time course of facilitation.

The time course of facilitation we report here is comparable to that reported at several other synapses (e. g., [105–110]). Several models of STP have been proposed (reviewed in: [29, 111]): the classical “residual calcium hypothesis” [112], which posits that accumulation of free calcium in the presynaptic terminals facilitates subsequent release of neurotransmitters; presence of high-affinity calcium binding sites with slow recovery, that would either cooperate with the main release sensor or that would facilitate presynaptic calcium current [95, 107, 113–116]; and saturation of endogenous calcium buffers [94, 117].

We found that the time constant of recovery from facilitation was longer with higher calcium concentration (Figs 6 and 7). Although it is well established that changing extracellular calcium concentration determines that amplitude of facilitation, we are unaware of studies demonstrating that such manipulation also affects the time course of facilitation. This calcium dependency suggests that the free residual calcium model is not sufficient to explain facilitation: extrusion of free calcium should display a single time constant independently of intracellular calcium concentration. Jackson and Redman (2003) [118] showed that the time constant of calcium concentration decay in synaptic terminals, τ , can associate two mechanisms, summarized by the equation: $\tau = \tau_0 \times (1 + \kappa_E)$, where τ_0 corresponds to the time constant of the calcium extrusion mechanism and κ_E to the calcium binding capacity of an endogenous calcium binding protein. An increase in τ_f would readily be explained if κ_E increases with extracellular calcium concentration.

Our results also suggest that two different depression mechanisms operate at the LOT-layer Ia synapse in our experimental conditions (Figs 6 and 7): the first one, observed in all cases, was characterized by a fast recovery time constant (<20 msec on average); the second one, whose involvement depended on extracellular calcium concentration, displayed a slower recovery time constant (100–200 msec). As these two mechanisms were revealed with relatively few stimuli, we cannot exclude additional depression mechanisms that would be revealed with longer stimulus trains. Actually, an additional depression mechanism recovering within 100 sec has been evidenced in piriform cortex with stimuli consisting in trains of hundreds of pulses [97, 102].

As for facilitation, several models have been proposed for explaining STD. Few of these mechanisms are postsynaptic and most are presynaptic. As these different mechanisms are associated with different time courses, several may operate at a given synapse.

One postsynaptic mechanism of STD, namely AMPA receptor desensitization, has been proposed to operate at some central synapses [119, 120]. Interestingly, the time constant of

recovery for this mechanism is quite fast [120–122] and appears to be similar to the time constant of recovery for the fast depression mechanism we report for the LOT-layer Ia synapse.

More traditionally, STD has been attributed to presynaptic mechanisms (reviewed in: [29, 111, 123, 124]). Among these, a fast mechanism recovering also in a few tens of msec has been reported at various synapses (e. g., [125–128]). One possible explanation for this short-lasting STD is a refractoriness of the release sites: once the immediately releasable vesicle pool has been exocytosed, release sites would be unavailable for a second release. Short-lasting inactivation of calcium currents has been proposed as an alternative mechanism [126].

Another presynaptic mechanism of STD corresponds to the emptying of the readily releasable pool of synaptic vesicles. This well documented mechanism has been demonstrated mostly in protocols based on large number of stimuli (e. g., [129–131]). Furthermore, recovery of the readily releasable pool appears to be a slow process characterized by time constants of seconds to minutes (e. g., [102, 132–134]). Our stimulation protocol was based on few stimulating pulses, and the recovery from depression was complete in much less than one second. This suggests that exhaustion of the readily releasable pool of vesicles was not the mechanism involved in our data.

In between fast and slow recovery mechanisms, depression mechanisms recovering with a time constant of the order of a few hundred msec, as our second depression mechanism, have been reported in multiple structures (e. g., [82, 108, 121, 135–137]). In our experiments we found that the strength of this type of depression increased with higher calcium concentration. Comparable calcium dependency has been reported at other synapses. In particular, at the climbing fiber to Purkinje cell synapse, Dittman and Regehr (1998) [135] demonstrated the presence of a depression mechanism, nearly lacking in 1 mM extracellular calcium, whose recovery accelerated in proportion of the extracellular calcium concentration. A calcium-dependent recovery process has also been observed in neocortex [136]. Beside, studies demonstrated that inactivation of voltage-dependent calcium channels can contribute to STD (reviewed in: [95, 111, 124]). As for facilitation, calcium-dependent STD could implicate calcium binding proteins, that could in turn regulate various processes such as voltage-dependent calcium channel inactivation or recovery of the immediately releasable vesicle pool [95, 114, 115, 135].

Effects of animal age and of extracellular calcium on short-term plasticity

Developmental stage, ionic concentrations and temperature are important variables in STP. We wished to examine STP in experimental conditions that were as close as possible to those prevailing in the adult brain *in vivo*. For this purpose we used brain slices, maintained at near physiological temperature, from adult mice and we took care to use extracellular ionic concentrations as close as possible to those reported in the interstitial fluid *in vivo* (see [Methods](#)).

A number of studies examining STP have been performed at room temperature, yet STP mechanisms may be differently affected by temperature. For example, Klyachko and Stevens (2006) [109] revealed profound effect of temperature on STP in hippocampus: depression dominated at room temperature but facilitation and augmentation prevailed when temperature $\geq 33^{\circ}\text{C}$.

It is also now well established that STP is strongly impinged by the developmental stage. For example, studies in neocortex demonstrated that STD, which prevails in immature animals, is reduced in adults while STF becomes more prominent [108, 138–143]. These developmental changes may be the consequence of an increase in endogenous adenosine concentration [137]. Developmental changes in STP have been reported also in a number of other structures, for example in the hippocampus (e. g., [144, 145]) and at the calyx of Held synapse [146].

Yet, even with adult animals, studies examining STP *in vivo* [110, 147–151] typically reported more facilitation and/or less depression than in analogue structures studied *in vitro*. Part of the difference might be explained by the presence of spontaneous activity that results in a steady state depression *in vivo* [148, 150, 152]. Another difference between *in vivo* and classical *in vitro* studies is calcium concentration: 1–1.2 mM *in vivo* vs. 2–2.5 mM in most *in vitro* studies. One reason initially invoked for justifying the use of high calcium concentration *in vitro* was that it improved the stability of intracellular recordings [153]. Hence a number of studies also demonstrated strong effects of calcium concentration on STP. In particular studies comparing STP in “classical” *in vitro* calcium concentration and in *in vivo*-like calcium concentration showed larger facilitation and/or reduced depression with the latter [109, 110, 135, 150, 151, 154–156].

Our study is a further demonstration of the importance of calcium concentration in STP, here in piriform cortex. Noticeably, had we stuck to the traditional approach of using young animals and high calcium concentration, we would have missed the large response enhancement in response to stimuli delivered in the beta frequency. Linking short-term plasticity in piriform cortex to rhythmic activity in the olfactory bulb would have then been more tentative.

Conclusion

Our results indicate that the interplay of three short-term plasticity mechanisms results in a frequency dependent enhancement of postsynaptic response amplitude at the LOT-layer Ia synapse in piriform cortex. In the *in vivo*-like ACSF the maximal enhancement was observed in the beta frequency range but was still large in the gamma frequency range (Fig 8). Beta and gamma oscillations are typically associated with olfactory stimulation in the olfactory bulb [13, 35–49]. Thus, in contrast to the hypothesis that oscillations are simply an epiphenomenon of circuit architecture, our results suggest that oscillations in the olfactory bulb have a functional impact on information transfer in downstream structures. More generally, beta and gamma oscillations are observed in a number of cortical and subcortical structures and are associated with sensory perception and with various cognitive tasks. It remains to be determined whether postsynaptic response enhancement in response to afferent stimulation at beta and gamma frequencies also takes place in these structures.

Supporting information

S1 Dataset. Individual data (n-wave amplitude as a function of calcium concentration, stimulation frequency and pulse ordinal number) are made available in the supporting information file S1_dataset.xls.

(XLS)

Acknowledgments

Thanks to Inès Carrasco, Muriel Mescam and Gianluigi Mongillo for helpful discussions and help in short-term plasticity model development. This research was supported by CNRS and by University of Toulouse 3 (IDEX transversalité 2015).

Author Contributions

Conceptualization: Caroline Fonta, Lionel G. Nowak.

Data curation: Marie Gleizes, Simon P. Perrier, Lionel G. Nowak.

Formal analysis: Marie Gleizes, Simon P. Perrier, Lionel G. Nowak.

Funding acquisition: Caroline Fonta.

Investigation: Marie Gleizes, Simon P. Perrier, Lionel G. Nowak.

Methodology: Simon P. Perrier, Lionel G. Nowak.

Project administration: Caroline Fonta, Lionel G. Nowak.

Resources: Caroline Fonta, Lionel G. Nowak.

Software: Simon P. Perrier, Lionel G. Nowak.

Supervision: Caroline Fonta, Lionel G. Nowak.

Validation: Simon P. Perrier, Caroline Fonta, Lionel G. Nowak.

Visualization: Marie Gleizes, Simon P. Perrier, Caroline Fonta, Lionel G. Nowak.

Writing – original draft: Marie Gleizes, Simon P. Perrier, Lionel G. Nowak.

Writing – review & editing: Caroline Fonta, Lionel G. Nowak.

References

1. Adrian ED, Matthews BHC. The interpretation of potential waves in the cortex. *J Physiol*. 1934; 81(4):440–71. PMID: [16994555](#)
2. Steriade M, McCormick DA, Sejnowski TJ. Thalamocortical oscillations in the sleeping and aroused brain. *Science*. 1993; 262(5134):679–85. PMID: [8235588](#)
3. O'Keefe J. Hippocampus, theta, and spatial memory. *Curr Opin Neurobiol*. 1993; 3(6):917–24. PMID: [8124075](#)
4. McCormick DA, McGinley MJ, Salkoff DB. Brain state dependent activity in the cortex and thalamus. *Curr Opin Neurobiol*. 2015; 31:133–40. <https://doi.org/10.1016/j.conb.2014.10.003> PMID: [25460069](#)
5. Buzsáki G. Theta rhythm of navigation: Link between path integration and landmark navigation, episodic and semantic memory. *Hippocampus*. 2005; 15:827–40. <https://doi.org/10.1002/hipo.20113> PMID: [16149082](#)
6. Berger H. Über das Elektroenzephalogramm des Menschen. *Arch für Psychiatrie*. 1929; 87:527–70.
7. VanRullen R, Zoefel B, İlhan B. On the cyclic nature of perception in vision versus audition. *Philos Trans R Soc Lond B Biol Sci*. 2014; 369:20130214. <https://doi.org/10.1098/rstb.2013.0214> PMID: [24639585](#)
8. Jasper H, Penfield W. Electrocorticograms in man: Effect of voluntary movement upon the electrical activity of the precentral gyrus. *Arch für Psychiatr und Nervenkrankheiten*. 1949; 183(1–2):163–74.
9. Murthy VN, Fetz EE. Coherent 25- to 35-Hz oscillations in the sensorimotor cortex of awake behaving monkeys. *Proc Natl Acad Sci U S A*. 1992; 89(12):5670–4. PMID: [1608977](#)
10. Kilavik BE, Zaepffel M, Brovelli A, Mackay WA, Riehle A. The ups and downs of beta oscillations in sensorimotor cortex. *Experimental Neurology*. 2013; 245:15–26. <https://doi.org/10.1016/j.expneuro.2012.09.014> PMID: [23022918](#)
11. Lopes da Silva FH, van Rotterdam A, Storm van Leeuwen W, Tielen AM. Dynamic characteristics of visual evoked potentials in the dog. II. Beta frequency selectivity in evoked potentials and background activity. *Electroencephalogr Clin Neurophysiol*. 1970; 29(3):260–8. PMID: [4195648](#)
12. Rougeul A, Bouyer JJ, Dédet L, Debray O. Fast somato-parietal rhythms during combined focal attention and immobility in baboon and squirrel monkey. *Electroencephalogr Clin Neurophysiol*. 1979; 46(3):310–9. PMID: [85524](#)
13. Chatrian GE, Bickford RG, Uihlein A. Depth electrographic study of a fast rhythm evoked from the human calcarine region by steady illumination. *Electroencephalogr Clin Neurophysiol*. 1960; 12:167–76. PMID: [13809431](#)
14. Eckhorn R, Bauer R, Jordan W, Brosch M, Kruse W, Munk M, et al. Coherent oscillations: A mechanism of feature linking in the visual cortex?—Multiple electrode and correlation analyses in the cat. *Biol Cybern*. 1988; 60(2):121–30. PMID: [3228555](#)
15. Gray CM, König P, Engel AK, Singer W. Oscillatory responses in cat visual cortex exhibit inter-columnar synchronization which reflects global stimulus properties. *Nature*. 1989; 338(6213):334–7. <https://doi.org/10.1038/338334a0> PMID: [2922061](#)

16. Henrie JA, Shapley R. LFP Power Spectra in V1 Cortex: The Graded Effect of Stimulus Contrast. *J Neurophysiol.* 2005; 94(1):479–90. <https://doi.org/10.1152/jn.00919.2004> PMID: [15703230](#)
17. Ahissar E, Vaadia E. Oscillatory activity of single units in a somatosensory cortex of an awake monkey and their possible role in texture analysis. *Proc Natl Acad Sci U S A.* 1990; 87(22):8935–9. PMID: [2247469](#)
18. Gross J, Schnitzler A, Timmermann L, Ploner M. Gamma oscillations in human primary somatosensory cortex reflect pain perception. *PLoS Biol.* 2007; 5(5):1168–73.
19. Joliot M, Ribary U, Llinás R. Human oscillatory brain activity near 40 Hz coexists with cognitive temporal binding. *Proc Natl Acad Sci U S A.* 1994; 91(24):11748–51. PMID: [7972135](#)
20. Brosch M, Budinger E, Scheich H. Stimulus-related gamma oscillations in primate auditory cortex. *J Neurophysiol.* 2002; 87(6):2715–25. PMID: [12037173](#)
21. Tallon-Baudry C. On the neural mechanisms subserving consciousness and attention. *Frontiers in Psychology.* 2012; 2:397. <https://doi.org/10.3389/fpsyg.2011.00397> PMID: [22291674](#)
22. Bosman CA, Lansink CS, Pennartz CMA. Functions of gamma-band synchronization in cognition: From single circuits to functional diversity across cortical and subcortical systems. *Eur J Neurosci.* 2014; 39(11):1982–99. <https://doi.org/10.1111/ejn.12606> PMID: [24809619](#)
23. Wilson MA, Bower JM. A computer simulation of oscillatory behavior in primary visual cortex. *Neural Computation* 1991; 3:498–509.
24. Shadlen MN, Movshon JA. Synchrony unbound: A critical evaluation of the temporal binding hypothesis. *Neuron.* 1999; 24(1):67–77. PMID: [10677027](#)
25. Merker B. Cortical gamma oscillations: The functional key is activation, not cognition. *Neuroscience and Biobehavioral Reviews.* 2013; 37:401–17. <https://doi.org/10.1016/j.neubiorev.2013.01.013> PMID: [23333264](#)
26. von der Malsburg C. The correlation theory of brain function. Internal Report 81–2, Dept. of Neurobiology, Max-Plank-Institute for Biophysical Chemistry, 3400 Göttingen, W- Germany. 1981.
27. Llinás R, Ribary U, Joliot M, Wang XJ. Content and context in temporal thalamocortical binding. In: *Temporal coding in the brain.* Buzsáki et al. editors, Springer-Verlag; 1994. pp. 251–272.
28. Engel AK, Roelfsema PR, Fries P, Brecht M, Singer W. Role of the temporal domain for response selection and perceptual binding. *Cereb Cortex.* 1997; 7(6):571–82. PMID: [9276181](#)
29. Zucker RS, Regehr WG. Short-Term Synaptic Plasticity. *Annu Rev Physiol.* 2002; 64(1):355–405.
30. Price JL. An autoradiographic study of complementary laminar patterns of termination of afferent fibers to the olfactory cortex. *J Comp Neurol.* 1973; 150(1):87–108. <https://doi.org/10.1002/cne.901500105> PMID: [4722147](#)
31. Haberly LB, Price JL. The axonal projection patterns of the mitral and tufted cells of the olfactory bulb in the rat. *Brain Res.* 1977; 129(1):152–7. PMID: [68803](#)
32. Igarashi KM, Ieki N, An M, Yamaguchi Y, Nagayama S, Kobayakawa K, et al. Parallel Mitral and Tufted Cell Pathways Route Distinct Odor Information to Different Targets in the Olfactory Cortex. *J Neurosci.* 2012; 32(23):7970–85. <https://doi.org/10.1523/JNEUROSCI.0154-12.2012> PMID: [22674272](#)
33. Buonviso N, Amat C, Litaudon P, Roux S, Royet JP, Farget V, et al. Rhythm sequence through the olfactory bulb layers during the time window of a respiratory cycle. *Eur J Neurosci.* 2003; 17(9):1811–9. PMID: [12752780](#)
34. Wesson DW, Donahou TN, Johnson MO, Wachowiak M. Sniffing behavior of mice during performance in odor-guided tasks. *Chem Senses.* 2008; 33(7):581–96. <https://doi.org/10.1093/chemse/bjn029> PMID: [18534995](#)
35. Manabe H, Mori K. Sniff rhythm-paced fast and slow gamma-oscillations in the olfactory bulb: relation to tufted and mitral cells and behavioral states. *J Neurophysiol.* 2013; 110(7):1593–9. <https://doi.org/10.1152/jn.00379.2013> PMID: [23864376](#)
36. Adrian ED. Olfactory reactions in the brain of the hedgehog. *J Physiol.* 1942; 100(4):459–73. PMID: [16991539](#)
37. Chapman CA, Xu Y, Haykin S, Racine RJ. Beta-frequency (15–35 Hz) electroencephalogram activities elicited by toluene and electrical stimulation in the behaving rat. *Neuroscience.* 1998; 86(4):1307–19. PMID: [9697135](#)
38. Neville KR, Haberly LB. Beta and gamma oscillations in the olfactory system of the urethane-anesthetized rat. *J Neurophysiol.* 2003; 90(6):3921–30. <https://doi.org/10.1152/jn.00475.2003> PMID: [12917385](#)
39. Ravel N, Chabaud P, Martin C, Gaveau V, Hugues E, Tallon-Baudry C, et al. Olfactory learning modifies the expression of odour-induced oscillatory responses in the gamma (60–90 Hz) and beta (15–40 Hz) bands in the rat olfactory bulb. *Eur J Neurosci.* 2003; 17(2):350–8. PMID: [12542672](#)

40. Tristan C, François D, Philippe L, Samuel G, Corine A, Nathalie B. Respiration-gated formation of gamma and beta neural assemblies in the mammalian olfactory bulb. *Eur J Neurosci.* 2009; 29(5):921–30. <https://doi.org/10.1111/j.1460-9568.2009.06651.x> PMID: 19291223
41. Lepousez G, Lledo PM. Odor Discrimination Requires Proper Olfactory Fast Oscillations in Awake Mice. *Neuron.* 2013; 80(4):1010–24. <https://doi.org/10.1016/j.neuron.2013.07.025> PMID: 24139818
42. Fourcaud-Trocmé N, Courtiol E, Buonviso N. Two distinct olfactory bulb sublaminar networks involved in gamma and beta oscillation generation: a CSD study in the anesthetized rat. *Front Neural Circuits.* 2014; 8:88. <https://doi.org/10.3389/fncir.2014.00088> PMID: 25126057
43. Frederick DE, Brown A, Brim E, Mehta N, Vujovic M, Kay LM. Gamma and Beta Oscillations Define a Sequence of Neurocognitive Modes Present in Odor Processing. *J Neurosci.* 2016; 36(29):7750–67. <https://doi.org/10.1523/JNEUROSCI.0569-16.2016> PMID: 27445151
44. Adrian ED. The electrical activity of the mammalian olfactory bulb. *Electroencephalogr Clin Neurophysiol.* 1950; 2(1–4):377–88.
45. Hughes JR, Mazurowski JA. Studies on the supracallosal mesial cortex of unanesthetized, conscious mammals. II. Monkey. C. Frequency analysis of responses from the olfactory bulb. *Electroencephalogr Clin Neurophysiol.* 1962; 14:646–653. PMID: 13955562
46. Boudreau JC. Computer analysis of electrical activity in the olfactory system of the cat. *Nature.* 1964; 201:155–158. PMID: 14118262
47. Bressler SL, Freeman WJ. Frequency analysis of olfactory system EEG in cat, rabbit, and rat. *Electroencephalogr Clin Neurophysiol.* 1980; 50(1–2):19–24. PMID: 6159187
48. Gray CM, Skinner JE. Centrifugal regulation of neuronal activity in the olfactory bulb of the waking rabbit as revealed by reversible cryogenic blockade. *Exp brain Res.* 1988; 69(2):378–86. PMID: 3345814
49. Kashiwadani H, Sasaki YF, Uchida N, Mori K. Synchronized oscillatory discharges of mitral/tufted cells with different molecular receptive ranges in the rabbit olfactory bulb. *J Neurophysiol.* 1999; 82(4):1786–92. PMID: 10515968
50. Eeckman FH, Freeman WJ. Correlations between unit firing and EEG in the rat olfactory system. *Brain Res.* 1990; 528(2):238–44. PMID: 2271924
51. Haberly LB, Shepherd GM. Current-density analysis of summed evoked potentials in opossum prepiriform cortex. *J Neurophysiol.* 1973; 36(4):789–802. PMID: 4713320
52. Shipley MT, Adamek GD. The connections of the mouse olfactory bulb: A study using orthograde and retrograde transport of wheat germ agglutinin conjugated to horseradish peroxidase. *Brain Res Bull.* 1984; 12(6):669–88. PMID: 6206930
53. Tsodyks MV., Markram H. The neural code between neocortical pyramidal neurons depends on neurotransmitter release probability. *Proc Natl Acad Sci U S A.* 1997; 94(2):719–23. PMID: 9012851
54. Nowak LG, Bullier J. Spread of stimulating current in the cortical grey matter of rat visual cortex studied on a new *in vitro* slice preparation. *J Neurosci Methods.* 1996; 67(2):237–48. PMID: 8872891
55. Nowak LG, Rosay B, Czégé D, Fonta C. Tetramisole and levamisole suppress neuronal activity independently from their inhibitory action on tissue non-specific alkaline phosphatase in mouse cortex. *Subcell Biochem.* 2015; 76:239–81. https://doi.org/10.1007/978-94-017-7197-9_12 PMID: 26219715
56. Nagayama S. Differential Axonal Projection of Mitral and Tufted Cells in the Mouse Main Olfactory System. *Front Neural Circuits.* 2010; 4:1–8.
57. Vyskocil F, Kritz N, Bures J. Potassium-selective microelectrodes used for measuring the extracellular brain potassium during spreading depression and anoxic depolarization in rats. *Brain Res.* 1972; 39(1):255–9. PMID: 5025649
58. Nicholson C, Bruggencate GT, Steinberg R, Stöckle H. Calcium modulation in brain extracellular microenvironment demonstrated with ion-selective micropipette. *Proc Natl Acad Sci U S A.* 1977; 74(3):1287–90. PMID: 2655573
59. Hansen AJ. The extracellular potassium concentration in brain cortex following ischemia in hypo- and hyperglycemic rats. *Acta Physiol Scand.* 1978; 102(3):324–9. <https://doi.org/10.1111/j.1748-1716.1978.tb06079.x> PMID: 645376
60. Astrup J, Rehncrona S, Siesjö BK. The increase in extracellular potassium concentration in the ischemic brain in relation to the preischemic functional activity and cerebral metabolic rate. *Brain Res.* 1980; 199(1):161–74. PMID: 7407619
61. Hansen AJ, Zeuthen T. Extracellular ion concentrations during spreading depression and ischemia in the rat brain cortex. *Acta Physiol Scand.* 1981; 113(4):437–45. <https://doi.org/10.1111/j.1748-1716.1981.tb06920.x> PMID: 7348028
62. Gardner-Medwin AR, Nicholson C. Changes of extracellular potassium activity induced by electric current through brain tissue in the rat. *J Physiol.* 1983; 335:375–92. PMID: 6875884

63. Yamaguchi T. Cerebral extracellular potassium concentration change and cerebral impedance change in short-term ischemia in gerbil. *Bull Tokyo Med Dent Univ.* 1986; 33(1):1–8. PMID: [3457643](#)
64. Jones HC, Keep RF. The control of potassium concentration in the cerebrospinal fluid and brain interstitial fluid of developing rats. *J Physiol.* 1987; 383:441–53. PMID: [3656129](#)
65. Jones HC, Keep RF. Brain fluid calcium concentration and response to acute hypercalcemia during development in the rat. *J Physiol.* 1988; 402:579–93. PMID: [3236250](#)
66. Zhang ET, Hansen AJ, Wieloch T, Lauritzen M. Influence of MK-801 on brain extracellular calcium and potassium activities in severe hypoglycemia. *J Cereb Blood Flow Metab.* 1990; 10(1):136–9. <https://doi.org/10.1038/jcbfm.1990.18> PMID: [2404997](#)
67. Nilsson P, Hillered L, Olsson Y, Sheardown MJ, Hansen AJ. Regional changes in interstitial K⁺ and Ca²⁺ levels following cortical compression contusion trauma in rats. *J Cereb Blood Flow Metab.* 1993; 13(2):183–92. <https://doi.org/10.1038/jcbfm.1993.22> PMID: [8436609](#)
68. Puka-Sundvall M, Hagberg H, Andine P. Changes in extracellular calcium concentration in the immature rat cerebral cortex during anoxia are not influenced by MK-801. *Dev Brain Res.* 1994; 77(1):146–50.
69. Nilsson P, Laursen H, Hillered L, Hansen AJ. Calcium movements in traumatic brain injury: the role of glutamate receptor-operated ion channels. *J Cereb Blood Flow Metab.* 1996; 16(2):262–70. <https://doi.org/10.1097/00004647-199603000-00011> PMID: [8594058](#)
70. Stiefel MF, Marmarou A. Cation dysfunction associated with cerebral ischemia followed by reperfusion: a comparison of microdialysis and ion-selective electrode methods. *J Neurosurg.* 2002; 97(1):97–103. <https://doi.org/10.3171/jns.2002.97.1.0097> PMID: [12134939](#)
71. Sun L, Kosugi Y, Kawakami E, Piao YS, Hashimoto T, Oyanagi K. Magnesium concentration in the cerebrospinal fluid of mice and its response to changes in serum magnesium concentration. *Magnes Res.* 2009; 22(4):266–72. <https://doi.org/10.1684/mrh.2009.0186> PMID: [20228005](#)
72. Hunter G, Smith HV. Calcium and magnesium in human cerebrospinal fluid. *Nature.* 1960; 186:161–162. PMID: [14405454](#)
73. Oppelt WW, MacIntyre I, Rall DP. Magnesium exchange between blood and cerebrospinal fluid. *Am J Physiol.* 1963; 205: 959–962. PMID: [5877425](#)
74. Davson H. The blood-brain barrier. *J Physiol.* 1976; 255: 1–28. PMID: [1255511](#)
75. Reed DJ, Yen MH. The role of the cat choroid plexus in regulating cerebrospinal fluid magnesium. *J Physiol.* 1978; 281:477–85. PMID: [702402](#)
76. Frosini M, Gorelli B, Matteini M, Palmi M, Valoti M, Sgaragli G Pietro. HPLC determination of inorganic cation levels in CSF and plasma of conscious rabbits. *J Pharmacol Toxicol Methods.* 1993; 29(2):99–104. PMID: [8318720](#)
77. Milhorat TH, Hammock KM. Cerebrospinal fluid as a reflection of internal milieu of the brain. In: *Neurobiology of Cerebrospinal Fluid*, vol 2, Wood JH editor. Plenum press. 1983, pp. 1–23.
78. Mulroney SE, Woda CB, Halaihel N, Louie B, McDonnell K, Schulkin J, et al. Central control of renal sodium-phosphate (NaPi-2) transporters. *Am J Physiol Renal Physiol.* 2004; 286(4):F647–52. <https://doi.org/10.1152/ajprenal.00354.2002> PMID: [14644753](#)
79. Yamamoto C, McIlwain H. Potentials evoked in vitro in preparation from the mammalian brain. *Nature.* 1966; 210:1055–6. PMID: [5914903](#)
80. Richards CD, Sercombe R. Electrical activity observed in guinea-pig olfactory cortex maintained in vitro. *J Physiol.* 1968; 197: 667–683. PMID: [5666180](#)
81. Tsodyks M, Pawelzik K, Markram H. Neural networks with dynamic synapses. *Neural Comput.* 1998; 10(4):821–35. PMID: [9573407](#)
82. Oswald A-MM, Urban NN. Interactions between behaviorally relevant rhythms and synaptic plasticity alter coding in the piriform cortex. *J Neurosci.* 2012; 32(18):6092–104. <https://doi.org/10.1523/JNEUROSCI.6285-11.2012> PMID: [22553016](#)
83. Nelder JA, Mead R. A simplex algorithm for function minimization. *Computer Journal.* 1965; 7:308–13.
84. Suzuki N, Bekkers JM. Neural coding by two classes of principal cells in the mouse piriform cortex. *J Neurosci.* 2006; 26(46):11938–47. <https://doi.org/10.1523/JNEUROSCI.3473-06.2006> PMID: [17108168](#)
85. Thomson AM, Girdlestone D, West DC. A local circuit neocortical synapse that operates via both NMDA and non-NMDA receptors. *Br J Pharmacol.* 1989; 96(2):406–8. PMID: [2564292](#)
86. Stafstrom CE, Schwindt PC, Chubb MC, Crill WE. Properties of persistent sodium conductance and calcium conductance of layer V neurons from cat sensorimotor cortex in vitro. *J Neurophysiol.* 1985; 53(1):153–70. PMID: [2579215](#)

87. Dodge FA, Rahamimoff R, Rahamimoff R. Co-operative action of calcium ions in transmitter release at the neuromuscular junction. *J Physiol.* 1967; 193(2):419–32. PMID: [6065887](#)
88. Hubbard JI, Jones SF, Landau EM. On the mechanism by which calcium and magnesium affect the release of transmitter by nerve impulses. *J Physiol.* 1968; 196(1):75–86. PMID: [4297537](#)
89. Katz B, Miledi R. Further study of the role of calcium in synaptic transmission. *J Physiol.* 1970; 207(3):789–801. PMID: [5499746](#)
90. Richards CD, Sercombe R. Calcium, magnesium and the electrical activity of guinea-pig olfactory cortex in vitro. *J Physiol.* 1970; 211(3):571–84. PMID: [5501052](#)
91. Dingledine R, Somjen G. Calcium dependence of synaptic transmission in the hippocampal slice. *Brain Res.* 1981; 207(1):218–22. PMID: [6258732](#)
92. Borst JG, Sakmann B. Calcium influx and transmitter release in a fast CNS synapse. *Nature.* 1996; 383:431–4. <https://doi.org/10.1038/383431a0> PMID: [8837774](#)
93. Reid CA, Bekkers JM, Clements JD. N- and P/Q-type Ca^{2+} channels mediate transmitter release with a similar cooperativity at rat hippocampal autapses. *J Neurosci.* 1998; 18(8):2849–55. PMID: [9526002](#)
94. Rozov A, Burnashev N, Sakmann B, Neher E. Transmitter release modulation by intracellular Ca^{2+} buffers in facilitating and depressing nerve terminals of pyramidal cells in layer 2/3 of the rat neocortex indicates a target cell-specific difference in presynaptic calcium dynamics. *J Physiol.* 2001; 531(3):807–26.
95. Xu J, He L, Wu L-G. Role of Ca^{2+} channels in short-term synaptic plasticity. *Curr Opin Neurobiol.* 2007; 17(3):352–9. <https://doi.org/10.1016/j.conb.2007.04.005> PMID: [17466513](#)
96. Yamamoto C, McIlwain H. Electrical activities in thin sections from the mammalian brain maintained in chemically-defined media in vitro. *J Neurochem.* 1966; 13(12):1333–43. PMID: [5962016](#)
97. Richards CD. Potentiation and depression of synaptic transmission in the olfactory cortex of the guinea-pig. *J Physiol.* 1972; 222(1):209–31. PMID: [4338692](#)
98. Schwob JE, Haberly LB, Price JL. The development of physiological responses of the piriform cortex in rats to stimulation of the lateral olfactory tract. *J Comp Neurol.* 1984; 223(2):223–37. <https://doi.org/10.1002/cne.902230206> PMID: [6707249](#)
99. Bower J, Haberly L. Facilitating and nonfacilitating synapses on pyramidal cells: a correlation between physiology and morphology. *Proc Natl Acad Sci U S A.* 1986; 83(4):1115–9. PMID: [3081890](#)
100. McNamara AM, Cleland TA, Linster C. Characterization of the synaptic properties of olfactory bulb projections. *Chem Senses.* 2004; 29(3):225–33. PMID: [15047597](#)
101. Yang S-C, Chiu T-H, Yang H-W, Min M-Y. Presynaptic adenosine A1 receptors modulate excitatory synaptic transmission in the posterior piriform cortex in rats. *Brain Res.* 2007; 1156:67–79. <https://doi.org/10.1016/j.brainres.2007.04.049> PMID: [17512911](#)
102. Best AR, Wilson DA. Coordinate synaptic mechanisms contributing to olfactory cortical adaptation. *J Neurosci.* 2004; 24(3):652–60. <https://doi.org/10.1523/JNEUROSCI.4220-03.2004> PMID: [14736851](#)
103. Suzuki N, Bekkers JM. Two layers of synaptic processing by principal neurons in piriform cortex. *J Neurosci.* 2011; 31(6):2156–66. <https://doi.org/10.1523/JNEUROSCI.5430-10.2011> PMID: [21307252](#)
104. Suzuki N, Bekkers JM. Microcircuits Mediating Feedforward and Feedback Synaptic Inhibition in the Piriform Cortex. *J Neurosci.* 2012; 32(3):919–31. <https://doi.org/10.1523/JNEUROSCI.4112-11.2012> PMID: [22262890](#)
105. Curtis DR, Eccles JC. Synaptic action during and after repetitive stimulation. *J Physiol.* 1960; 150:374–98. PMID: [13813399](#)
106. Lømo T. Potentiation of monosynaptic EPSPs in the perforant path-dentate granule cell synapse. *Exp Brain Res.* 1971; 12:46–63. PMID: [5543201](#)
107. Atluri PP, Regehr WG. Determinants of the Time Course of Facilitation at the Granule Cell to Purkinje Cell Synapse. *J Neurosci.* 1996; 16(18):5661–71. PMID: [8795622](#)
108. Varela JA, Sen K, Gibson J, Fost J, Abbott LF, Nelson SB. A quantitative description of short-term plasticity at excitatory synapses in layer 2/3 of rat primary visual cortex. *J Neurosci.* 1997; 17(20):7926–40. PMID: [9315911](#)
109. Klyachko VA, Stevens CF. Temperature-dependent shift of balance among the components of short-term plasticity in hippocampal synapses. *J Neurosci.* 2006; 26(26):6945–57. <https://doi.org/10.1523/JNEUROSCI.1382-06.2006> PMID: [16807324](#)
110. Reig R, Sanchez-Vives M V. Synaptic transmission and plasticity in an active cortical network. *PLoS One.* 2007; 2(8):e670.
111. Fioravante D, Regehr WG. Short-term forms of presynaptic plasticity. *Curr Opin Neurobiol.* 2011; 21:269–74. <https://doi.org/10.1016/j.conb.2011.02.003> PMID: [21353526](#)

112. Katz B, Miledi R. The role of calcium in neuromuscular facilitation. *J Physiol.* 1968; 195(2):481–92. PMID: [4296699](#)
113. Sippy T, Cruz-Martín A, Jeromin A, Schweizer FE. Acute changes in short-term plasticity at synapses with elevated levels of neuronal calcium sensor-1. *Nat Neurosci.* 2003; 6(10):1031–8. <https://doi.org/10.1038/nn1117> PMID: [12947410](#)
114. Mochida S, Few AP, Scheuer T, Catterall WA. Regulation of Presynaptic Ca_v2.1 Channels by Ca²⁺ Sensor Proteins Mediates Short-Term Synaptic Plasticity. *Neuron.* 2008; 57(2):210–6. <https://doi.org/10.1016/j.neuron.2007.11.036> PMID: [18215619](#)
115. de Jong APH, Fioravante D. Translating neuronal activity at the synapse: presynaptic calcium sensors in short-term plasticity. *Front Cell Neurosci.* 2014; 8:356. <https://doi.org/10.3389/fncel.2014.00356> PMID: [25400547](#)
116. Nanou E, Sullivan JM, Scheuer T, Catterall WA. Calcium sensor regulation of the Ca_v2.1 Ca²⁺ channel contributes to short-term synaptic plasticity in hippocampal neurons. *Proc Natl Acad Sci U S A.* 2016; 113(4):1062–7. <https://doi.org/10.1073/pnas.1524636113> PMID: [26755594](#)
117. Scott R, Rusakov DA. Main determinants of presynaptic Ca²⁺ dynamics at individual mossy fiber-CA3 pyramidal cell synapses. *J Neurosci.* 2006; 26(26):7071–81. <https://doi.org/10.1523/JNEUROSCI.0946-06.2006> PMID: [16807336](#)
118. Jackson MB, Redman SJ. Calcium dynamics, buffering, and buffer saturation in the boutons of dentate granule-cell axons in the hilus. *J Neurosci.* 2003; 23(5):1612–21. PMID: [12629165](#)
119. Jones M V., Westbrook GL. The impact of receptor desensitization on fast synaptic transmission. *Trends Neurosci.* 1996; 19(3):96–101. PMID: [9054063](#)
120. Trussell LO, Zhang S, Ramant IM. Desensitization of AMPA receptors upon multiquantal neurotransmitter release. *Neuron.* 1993; 10(6):1185–96. PMID: [7686382](#)
121. Wong AYC, Graham BP, Billups B, Forsythe ID. Distinguishing between presynaptic and postsynaptic mechanisms of short-term depression during action potential trains. *J Neurosci.* 2003; 23(12):4868–77. PMID: [12832509](#)
122. Xu-Friedman MA, Regehr WG. Ultrastructural contributions to desensitization at cerebellar mossy fiber to granule cell synapses. *J Neurosci.* 2003; 23(6):2182–92. PMID: [12657677](#)
123. Thomson AM, Deuchars J. Synaptic interactions in neocortical local circuits: Dual intracellular recordings in vitro. *Cereb Cortex.* 1997; 7(6):510–22. PMID: [9276176](#)
124. Hennig MH. Theoretical models of synaptic short term plasticity. *Front Comput Neurosci.* 2013; 7:45. <https://doi.org/10.3389/fncom.2013.00045> PMID: [23626536](#)
125. Stevens CF, Wang Y. Facilitation and depression at single central synapses. *Neuron.* 1995; 14(4):795–802. PMID: [7718241](#)
126. Dobrunz LE, Huang EP, Stevens CF. Very short-term plasticity in hippocampal synapses. *Proc Natl Acad Sci U S A.* 1997; 94(26):14843–7. PMID: [9405701](#)
127. Thomson AM, West DC. Presynaptic frequency filtering in the gamma frequency band; dual intracellular recordings in slices of adult rat and cat neocortex. *Cereb Cortex.* 2003; 13(2):136–43. PMID: [12507944](#)
128. Kobayashi M, Hamada T, Kogo M, Yanagawa Y, Obata K, Kang Y. Developmental profile of GABA_A-mediated synaptic transmission in pyramidal cells of the somatosensory cortex. *Eur J Neurosci.* 2008; 28(5):849–61. <https://doi.org/10.1111/j.1460-9568.2008.06401.x> PMID: [18691332](#)
129. del Castillo J, Katz B. Statistical factors involved in neuromuscular facilitation and depression. *J Physiol.* 1954; 124(3): 574–85. PMID: [13175200](#)
130. Betz WJ. Depression of transmitter release at the neuromuscular junction of the frog. *J Physiol.* 1970; 206(3): 629–644. PMID: [5498509](#)
131. Korn H, Mallet A, Triller A, Faber DS. Transmission at a central inhibitory synapse. II Quantal description of release, with a physical correlate for binomial n. *J Neurophysiol.* 1982; 48(3):679–707. PMID: [6127375](#)
132. Stevens CF, Tsujimoto T. Estimates for the pool size of releasable quanta at a single central synapse and for the time required to refill the pool. *Proc Natl Acad Sci U S A.* 1995; 92(3):846–9. PMID: [7846064](#)
133. Dobrunz LE, Stevens CF. Heterogeneity of release probability, facilitation, and depletion at central synapses. *Neuron.* 1997; 18(6):995–1008. PMID: [9208866](#)
134. Beck O, Chistiakova M, Obermayer K, Volgushev M. Adaptation at synaptic connections to layer 2/3 pyramidal cells in rat visual cortex. *J Neurophysiol.* 2005; 94(1):363–76. <https://doi.org/10.1152/jn.01287.2004> PMID: [15758049](#)

135. Dittman JS, Regehr WG. Calcium dependence and recovery kinetics of presynaptic depression at the climbing fiber to Purkinje cell synapse. *J Neurosci*. 1998; 18(16):6147–62. PMID: [9698309](#)
136. Fuhrmann G, Cowan A, Segev I, Tsodyks M, Stricker C. Multiple mechanisms govern the dynamics of depression at neocortical synapses of young rats. *J Physiol*. 2004; 557(Pt 2):415–38. <https://doi.org/10.1113/jphysiol.2003.058107> PMID: [15020700](#)
137. Kerr MI, Wall MJ, Richardson MJE. Adenosine A1 receptor activation mediates the developmental shift at layer 5 pyramidal cell synapses and is a determinant of mature synaptic strength. *J Physiol*. 2013; 591(13):3371–80. <https://doi.org/10.1113/jphysiol.2012.244392> PMID: [23613526](#)
138. Reyes A, Sakmann B. Developmental switch in the short-term modification of unitary EPSPs evoked in layer 2/3 and layer 5 pyramidal neurons of rat neocortex. *J Neurosci*. 1999; 19(10):3827–35. PMID: [10234015](#)
139. Angulo MC, Staiger JF, Rossier J, Audinat E. Developmental synaptic changes increase the range of integrative capabilities of an identified excitatory neocortical connection. *J Neurosci*. 1999; 19(5):1566–76. PMID: [10024344](#)
140. Frick A, Feldmeyer D, Sakmann B. Postnatal development of synaptic transmission in local networks of L5A pyramidal neurons in rat somatosensory cortex. *J Physiol*. 2007; 585(Pt 1):103–16. <https://doi.org/10.1113/jphysiol.2007.141788> PMID: [17916610](#)
141. Oswald A-MM, Reyes AD. Maturation of intrinsic and synaptic properties of layer 2/3 pyramidal neurons in mouse auditory cortex. *J Neurophysiol*. 2008; 99(6):2998–3008. <https://doi.org/10.1152/jn.01160.2007> PMID: [18417631](#)
142. Cheetham CEJ, Fox K. Presynaptic development at L4 to I2/3 excitatory synapses follows different time courses in visual and somatosensory cortex. *J Neurosci*. 2010; 30(38):12566–71. <https://doi.org/10.1523/JNEUROSCI.2544-10.2010> PMID: [20861362](#)
143. Etherington SJ, Williams SR. Postnatal development of intrinsic and synaptic properties transforms signaling in the layer 5 excitatory neural network of the visual cortex. *J Neurosci*. 2011; 31(26):9526–37. <https://doi.org/10.1523/JNEUROSCI.0458-11.2011> PMID: [21715617](#)
144. Mori-Kawakami F, Kobayashi K, Takahashi T. Developmental decrease in synaptic facilitation at the mouse hippocampal mossy fibre synapse. *J Physiol*. 2003; 553(Pt 1):37–48. <https://doi.org/10.1113/jphysiol.2003.045948> PMID: [12963803](#)
145. Speed HE, Dobrunz LE. Developmental changes in short-term facilitation are opposite at temporoammonic synapses compared to schaffer collateral synapses onto CA1 pyramidal cells. *Hippocampus*. 2009; 19(2):187–204. <https://doi.org/10.1002/hipo.20496> PMID: [18777561](#)
146. Crins TTH, Rusu SI, Rodríguez-Contreras A, Borst JGG. Developmental changes in short-term plasticity at the rat calyx of held synapse. *J Neurosci*. 2011; 31(32):11706–17. <https://doi.org/10.1523/JNEUROSCI.1995-11.2011> PMID: [21832200](#)
147. Kang Y, Endo K, Araki T. Differential connections by intracortical axon collaterals among pyramidal tract cells in the cat motor cortex. *J Physiol*. 1991; 435:243–56. PMID: [1770438](#)
148. Boudreau E, Ferster D. Short-Term Depression in Thalamocortical Synapses of Cat Primary Visual Cortex. *J Neurosci*. 2005; 25(31):7179–90. <https://doi.org/10.1523/JNEUROSCI.1445-05.2005> PMID: [16079400](#)
149. Crochet S, Fuentealba P, Cissé Y, Timofeev I, Steriade M. Synaptic plasticity in local cortical network in vivo and its modulation by the level of neuronal activity. *Cereb Cortex*. 2006; 16(5):618–31. <https://doi.org/10.1093/cercor/bhj008> PMID: [16049189](#)
150. Reig R, Gallego R, Nowak LG, Sanchez-Vives MV. Impact of cortical network activity on short-term synaptic depression. *Cereb Cortex*. 2006; 16(5):688–95. <https://doi.org/10.1093/cercor/bhj014> PMID: [16107589](#)
151. Borst JGG. The low synaptic release probability in vivo. *Trends Neurosci*. 2010; 33(6):259–66. <https://doi.org/10.1016/j.tins.2010.03.003> PMID: [20371122](#)
152. Stoelzel CR, Bereshpolova Y, Gusev AG, Swadlow HA. The impact of an LGNd impulse on the awake visual cortex: synaptic dynamics and the sustained/transient distinction. *J Neurosci*. 2008; 28(19):5018–28. <https://doi.org/10.1523/JNEUROSCI.4726-07.2008> PMID: [18463255](#)
153. Benninger C, Kadis J, Prince DA. Extracellular calcium and potassium changes in hippocampal slices. *Brain Res*. 1980; 187(1):165–82. PMID: [7357467](#)
154. Williams SR, Atkinson SE. Pathway-specific use-dependent dynamics of excitatory synaptic transmission in rat intracortical circuits. *J Physiol*. 2007; 585(3):759–77.
155. Holohan AM, Magleby KL (2011) The number of components of enhancement contributing to short-term synaptic plasticity at the neuromuscular synapse during patterned nerve stimulation progressively decreases as basal release probability is increased from low to normal levels by changing

- extracellular Ca^{2+} . *J Neurosci*. 2011; 31(19):7060–7072. <https://doi.org/10.1523/JNEUROSCI.0392-11.2011> PMID: [21562268](#)
156. Díaz-Quesada M, Martini FJ, Ferrati G, Bureau I, Maravall M. Diverse thalamocortical short-term plasticity elicited by ongoing stimulation. *J Neurosci*. 2014; 34(2):515–26. <https://doi.org/10.1523/JNEUROSCI.2441-13.2014> PMID: [24403151](#)

D. Effect of adenosine on short-term plasticity in mouse piriform cortex in vitro: adenosine acts as a high-pass filter. Simon P. Perrier, Marie Gleizes, Caroline Fonta, Lionel G. Nowak. En préparation.

1. Résumé

L'objectif de cette étude était d'examiner l'effet de l'adénosine sur la plasticité à court terme chez dans le cortex de la souris adulte. L'adénosine joue sur la transmission synaptique en particulier via ses propriétés anticonvulsives par l'intermédiaire des récepteurs A1 présynaptiques en inhibant la libération de glutamate. Par ailleurs, la plasticité synaptique à court terme peut être modulée par la probabilité de libération des neurotransmetteurs. Ainsi l'adénosine a une influence directe à la fois sur la transmission synaptique et sur la plasticité synaptique à court terme.

La transmission synaptique a été étudiée en réalisant des enregistrements électrophysiologiques dans la couche Ia du cortex piriforme de la souris à une fréquence de stimulation de 0.5 Hz. L'effet de l'adénosine exogène sur la transmission synaptique a été testé en supplémentant le milieu d'incubation avec différentes concentrations d'adénosine (10, 30, 100, 300 et 1000 µM). L'effet de l'adénosine endogène sur la transmission synaptique a également été étudié en bloquant les récepteurs A1 avec un antagoniste spécifique de ces récepteurs, le CPT (0.2 µM, 1 µM). Nos résultats montrent que la transmission synaptique est d'autant plus diminuée que la concentration en adénosine augmente. À l'inverse, le blocage du récepteur A1 à l'adénosine par le CPT augmente la transmission synaptique.

Dans un deuxième temps, nous avons étudié l'effet de l'adénosine (exogène et endogène) sur la plasticité synaptique à court terme dans la couche Ia du cortex piriforme chez la souris. Le protocole de stimulation consistait à appliquer des trains de stimulation, composés de 5 pulses consécutifs, à différentes fréquences (entre 3.125 et 100 Hz) au niveau du tractus olfactif latéral. Nos résultats montrent que l'augmentation de la concentration d'adénosine pour des fréquences supérieures à 25 Hz augmente la contribution de la facilitation. Ainsi, l'effet de l'adénosine pourrait

s'apparenter à un filtre passe-haut. A l'inverse, le blocage des récepteurs de l'adénosine A1 augmente la contribution de la dépression par rapport à la facilitation.

Par ailleurs, un modèle de plasticité synaptique (Gleizes et al., 2017) a été adapté à nos données expérimentales. Ce modèle permet de fournir une description phénoménologique des dynamiques à court terme des réponses synaptiques au moyen de divers paramètres. En situation contrôle, la plasticité que nous observions s'expliquait par 3 mécanismes : une facilitation et deux dépressions (Gleizes et al., 2017). Dans l'étude présente, nos résultats révèlent que des concentrations croissantes d'adénosine réduisent l'impact de la dépression. En effet, avec de fortes concentrations en adénosine la plasticité observée ne s'explique plus que par un seul mécanisme de facilitation. Le modèle révèle également que le facteur U, défini comme étant la probabilité initiale de libération des neurotransmetteurs, est modifié en fonction de nos conditions expérimentales. La probabilité initiale de libération des neurotransmetteurs est augmentée en présence de CPT tandis qu'elle est diminuée en présence de concentrations croissantes d'adénosine. Le facteur U serait proportionnel à la concentration intracellulaire de calcium dans le bouton présynaptique. L'adénosine et le CPT joueraient ainsi de manière opposée sur la concentration intracellulaire de calcium, qui a son tour induit une consommation plus ou moins importante de ressources vésiculaires.

2. Article

Effect of adenosine on short-term plasticity in mouse piriform cortex in vitro: adenosine acts as a high-pass filter.

Simon P. Perrier¹, Marie Gleizes¹, Caroline Fonta^{1*}, Lionel G. Nowak^{1*}

¹ CerCo, Université Toulouse 3, CNRS, Pavillon Baudot, CHU Purpan, BP 25202, 31052 Toulouse Cedex.

* Corresponding authors: lionel.nowak@cnrs.fr, caroline.fonta@cnrs.fr

Short Title: adenosine and short-term plasticity in adult mouse piriform cortex

ABSTRACT

Neuronal activity in the brain is characterized by a diversity of oscillatory phenomena, some associated with the sleep/waking cycle and others with diverse behavioral and cognitive processes. Single-unit activity is often phase-locked with oscillations recorded in the local field potential. We examined whether and how different oscillatory activities affect short-term plasticity and how adenosine controls this short-term plasticity. For this purpose we used the olfactory system as a model. Indeed, during odorant stimulation, the olfactory bulb displays a slow (1-10 Hz) respiratory rhythms as well as prominent beta and gamma oscillations. Furthermore, studies showed that the firing of mitral and tufted cells, which project to the anterior piriform cortex, is phase-locked with both beta and gamma oscillations. We examined short-term plasticity in slices of adult mouse piriform cortex maintained *in vitro* in an *in vivo*-like ACSF. In our *in vitro* study, we replaced the presynaptic neuronal firing rate by controlled and repeated electrical stimulation (trains consisting in 5 pulses, frequency between 3.125 and 100 Hz) applied to the lateral olfactory tract. Postsynaptic responses were recorded in layer 1a of the piriform cortex. Our results revealed a considerable enhancement of postsynaptic response amplitude for stimulation frequencies in the beta and gamma range. The data were fit with a phenomenological model of short-term plasticity adapted from that of Tsodyks et al. (1998). The parameters of the model indicate that the observed results can be explained by the interplay between a short-term facilitation mechanism (time constant 184 msec) and two short-term depression mechanisms, with fast (less than 20 msec on average) and slow (101 msec) recovery time constants. In the presence of adenosine (10-1000 µM), response amplitude decreased while short-term plasticity became more dominated by facilitation and less antagonized by depression. Both changes compensated for the decreased response amplitude in a frequency dependent manner: compensation was strongest at high frequency, up to restoring response amplitude to that measured in control conditions. The model suggested that the principal effect of adenosine was to decrease initial release probability; increased facilitation hereby ensued due to increased available resources. Altogether these results suggest that adenosine acts as a high-pass filter.

INTRODUCTION

Neuronal activity in the brain is associated with various oscillatory phenomena. Different kinds of oscillation have been categorized as a function of their frequency ranges and their association with cognitive, perceptive or vegetative processes. A slow rhythm (< 1Hz), delta oscillations (1-4 Hz) and

spindles (11-15 Hz) are characteristic of non-REM sleep (Adrian and Matthews 1934; Steriade et al. 1993; McCormick et al. 2015). Alpha waves (8-12 Hz) are observed during quite rest (Berger 1929) and are associated to attentional processing (VanRullen et al. 2014). Beta oscillations (13-35 Hz) were mainly associated to motor preparation (Jasper and Penfield 1949; Kilavik et al. 2013). Gamma waves (>35 Hz) have been abundantly studied in visual integration domain (Chatrian et al. 1960; Eckhorn et al. 1998, Gray et al. 1989) and are also associated with a variety of cognitive processes (reviewed in: Tal-lon-Baudry 2012; Bosman et al. 2014). The functional meanings and consequences of oscillations are presently little understood (e. g., Shadlen and Movshon 1999; Merker 2013). Our hypothesis is that oscillatory activities dynamically regulate information flow through short-term synaptic plasticity.

Short-term synaptic plasticity refers to the modulation of synaptic efficiency that takes place on a fast time scale (a few msec to < 1 min). Increase or decrease of synaptic response amplitude are referred to as facilitation and depression, respectively. Both facilitation and depression rest on several mechanisms, usually presynaptic, and with different time scales (reviewed in Zucker & Regehr 2002; Fioravante and Regehr 2011; de Jong and Fioravante 2014). Several models have been developed to determine time constants associated to different plasticity mechanisms (Hening 2013 for a review).

In a previous study (Gleizes et al. 2017), we studied short-term plasticity (STP) in the mouse olfactory system, at the connection between the olfactory bulb output and layer Ia of the anterior piriform cortex. In the olfactory bulb, odorant stimulation triggers three kinds of oscillations: a slow rhythm that corresponds to breathing as well as beta and gamma fluctuations that are superimposed over the breathing rhythm (e. g., Buonviso et al. 2003; Neville and Haberly 2003; Wesson et al. 2008; Fourcaud-Trocmé et al. 2014). Efferent axons of the olfactory bulb form the lateral olfactory tract (LOT). The LOT hence conveys these rhythmic activities to several brain regions (Price 1973; Haberly and Price 1977), of which the anterior piriform cortex is the largest. Our study demonstrated that, provided extracellular calcium is at physiological concentration, STP leads to a considerable enhancement of the postsynaptic response, especially when elicited at frequencies corresponding to beta and gamma oscillations.

Using the same approach, we focused here on the effects of adenosine on STP. Adenosine is a ubiquitous molecule with multiple physiological functions. Originally described as a powerful vasodilatator, adenosine has later been shown to possess anti-convulsive, anti-inflammatory, anti-nociceptive, neuro-protective and hypnogenic effects. Part of these effects results from the action of adenosine as a neuromodulator. In many cerebral regions, adenosine has a depressant action on neuronal activity. In cortical regions, this is mostly due to the activation of adenosine A1 receptor (reviewed in: Fredholm et al. 2005; Gomes et al. 2011). A1 receptors are preferentially expressed on synaptic terminals of excitatory neurons (Goodman et al. 1983) where they produce presynaptic inhibition by reducing calcium currents (Wu and Saggau 1994).

Adenosine contributes to couple cell metabolism to synaptic transmission. Hence, prolonged high frequency firing leads to an increase in intracellular adenosine that is externalized through equilibrative nucleotide transporters (ENTs) (King et al. 2006). Externalized adenosine acting through A1 receptors then provides a negative feedback by reducing synaptic transmission. Degradation of extracellular ATP provides the second source of extracellular adenosine: at the synaptic cleft, ATP released by neurons and/or astrocytes, is catabolized in ADP, AMP and adenosine by four families of ecto-nucleotidases called ecto-nucleoside triphosphate diphosphohydrolases, ecto-nucleotide pyrophosphatase/phosphodiesterases, ecto-5'-nucleotidase and tissue non-specific alkaline phosphatase (Zimmerman et al. 2012; Cruz et al. 2017).

Extracellular adenosine level is also determined by the sleep-waking cycle, a domain in which the hyp-

nogenic role of adenosine has long been studied (e. g., Porkka-Heiskanen et al. 1997). In cortex, hippocampus and basal forebrain, adenosine levels increase after sleep deprivation and are normalized after recovery sleep. Reducing adenosine deaminase activity, which results in an increase in extracellular adenosine, has been associated with prolonged slow wave sleep and enhanced EEG delta activity (4-8 Hz) in non-REM sleep. On the opposite, increasing adenosine kinase activity, which deplete intracellular adenosine and, through ENTs, reduces extracellular adenosine concentration, leads to reduced EEG delta power. These studies suggest that adenosine contributes to slow oscillation genesis or persistence.

In short, adenosine could enhance prevalence of slow oscillation, as shown in genetic studies, and could counteract fast activities, due to its negative feedback action. Using adapted stimulation protocol to study consequences of oscillations on signal transmission, we explored in this paper the effects of adenosine on STP at the LOT-layer Ia synapse of the anterior piriform cortex. To quantify STP mechanism parameters, we relied on a model adapted from that of Tsodyks et al. (1998).

MATERIALS AND METHODS

Ethics statement

All procedures were conducted in accordance with the guidelines from the French Ministry of Agriculture (décret 87/848) and from the European Community (directive 86/609) and was approved by the local ethical committee (comité d'éthique Midi-Pyrénées pour l'expérimentation animale, N° MP/06/79/11/12).

Brain slices preparation and ACSF composition

Brain slices were prepared as previously described (Gleizes et al. 2017). In short: brains of two- to 4-month-old C57BL/6 female mice were extracted after deep anesthetization with isoflurane. Brain extraction and brain slicing were performed in an ice-cold, oxygenated (95% O₂ / 5% CO₂), high magnesium / calcium free ACSF of the following composition (mM): NaCl 124, NaHCO₃ 26, KCl 3.2, MgSO₄ 1, NaH₂PO₄ 0.5, MgCl₂ 9, Glucose 10. Four-hundred μm thick slices were obtained with a vibratome. The cutting angle allowed preserving the axons issued from the LOT and innervating the anterior piriform cortex. After cutting, the slices were fully submerged in a storage chamber in oxygenated, *in vivo*-like ACSF, for at least 1 hour at room temperature. The *in vivo*-like ACSF composition, based on ionic concentrations measured in rodent interstitial fluid and CSF *in vivo* (for references see Gleizes et al. 2017), was (in mM): NaCl 124, NaHCO₃ 26, KCl 3.2, MgSO₄ 1, NaH₂PO₄ 0.5, CaCl₂ 1.1, and glucose 10. This ACSF was continuously bubbled with a 95 % O₂ / 5 % CO₂ mixture (pH 7.4).

Stimulation and recording

For recording, a slice was transferred to a submersion-type chamber continuously perfused with oxygenated *in vivo*-like ACSF (flow rate 3-3.5 ml/min). All recordings were performed at 34-35°C. Both electrical stimulation and extracellular LFP recordings were performed through tungsten-in-epoxylite microelectrodes (FHC, 0.2-0.3 MΩ). “Sharp” intracellular recordings were performed through glass micropipettes filled with 3 M K-Acetate (50-90 MΩ). The micropipettes were made from 1.2 mm OD medium walled capillaries with filament (GC120F, Harvard Apparatus) pulled on a P97 Flaming Brown puller. Stimulating electrodes were implanted in the LOT. Stimulation consisted in monopolar cathodal square current pulses delivered by an isolated stimulator (A365 stimulus Isolator, WPI). Local field potentials were recorded in layer Ia of the piriform cortex. The signal was amplified ($\times 1000$) and

filtered (0.1 Hz-10 kHz) with a NeuroLog system (Digitimer, UK). Intracellular recording targeted layer 2 of the anterior piriform cortex. Signals were amplified with the AxoClamp 2B amplifier (gain $\times 10$). Intracellular recording data were excluded if the membrane potential was more positive than -60 mV, if the input resistance was $<20\text{ M}\Omega$ and if the cells were unable to repetitively fire overshooting action potentials during depolarizing square current pulses lasting 120-300 msec. For both intra- and extracellular recordings, fifty Hz noise was filtered-out with a Humbug system (Quest Scientific, Canada). Signals were displayed in real-time on an oscilloscope and with Spike2 software (CED, UK). Signals were digitized at 20 kHz (1401plus or power1401, CED, UK) for off-line analysis.

The LFPs evoked in layer Ia after LOT stimulation are composed of a fiber volley followed by a slow negative wave (N-wave) (Yamamoto and McIlwain 1966). The fiber volley reflects the propagation of action potentials in axons synchronously activated by the stimulation while the N-wave corresponds to the monosynaptic excitatory postsynaptic potentials generated in the vicinity of the recording electrode. N-wave amplitude and fiber volley amplitude were measured as their peak amplitudes relative to pre-stimulus baseline. Stimulation intensity impacts on current spread and determines the stimulated volume (Nowak et al. 1996). It was kept relatively low ($6\text{-}35\text{ }\mu\text{A}$, 200 μs duration) in an attempt to avoid contamination of the N-wave by fast positive components likely due to postsynaptic action potentials generation (Richards and Sercombe 1968).

In order to examine the effect of adenosine on synaptic response amplitude and short-term synaptic plasticity, five *exogenous* adenosine concentrations have been tested (10, 30, 100, 300 and 1000 μM). In addition, the influence of *endogenous* adenosine was examined using the A1 receptor antagonist 8-cyclopentyl-1,3-dipropylxanthine (CPT). Two concentrations of CPT (0.2 and 1 μM) have been used. Since they elicited similar effects, results obtained with the two concentrations have been pooled. Adenosine and CPT were purchased from Sigma.

Dose-response relationship

Signal was processed using Spike2 software and user-written scripts. The effect of adding adenosine or CPT on field potential amplitude was monitored using electrical stimulation delivered at 0.5 Hz for 10-20 minutes. The time-course of the effect was examined by averaging the data over each consecutive minute (30 responses per average). This analysis revealed that adenosine and CPT exerted their maximal effect within 5 minutes. The last minute of the series was used for constructing the dose-response relationship (Fig 1). One to three adenosine concentrations were tested between one control and one recovery test. CPT was tested individually between one control and one recovery. Data were included only if the value during recovery differed by less than $\pm 15\%$ from that obtained in the control. For population data analysis, the data were normalized prior to averaging, with the normalized response amplitudes, NRA , corresponding to the peak amplitude of the N-wave in a given situation expressed as a fraction of the response amplitude in the control condition. The mean NRA as a function of extracellular adenosine concentration, $[Ado]$, was then fitted with Prince and Stevens (1992) model:

$$NRA = \frac{NRA_{Max}}{1 + \frac{c_0 + [Ado]}{K_d}}$$

where NRA_{max} represents the response amplitude in the presence of CPT, that is, without endogenous adenosine action, c_0 the estimated endogenous adenosine concentration, and K_d the dissociation constant of the complex formed by adenosine and adenosine A1 receptor.

Short-term plasticity

The STP protocol was applied after the 0.5 Hz stimulation period. STP was tested using stimulation trains consisting of five consecutive stimuli delivered at 6 different frequencies: 3.125, 6.25, 12.5, 25, 50 and 100 Hz. Stimulation trains were limited to 5 successive pulses for two reasons: first because the number of successive cycles in the olfactory bulb oscillation is typically between 4 and 10 (e.g., Buonviso et al 2003; Neville and Haberly 2003; Fourcaud-Trocmé et al. 2014), and second, because large number of pulses may recruit a slow adaptation (Richards 1972; Best and Wilson 2004) that would have complicated our model-based analysis. Ten seconds without stimulation followed each train to ensure recovery of synaptic resources. Each train was repeated 10 times to allow for averaging. The 10 traces obtained at a given frequency were averaged as a function of pulse ordinal number.

Individual-level data are represented as the mean \pm SEM. At the population-level and for model fitting, the *relative response amplitude* (RA_n) were calculated by dividing the amplitude of the N-wave obtained at the n^{th} stimulation (A_n) by that obtained with the first response (A_1) of each stimulation train in the *control* condition ($RA_n = A_n / A_1$, n between 1 and 5).

Short-term plasticity model

We used a phenomenological model to achieve a quantitative description of the influence of adenosine on STP parameters at the LOT-layer Ia synapse. This model, initially adapted from that developed by Tsodyks and Markram (1997) and Tsodyks et al. (1998), has been described previously (Gleizes et al. 2017). Two versions of the model were used in the present study: the first stipulates that one single facilitation mechanism can account for the data while the second allows for the presence of either one or two depression mechanisms in addition to facilitation.

In response to the first stimulation of a train, the relative response amplitude is:

$$RA_1 = E \cdot U = 1$$

where E depicts the global synaptic efficacy and U , the utilization of efficacy E , which corresponds to the proportion of E that is used at the first stimulation. U may be conceived as the calcium entry in presynaptic terminals, which leads to neurotransmitter release, while E would correspond to the theoretical maximal value obtained if the synapses released all their synaptic vesicles and/or if all postsynaptic receptors saturated.

In its full version, the aim of the model was to fit, for each stimulation rank $n > 1$, RA as the product of four terms:

$$RA_n = E \cdot r_{1,n}^- \cdot r_{2,n}^- \cdot u_n^+$$

where '*minus*' and '*plus*' indicate values, respectively, just before the stimulation and at stimulation time. u , the utilization of efficacy, implements the amount of facilitation as a fraction of E : for a pulse, u rises by a fraction of its value at the first pulse, U ; then, during the interpulse interval (IPI), u decays back to zero according to the time constant of facilitation (τ_F) as follows:

$$\text{at stimulation time: } u_{n+1}^+ = u_{n+1}^- + U \cdot (1 - u_{n+1}^-);$$

$$\text{during } IPI: u_{n+1}^- = u_n^+ \cdot e^{\frac{-IPI}{\tau_F}}$$

r_1 and r_2 represents two reserves of available synaptic resources E , such as pools of neurotransmitters vesicles or efficacy of postsynaptic receptors. At rest, $r_1 = r_2 = 1$. Then, at each stimulation, utilization of efficacy u impacts on both reserves. However, to avoid an equal influence on the two synaptic reserves, u is assumed to be distributed by factors k and $(1-k)$, respectively:

$$r_{1,n+1}^+ = r_{1,n}^- - r_{1,n}^- \cdot u_{n+1}^+ \cdot k ; r_{2,n+1}^+ = r_{2,n}^- - r_{2,n}^- \cdot u_{n+1}^+ \cdot (1-k)$$

During the IPI , r_1 and r_2 recover with time constants that correspond to two distinct time constants of recovery from depression (respectively, τ_{R1} and τ_{R2}), as follows:

$$r_{1,n+1}^- = (r_{1,n}^+ - 1) \cdot e^{\frac{-IPI}{\tau_{R1}}} + 1 ; r_{2,n+1}^- = (r_{2,n}^+ - 1) \cdot e^{\frac{-IPI}{\tau_{R2}}} + 1$$

By construction the first depression mechanism was assumed to be faster than the second one. The slowest depression mechanism was dismissed when $k=1$.

In some cases, neither fast nor slow depressions were required to fit the data and the model was simplified by removing the r terms as follows: $RA_n = E \cdot u_n^+$.

The model was adjusted to several datasets at the same time, with E as a shared parameters. Datasets corresponded to one control and one to three adenosine concentrations, or to one control and one CPT condition issued from the same experiment. Hence, one set of parameters was returned for each control, adenosine or CPT condition except for E that was assumed to be constant across experimental condition. The model fit was optimized by an iterative procedure that minimized the mean-squared error (MSE) between measured and estimated amplitudes. During parameters optimization, E , U , τ_F , τ_{R1} , τ_{R2} and k were constrained as follows: E , U and k between 0 and, respectively, 10, 1 and 1; time constants between 0 and 3 seconds with the supplementary constraint that τ_{R1} had to be inferior to τ_{R2} . When optimal k was equal to 1, τ_{R2} had no more influence and was withheld from further analysis. Robustness of fitting was estimated using root mean-squared error (RMSE).

Statistics

Paired t-test was used to compare model parameter values. Unless otherwise stated, raw population data are summarized by their means \pm SEM and comparisons (expressed as percentages) are summarized by means and 95% confidence intervals (between brackets).

RESULTS

Thirty three experiments have been performed, an experiment corresponding to one slice and, as one slice was used per mouse, to one mouse. Up to four different adenosine concentrations have been tested in each experiment, while CPT effect have been tested in 20 experiments. The total number of “tests” (one single adenosine or CPT concentration) was 66. CPT administration was systematically preceded by a control and followed by a recovery, yet between one and three adenosine concentrations were tested between one control and one recovery, such the total number of controls ($N=49$) is less than the total number of tests. Five different adenosine concentrations have been tested: 10 μ M ($N=6$), 30 μ M ($N=12$), 100 μ M ($N=13$), 300 μ M ($N=10$) and 1000 μ M ($N=5$), as well as two CPT concentrations (0.2 and 1 μ M) for which data were pooled ($N=20$).

Effect of adenosine on response amplitude

Previous studies established that adenosine inhibits synaptic transmission at the LOT-layer 1a synapse (Kuroda et al. 1976; Scholfield 1978b; Yang et al. 2007) and that this inhibitory action is mediated by presynaptic A1 receptor activation (Collins and Anson 1985; McCabe and Scholfield 1985). We first wished to confirm and quantify adenosine inhibitory effect by recording LFPs in layer Ia of the anterior or piriform cortex while the LOT was stimulated at 0.5 Hz, a stimulation frequency that minimally recruited STP mechanisms – Gleizes et al. (2017) reported a 3% difference in amplitude between responses evoked at the beginning and at the end of a 0.5 Hz stimulation train.

Fig 1A shows examples of adenosine effects on LFP in layer Ia. Two concentrations are represented: 30 and 100 μ M. Adenosine at 100 μ M reduced N-wave amplitude to about 80% of the control value. Adenosine at 30 μ M produced a weaker inhibition, with a response decrease of about 30%.

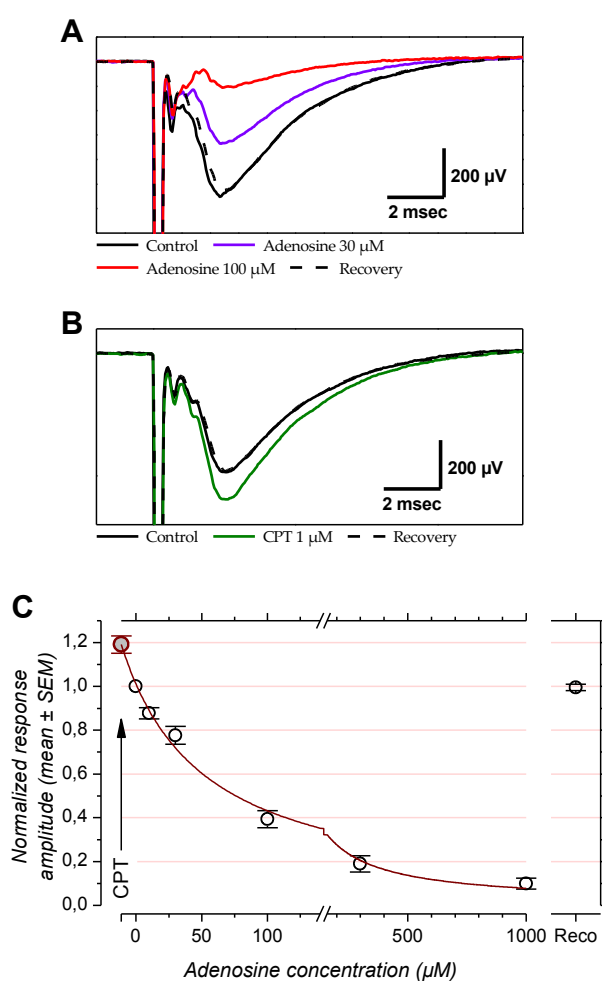


Figure 1. Effect of endogenous and exogenous adenosine on response amplitude evoked at 0.5 Hz at the LOT-layer Ia synapse. A: Example of LFP recorded in layer Ia of the piriform cortex with 2 different extracellular adenosine concentrations (30 and 100 μ M) compared to control conditions. B: Example of LFP recorded in presence or absence of CPT. C: Population data fitted with the model of Prince and Stevens (1992). Data points correspond to the mean and error bars to ± 1 SEM computed after normalizing the individual amplitudes to their corresponding control values. Red line corresponds to the fit ($R^2 = 0.99$). Note that the value obtained in presence of CPT (arrow, $c_0 = -11 \mu$ M, $NRA_{max} = 1.19$) was plotted after fitting. For enhancing data visibility, the x-axis has been divided and is presented with different scales before and after the break.

Previous studies revealed an inhibitory tone exerted by endogenous adenosine (McCabe and Scholfield 1985; Yang et al. 2007). We used CPT, an A1 receptor antagonist, to reveal this inhibitory tone. Fig 1B presents an example where CPT (1 μ M) led to an increase of N-wave amplitude by +20% relative to the control situation.

Constancy of fiber volley amplitude (Figs 1A and 1B) indicates that neither adenosine nor CPT affected action potential propagation in axons. Hence changes in N-wave amplitude can be attributed to changes taking place at the synapse.

Population data are displayed in Fig 1C. Data were normalized to the amplitude in control condition before averaging (see Methods). The NRA as a function of adenosine concentration has been fitted with Prince and Stevens (1992) model (see Methods). In the presence of CPT, the mean response amplitude was 19% above the control value. The x-value associated to CPT was estimated at $-c_0$ with a value of -11μ M (note that the data point corresponding to the CPT data in Fig 1C was plotted after fitting). In other words, the endogenous adenosine concentration in our experimental condition is equivalent to 11 μ M of bath applied adenosine. The actual endogenous concentration is likely to be much lower due to the presence of potent uptake mechanisms for adenosine (see Discussion). Including endogenous adenosine, the concentration which leads to 50% of the maximal inhibition (IC_{50}) was determined at a value of 52 μ M; it was 76 μ M if endogenous adenosine is not included.

Intracellular recordings ($N=5$, not illustrated) confirmed that adenosine exerted its inhibitory action at

the synaptic level: perfusion of adenosine ($100 \mu\text{M}$) resulted in a minor hyperpolarization by 1.75 mV (SEM 0.78 mV). This hyperpolarization should have increased the driving force for excitatory synaptic potentials, leading to a (probably insignificant) *increase* in synaptic response amplitude.

Effects of adenosine on short-term plasticity

For examining the effect of adenosine on STP at the LOT-layer 1a synapse, we used a stimulation protocol that consisted in 5-pulse trains delivered at six different frequencies between 3.125 Hz and 100 Hz

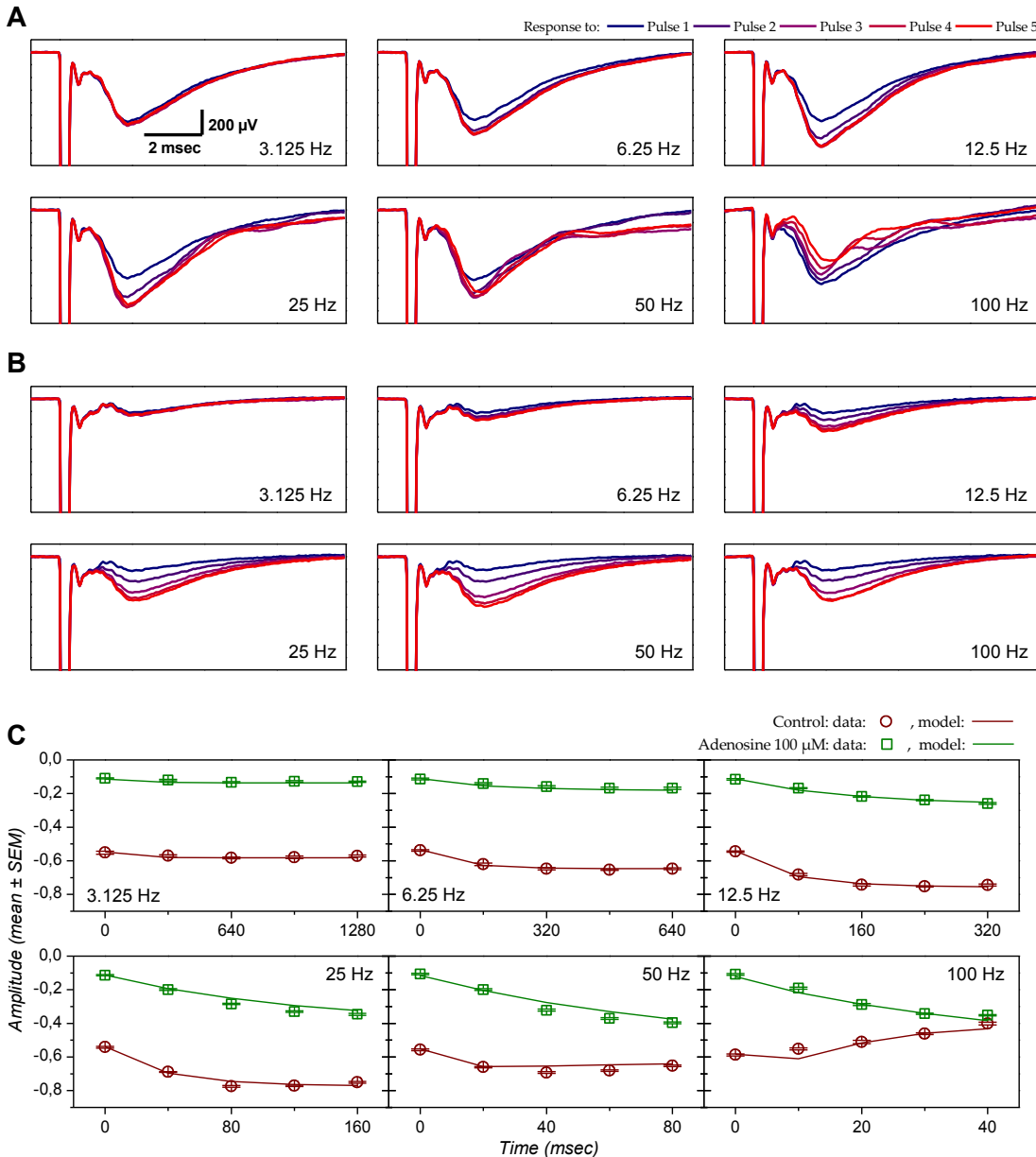


Figure 2. Example of adenosine ($100 \mu\text{M}$) effect on short-term synaptic plasticity. A and B: The 6 panels correspond to the 6 stimulation frequencies (from 3.125 to 100 Hz , annotated in each panel). Each panel shows the mean LFP traces for each of the five consecutive stimuli of a stimulation train at a given frequency. Pulse ranks are colored coded from the first (blue) to the fifth one (red). Results obtained in the control condition and in presence of adenosine $100 \mu\text{M}$ are represented in A and B respectively. Scale in the 3.125 Hz panel in A applies to all other panels. C: Maximal N-wave amplitudes (in mV) as a function of stimulus timing and frequency. Points represent experimental data (error bars denote SEM) while solid lines represent STP model fits. Red symbols and lines correspond to control situation, while green ones are associated to adenosine $100 \mu\text{M}$. Model parameters: shared parameter, $E = 1.948$. Control: $U = 0.51$, $\tau_F = 155 \text{ ms}$, $k = 0.829$, $\tau_{R1} = 17 \text{ ms}$, $\tau_{R2} = 27 \text{ ms}$; adenosine $100 \mu\text{M}$: $U = 0.106$; $\tau_F = 188 \text{ ms}$; $k = 1$; $\tau_{R1} = 10 \text{ ms}$ (τ_{R2} irrelevant as $k=1$). MSE = 0.001.

Hz. Examples of averaged LFPs for each frequency and each pulse ordinal number are presented in Figs 2 and 3. The data illustrate two experiments, one on the effect of adenosine 100 μ M (Fig 2) and the other on the effect of CPT 1 μ M (Fig 3). Fiber-volleys were stable across successive pulses in a train, allowing to conclude that variations in N-wave amplitude were not due to variations in axonal transmission. For both experiments, the peak amplitude of the N-wave was extracted and was represented as a function of stimulus time in Fig 2C and Fig 3C.

Results for both control conditions (Figs 2A, 2C and 3A, 3C) appear similar. Response amplitude remained fairly constant when stimuli were delivered at 3.125 Hz. With stimulation train between 6.25 Hz and 25 Hz, N-wave amplitudes were progressively enhanced in proportion to the stimulation frequency. The maximal amplitude was reached with the third pulse of the train at 25 Hz ($\times 1.4$ relative to the first response amplitude in Fig 2A, $\times 1.3$ in Fig 3A). Response enhancement was less pronounced at 50 Hz than at 25 Hz and it was no longer visible at 100 Hz. At 100 Hz response amplitude instead

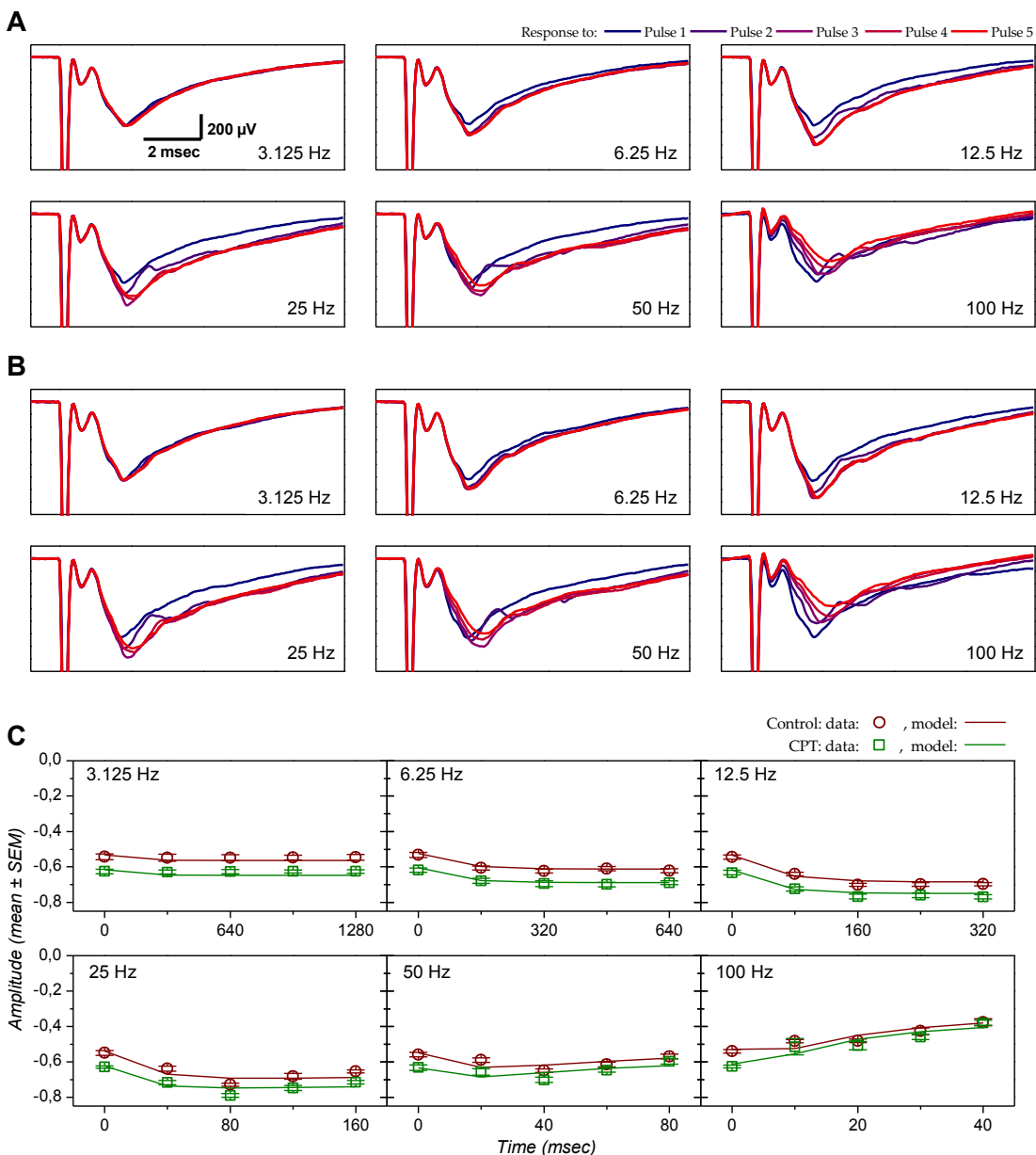


Figure 3. Example of CPT (1 μ M) effect on short-term synaptic plasticity. Same conventions as in Fig. 2. A, control LFPs. B, LFPs in CPT 1 μ M. C, N-wave amplitude, experimental data and model fit. Red symbols and line: control; green symbols and line: CPT. Model parameters: shared parameter, $E_i = 1.686$. Control: $U = 0.582$, $\tau_F = 160$ ms, $k = 0.894$, $\tau_{R1} = 14$ ms, $\tau_{R2} = 75$ ms; CPT 1 μ M: $U = 0.673$; $\tau_F = 169$ ms; $k = 0.882$; $\tau_{R1} = 12$ ms, $\tau_{R2} = 58$ msec. MSE = 0.001.

declined during the stimulation to reach a value representing 68% (Fig 2A) or 70% (Fig 3A) of first pulse amplitude at the end of the train.

The addition of 100 μM of adenosine (fig 2B, 2C) resulted in a strong reduction of first pulse response amplitudes, as expected (Fig 1). Response enhancement was visible at 6.25 Hz. It persisted with all tested frequencies including 100 Hz. Maximal enhancement was reached at 50 Hz and was much larger than the maximal enhancement in control condition ($\times 3.75$ relative to first pulse amplitude *vs.* $\times 1.4$). It has to be noticed that, in spite of the initial inhibition, response enhancement at 100 Hz was such that the response amplitude was equivalent to that observed in the control situation at the end of the stimulation train.

In the presence of CPT, response amplitude for the first pulse was larger than in control (fig 3B, 3C). Response amplitude changes as a function of stimulation frequency and pulse ordinal number for the next pulses then paralleled that observed in control condition for the three lowest frequencies. Yet for frequencies between 25 and 100 Hz condition, response amplitude differences progressively weakened; at 100 Hz the initial difference vanished during the stimulation train, as if response decline was stronger in the presence of CPT.

The examples presented in Figs 2 and 3 are representative of the mean observations. Data from STP protocols have been kept in the final sample on the basis of the goodness of STP model fit (see below) and is distributed as follows: control: N=39; CPT: N=16; adenosine 10 μM : N=5; adenosine 30 μM : N=12; adenosine 100 μM : N=8; adenosine 300 μM : N=9; adenosine 1000 μM : N=5. The dots in Fig 4 represents experimental data at the population level. Before averaging, data were normalized as a function of the first response amplitude measured in *control* situation. Relative amplitudes are plotted with colored dots, one color per condition.

As in the examples, stimulation at 3.125 Hz induced only weak increase in relative amplitudes (<10%), whatever the condition. In control condition (magenta dots in Fig 4), relative amplitudes progressively increased with the increase of stimulation frequency up to 25 Hz, at which frequency the maximal enhancement (+51%) was reached. At 50 Hz responses were still enhancement, although less than at 25 Hz (+37%). For all frequencies between 6.25 and 50 Hz, amplitudes reached their highest values with the 3rd or 4th stimulus and plateaued beyond. Responses obtained at 100 Hz showed only a weak enhancement with the second and third stimulation pulse; relative amplitudes beyond declined until reaching, at the end of stimulation train, an amplitude inferior to the initial one (-11%).

In adenosine 10 μM condition (purple dots in Fig 4), STP appeared essentially similar to that in control condition. Response amplitude appeared slightly lower than in control condition for the lowest stimulation frequencies. Yet these weak differences receded from the second pulse with stimulation frequencies between 25 and 100 Hz. Thus the initial weak inhibition induced by adenosine was counteracted by STP.

With higher adenosine concentration, STP behavior became clearly distinct from that in control situation. In adenosine 30 μM (blue dots in Fig 4), relative amplitude enhancement reached a maximum with the 4th stimulus at 25 Hz as in control situation, yet signal modulation was stronger (+70 % relative to first amplitude *vs.* +51 % in control condition). Although less pronounced at 50 and 100 Hz, this modulation persisted at a level higher than in control condition. At the end of 100 Hz stimulation train, response amplitude actually reached values comparable to those in the control condition.

In adenosine 100 μM (dark cyan dots in Fig 4), relative amplitude was enhanced with successive stimuli and reached an equivalent maximum at 25 and 50 Hz. This modulation was much bigger ($>\approx 200\%$ rel-

ative to first pulse amplitude) than in control condition and in lower adenosine concentration conditions. Furthermore, the maximal amplitude was reached, not with the 3rd or 4th stimulus but with the last pulse of the train – the plateau was less marked than in previous conditions. At 100 Hz, response enhancement persisted, although slightly weaker than with lower stimulation frequencies. This persistent enhancement was sufficient to lead to a relative amplitude similar to the control one at the end of the stimulation train.

With adenosine between 10 and 100 μM , the initial inhibition induced by adenosine seemed to be counteracted by a stronger response enhancement. STP allowed preserving an equivalent synaptic transmission in the highest frequency bands. In particular at 100 Hz all response amplitudes converged to the one obtained in the control condition. A trend toward such convergence was also noticeable at 50 Hz.

With 300 and 1000 μM of added adenosine (dark green and green dots in Fig 4), STP behavior appeared to be identical, as if a floor effect for adenosine was reached. Initial amplitudes were at the same level (14–15% of control amplitude). Response enhancement became visible at 12.5 Hz and was less prominent than in the other conditions. With higher stimulation frequencies and in contrast to the other conditions, response amplitude did not plateau and increased linearly instead. The strongest response enhancements was observed at 50 and 100 Hz and reached values between +230 and +245% of first response amplitude, yet, despite this considerable enhancement, response amplitude at the end of the 100 Hz train remained at 45% of the response amplitude at the end of the 100 Hz train in the control condition.

We used CPT to examine the influence of endogenous adenosine on STP (red dots in Fig 4). Antagonist effect was visible at the first pulse with an increase of about +17 % relative to control response amplitude. Then, as in the example in Fig 3, relative amplitudes were enhanced with stimulation frequencies between 6.25 Hz and 50 Hz. Relative amplitude reached a comparable maximum at 12.5 and

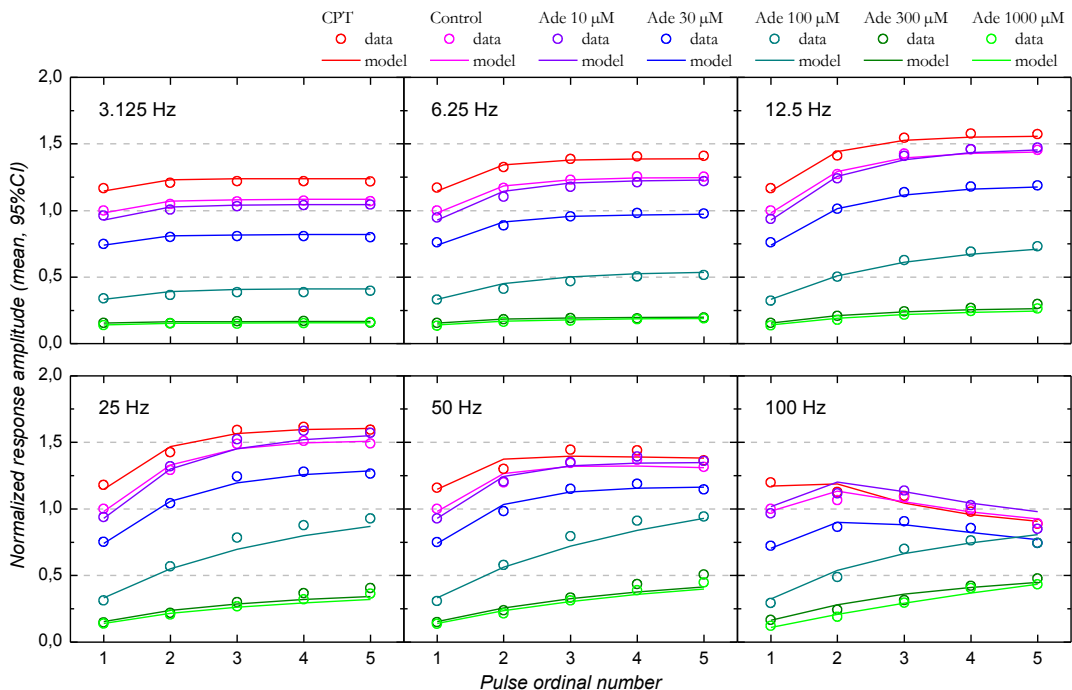


Figure 4. Effect of adenosine and CPT on short-term synaptic plasticity at the population level. CPT (adenosine A1 receptor antagonist) and different extracellular adenosine concentrations (10, 30, 100, 300 and 1000 μM) were tested with a short-term synaptic plasticity protocol. Relative amplitudes associated to each condition (colored dots) are plotted as a function of stimulation pulse ranks and of stimulation frequency (3.125 to 100 Hz, annotated above each graph). Predicted values by the STP model are represented by solid lines. $N_{\text{CPT}} = 16$; $N_{\text{Ctrl}} = 39$; $N_{\text{Ade}10\mu\text{M}} = 5$; $N_{\text{Ade}30\mu\text{M}} = 12$; $N_{\text{Ade}100\mu\text{M}} = 8$; $N_{\text{Ade}300\mu\text{M}} = 9$; $N_{\text{Ade}1000\mu\text{M}} = 5$. Error bars are not presented for preserving visibility of the data.

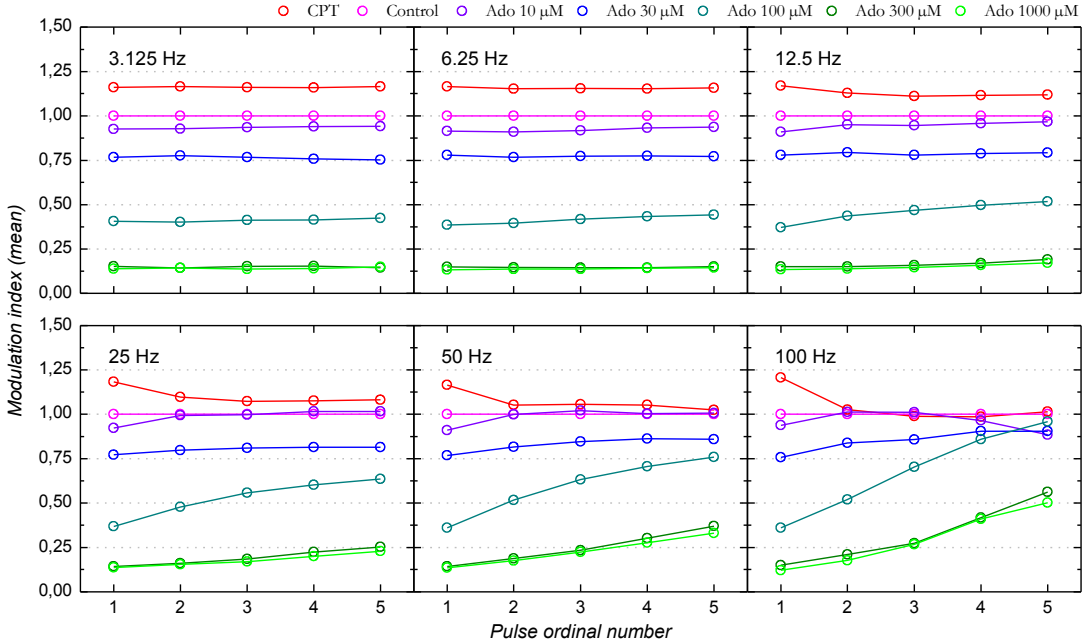


Figure 5. Changes in similitude index indicate that short-term synaptic plasticity counteracts adenosine inhibition at high stimulation frequency. The similitude index corresponds, for a stimulus of order n , to the ratio of N-wave amplitude in a given condition (adenosine or CPT) divided by the control N-wave amplitude. Similitude indices associated to each condition are plotted as a function of stimulation pulse ranks and of stimulation frequency (3.125 to 100 Hz, annotated above each graph). Colored dots indicates the different tests (CPT and adenosine at 10, 30, 100, 300 and 1000 μ M). Error bars are not presented for preserving data visibility.

25 Hz, with a signal modulation of +35 and +38% relative to first response amplitude. Most notably, differences between CPT and control condition weakened at 25-50 Hz and disappeared at 100 Hz.

These results show that, in addition to dose effect visible with the first pulse, adenosine had two further actions on signal modulation during the stimulation trains: first, the relative enhancement during stimulation trains was stronger with higher adenosine concentration; second, the frequency at which modulation was the strongest appeared to shift toward higher values with the increase in extracellular adenosine concentration. A consequence of these effects was that the inhibition induced by adenosine lost a great part of its influence during high frequency stimulation.

Hence the initial loss in response amplitude seemed to be compensated by short-term synaptic plasticity. This frequency-dependent counterbalance is further illustrated in Fig 5, which represents the “similitude index” with respect to adenosine concentration and stimulation frequency. The similitude index, SI , is calculated as the response amplitude obtained with a stimulus of rank n in one condition ($cond$) divided by the response amplitude obtained with the *same* stimulus rank in the control ($cont$) condition: $SI_n = A_{cond,n} / A_{cont,n}$. In the presence of adenosine, the SI remained at a steady level below unity for all stimuli at low frequency (3.125 and 6.25 Hz); conversely, in the presence of CPT the SI remained at a constant value above unity for all stimuli. For frequencies between 12.5 Hz and 50 Hz, the SI tended to increase, in particular with adenosine at 100 μ M, while it tended to decrease in the presence of CPT. At 100 Hz the SI at the end of the stimulation trains reached a value close to 1 for CPT and for adenosine at 10, 30 and 100 μ M: at this frequency the effect of adenosine or of adenosine receptor blockade were fully compensated by STP.

Short-term plasticity model

To quantify the effect of adenosine on STP, we fitted the data with the model we previously used to explore the influence of calcium on STP in piriform cortex (Gleizes et al. 2017). This model (see Methods) was derived from those of Tsodyks and Markram (1997) and Tsodyks et al. (1998). STP is a combination of facilitation and depression mechanisms. These mechanisms possess different time constants that determine the speed of recovery to the steady state. Depending on stimulation frequency, these phenomenological rules directly influence relative amplitude evolution.

To fit the present data, we used two variants of our model: one with facilitation only and another that, in addition to facilitation, included up to two depression mechanisms. Fittings were made at once on experimental datasets consisting in one control and one CPT condition, or one control and 1-3 adenosine conditions, with E , the global synaptic efficacy, shared across conditions.

As highlighted in the examples in Figs 2C and 3C, the STP model reproduced the observed STP behaviors in both control condition and in CPT and adenosine 100 μM conditions (solid lines for model compared to dots in same color for observed data). In the control condition, the modeled STP rests on three mechanisms: a facilitation mechanism with a recovery time constant around 155-160 ms, and two depression mechanisms that recovered with different time constants. The fastest was similar in both examples around 14-17 ms; the slowest appeared quite distinct with values of 27 and 75 ms. This difference was visible by difference in the persistence of the plateau effect that appeared at 50 Hz of stimulation. k , in both cases, displayed high values, 0.83 and 0.89, indicating more importance for the depression associated to the fastest recovery time constant. Thus, enhancement up to 25 Hz can be explained by the dominance of a facilitation mechanism with a long time constant of recovery. For higher frequencies the fast depression counteracted facilitation and led to a decrease of relative amplitude.

In CPT condition (Fig 3C), data were fitted by a model composed of the same three components. The difference with the control situation was mostly explained by an increase by about 15% in synaptic resource utilization at the first pulse, U ($U_{\text{ctrl}}=0.580$ vs. $U_{\text{CPT}}=0.673$). A small decrease of slow depression recovery time constant was also noticed (from 75 ms in control situation to 58 ms in CPT condition).

The model fit obtained in the presence of adenosine 100 μM returned a value of 1 for parameter k . This indicates that two mechanisms (facilitation and fast depression) were sufficient to fit the data in this case. The recovery time constant for facilitation was increased by about 20 %. A large decrease of U was obtained (-79%), which indicates a strong decrease in resource utilization that in turn resulted in a reduced influence of depression through rapid synaptic reserve recovery. Thus facilitation was predominant to explained STP in this example.

Model optimization rested on MSE minimization. The model fit quality was evaluated with the root mean square error (RMSE), which have the same dimension as the relative amplitude. Data have been excluded from further consideration when RMSE was >0.1 . For the remaining 39 datasets, the mean RMSE was 0.048 [95%CI: 0.043 – 0.054] – that is, a <5% difference between observed and predicted data on average.

At the population level, relative amplitudes predicted by the model were averaged then represented in Fig 4 by solid lines. Mean predicted values appear to be quite similar to the mean observed values. Goodness of fit is further illustrated in Fig 6, which represents the predicted data as a function of the observed data. The alignment to the diagonal of equality and the global correlation coefficient, r^2 , of 0.986 attest for the model fit quality.

For a given dataset both models, *i.e.*, with or without depression, could be used. The model without

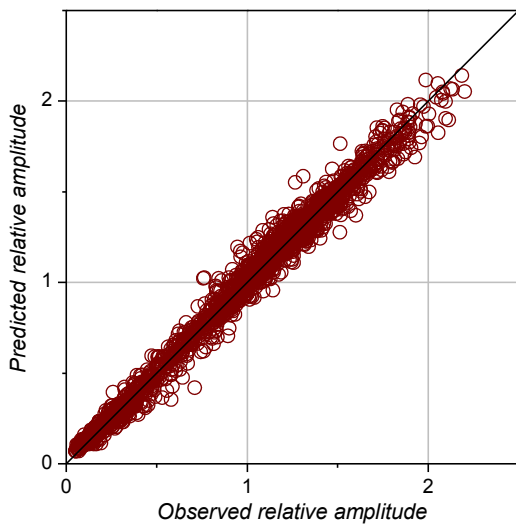


Figure 6. Scatterplot of predicted relative amplitudes as a function of observed values. In total, 2620 values are represented. Perfect prediction is represented by the diagonal in black. A linear correlation was calculated to compare best theoretical predictions to the observed, which gave an r^2 of 0.986.

of the slow depression mechanism, then to that of the highest extracellular adenosine concentration tested, the model did not require depression to explain the observed STP.

Distribution of STP parameters are represented as cumulative distribution in Fig 7.

E , as the maximal potential of synaptic transmission, is a ceiling level for response amplitude. Among the 39 datasets, E was distributed from 1.41 to 5.08 with a mean of 2.43 ± 0.14 (SEM).

U is defined as initial probability of release. In control condition U averaged 0.447 ± 0.021 (SEM). In the presence of CPT, U increased significantly ($P=0.0003$) by 17% [10%-24%] in comparison to paired control. Conversely, U decreased significantly with increasing adenosine concentration except for adenosine at 10 μM ($P=0.35$). The decrease of U was proportional to adenosine concentration. In adenosine 30 μM , U reached a value representing 75% [65%-85%] of the control value ($P=0.0005$). In adenosine 100 μM , U reached a value representing 34% [24%-44%] of the control value ($P=0.0002$). In adenosine 300 μM , U reached a value representing 15% [10%-21%] of the control value ($P=0.00002$) and a value representing 14% [6%-23%] of the control value ($P=0.0003$) in adenosine 1 mM. As U reflects the first synaptic resource utilization, it varied in the same way as the initial relative amplitude; in other words, its variation merely reflects the dose-response effect of adenosine (Fig 1).

In contrast to U , other model parameters did not appear to be significantly affected by CPT or adenosine and their cumulative distribution all overlapped to some extent (Fig 7). The recovery time constant for facilitation, τ_F , presented a mean value of $0.184 \text{ msec} \pm 0.012$ (SEM) in control conditions. As shown in Fig 7, the same range of values were observed in the different experimental condition and no significant difference could be detected except for a small, although significant ($P=0.003$), increase (+9%) in adenosine 10 μM .

For data fitted with the two-depression model, the parameter k determines the allocation of the synaptic resources into two subgroups, one that shows a fast and the other a slow recovery from depression. When k is equal to 1, only rapid depression was required for fitting the data. At the population level, k was not significantly affected by CPT or adenosine ($P>0.05$ for all comparisons). However, as

depression yielded better fits only with the highest adenosine concentrations (100-1000 μM), and the proportion of fits without depression increased with adenosine concentration: 25% (2/8 cases) with adenosine 100 μM , 78% (7/9) with adenosine 300 μM , and 100% (5/5 cases) with adenosine 1000 μM . Adequate fit of STP data for adenosine concentrations $<100 \mu\text{M}$, as well as for control and for CPT conditions, required models with at least the fast depression in addition to the facilitation mechanism in all cases. For control, CPT and adenosine 10 μM , the model with two depressions returned better MSE than the model with one depression in the majority of cases (64%, 56% and 60% respectively). Yet for adenosine concentrations of 30, 100 and 300 μM the converse was observed, with a minority of cases requiring two depressions (42, 25 and 0% respectively). Altogether these results suggest that increasing adenosine concentration leads first to the disengagement of the fast depression mechanism. Hence, with the highest extracellular adenosine concentration tested, the model did not require depression to explain the observed STP.

Distribution of STP parameters are represented as cumulative distribution in Fig 7.

E , as the maximal potential of synaptic transmission, is a ceiling level for response amplitude. Among the 39 datasets, E was distributed from 1.41 to 5.08 with a mean of 2.43 ± 0.14 (SEM).

U is defined as initial probability of release. In control condition U averaged 0.447 ± 0.021 (SEM). In the presence of CPT, U increased significantly ($P=0.0003$) by 17% [10%-24%] in comparison to paired control. Conversely, U decreased significantly with increasing adenosine concentration except for adenosine at 10 μM ($P=0.35$). The decrease of U was proportional to adenosine concentration. In adenosine 30 μM , U reached a value representing 75% [65%-85%] of the control value ($P=0.0005$). In adenosine 100 μM , U reached a value representing 34% [24%-44%] of the control value ($P=0.0002$). In adenosine 300 μM , U reached a value representing 15% [10%-21%] of the control value ($P=0.00002$) and a value representing 14% [6%-23%] of the control value ($P=0.0003$) in adenosine 1 mM. As U reflects the first synaptic resource utilization, it varied in the same way as the initial relative amplitude; in other words, its variation merely reflects the dose-response effect of adenosine (Fig 1).

In contrast to U , other model parameters did not appear to be significantly affected by CPT or adenosine and their cumulative distribution all overlapped to some extent (Fig 7). The recovery time constant for facilitation, τ_F , presented a mean value of $0.184 \text{ msec} \pm 0.012$ (SEM) in control conditions. As shown in Fig 7, the same range of values were observed in the different experimental condition and no significant difference could be detected except for a small, although significant ($P=0.003$), increase (+9%) in adenosine 10 μM .

For data fitted with the two-depression model, the parameter k determines the allocation of the synaptic resources into two subgroups, one that shows a fast and the other a slow recovery from depression. When k is equal to 1, only rapid depression was required for fitting the data. At the population level, k was not significantly affected by CPT or adenosine ($P>0.05$ for all comparisons). However, as

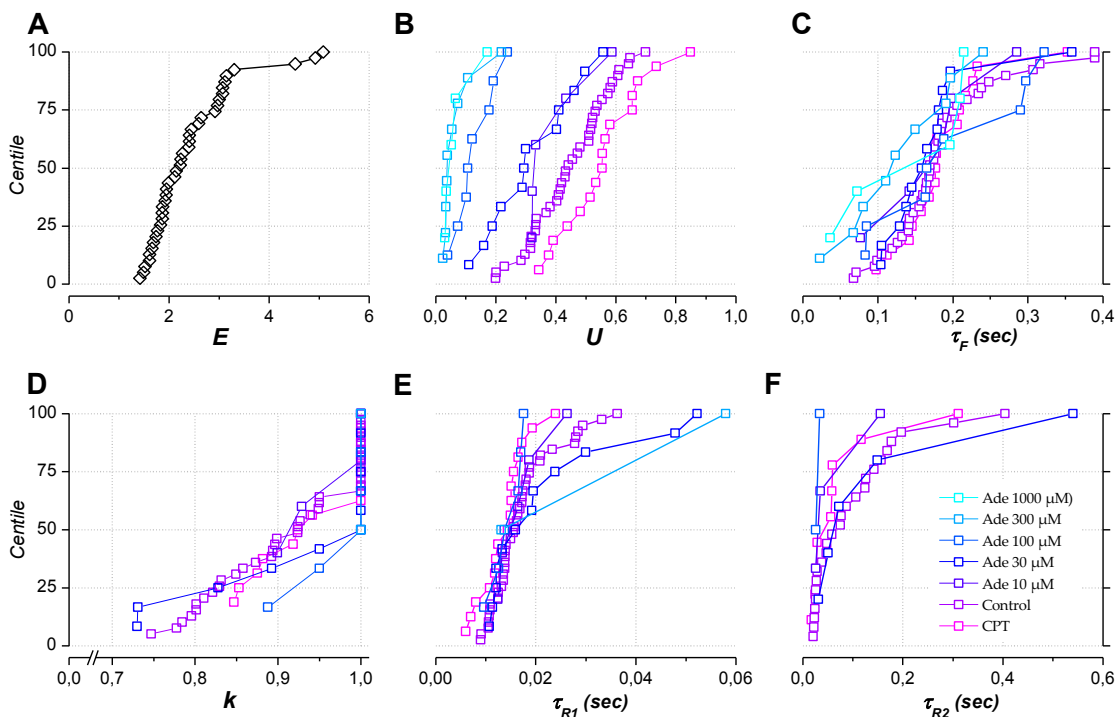


Figure 7. Short-term synaptic plasticity parameters: cumulative distribution at the population level. Parameters were determined by fitted datasets containing one control and one to three tested conditions (only one for CPT condition). For each dataset, E is independent from the experimental condition, and its values are represented in first panel in black. The other parameters form a set associated for a condition.

mentioned above, increasing adenosine reduced the proportion of models requiring 2 vs. 1 depression mechanism.

Time constants for fast and slow depression recovery also seemed to be independent of the tested condition (Fig 7; $P>0.05$ for all comparisons). In control condition the recovery time constant for the fast depression mechanism averaged $17 \text{ ms} \pm 1 \text{ msec}$ (SEM). For the slow depression mechanism the recovery time constant averaged $101 \pm 19 \text{ msec}$.

Altogether these experiments allowed determining which mechanisms of STP at the LOT-layer Ia synapse were affected by extracellular adenosine concentration. Globally, increasing extracellular adenosine concentration reduced the impact of depression on synaptic transmission. The model suggests that differences in STP behaviours were mostly explained by two phenomena: 1) a reduction of the number of depression mechanisms and 2) a decrease of initial release probability (U) with increased adenosine concentration. The consequence is that, despite the initial inhibition induced by adenosine (decrease in U), changes in STP dynamics led to an increase in response amplitude especially for signal transmitted at high frequency. This way, adenosine could be envisioned as a high-pass filter, efficiently inhibiting synaptic transmission at low frequency but letting through high-frequency signals.

DISCUSSION

Dose-response relationship

In the first part of this study, we examined the dose-response effect of adenosine on synaptic transmission at the LOT-layer 1a synapse. The inhibitory action of adenosine has been established long ago in various structures including the neuromuscular junction (Ginsborg and Hirst 1972), neocortex (Phillis et al. 1975), hippocampus (Schubert and Mitzdorf 1979; Dunwiddie and Hoffer 1980) and piriform

cortex (Kuroda et al. 1976; Scholfield 1978). In piriform cortex, the inhibitory action of adenosine at the LOT-layer Ia synapse has been attributed to A1 receptor activation (Collins and Anson 1985; McCabe and Scholfield 1985). The dose-response relationship we constructed using Prince and Stevens (1992) model returned an IC_{50} of 76 μ M. This value is in between those reported in previous piriform cortex studies: McCabe and Scholfield (1985) and Yang et al. (2007) reported IC_{50} s of the order of 7-8 μ M while at the other extreme Collins and Anson (1985) reported an IC_{50} of 139 μ M. Several factors may explain these discrepancies. In particular, powerful adenosine uptake (through ENTs) and adenosine degradation (by adenosine deaminase) mechanisms are capable to strongly reduce bath-applied adenosine concentration as it diffuses through the brain tissue; as a result of this reduction, Dunwiddie and Diao (1994) estimated that the “real” IC_{50} for adenosine action in hippocampus was between 0.60 and 0.76 μ M only. Any environmental factor that affects adenosine diffusion, uptake and degradation would therefore affect the apparent IC_{50} . For example, experiments conducted at room temperature, as in Yang et al. (2007) study, would slow down uptake and degradation mechanisms and decrease the apparent IC_{50} .

In our experiments, postsynaptic response amplitude were increased by about 20% in the presence of CPT, an A1 receptor antagonist. This reveals the presence of endogenous adenosine that generates a sustained inhibitory tone at the LOT-layer 1a synapse. In piriform cortex, a +15% response increase was previously reported by McCabe and Scholfield (1985) after blocking endogenous adenosine intracellular signaling pathway. Yang et al. (2007), on the other hand, reported a +84% increase of postsynaptic response amplitude after blocking endogenous adenosine action with DPCPX, another A1 receptor antagonist. Using Prince and Stevens (1992) model, we could extrapolate that the endogenous adenosine concentration is equivalent to 11 μ M of bath-applied adenosine. The same value was extrapolated by Prince and Stevens (1992) in the dentate gyrus. Using the same approach, Kerr et al. (2013) extrapolated the endogenous adenosine concentration to be equivalent to 23 μ M of bath applied adenosine layer 5 of neocortex. For the reason given above, the “real” endogenous adenosine concentration is likely to be much lower. In hippocampus, Dunwiddie and Diao (1994) estimated that this concentration would be around 0.14-0.20 μ M.

Effect of adenosine on short-term plasticity

The main purpose of this study was to examine the effect of adenosine on short-term synaptic plasticity at the LOT-layer Ia synapse of the adult mouse piriform cortex *in vitro* using environmental conditions (temperature, ionic concentrations) as close as possible to those that prevail *in vivo*. For this purpose, we use 5-pulse trains of stimuli emitted at frequencies between 3.125 and 100 Hz frequency. This frequency range allowed us to approximate the influence of oscillations identified *in vivo*, including those emitted by the olfactory bulb: respiratory rhythm, β and γ fluctuations. In agreement with our previous study (Gleizes et al. 2017), we observed that, in the control situation, repeated stimulation led to a enhancement of postsynaptic responses, which was maximal at 25 Hz. This enhancement was barely visible with the lowest frequency tested (3.125 Hz) and was eventually replaced by a response decline at the highest frequency tested (100 Hz). As described in Gleizes et al. (2017), response enhancement at β and γ frequencies would have been missed, had we used the environmental factors that are traditionally used in *in vitro* studies – in particular extracellular calcium concentration.

As far as piriform cortex is concerned, only few studies reported the action of adenosine on short-term plasticity. Okada and Saito (1979) and Yang et al. (2007) restricted their exploration to the examination of paired-pulse ratios (PPR). Both studies reported that the PPR increased with adenosine, and Yang et al. (2007) reported a decrease of the PPR with DPCPX. Increase in PPR, attributed to the presynaptic action of adenosine acting on A1 receptors, has been reported in many

other brain regions.

The predominant effect of adenosine in the present study was to reinforce response enhancement in comparison to that in control condition. Conversely, blocking endogenous adenosine receptor had an opposite effect. Moreover, we showed that the strengthening of response enhancement depended on both stimulation frequency, pulse ordinal number and adenosine concentration (Fig 4). For example, maximal response enhancement in adenosine at 30 μ M occurred at 25 Hz, as in control condition whereas that obtained with adenosine 100 μ M was at 25-50 Hz and at 50-100 Hz with higher adenosine concentrations. To further examine the effects of adenosine concentration and stimulation frequencies, response amplitudes were compared pulse by pulse with those in control condition. The “similitude index” (Fig 5) thus computed revealed that responses obtained in CPT tended to converge toward those obtained in control condition during the stimulation train, and reached control amplitude at the second stimulation at 50 and 100 Hz. The same converging action was observed with adenosine at 10 μ M when stimulation frequency was \geq 25 Hz and with adenosine at 30 and 100 μ M when stimulation frequency was at 100 Hz.

Mechanisms involved in the action of adenosine on short-term plasticity

The results we obtained indicate two opposite action of adenosine: first a reduction of response amplitude at 0.5 Hz, that persisted at 3.125 and 6.25; second, a reinforcement of response enhancement, which was predominant with high stimulation frequencies. This last feature suggests that adenosine had an effect STP mechanisms with fast kinetics. The phenomenological model of STP we applied to the data allowed determining with mechanisms accounted for the effect of adenosine.

The main effect of changing adenosine concentration was a significant changes of the initial probability of release, U . U increased in the presence of CPT and decreased in proportion of the concentration of bath applied adenosine. This readily explains changes in response amplitude at the first stimulation pulse, as it is solely determined by U . Kerr et al. (2013), who analyzed STP between layer 5 pyramidal cells using Tsodyks/Markram model, also suggested that the main effect of endogenous and exogenous adenosine was to modify the initial release probability.

None of the other model parameters showed significant changes with changes in adenosine concentration. This is at variance with the results obtained in our previous study (Gleizes et al. 2017), where we found that changing calcium concentration impacted on two additional parameters in addition to U : the time constant of facilitation that increased when calcium concentration was doubled, and the sharing of synaptic resources, k , that decreased when calcium concentration was doubled.

In the present study, we nevertheless noticed another consequence of increasing adenosine concentration: the number of dynamic components required for fitting the data progressively decreased. Proportions of cases requiring 2 depressions (fast and slow) and one facilitation were the highest with CPT, in control, and with adenosine 10 μ M. With adenosine 30 and 100 μ M most cases required one fast depression and one facilitation mechanisms. In the end, with adenosine 300 and 1000 μ M, only the facilitation mechanism was required for fitting most datasets.

These results could be explained by the presence of a “threshold” below which the low use of synaptic resources (low values of U in high adenosine concentration) prevented the occurrence of depression. Provided exhaustion does not occur, then only facilitation takes place. Our model does not include such a threshold but future development could make it explicit.

Conclusions

The filtering of low, but not high, frequencies by adenosine is opposite to what was expected given the hypnogenic role of adenosine, and especially its influence on the genesis of the δ (slow waves) oscillations. On the basis of this observation, it could be anticipated that adenosine would tend to decrease the high frequencies on one hand, and increase the low frequencies on the other hand. Yet it is just the opposite that we have observed.

Adenosine is a hypnogenic agent, and it can be imagined that despite the sleepiness it induces, some information would still be important to treat even in the event of sleep necessity (e. g., a bear growl near the cave). This type of urgent information could induce high frequencies firing at the neuronal level. Then adenosine would leave communication at high frequency possible, and would allow us to perceive or become aware of the danger even if one is at the doors of sleep.

ACKNOWLEDGMENTS

Thanks to Inès Carrasco, Muriel Mescam and Gianluigi Mongillo for helpful discussions and help in short-term plasticity model development. This research was supported by CNRS and by University of Toulouse 3 (IDEX transversalité 2015).

REFERENCES

- Adrian ED, Matthews BHC (1934) The interpretation of potential waves in the cortex. *J Physiol* 81: 440-471.
- Berger H (1929) Über das elektrenkephalogramm des menschen. *Archiv für Psychiatrie und Nervenkrankheiten* 87: 527-570.
- Best AR, Wilson DA (2004) Coordinate synaptic mechanisms contributing to olfactory cortical adaptation. *J Neurosci* 24: 652-660.
- Bosman CA, Lansink CS, Pennartz CM (2014) Functions of gamma-band synchronization in cognition: from single circuits to functional diversity across cortical and subcortical systems. *Eur J Neurosci* 39: 1982-1999.
- Buonviso N, Amat C, Litaudon P, Roux S, Royet JP, Farget V, Sicard G (2003) Rhythm sequence through the olfactory bulb layers during the time window of a respiratory cycle. *Eur J Neurosci* 17: 1811-1819.
- Chatrian GE, Bickford RG, Uihlein A (1960) Depth electrographic study of a fast rhythm evoked from the human calcarine region by steady illumination. *Electroencephalogr Clin Neurophysiol* 12: 167-176.
- Collins GG, Anson J (1985) Adenosine A₁ receptors mediate the inhibitory effects of exogenous adenosine in the rat olfactory cortex slice. *Neuropharmacology* 24: 1077-1084.
- Cruz T, Gleizes M, Balayssac S, Moronet E, Marsal G, Millán JL, Malet-Martino M, Nowak LG, Gilard V, Fonta C (2017) Identification of altered brain metabolites associated with TNAP activity in a mouse model of hypophosphatasia using untargeted NMR-based metabolomics analysis. *J Neurochem* 140: 919-940.
- de Jong AP, Fioravante D (2014) Translating neuronal activity at the synapse: presynaptic calcium sensors in short-term plasticity. *Front Cell Neurosci* 8:356.
- Dunwiddie TV, Diao L (1994) Extracellular adenosine concentrations in hippocampal brain slices and the tonic inhibitory modulation of evoked excitatory responses. *J Pharmacol Exp Ther* 268: 537-545.
- Dunwiddie TV, Hoffer BJ (1980) Adenine nucleotides and synaptic transmission in the in vitro rat hippocampus. *Br J Pharmacol* 69: 59-68.
- Eckhorn R, Bauer R, Jordan W, Brosch M, Kruse W, Munk M, Reitboek HJ (1988) Coherent oscillations: a mechanism of feature linking in the visual cortex? *Biol Cybern* 60: 121-130.
- Fioravante D, Regehr WG (2011) Short-term forms of presynaptic plasticity. *Curr Opin Neurobiol* 21: 269-274.
- Fourcaud-Trocmé N, Courtiol E, Buonviso N (2014) Two distinct olfactory bulb sublaminar networks involved in gamma and beta oscillation generation: a CSD study in the anesthetized rat. *Front Neural Circuits* 8: 88.
- Fredholm BB, Chen JF, Masino SA, Vaugeois JM (2005) Actions of adenosine at its receptors in the CNS: insights from

- knockouts and drugs. *Annu Rev Pharmacol Toxicol* 45: 385-412.
- Ginsborg BL, Hirst GD (1972) The effect of adenosine on the release of the transmitter from the phrenic nerve of the rat. *J Physiol* 224: 629-645.
- Gleizes M, Perrier SP, Fonta C, Nowak LG (2017) Prominent facilitation at beta and gamma frequency range revealed with physiological calcium concentration in adult mouse piriform cortex in vitro. *PLoS One* 12: e0183246.
- Gomes CV, Kaster MP, Tomé AR, Agostinho PM, Cunha RA (2011) Adenosine receptors and brain diseases: neuroprotection and neurodegeneration. *Biochim Biophys Acta*. 2011 1808: 1380-1399.
- Goodman RR, Kuhar MJ, Hester L, Snyder SH (1983) Adenosine receptors: autoradiographic evidence for their location on axon terminals of excitatory neurons. *Science* 220: 967-969.
- Gray CM, König P, Engel AK, Singer W (1989) Oscillatory responses in cat visual cortex exhibit inter-columnar synchronization which reflects global stimulus properties. *Nature* 338: 334-337.
- Haberly LB, Price JL (1977) The axonal projection patterns of the mitral and tufted cells of the olfactory bulb in the rat. *Brain Res* 129: 152-157.
- Hennig MH (2013) Theoretical models of synaptic short term plasticity. *Front Comput Neurosci*. 7: 45.
- Jasper H, Penfield W (1949) Electrocorticograms in man: Effect of voluntary movement upon the electrical activity of the precentral gyrus. *Arch F Psychiatr U Z Neur* 183: 163-174.
- Kilavik BE, Zaepffel M, Brovelli A, MacKay WA, Riehle A (2013) The ups and downs of beta oscillations in sensorimotor cortex. *Exp Neurol* 245: 15-26.
- King AE, Ackley MA, Cass CE, Young JD, Baldwin SA (2006) Nucleoside transporters: from scavengers to novel therapeutic targets. *Trends Pharmacol Sci* 27: 416-425.
- Kuroda Y, Saito M, Kobayashi K (1976) Concomitant changes in cyclic AMP level and postsynaptic potentials of olfactory cortex slices induced by adenosine derivatives. *Brain Res* 109: 196-201.
- McCabe J, Scholfield CN (1985) Adenosine-induced depression of synaptic transmission in the isolated olfactory cortex: receptor identification. *Pflugers Arch* 403: 141-145.
- McCormick DA, McGinley MJ, Salkoff DB (2015) Brain state dependent activity in the cortex and thalamus. *Curr Opin Neurobiol* 31: 133-140.
- Merker B (2013) Cortical gamma oscillations: the functional key is activation, not cognition. *Neurosci Biobehav Rev* 37: 401-417.
- Neville KR, Haberly LB (2003) Beta and gamma oscillations in the olfactory system of the urethane-anesthetized rat. *J Neurophysiol* 90: 3921-3930.
- Nowak LG, Bullier J (1996) Spread of stimulating current in the cortical grey matter of rat visual cortex studied on a new in vitro slice preparation. *J Neurosci Methods* 67: 237-248.
- Okada Y, Saito M (1979) Inhibitory action adenosine, 5-HT (serotonin) and GABA (gamma-aminobutyric acid) on the postsynaptic potential (PSP) or slices from olfactory cortex and superior colliculus in correlation to the level of cyclic AMP. *Brain Res* 160: 368-371.
- Phillis JW, Edstrom JP, Kostopoulos GK, Kirkpatrick JR (1979) Effects of adenosine and adenine nucleotides on synaptic transmission in the cerebral cortex. *Can J Physiol Pharmacol* 57: 1289-1312.
- Porkka-Heiskanen T, Strecker R, Thakkar M, Bjorkum AA, Greene RW, McCarley RW (1997) Adenosine: A mediator of the sleep-inducing effects of prolonged wakefulness. *Science* 276: 1265-1268.
- Price JL (1973) An autoradiographic study of complementary laminar patterns of termination of afferent fibers to the olfactory cortex. *J Comp Neurol* 150: 87-108.
- Prince DA, Stevens CF (1992) Adenosine decreases neurotransmitter release at central synapses. *Proc Natl Acad Sci U S A* 89: 8586-8590.
- Richards CD (1972) Potentiation and depression of synaptic transmission in the olfactory cortex of the guinea-pig. *J Physiol* 222: 209-231.
- Richards CD, Sercombe R (1968) Electrical activity observed in guinea-pig olfactory cortex maintained in vitro. *J Physiol* 197: 667-683.
- Scholfield CN (1978) Depression of evoked potentials in brain slices by adenosine compounds. *Br J Pharmacol* 63: 239-244.
- Schubert P, Mitzdorf U (1979) Analysis and quantitative evaluation of the depressive effect of adenosine on evoked potentials in hippocampal slices. *Brain Res* 172: 186-190.

- Shadlen MN, Movshon JA (1999) Synchrony unbound: a critical evaluation of the temporal binding hypothesis. *Neuron* 24: 67-77.
- Steriade M, McCormick DA, Sejnowski TJ (1993) Thalamocortical oscillations in the sleeping and aroused brain. *Science* 262: 679-685.
- Tallon-Baudry C (2012) On the neural mechanisms subserving consciousness and attention. *Front Psychol* 2:397.
- Tsodyks M, Pawelzik K, Markram H (1998) Neural networks with dynamic synapses. *Neural Comput* 10: 821-835.
- Tsodyks MV, Markram H (1997) The neural code between neocortical pyramidal neurons depends on neurotransmitter release probability. *Proc. Natl. Acad. Sci.* 94: 719-723.
- VanRullen R, Zoefel B, Ilhan B (2014) On the cyclic nature of perception in vision versus audition. *Phil Trans R Soc B* 369: 20130214.
- Wesson DW, Donahou TN, Johnson MO, Wachowiak M (2008) Sniffing behavior of mice during performance in odor-guided tasks. *Chem Senses* 33: 581-596.
- Wu LG, Saggau P (1994) Adenosine inhibits evoked synaptic transmission primarily by reducing presynaptic calcium influx in area CA1 of hippocampus. *Neuron* 12: 1139-1148.
- Yamamoto C, McIlwain H (1966) Potentials evoked in vitro in preparation from the mammalian brain. *Nature* 210: 1055-1056.
- Yang SC, Chiu TH, Yang HW, Min MY (2007) Presynaptic adenosine A1 receptors modulate excitatory synaptic transmission in the posterior piriform cortex in rats. *Brain Res* 1156: 67-79.
- Zimmermann H, Zebisch M, Strater N (2012) Cellular function and molecular structure of ecto-nucleotidases. *Purinergic signalling* 8: 437-502.
- Zucker RS, Regehr WG (2002) Short-term synaptic plasticity. *Annu Rev Physiol* 64: 355-405.

CHAPITRE IV : DISCUSSION GENERALE ET PERSPECTIVES

Cette thèse repose sur l'étude du rôle de la TNAP dans la production d'adénosine dans le cerveau et de l'effet de l'adénosine sur la plasticité synaptique à court terme dans le cortex piriforme de la souris adulte. Plusieurs approches et divers systèmes d'étude ont été utilisés afin de répondre à ces deux problématiques : une approche métabolomique sur des cerveaux de souris KO pour le gène de la TNAP, une approche électrophysiologique couplée à une approche pharmacologique sur des tranches de cerveaux de souris adultes. Les données électrophysiologiques ont été exploitées à l'aide d'un modèle de la plasticité à court terme en collaboration avec Simon Perrier. J'aborderai en premier lieu l'étude métabolomique réalisée dans le cadre d'une collaboration avec l'équipe de chimistes de Myriam Malet-Martino du laboratoire de Synthèse et Physico-Chimie des Molécules d'Intérêt Biologique (Université Paul Sabatier, Toulouse), puis les études électrophysiologiques et pharmacologiques menées dans le cortex piriforme chez la souris adulte.

A. Etude métabolomique

Ce travail avait pour but d'identifier les métabolites dont les niveaux seraient modifiés suite à un défaut d'activité de la TNAP dans le cerveau. Ces métabolites pourraient donc constituer des substrats et produits directs ou indirects de la TNAP qui étaient jusqu'alors peu connus dans le tissu cérébral. Néanmoins 3 métabolites avaient déjà été proposés dans la littérature comme étant des substrats de la TNAP : la phosphoéthanolamine (PE), le pyrophosphate (PPi) et le pyridoxal-5-phosphate (PLP).

L'analyse des spectres RMN par Thomas Cruz a permis d'identifier et de quantifier 39 métabolites dans les cerveaux de souris. Ainsi, nous avons pu mettre en évidence qu'une invalidation du gène codant pour la TNAP modifie la concentration de 8 métabolites dans le cerveau : le GABA, l'adénosine, la cystathionine, la méthionine, l'histidine, la 3-méthylhistidine, le N-acétylaspartate (NAA) et le N-acétyl-aspartylglutamate (NAAG). Parmi ces 8 métabolites,

seul le GABA avait déjà été décrit comme diminué chez des souris KO pour la TNAP (Waymire et al., 1995 ; Fonta et al., 2012b). Cette étude est donc la première à mettre en évidence une modification des concentrations de 7 autres métabolites dans le cerveau de souris KO pour la TNAP. Les métabolites les plus impactés sont le GABA, l'adénosine et la cystathionine.

Dans cette étude métabolomique, le PLP et le PPi, qui sont des substrats connus de la TNAP, n'ont pas pu être détectés dans nos échantillons en raison de leur concentration trop faible par rapport à la limite de détection de la technique RMN. Par ailleurs la PE, qui est aussi un substrat de la TNAP, a pu être détectée dans les échantillons de cerveaux mais aucune variation de concentration n'a pas été mise en évidence.

Nous observons une diminution d'environ 40% de la concentration en GABA lorsque les animaux sont dépourvus d'activité TNAP. Ceci s'explique par le fait que le PLP, qui n'est plus déphosphorylé en PL en l'absence de TNAP, ne peut plus pénétrer dans la cellule et servir de cofacteur à la synthèse de GABA (*Figure 16*). Etant donné que le GABA est le principal neurotransmetteur inhibiteur dans le cerveau et qu'il empêche ainsi l'excitation neuronale, une diminution de sa concentration pourrait entraîner des troubles neurologiques comme des crises d'épilepsie que l'on observe chez les souris KO pour la TNAP.

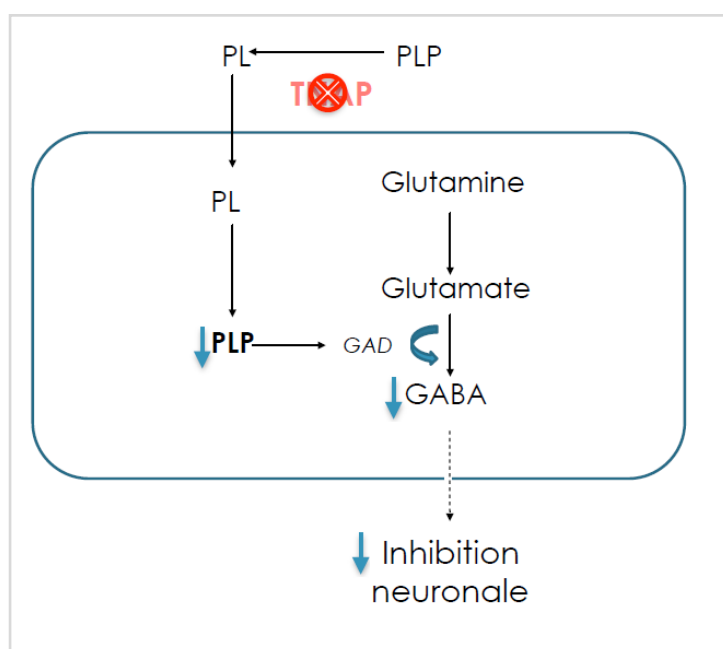


Figure 16 : Schéma de la voie de synthèse de GABA. Le PLP extracellulaire est déphosphorylé par la TNAP, rentre dans la cellule et est rephosphorylé pour servir de cofacteur aux enzymes responsables de la synthèse de GABA. Si la TNAP n'est plus fonctionnelle, on observe une diminution de PLP intracellulaire qui induit une diminution de synthèse de GABA. Par conséquent, on observe moins d'inhibition neuronale.

A l'inverse du GABA, la concentration de cystathionine mesurée dans les extraits de cerveaux de souris KO pour la TNAP est multipliée par 4. Les enzymes responsables de la synthèse de

la cystathionine (Cystathionine bêta-synthase, CBS) et de la dégradation La (Cystathionine gamma-lyase, CGL) de la cystathionine sont dépendantes du PLP (*Figure 17*). Toutefois, la CGL est plus fortement impactée par un défaut en PLP. Ce qui expliquerait la diminution de la concentration de ce composé dans nos conditions expérimentales.

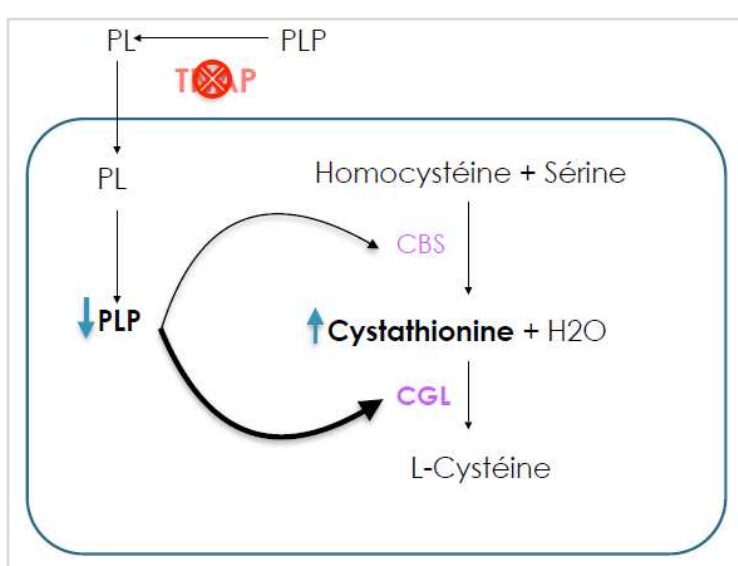


Figure 17 : Schéma de la voie de synthèse et de dégradation de la cystathionine. La synthèse de cystathionine se fait à partir d'homocystéine et de sérine et est réalisée par une cystathionine bêta synthase (CBS). La dégradation de la cystathionine en L-cystéine est réalisée par une cystathionine gamma lyase (CGL). Ces deux réactions sont dépendantes du PLP. Un défaut en PLP conduit à l'accumulation de cystathionine dans la cellule.

Cependant, la littérature ne nous renseigne pas sur le rôle de la cystathionine dans l'épilepsie. La TNAP pourrait réguler de manière extracellulaire la concentration en nucléotides et nucléosides, via une activité ectonucléotidase, en hydrolysant les nucléotides en nucléosides. Dans l'étude métabolomique, nous observons une diminution d'environ 80% de la concentration d'adénosine dans les cerveaux de souris KO pour la TNAP par rapport aux souris sauvages. Connaissant les propriétés anticonvulsives de l'adénosine, il se pourrait que l'absence d'adénosine contribue également aux crises d'épilepsie.

Outre les crises d'épilepsie, la maladie peut être associée à des phénomènes d'inflammation osseuse (Girshick et al., 2007 ; Whyte et al., 2009). Ainsi l'absence de TNAP pourrait contribuer aux mécanismes d'inflammation via l'ATP et la cystathionine. En effet, si la TNAP n'est plus fonctionnelle, alors les nucléotides, notamment l'ATP, ne sont plus déphosphorylés. L'accumulation d'ATP dans la cellule conduit à l'activation du récepteur P2X7 qui induit la production de cytokines pro-inflammatoires dont l'interleukine 1-bêta (*Figure 18*). De ce fait, on peut supposer que la TNAP contribue à l'inflammation.

D'autre part, la dégradation de la cystathionine par la CGL conduit à la production d'un composé anti-inflammatoire l'hydrogène sulfuré (H₂S) (*Figure 18*). Dans le cas d'un défaut d'expression de la TNAP, la cystathionine s'accumule limitant ainsi la production d'hydrogène sulfuré. Par les deux mécanismes que je viens de décrire, l'absence de TNAP pourrait ainsi favoriser les mécanismes d'inflammation.

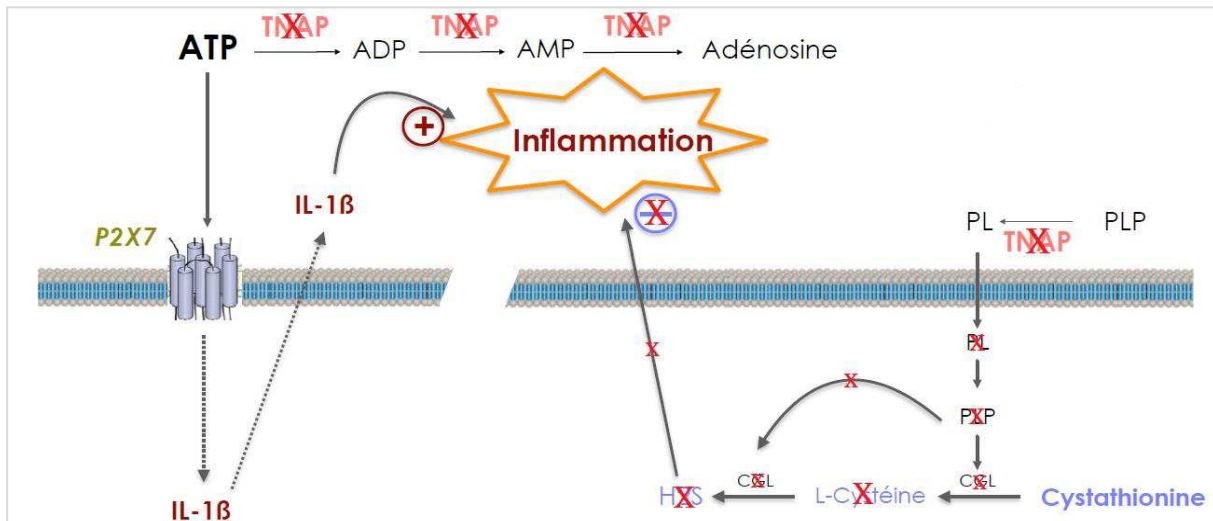


Figure 18 : Hypothèses du rôle de la TNAP dans les processus inflammatoires via sa fonction d'ectonucléotidase avec l'ATP et via le PLP avec la cystathionine. A gauche, l'activation du récepteur P2X7, suite à une accumulation d'ATP provoquée par un défaut d'activité de la TNAP, induit la production d'IL-1 β contribuant aux processus inflammatoires. A droite, suite à un défaut de l'activité TNAP, la cystathionine n'est plus dégradée ce qui limite la production d'hydrogène sulfuré H₂S (composé anti-inflammatoire) et contribue également aux processus inflammatoires.

Par ailleurs, l'accumulation de NAA et de NAAG chez les souris KO TNAP pourrait expliquer le retard de myélinisation observé chez ces souris. Le catabolisme de ces deux métabolites étant requis pour la synthèse de myéline.

Tous ces résultats sont autant d'éléments cohérents avec les principales caractéristiques phénotypiques de l'hypophosphatasie (neuronale) à savoir des crises d'épilepsie ou encore des retards de myélinisation que l'on peut observer chez les souris KO pour la TNAP.

Deux autres études pourraient nous permettre de compléter les résultats obtenus dans l'étude métabolomique. Premièrement, une étude métabolomique sur des cultures de cellules

neuronales qui est en cours de réalisation et de mise au point, en collaboration avec l'équipe de Davide Magne (Lyon) et l'équipe de Myriam Malet-Martino (Toulouse). A la différence de l'étude sur des cerveaux de souris KO pour la TNAP, cette étude est réalisée sur des cellules neuronales traitées avec l'inhibiteur spécifique de la TNAP, le MLS-0038949. Cela pourrait permettre la mise en évidence d'une modification de certains métabolites connus comme le PLP, le PPi et d'en identifier d'autres.

Deuxièmement, une étude électrophysiologique et pharmacologique via le contrôle de l'activité enzymatique des ectonucléotidases (TNAP et NT5E) par des inhibiteurs et le contrôle du transport de l'adénosine du milieu intracellulaire vers le milieu extracellulaire par le blocage des transporteurs. Cela permettrait d'analyser uniquement la voie des ectonucléotidases impliquées dans la synthèse d'adénosine. C'est l'objet du deuxième article intitulé "*Unexpected effect of TNAP and NT5E inhibition suggest that AMP acts as a A1 receptor agonist in the mouse piriform cortex*" dont la discussion suit.

B. Etudes électrophysiologiques et pharmacologiques

1. Etude de la contribution de la TNAP dans la synthèse d'adénosine dans le cortex piriforme chez la souris adulte.

Afin d'étudier la contribution de la TNAP dans la production d'adénosine, nous nous sommes intéressés, en particulier, à la dernière étape de production de l'adénosine extracellulaire, c'est-à-dire l'hydrolyse de l'AMP en adénosine. Nous avons enregistré les réponses électrophysiologiques dans le cortex piriforme de la souris adulte suite à divers traitements pharmacologiques. D'une part en bloquant l'activité de la TNAP et de la NT5E avec des inhibiteurs d'enzymes, le MLS-0038949 et l'AOPCP, respectivement. D'autre part en bloquant le transport de l'adénosine du milieu intracellulaire vers le milieu extracellulaire au moyen d'un inhibiteur des transporteurs, le NBTI. Le récepteur A1 par lequel l'adénosine exerce son rôle d'inhibiteur présynaptique a également été bloqué avec un antagoniste compétitif du récepteur A1, le CPT (*Figure 18*).

Deux conditions ont été testées : une condition dite « exogène » où nous avons ajouté de l'AMP (100 µM) dans le milieu d'incubation et une condition dite « endogène » où aucune source exogène d'AMP n'a été ajoutée dans le milieu d'incubation. Dans cette dernière condition, nous étudions le niveau basal d'activité des ectonucléotidases.

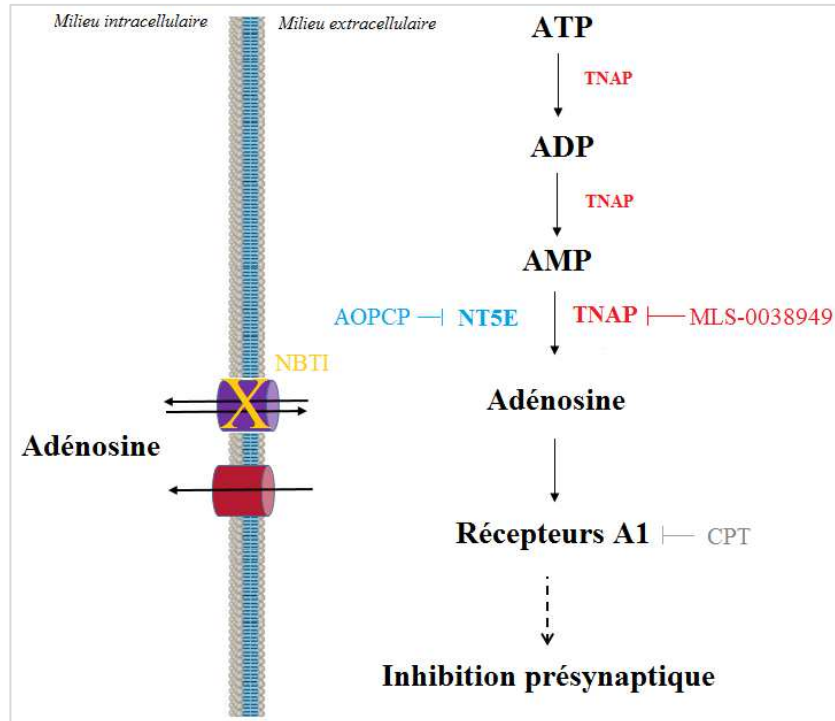


Figure 19 : Schéma récapitulatif de la signalisation purinergique associée à l'adénosine. Le transporteur ENT est représenté en violet, le transporteur CNT est représenté en rouge.

En bloquant l'activité TNAP par le MLS-0038949, que ce soit en condition endogène ou en condition exogène, nous avons observé que l'inhibition présynaptique était toujours présente. Et ce malgré que nos marquages histochimiques, révélant l'activité TNAP, montrent que le MLS-0038949 inhibe toute l'activité TNAP dans le cerveau. Le blocage de l'activité de la NT5E avec un inhibiteur spécifique, l'AOPCP, donne les mêmes résultats que précédemment. Le blocage simultané des deux enzymes ne permettait pas non plus de supprimer l'inhibition présynaptique. Cependant lorsque les récepteurs A1 étaient bloqués avec le CPT, un antagoniste compétitif des récepteurs A1, l'inhibition présynaptique était totalement supprimée dans la condition endogène et très majoritairement supprimée dans la condition exogène. Ces résultats nous ont amenés à poser plusieurs hypothèses permettant d'expliquer la persistance de l'inhibition présynaptique observée (*Figure 19*) : (1) outre la NT5E et la TNAP, une autre

enzyme pourrait synthétiser de l'adénosine : la phosphatase prostatique acide (PAP); (2) l'inhibition proviendrait du transport de l'adénosine intracellulaire qui se retrouverait directement dans le milieu extracellulaire ; (3) l'AMP agirait directement sur les récepteurs A1.

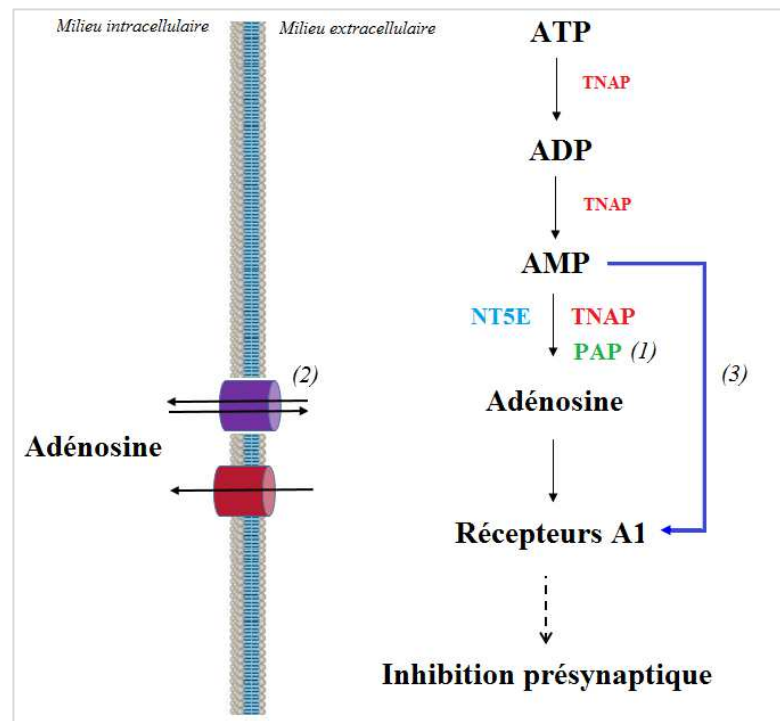


Figure 20 : Schéma récapitulatif de la signalisation purinergique associée à l'adénosine et des différentes hypothèses énoncées.

(1) *Hypothèse de la PAP.*

La persistance de l'inhibition observée pourrait être médiée par la PAP qui, via sa fonction ectonucléotidase, est impliquée dans l'hydrolyse de l'AMP en adénosine (Zylka et al., 2008) au niveau des ganglions de la racine dorsale. De plus, Street et al. (2013) ont montré, chez des souris doubles KO pour la NTSE et la PAP et où la TNAP est inactivée avec le MLS-0038949, que l'effet inhibiteur de l'AMP (250 µM) est totalement supprimé dans la moelle épinière. Leurs résultats suggèrent donc que ces trois enzymes sont responsables de l'hydrolyse de l'AMP en adénosine au niveau de la moelle épinière. La PAP pourrait donc expliquer l'effet inhibiteur indirect de l'AMP endogène et exogène (100 µM) qui persiste dans nos conditions. Peu d'informations sont disponibles concernant la présence de cette enzyme dans le cerveau notamment dans le cortex piriforme, où aucune étude n'a été réalisée à ce jour. Nousiainen et al. (2014) ont récemment mis en évidence par immunohistochimie que la

PAP est exprimée dans la région CA1 dans l'hippocampe et le striatum de la souris. Dans l'hippocampe, cette enzyme co-localise avec les neurones GABAergiques (Nousiainen et al., 2014). Dans le cas présent nous examinons les réponses excitatrices, on peut donc supposer que la PAP ne participerait pas à la production d'adénosine dans la synapse que nous étudions.

(2) Hypothèse du transport de l'adénosine.

L'adénosine intracellulaire peut être libérée en tant que telle dans le milieu extracellulaire au moyen d'un type de transporteur : les ENTs (*cf Partie I. C*). Le blocage des deux enzymes (TNAP et NT5E) pourrait provoquer un déséquilibre entre la concentration intracellulaire et extracellulaire en adénosine. Street et al. (2013) ont mis en évidence que la triple inhibition de la TNAP, NT5E et PAP dans la moelle épinière supprime quasiment l'hydrolyse de l'AMP en adénosine. Grâce à la technique de la voltamétrie (FSCV) qui permet la mesure de la production de l'adénosine, ils ont mis en évidence qu'une faible quantité d'adénosine est tout de même présente dans le milieu. Étant donné que les concentrations sont sensiblement équivalentes entre ces deux compartiments, il est donc envisageable que de l'adénosine intracellulaire soit libérée dans le milieu extracellulaire afin de rééquilibrer les concentrations. Ainsi la voie des ectonucléotidases pourrait être contournée.

Le blocage des transporteurs ENT1 et ENT2 par le NBTI ne modifie pas les réponses électrophysiologiques enregistrées. Etant donné que la concentration de NBTI est suffisante pour bloquer à la fois l'ENT1 et l'ENT2 (Belt et al., 1993) nous supposons que les deux transporteurs sont efficacement bloqués et qu'il n'y aurait pas de libération d'adénosine intracellulaire.

(3) L'AMP agirait en tant qu'agoniste des récepteurs A1.

La dernière hypothèse qui pourrait expliquer la persistance de l'inhibition en présence de MLS-0038949 et d'AOPCP, serait que l'AMP active directement les récepteurs A1. En effet, nous

avons observé que, lorsque les récepteurs A1 sont bloqués avec le CPT (antagoniste compétitif des récepteurs A1), l'inhibition est totalement supprimée en condition endogène. En condition exogène, le blocage des récepteurs A1 supprime de façon majoritaire l'inhibition présynaptique. Ces résultats nous suggèrent que l'AMP agirait comme un agoniste des récepteurs A1.

Bien qu'aucun récepteur spécifique à l'AMP n'est, à ce jour, mis en évidence, il a déjà été rapporté que l'AMP agirait directement sur le récepteur A1 dans l'intestin (Moody et al., 1984). Dans cette étude, les ectonucléotidases responsables de la dégradation de l'AMP en adénosine n'avaient pas été inhibées. Ainsi, on peut se demander si l'effet observé était réellement le reflet d'une action de l'AMP *per se* sur le récepteur ou d'une action indirecte de l'AMP après son hydrolyse en adénosine. Rittiner et al. (2012) ont étudié l'effet direct et indirect de l'AMP sur les récepteurs à l'adénosine. Cette étude a été réalisée, d'une part, sur des cultures de cellules HEK transfectées de telle sorte qu'elles expriment le récepteur A1, le récepteur A2b, la PAP et la NT5E. De plus, ces cellules peuvent exprimer de façon endogène les récepteurs P2Y. D'autre part, l'action de l'AMP a aussi été étudiée sur des cultures de neurones corticaux embryonnaires de souris qui reflètent une condition plus physiologique que les cellules transfectées. En utilisant un analogue de l'AMP non hydrolysable (ACP, 1 mM), les auteurs ont montré que l'AMP active le récepteur A1 et non le récepteur A2b. De plus, l'activation du récepteur A1 par l'ACP entraîne le même mécanisme de transduction que l'adénosine puisque la concentration en AMP cyclique est diminuée (*cf Partie I.E pour le mécanisme de transduction*). Par ailleurs, l'AMP et l'adénosine ont une affinité équivalente pour le récepteur A1 puisque la concentration efficace pour laquelle 50 % de l'effet maximum observé de l'adénosine est de 1.41 µM et de 1.1 µM pour l'AMP.

En résumé, en bloquant la TNAP, on ne supprime pas l'effet inhibiteur de l'AMP médié par les récepteurs A1. Nos résultats suggèrent donc que l'AMP agirait en tant qu'agoniste des récepteurs A1.

Toutefois, on peut se demander quel est le rôle de ces ectonucléotidases (NT5E et TNAP) si l'AMP est aussi efficace que l'adénosine sur les récepteurs A1 ? D'une part ces enzymes

agiraient de manière redondante de sorte à compenser l'activité de l'une ou de l'autre en cas de défaut d'activité comme c'est le cas dans les travaux de Street et ses collaborateurs (2013). Leurs travaux dans la moelle épinière montrent que le blocage de deux enzymes uniquement (PAP/NT5E, TNAP/PAP ou TNAP/NT5E) n'est pas suffisant pour empêcher la production d'adénosine. D'autre part, ces enzymes permettent de réguler l'activité des différents récepteurs via la production d'adénosine. Par exemple, l'expression de la NT5E est élevée au niveau de régions riches en dopamine dont on sait qu'elles impliquées, entre autre, dans le contrôle de l'activité locomotrice. Ce contrôle se fait via l'interaction des récepteurs A2a et D2. Dans le striatum, il a été montré que la NT5E et les récepteurs A2a sont colocalisés au niveau du striatum (Augusto et al., 2013). Des souris KO pour la CD73 présentent des altérations de l'activité locomotrice (Kuleskaya et al., 2013). Cela suggère donc que l'adénosine issue de la dégradation de l'AMP via la NT5E joue un rôle important dans le contrôle d'une activité locomotrice normale.

Afin de statuer sur le rôle d'ectonucléotidase de la TNAP et sa contribution dans la production d'adénosine dans notre modèle, plusieurs approches pourraient être envisagées. L'idéal serait de réaliser des enregistrements électrophysiologiques sur des tranches de souris KO pour la TNAP pour voir si concrètement l'invalidation du gène Akp2 modifie la transmission synaptique. Etant donné que les souris KO pour la TNAP ne survivent pas plus d'une dizaines de jours, l'extraction du cerveau pourrait se révéler délicate et le cerveau n'étant pas encore arrivé à maturité cela pourrait compliquer l'analyse des données électrophysiologiques. Une méthode alternative au KO TNAP serait le knockdown au moyen d'ARN interférents. En 2006, Kermer et coll. ont appliqué ce type de protocole sur des cellules souches neurales en culture afin d'éteindre l'expression de la protéine codant pour la TNAP. Par ailleurs, il est possible d'utiliser cette technique knockdown sur des tranches de cerveau (Taliaz et al., 2010) où l'on peut localiser d'un point de vue spatial l'extinction de l'activité d'une protéine. Les ARN interférents (shRNA) sont exprimés dans un vecteur lentiviral qui peut être microinjecté localement dans une région du cerveau. Il pourrait être envisageable d'utiliser cette technique

pour supprimer l'activité de la TNAP spécifiquement dans le cortex piriforme et d'enregistrer les réponses électrophysiologiques afin d'examiner la transmission synaptique.

D'autre part, le modèle KO NT5E et knock-down pour la TNAP permettrait de s'affranchir de l'utilisation d'agents pharmacologiques pour lesquels les affinités et les spécificités ne peuvent pas être totalement exclusives que soit pour une enzyme, un transporteur, ou un récepteur donné et donc nous assurer que la totalité de l'activité est supprimée. On pourrait aussi imaginer que certains agents (inhibiteurs, antagonistes) puissent interagir entre eux entraînant ainsi une réponse qui ne reflèterait pas ce qu'il se passe en condition physiologique. Par ailleurs, il existe de nombreuses interactions entre le récepteur A1 et d'autres récepteurs comme par exemple les récepteurs A2a (Ciruela et al., 2006), A2b (Gonçalves et al., 2015), les récepteurs au glutamate (Ferré et al., 2002) ou bien les récepteurs P2Y1 (Yoshioka et al., 2001). Cependant, il n'existe à notre connaissance aucune étude dans le cortex piriforme faisant état de telles interactions. Le fait que les effets de l'AMP et de l'ATP soient totalement supprimés lorsque l'on bloque les récepteurs A1 laisse penser que seul ce récepteur serait impliqué dans nos conditions expérimentales. Mais on ne peut exclure que les effets de l'adénosine sur les récepteur A1 (inhibition neuronale) et sur les récepteurs A2a (excitation neuronale) puissent s'additionner. En effet, ces deux récepteurs sont les plus abondants dans le système nerveux central. Afin de s'assurer que seuls les effets inhibiteurs sont présents dans notre système, il faudrait bloquer les récepteurs A2a avec un antagoniste sélectif, le SCH 58261 (Cunha, 2005).

Pour résumer, l'étude métabolomique et l'étude électrophysiologique nous apportent des éléments nouveaux concernant la contribution de la TNAP dans la production d'adénosine. L'étude métabolomique montre que la quantité d'adénosine est associée à l'activité de la TNAP. L'étude électrophysiologique réalisée dans le cortex piriforme révèle que le TNAP régule la signalisation purinergique via la dégradation des nucléotides et la production d'adénosine. Un rôle indirect de la TNAP pourrait être un rôle de « détoxication » via la déphosphorylation de l'ATP. En effet, une accumulation d'ATP est responsable de phénomènes d'inflammation via l'activation des récepteurs P2X7 qui induit la production

d'interleukine 1bêta (Griffiths et al., 1995). On pourrait trouver une certaine homologie avec le pyrophosphate (PPi) qui inhibe la minéralisation osseuse. Par ailleurs, on peut envisager que le phosphate inorganique, issu de la dégradation du PPi par la TNAP et qui entre dans la cellule via des transporteurs, puisse être réintégré dans divers processus biochimiques. Enfin, la TNAP pourrait également avoir un rôle dans le passage des molécules du milieu extracellulaire vers le milieu intracellulaire comme c'est le cas avec le pyridoxal-5'-phosphate (PLP).

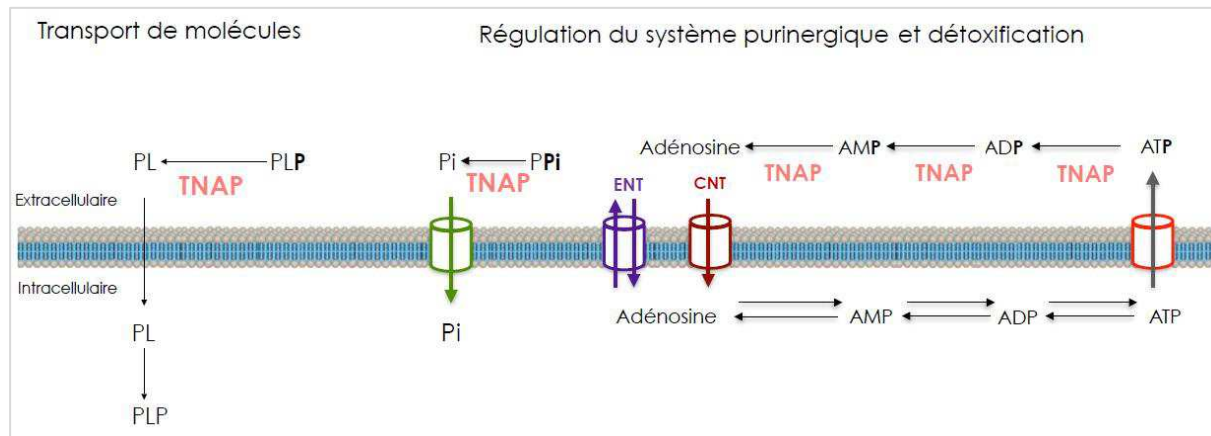


Figure 21 : Schéma récapitulatif des différents rôles de la TNAP dans le cerveau. A gauche, la TNAP pourrait jouer un rôle dans le passage des molécules (cas du PLP). A droite, la TNAP joue un rôle dans la régulation de la signalisation purinergique via sa fonction d'ectonucléotidase en dégradant les nucléotides et nucléosides. Toujours via cette fonction ectonucléotidase, elle jouerait un rôle de « détoxicification » en déphosphorylant l'ATP, composé pro-inflammatoire, ou encore le pyrophosphate (PPi) qui inhibe la minéralisation osseuse.

2. Etude de l'influence du calcium extracellulaire sur la transmission synaptique et sur la plasticité synaptique à court terme dans le cortex piriforme chez la souris adulte.

Cette étude avait pour but de valider les conditions expérimentales de nos enregistrements électrophysiologiques dans le cortex piriforme dans lesquels la concentration de calcium dans le liquide céphalo-rachidien artificiel est de 1.1 mM. La plupart des études sur la plasticité en électrophysiologie utilisent des concentrations de calcium comprises entre 2 et 2.5 mM. Cette étape préliminaire était donc nécessaire étant donné la différence de concentrations de

calcium que nous utilisons dans nos études électrophysiologiques et l'importance du calcium dans la transmission et la plasticité synaptique.

Nous avons observé que la concentration de calcium intracellulaire augmente l'amplitude de la réponse de façon dose-dépendante avec un effet de saturation atteint pour une concentration d'environ 5 mM de calcium. Par ailleurs, on observe que l'amplitude de la réponse est augmentée de 40 % en présence de 2,2 mM de calcium comparée à celle que nous observons en présence de 1,1 mM de calcium.

Concernant les phénomènes de plasticité synaptique pour une concentration de 1,1 mM de calcium, nous avons observé que le maximum de facilitation est atteint pour une valeur de 25 Hz. Une stimulation de 50 Hz induit des amplitudes de réponse plus faibles qu'à 25 Hz ce qui révèlerait l'apparition du phénomène de dépression à court terme. Les stimulations à 100 Hz sont associées à une perte importante voire totale de facilitation suggérant une prédominance de la dépression. Pour une concentration de 2,2 mM de calcium, on observe que la dynamique de la plasticité est modifiée. En effet, le maximum de facilitation est déplacé vers des fréquences plus basses, 12.5 Hz. Plus la fréquence augmente, plus la facilitation devient déficitaire au profit de la dépression. Enfin à 100 Hz, on observe une disparition totale de la facilitation de la réponse. Ces résultats ont mis en évidence que la plasticité synaptique dans le cortex piriforme fait intervenir à la fois des mécanismes de facilitation et de dépression avec des caractéristiques temporelles différentes. Ces observations n'auraient pas été possible si nous nous avions utilisé des stimulations par paires de pulses, qui est la méthode classique d'analyse de la plasticité synaptique. En effet, cette approche ne permet pas forcément d'observer la chronologie du phénomène de plasticité et ne nous aurait permis d'observer ni la saturation de l'augmentation de la réponse à 25 Hz, ni la dominance de la dépression en fin de train de stimulation à 50 et 100 Hz.

De plus, le modèle de la plasticité adapté à nos données nous permet de déterminer des constantes de temps de récupération associées à chaque mécanisme. Cela permet de préciser la contribution de la facilitation et de la dépression en fonction des conditions expérimentales et de dire quel mécanisme est affecté par la concentration de calcium. Dans

cette étude, la facilitation et la dépression lente sont affectées par la concentration de calcium, tandis que la dépression rapide ne l'est pas. Avec 1,1 mM de calcium, le modèle suggère que trois composantes de la plasticité sont impliquées : une facilitation dont la constante de temps de récupération est d'environ 160 ms, une dépression rapide (< à 20 ms) et une dépression lente (140 ms). Lorsque l'on est en présence de 2,2 mM de calcium, la constante de temps de récupération de la facilitation est augmentée (236 ms) comparée à celle obtenue à 1,1 mM de calcium. Par ailleurs, la constante de temps de récupération de la dépression lente présente une tendance à l'augmentation (266 ms) suggérant que la dépression lente est davantage sollicitée à 2,2 mM de calcium. En revanche la dépression rapide n'était pas affectée par la concentration de calcium.

En résumé, nos résultats montrent un maximum de facilitation pour des fréquences dans la gamme des oscillations beta et une facilitation, certes moindre, mais tout de même prédominante dans la gamme gamma. Les oscillations beta (15-40 Hz) et gamma (50-100 Hz) sont associées à la présentation de stimuli odorants dans le bulbe olfactif (Neville et Haberly 2003). C'est aussi dans ces gammes d'oscillations que nous observons une amplification de la facilitation. Ce phénomène d'amplification gamma a également été observé au niveau du bulbe olfactif par Manabe et Mori (2013). Les mécanismes de la plasticité augmentent le ratio signal/bruit de la transmission des signaux dans le cortex piriforme. Cela suggère une facilitation de la transmission des informations odorantes. Nos conditions expérimentales se rapprochent donc au mieux de ce que l'on peut observer en condition physiologique.

Par ailleurs, l'utilisation d'une concentration de 2,2 mM de calcium, comme le font la plupart des études classiques sur la plasticité synaptique, surestime la contribution de la dépression et sous-estime les mécanismes de facilitation. Ainsi, on peut se demander si l'étude, que ce soit de la transmission ou de la plasticité, à des concentrations beaucoup plus élevées en calcium est pertinente lorsque l'on veut examiner ce qu'il se passe en condition physiologique. Outre la transmission synaptique et la plasticité, d'autres mécanismes peuvent être modulés par le calcium. D'une part, l'activité spontanée générée dans le cortex cérébral *in vivo* peut aussi apparaître *in vitro* si les concentrations ioniques du milieu d'incubation sont très proches

de celles retrouvées *in vivo*. Cette activité spontanée disparaît si les concentrations ioniques du milieu sont lointaines de ce qui est retrouvé *in vivo*, notamment lorsqu'une concentration de calcium de 2 mM est utilisée (Sanchez-Vives, McCormick, 2000). D'autre part, en fonction de la concentration calcium, un type de neurones à haute fréquence de décharge (> 300 Hz) peut être observé ou non dans le cortex. En effet, en présence de 2 mM de calcium, un faible pourcentage de ces neurones a pu être observé tandis que lorsque la concentration de calcium est de 1.2 mM, le pourcentage de ce types de cellule est multiplié par 8 (Brumberg et al., 2000).

3. Etude de l'influence de l'adénosine extracellulaire sur la plasticité synaptique à court terme dans le cortex piriforme chez la souris adulte.

Cette étude a été réalisée avec les mêmes conditions expérimentales que dans l'article précédent. Les réponses électrophysiologiques dans le cortex piriforme de la souris ont été enregistrées suite à des trains (5 pulses) de stimulations à différentes fréquences (3, 125 Hz à 100 Hz). Plusieurs concentrations d'adénosine ont été utilisées (10, 30, 100, 300 et 1000 µM) et le CPT, qui est un antagoniste compétitif des récepteurs A1, ce qui a permis d'évaluer l'influence de l'adénosine endogène sur la plasticité synaptique. Le modèle (Gleizes et al., 2017) a également été utilisé afin d'adapter nos données expérimentales et de déterminer les caractéristiques de la plasticité synaptique à court terme en présence ou en absence totale d'adénosine.

Nos résultats expérimentaux montrent que l'adénosine produit une facilitation qui se renforce avec de fortes concentrations mais aussi en fonction de la fréquence. Plus on augmente la concentration en adénosine, plus le maximum de facilitation est observée pour des fréquences de stimulations élevées. En condition contrôle et pour de faibles concentrations en adénosine (10 et 30 µM), le maximum de facilitation est observé pour des fréquences égales à 25 Hz. En revanche pour des concentrations élevées en adénosine, le maximum de facilitation est déplacé vers des fréquences plus hautes, 50 Hz et 100 Hz. A l'inverse avec le CPT et pour des stimulations à 100 Hz, l'amplitude de la réponse diminue avec les stimulations. Ainsi il

semble que pour des hautes fréquences, l'inhibition de l'adénosine semble être contrecarrée par les mécanismes de plasticité car l'amplitude de la réponse tend à atteindre une valeur proche de celle obtenue en condition contrôle.

La modélisation de nos données expérimentales montre que plus la concentration d'adénosine augmente moins les mécanismes de dépression lente et rapide sont sollicités. C'est pour cela qu'avec la plus forte concentration d'adénosine le modèle ne fait intervenir qu'une constante de temps de facilitation.

Dans la condition avec le CPT, la modélisation de nos données expérimentales n'est pas très différente de celle obtenue en condition contrôle puisque le modèle suggère l'interaction de 3 mécanismes : une facilitation et deux dépressions avec une dépression lente et une dépression rapide. Par ailleurs, le seul paramètre qui semble être affecté en fonction des conditions expérimentales (adénosine et CPT) est U qui représente la probabilité de libération initiale. En condition avec le CPT, la valeur de U augmente. Ceci peut s'expliquer par le fait que l'inhibition des récepteurs A1 provoque une augmentation du signal dû à un apport de calcium plus important à l'intérieur de la synapse. Par conséquent, cela induit une libération accrue de vésicules de neurotransmetteurs. Ce qui expliquerait pourquoi à hautes fréquences le signal déprime. En effet, à ces fréquences la synapse n'aurait pas le temps de reformer la réserve de vésicule d'où l'apparition de la dépression. A l'inverse, on observe que plus la concentration d'adénosine augmente plus le paramètre U diminue. L'apport de calcium étant moindre dans la synapse en présence d'adénosine, la réserve de vésicules ne s'épuiserait pas aussi vite qu'en condition contrôle ou sans adénosine. En d'autre terme, dans ces conditions la dépression est de moins en moins sollicitée à hautes fréquences. Ce qui explique pourquoi la modélisation de nos données ne fait intervenir que de la facilitation.

Tous ces résultats nous indiquent que d'une part, l'augmentation de la concentration en adénosine réduit l'impact des mécanismes de dépression. D'autre part, l'adénosine diminue la probabilité initiale de libération de neurotransmetteurs. Une des conséquences d'une telle modulation par l'adénosine serait que malgré l'inhibition qu'elle procure (en diminuant la probabilité initiale de libération), les modifications qu'elle induit sur les caractéristiques de la

plasticité contrecarrent l'inhibition pour de hautes fréquences. En effet, de nombreux neuromodulateurs activent des récepteurs présynaptiques, et il en résulte le plus souvent une diminution de la probabilité de libération des neurotransmetteurs. À la suite de cette diminution, les caractéristiques de « filtrage » de la synapse sont modifiées de sorte que la dépression diminue la contribution à la dynamique synaptique et la facilitation devient plus importante (Abbott et Regehr, 2004). De cette façon, l'adénosine pourrait donc agir comme un « filtre passe-haut », permettant la transmission des signaux à haute fréquence.

Cet effet de filtre de l'adénosine est opposé à celui que nous avions supposé au départ. En effet, avec la fonction hypnogène attribuée à l'adénosine, cela laissait supposer qu'elle jouerait un rôle de sélection des fréquences et notamment des basses fréquences. Par ailleurs, des études faites chez le rat d'une part, et chez l'Homme d'autre part, ont permis de faire un lien entre l'adénosine et les oscillations lentes de certaines phases du sommeil. Une étude chez le rat, a montré que le CPA (un agoniste des récepteurs A1) augmentait la puissance des ondes lentes, **δ**, de manière dépendante de la dose, et ce, dès l'injection (Benington et al., 1995). Par ailleurs, chez l'Homme, un polymorphisme du gène codant pour la protéine ADA (responsable de la dégradation de l'adénosine en inosine) a été associé à des modifications des phases de sommeil. En effet, chez les individus dépourvus de ADA fonctionnelle, la phase de sommeil à ondes lentes est allongée et l'activité des ondes **δ** pendant les phases de sommeil - hors sommeil paradoxal (REM) - est augmentée (Retey et al., 2005). Ainsi, l'effet hypnogène de l'adénosine est souvent associé à la genèse des ondes **δ**. Comme l'injection d'adénosine augmente la puissance des basses fréquences, nous aurions pu penser que l'adénosine ait pour rôle d'augmenter l'effet des basses fréquences et à l'inverse de diminuer l'effet des hautes fréquences. Or ce n'est pas ce que nous avons observé dans notre étude. On peut supposer que l'effet de filtre passe haut de l'adénosine permettrait la transmission d'informations « importantes », comme un signal de danger, liées à l'induction de hautes fréquences.

Le rôle de filtre passe-haut que nous avons mis en évidence dans cette étude va à l'encontre de l'effet anticonvulsivant de l'adénosine. Cependant, notre protocole de stimulation est limité puisqu'il est composé de 5 pulses et ne rendrait donc pas compte de ce qu'il peut se passer

en condition épileptique. En effet, au-delà de 5 pulses, d'autres mécanismes de plasticité pourraient entrer en jeu, et on ne sait pas quel serait l'impact de l'adénosine dans ces conditions. Il pourrait être envisagé de tester notre protocole de stimulation sur des préparations de tranches épileptiques (en supprimant le magnésium du liquide céphalorachidien, par exemple). Une autre solution serait de tester des trains de stimulation composés de nombreux pulses afin de mimer ce qu'il pourrait se passer lors d'une crise d'épilepsie.

CHAPITRE V : CONCLUSION

L'ensemble des résultats obtenus au cours de mes trois années de thèse a permis de montrer pour la première fois qu'un défaut d'activité de la TNAP dans le cerveau entraîne une modification de la concentrations de 8 métabolites dans le cerveau de la souris : le GABA, l'adénosine, la cystathionine, la méthionine, l'histidine, la 3-méthylhistidine, le NAA et le NAAG. Parmi ces métabolites, l'adénosine est le point central de cette thèse. En effet, c'est un neuromodulateur puissant qui a une influence sur la transmission synaptique et sur la plasticité synaptique. La diminution drastique de 80 % de la concentration d'adénosine chez les souris KO pour la TNAP observée dans l'étude métabolomique, suggère qu'elle pourrait contribuer à l'aggravation des crises d'épilepsies générées par l'absence de GABA et que l'on observe chez ces souris.

Avec une approche électrophysiologique et pharmacologique, l'inhibition des ectonucléotidases impliquées dans la synthèse d'adénosine ne supprime pas l'effet inhibiteur de l'AMP suggérant que l'AMP pourrait agir en tant qu'agoniste des récepteurs A1. Etant donné qu'il a la même affinité que l'adénosine et qu'il induit le même mécanisme de transduction du signal que l'adénosine, l'AMP peut être considérée comme un anticonvulsivant endogène (Muzzi et al., 2013). Cependant dans des cas d'épilepsies sévères, l'AMP ne serait pas suffisant pour contrecarrer les crises d'épilepsies (Muzzi et al., 2013). Ceci pourrait être une explication concernant la persistance des crises létales chez les souris KO pour la TNAP. La TNAP pourrait être impliquée dans des mécanismes d'inflammation médiée par l'ATP. En effet, la TNAP étant capable de dégrader l'ATP, il se peut donc que ce nucléotide aussi s'accumule chez les souris KO pour la TNAP. L'ATP est connue pour avoir des propriétés pro-inflammatoires via l'activation du récepteur P2X7 (Sperlagh, 2006). L'épilepsie engendre aussi de l'inflammation, il se pourrait que l'ATP accumulé en raison d'un défaut d'activité de la TNAP favorise le maintien des processus épileptiques via l'ATP. Il pourrait être envisagé d'analyser les facteurs d'inflammation (interleukines, et facteurs de nécrose) dans le cerveau suite à un défaut d'activité de la TNAP. Cela pourrait être une autre voie à explorer quant aux crises d'épilepsies létales observées chez les souris KO pour la TNAP.

CHAPITRE VI : REFERENCES BIBLIOGRAPHIQUES

- Abbott, L. F., and Wade G. Regehr. 2004. "Synaptic Computation." *Nature* 431 (7010): 796.
- Abbracchio, M. P. 2006. "International Union of Pharmacology LVIII: Update on the P2Y G Protein-Coupled Nucleotide Receptors: From Molecular Mechanisms and Pathophysiology to Therapy." *Pharmacological Reviews* 58 (3): 281–341. <https://doi.org/10.1124/pr.58.3.3>.
- Abbracchio, Maria P., and Geoffrey Burnstock. 1994. "Purinoceptors: Are There Families of P2X and P2Y Purinoceptors?" *Pharmacology & Therapeutics* 64 (3): 445–75. [https://doi.org/10.1016/0163-7258\(94\)00048-4](https://doi.org/10.1016/0163-7258(94)00048-4).
- Abbracchio, Maria P, Gabriella Rainaldi, Anna Maria Giammarioli, Stefania Ceruti, Roberta Brambilla, Flaminio Cattabeni, Daniela Barbieri, Claudio Franceschi, Kenneth A Jacobson, and Walter Malorni. 1997. "The A(3) Adenosine Receptor Mediates Cell Spreading, Reorganization of Actin Cytoskeleton, and Distribution of Bcl-x(L): Studies in Human Astrogloma Cells." *Biochemical and Biophysical Research Communications* 241 (2): 297–304. <https://doi.org/10.1006/bbrc.1997.7705>.
- Abraham, E H, A G Prat, L Gerweck, T Seneviratne, R J Arceci, R Kramer, G Guidotti, and H F Cantiello. 1993. "The Multidrug Resistance (mdr1) Gene Product Functions as an ATP Channel." *Proceedings of the National Academy of Sciences* 90 (1): 312–16.
- Anderson, Christopher M., Stephen A. Baldwin, James D. Young, Carol E. Cass, and Fiona E. Parkinson. 1999. "Distribution of mRNA Encoding a Nitrobenzylthioinosine-Insensitive Nucleoside Transporter (ENT2) in Rat Brain." *Molecular Brain Research* 70 (2): 293–297.
- Anderson, Christopher M., and Raymond A. Swanson. 2000. "Astrocyte Glutamate Transport: Review of Properties, Regulation, and Physiological Functions." *Glia* 32 (1): 1–14. [https://doi.org/10.1002/1098-1136\(200010\)32:1<1::AID-GLIA10>3.0.CO;2-W](https://doi.org/10.1002/1098-1136(200010)32:1<1::AID-GLIA10>3.0.CO;2-W).
- Anderson, Christopher M., Wei Xiong, James D. Young, Carol E. Cass, and Fiona E. Parkinson. 1996. "Demonstration of the Existence of mRNAs Encoding N1/Cif and N2/Cit Sodium/Nucleoside Cotransporters in Rat Brain." *Molecular Brain Research* 42 (2): 358–61. [https://doi.org/10.1016/S0169-328X\(96\)00244-6](https://doi.org/10.1016/S0169-328X(96)00244-6).
- Angulo, Ester, Vicent Casadó, Josefa Mallol, Enric I. Canela, Francesc Viñals, Isidre Ferrer, Carmen Lluis, and Rafael Franco. 2003. "A1 Adenosine Receptors Accumulate in Neurodegenerative Structures in Alzheimer's Disease and Mediate Both Amyloid Precursor Protein Processing and Tau Phosphorylation and Translocation." *Brain Pathology* 13 (4): 440–451.
- Atkinson, L, T.F.C Batten, T.S Moores, H Varoqui, J.D Erickson, and J Deuchars. 2004. "Differential Co-Localisation of the P2X7 Receptor Subunit with Vesicular Glutamate Transporters VGLUT1 and VGLUT2 in Rat CNS." *Neuroscience* 123 (3): 761–68. <https://doi.org/10.1016/j.neuroscience.2003.08.065>.
- Atkinson, Lucy, Carol. J. Milligan, Noel J. Buckley, and Jim Deuchars. 2002. "Purinergic Receptors: An ATP-Gated Ion Channel at the Cell Nucleus." *Nature* 420 (6911): 42–42. <https://doi.org/10.1038/420042a>.
- Atluri, Pradeep P., and Wade G. Regehr. 1998. "Delayed Release of Neurotransmitter from Cerebellar Granule Cells." *The Journal of Neuroscience* 18 (20): 8214.
- Augusto, Elisabete, Marco Matos, Jean Sévigny, Ali El-Tayeb, Margaret S Bynoe, Christa E Müller, Rodrigo A Cunha, and Jiang-Fan Chen. 2013. "Ecto-5'-Nucleotidase (CD73)-Mediated Formation of Adenosine Is Critical for the Striatal Adenosine A(2A) Receptor Functions." *The*

Journal of Neuroscience 33 (28): 11390–99. <https://doi.org/10.1523/JNEUROSCI.5817-12.2013>.

- Barsotti, Catia, and Piero L. Ipata. 2004. "Metabolic Regulation of ATP Breakdown and of Adenosine Production in Rat Brain Extracts." *The International Journal of Biochemistry & Cell Biology* 36 (11): 2214–25. <https://doi.org/10.1016/j.biocel.2004.04.015>.
- Baxter, Andrew W., Se Joon Choi, Joan A. Sim, and R. Alan North. 2011. "Role of P2X4 Receptors in Synaptic Strengthening in Mouse CA1 Hippocampal Neurons: P2X4 Receptors and Hippocampal Synaptic Transmission." *European Journal of Neuroscience* 34 (2): 213–20. <https://doi.org/10.1111/j.1460-9568.2011.07763.x>.
- Bekkers, John M., and Norimitsu Suzuki. 2013. "Neurons and Circuits for Odor Processing in the Piriform Cortex." *Trends in Neurosciences* 36 (7): 429–38. <https://doi.org/10.1016/j.tins.2013.04.005>.
- Belcher, S.M., A. Zsarnovszky, P.A. Crawford, H. Hemani, L. Spurling, and T.L. Kirley. 2006. "Immunolocalization of Ecto-Nucleoside Triphosphate Diphosphohydrolase 3 in Rat Brain: Implications for Modulation of Multiple Homeostatic Systems Including Feeding and Sleep-wake Behaviors." *Neuroscience* 137 (4): 1331–46. <https://doi.org/10.1016/j.neuroscience.2005.08.086>.
- Belt, Judith A., Neyssa M. Marina, Doris A. Phelps, and Charles R. Crawford. 1993. "Nucleoside Transport in Normal and Neoplastic Cells." *Advances in Enzyme Regulation* 33 (January): 235–52. [https://doi.org/10.1016/0065-2571\(93\)90021-5](https://doi.org/10.1016/0065-2571(93)90021-5).
- Benington, Joel H., Susheel K. Kodali, and H. Craig Heller. 1995. "Stimulation of A1 Adenosine Receptors Mimics the Electroencephalographic Effects of Sleep Deprivation." *Brain Research* 692 (1): 79–85. [https://doi.org/10.1016/0006-8993\(95\)00590-M](https://doi.org/10.1016/0006-8993(95)00590-M).
- Bennett, Gillian C., and Michael R. Boarder. 2000. "The Effect of Nucleotides and Adenosine on Stimulus-Evoked Glutamate Release from Rat Brain Cortical Slices." *British Journal of Pharmacology* 131 (3): 617–623.
- Bertram, R., A. Sherman, and E. F. Stanley. 1996. "Single-Domain/Bound Calcium Hypothesis of Transmitter Release and Facilitation." *Journal of Neurophysiology* 75 (5): 1919.
- Bigonnesse, Fran?ois, S?bastien A. L?vesque, Filip Kukulski, Joanna Lecka, Simon C. Robson, Maria J. G. Fernandes, and Jean S?vigny. 2004. "Cloning and Characterization of Mouse Nucleoside Triphosphate Diphosphohydrolase-8 ? , ?" *Biochemistry* 43 (18): 5511–19. <https://doi.org/10.1021/bi0362222>.
- Bjelobaba, Ivana, Nadezda Nedeljkovic, Sanja Subasic, Irena Lavrnja, Sanja Pekovic, Danijela Stojkov, Ljubisav Rakic, and Mirjana Stojiljkovic. 2006. "Immunolocalization of Ecto-Nucleotide Pyrophosphatase/Phosphodiesterase 1 (NPP1) in the Rat Forebrain." *Brain Research* 1120 (1): 54–63. <https://doi.org/10.1016/j.brainres.2006.08.114>.
- Bjelobaba, Ivana, Mirjana Stojiljkovic, Sanja Pekovic, Sanja Dacic, Irena Lavrnja, Danijela Stojkov, Ljubisav Rakic, and Nadezda Nedeljkovic. 2007. "Immunohistological Determination of Ecto-Nucleoside Triphosphate Diphosphohydrolase1 (NTPDase1) and 5'-Nucleotidase in Rat Hippocampus Reveals Overlapping Distribution." *Cellular and Molecular Neurobiology* 27 (6): 731–43. <https://doi.org/10.1007/s10571-007-9159-8>.
- Blass-Kampmann, Sabine, Andrea Kindler-Röhrborn, Helmut Deissler, Donatella D'Urso, and Manfred F. Rajewsky. 1997. "In Vitro Differentiation of Neural Progenitor Cells from Prenatal Rat Brain: Common Cell Surface Glycoprotein on Three Glial Cell Subsets." *Journal of Neuroscience Research* 48 (2): 95–111. [https://doi.org/10.1002/\(SICI\)1097-4547\(19970415\)48:2<95::AID-JNR2>3.0.CO;2-7](https://doi.org/10.1002/(SICI)1097-4547(19970415)48:2<95::AID-JNR2>3.0.CO;2-7).

- Bollen, Mathieu, Rik Gijsbers, Hugo Ceulemans, Willy Stalmans, and Cristiana Stefan. 2000. "Nucleotide Pyrophosphatases/Phosphodiesterases on the Move." *Critical Reviews in Biochemistry and Molecular Biology* 35 (6): 393–432. <https://doi.org/10.1080/10409230091169249>.
- Boucsein, Clemens, Robert Zacharias, Katrin Färber, Sanja Pavlovic, Uwe-Karsten Hanisch, and Helmut Kettenmann. 2003. "Purinergic Receptors on Microglial Cells: Functional Expression in Acute Brain Slices and Modulation of Microglial Activation in Vitro." *European Journal of Neuroscience* 17 (11): 2267–2276. <https://doi.org/10.1046/j.1460-9568.2003.02663.x>.
- Bower, J M, and L B Haberly. 1986. "Facilitating and Nonfacilitating Synapses on Pyramidal Cells: A Correlation between Physiology and Morphology." *Proceedings of the National Academy of Sciences of the United States of America* 83 (4): 1115–19.
- Braun, Norbert, Jean Sévigny, Santosh K. Mishra, Simon C. Robson, Stephan W. Barth, Ruediger Gerstberger, Klaus Hammer, and Herbert Zimmermann. 2003. "Expression of the Ecto-ATPase NTPDase2 in the Germinal Zones of the Developing and Adult Rat Brain: Ecto-ATPase in Germinal Zones of the Rat Brain." *European Journal of Neuroscience* 17 (7): 1355–64. <https://doi.org/10.1046/j.1460-9568.2003.02567.x>.
- Brenowitz, Stephan, and Laurence O. Trussell. 2001. "Minimizing Synaptic Depression by Control of Release Probability." *The Journal of Neuroscience* 21 (6): 1857.
- Broch, Ole Jacob, and Per Magne Ueland. 1980. "Regional and Subcellular Distribution of S-Adenosylhomocysteine Hydrolase in the Adult Rat Brain." *Journal of Neurochemistry* 35 (2): 484–488.
- Brumberg, Joshua C., Lionel G. Nowak, and David A. McCormick. 2000. "Ionic Mechanisms Underlying Repetitive High-Frequency Burst Firing in Supragranular Cortical Neurons." *Journal of Neuroscience* 20 (13): 4829–4843.
- Brun-Heath, Isabelle, Myriam Ermonval, Elodie Chabrol, Jinsong Xiao, Miklós Palkovits, Ruth Lyck, Florence Miller, Pierre-Olivier Couraud, Etienne Mornet, and Caroline Fonta. 2011. "Differential Expression of the Bone and the Liver Tissue Non-Specific Alkaline Phosphatase Isoforms in Brain Tissues." *Cell and Tissue Research* 343 (3): 521–36. <https://doi.org/10.1007/s00441-010-1111-4>.
- Bruns, R F, G H Lu, and T A Pugsley. 1986. "Characterization of the A2 Adenosine Receptor Labeled by [3H]NECA in Rat Striatal Membranes." *Molecular Pharmacology* 29 (4): 331.
- Bruns, Robert F., James H. Fergus, Edward W. Badger, James A. Bristol, Lisa A. Santay, Jon D. Hartman, Sheryl J. Hays, and Che C. Huang. 1987. "Binding of the A1-Selective Adenosine Antagonist 8-Cyclopentyl-1,3-Dipropylxanthine to Rat Brain Membranes." *Naunyn-Schmiedeberg's Archives of Pharmacology* 335 (1): 59–63. <https://doi.org/10.1007/BF00165037>.
- Burnstock, Geoffrey. 2008. "Purinergic Signalling and Disorders of the Central Nervous System." *Nature Reviews Drug Discovery* 7 (7): 575–90. <https://doi.org/10.1038/nrd2605>.
- Calker, Dietrich van, Margarete Müller, and Bernd Hamprecht. 1979. "ADENOSINE REGULATES VIA TWO DIFFERENT TYPES OF RECEPTORS, THE ACCUMULATION OF CYCLIC AMP IN CULTURED BRAIN CELLS." *Journal of Neurochemistry* 33 (5): 999–1005. <https://doi.org/10.1111/j.1471-4159.1979.tb05236.x>.
- Cammer, Wendy, Francine A. Tansey, and Robert Sacchi. n.d. "Antibody against Mouse Liver 5'-Nucleotidase Immunostains White Matter in the Adult Mouse Central Nervous System." *Journal of the Neurological Sciences* 73 (2): 155–67. [https://doi.org/10.1016/0022-510X\(86\)90127-9](https://doi.org/10.1016/0022-510X(86)90127-9).

- Cass, Carol E., James D. Young, and Stephen A. Baldwin. 1998. "Recent Advances in the Molecular Biology of Nucleoside Transporters of Mammalian Cells." *Biochemistry and Cell Biology* 76 (5): 761–770.
- Cass, Carol E., James D. Young, Stephen A. Baldwin, Miguel A. Cabrita, Kathryn A. Graham, Mark Griffiths, Lori L. Jennings, et al. 2002. "Nucleoside Transporters of Mammalian Cells." In *Membrane Transporters as Drug Targets*, 313–352. Springer. http://link.springer.com/chapter/10.1007/0-306-46812-3_12.
- Catterall, William A., and Alexandra P. Few. 2008. "Calcium Channel Regulation and Presynaptic Plasticity." *Neuron* 59 (6): 882–901. <https://doi.org/10.1016/j.neuron.2008.09.005>.
- Chambers, Jon K., Lynn E. Macdonald, Henry M. Sarau, Robert S. Ames, Katie Freeman, James J. Foley, Yuan Zhu, Megan M. McLaughlin, Paul Murdock, and Lynette McMillan. 2000. "AG Protein-Coupled Receptor for UDP-Glucose." *Journal of Biological Chemistry* 275 (15): 10767–10771.
- Choi, Roy C. Y., Glanice K. Y. Chu, Nina L. Siow, Amanda W. Y. Yung, Lisa Y. Yung, Pinky S. C. Lee, Christopher C. W. Lo, et al. 2013. "Activation of UTP-Sensitive P2Y₂ Receptor Induces the Expression of Cholinergic Genes in Cultured Cortical Neurons: A Signaling Cascade Triggered by Ca²⁺ Mobilization and Extracellular Regulated Kinase Phosphorylation." *Molecular Pharmacology* 84 (1): 50. <https://doi.org/10.1124/mol.112.084160>.
- Ciccarelli, R, P Ballerini, G Sabatino, M.P Rathbone, M D'Onofrio, F Caciagli, and P Di Iorio. 2001. "Involvement of Astrocytes in Purine-Mediated Reparative Processes in the Brain." *International Journal of Developmental Neuroscience* 19 (4): 395–414. [https://doi.org/10.1016/S0736-5748\(00\)00084-8](https://doi.org/10.1016/S0736-5748(00)00084-8).
- Ciruela, F. 2006. "Presynaptic Control of Striatal Glutamatergic Neurotransmission by Adenosine A1-A2A Receptor Heteromers." *Journal of Neuroscience* 26 (7): 2080–87. <https://doi.org/10.1523/JNEUROSCI.3574-05.2006>.
- Citri, Ami, and Robert C. Malenka. 2008. "Synaptic Plasticity: Multiple Forms, Functions, and Mechanisms." *Neuropsychopharmacology* 33 (1): 18–41.
- Coburn, Stephen P. 2015. "Vitamin B-6 Metabolism and Interactions with TNAP." In *Neuronal Tissue-Nonspecific Alkaline Phosphatase (TNAP)*, edited by Caroline Fonta and László Négyessy, 76:207–38. Dordrecht: Springer Netherlands. https://doi.org/10.1007/978-94-017-7197-9_11.
- Collo, Ginetta, R. Alan North, Eric Kawashima, Emilio Merlo-Pich, Sybille Neidhart, Annmarie Surprenant, and Gary Buell. 1996. "Cloning of P2X5 and P2X6 Receptors and the Distribution and Properties of an Extended Family of ATP-Gated Ion Channels." *The Journal of Neuroscience* 16 (8): 2495–2507.
- Costenla, Ana Rita, Luísa V. Lopes, Alexandre de Mendonça, and Joaquim A. Ribeiro. 2001. "A Functional Role for Adenosine A3 Receptors: Modulation of Synaptic Plasticity in the Rat Hippocampus." *Neuroscience Letters* 302 (1): 53–57. [https://doi.org/10.1016/S0304-3940\(01\)01633-0](https://doi.org/10.1016/S0304-3940(01)01633-0).
- Cotrina, Maria Luisa, Jane H.-C. Lin, Alexandra Alves-Rodrigues, Shujun Liu, Jiang Li, Hooman Azmi-Ghadimi, Jian Kang, Christian CG Naus, and Maiken Nedergaard. 1998. "Connexins Regulate Calcium Signaling by Controlling ATP Release." *Proceedings of the National Academy of Sciences* 95 (26): 15735–15740.
- Cruz, Thomas, Marie Gleizes, Stéphane Bayayssac, Etienne Mornet, Grégory Marsal, José Luis Millán, Myriam Malet-Martino, Lionel G Nowak, Véronique Gilard, and Caroline Fonta. 2017. "Identification of Altered Brain Metabolites Associated with TNAP Activity in a Mouse Model of

Hypophosphatasia Using Untargeted NMR-Based Metabolomics Analysis." *Journal of Neurochemistry* 140 (6): 919–40. <https://doi.org/10.1111/jnc.13950>.

Cunha, R.A. 2001. "Adenosine as a Neuromodulator and as a Homeostatic Regulator in the Nervous System: Different Roles, Different Sources and Different Receptors." *Neurochemistry International* 38 (2): 107–25. [https://doi.org/10.1016/S0197-0186\(00\)00034-6](https://doi.org/10.1016/S0197-0186(00)00034-6).

Cunha, Rodrigo A. 2005. "Neuroprotection by Adenosine in the Brain: From A1 Receptor Activation to A2A Receptor Blockade." *Purinergic Signalling* 1 (2): 111–34. <https://doi.org/10.1007/s11302-005-0649-1>.

Cusack, N. J., J. D. Pearson, and J. L. Gordon. 1983. "Stereoselectivity of Ectonucleotidases on Vascular Endothelial Cells." *Biochemical Journal* 214 (3): 975–981.

Daly, John W., Pamela Butts-Lamb, and William Padgett. 1983. "Subclasses of Adenosine Receptors in the Central Nervous System: Interaction with Caffeine and Related Methylxanthines." *Cellular and Molecular Neurobiology* 3 (1): 69–80. <https://doi.org/10.1007/BF00734999>.

Daré, Elisabetta, Gunnar Schulte, Olga Karovic, Christian Hammarberg, and Bertil B. Fredholm. 2007. "Modulation of Glial Cell Functions by Adenosine Receptors." *Karolinska Institutet - Neuroscience* 92 (1): 15–20. <https://doi.org/10.1016/j.physbeh.2007.05.031>.

Deissler, Helmut, Sabine Blass-kampmann, Erik Bruyneel, Marc Mareel, and Manfred F. Rajewsky. 1999. "Neural Cell Surface Differentiation Antigen gp130RB13-6 Induces Fibroblasts and Glioma Cells to Express Astroglial Proteins and Invasive Properties." *The FASEB Journal* 13 (6): 657–666.

Delaney, KR, and DW Tank. 1994. "A Quantitative Measurement of the Dependence of Short-Term Synaptic Enhancement on Presynaptic Residual Calcium." *The Journal of Neuroscience* 14 (10): 5885.

Demenis, Marlene A., and Francisco A. Leone. 2000. "Kinetic Characteristics of ATP Hydrolysis by a Detergent-Solubilized Alkaline Phosphatase From Rat Osseous Plate." *IUBMB Life* 49 (2): 113–119. <https://doi.org/10.1080/15216540050022421>.

Dienel, Gerald A. 2013. "Astrocytic Energetics during Excitatory Neurotransmission: What Are Contributions of Glutamate Oxidation and Glycolysis?" *Neurochemistry International* 63 (4): 244–58. <https://doi.org/10.1016/j.neuint.2013.06.015>.

Díez-Zaera, María, Juan Ignacio Díaz-Hernández, Elena Hernández-Álvarez, H. Zimmermann, Miguel Díaz-Hernández, and María Teresa Miras-Portugal. 2011. "Tissue-Nonspecific Alkaline Phosphatase Promotes Axonal Growth of Hippocampal Neurons." *Molecular Biology of the Cell* 22 (7): 1014–1024.

Ding, Jun, Jayms D. Peterson, and D. James Surmeier. 2008. "Corticostriatal and Thalamostriatal Synapses Have Distinctive Properties." *The Journal of Neuroscience* 28 (25): 6483. <https://doi.org/10.1523/JNEUROSCI.0435-08.2008>.

Dixon, Alistair K., Amelie K. Gubitz, Dalip J.S. Sirinathsinghji, Peter J. Richardson, and Tom C. Freeman. 1996. "Tissue Distribution of Adenosine Receptor mRNAs in the Rat." *British Journal of Pharmacology* 118 (6): 1461–1468. <https://doi.org/10.1111/j.1476-5381.1996.tb15561.x>.

Dobrunz, Lynn E., and Charles F. Stevens. 1997. "Heterogeneity of Release Probability, Facilitation, and Depletion at Central Synapses." *Neuron* 18 (6): 995–1008.

Dreisig, Karin, Matilda Degn, Louise Sund, Piotr Hadaczek, Lluis Samaranach, Waldy San Sebastian, Krystof Bankiewicz, and Birgitte Rahbek Kornum. 2016. "Validation of Antibodies for

“Neuroanatomical Localization of the P2Y11 Receptor in Macaque Brain.” *Journal of Chemical Neuroanatomy* 78 (December): 25–33. <https://doi.org/10.1016/j.jchemneu.2016.08.002>.

Drury, A. N., and A. v Szent-Györgyi. 1929. “The Physiological Activity of Adenine Compounds with Especial Reference to Their Action upon the Mammalian Heart.” *The Journal of Physiology* 68 (3): 213–237.

Dubyak, GEORGE R., and CHAKIB el-Moatassim. 1993. “Signal Transduction via P2-Purinergic Receptors for Extracellular ATP and Other Nucleotides.” *American Journal of Physiology-Cell Physiology* 265 (3): C577–C606.

Dunwiddie, T V, and H L Haas. 1985. “Adenosine Increases Synaptic Facilitation in the in Vitro Rat Hippocampus: Evidence for a Presynaptic Site of Action.” *The Journal of Physiology* 369 (December): 365–77.

Dunwiddie, T. V., and B. J. Hoffer. 1980. “Adenine Nucleotides and Synaptic Transmission in the in Vitro Rat Hippocampus.” *British Journal of Pharmacology* 69 (1): 59–68.

Dunwiddie, T V, and T Worth. 1982. “Sedative and Anticonvulsant Effects of Adenosine Analogs in Mouse and Rat.” *Journal of Pharmacology and Experimental Therapeutics* 220 (1): 70.

Dunwiddie, Thomas V., and Susan A. Masino. 2001. “The Role and Regulation of Adenosine in the Central Nervous System.” *Annual Review of Neuroscience* 24 (1): 31–55.

Ermonval, Myriam, Anne Baudry, Florence Baychelier, Elodie Pradines, Mathéa Pietri, Kimimitsu Oda, Benoît Schneider, Sophie Mouillet-Richard, Jean-Marie Launay, and Odile Kellermann. 2009. “The Cellular Prion Protein Interacts with the Tissue Non-Specific Alkaline Phosphatase in Membrane Microdomains of Bioaminergic Neuronal Cells.” Edited by Patricia Bozza. *PLoS ONE* 4 (8): e6497. <https://doi.org/10.1371/journal.pone.0006497>.

Fausther, Michel, Joanna Lecka, Filip Kukulski, Sébastien A Lévesque, Julie Pelletier, Herbert Zimmermann, Jonathan A Dranoff, and Jean Sévigny. 2007. “Cloning, Purification, and Identification of the Liver Canalicular Ecto-ATPase as NTPDase8.” *American Journal of Physiology. Gastrointestinal and Liver Physiology* 292 (3): G785–95. <https://doi.org/10.1152/ajpgi.00293.2006>.

Felmy, Felix, Erwin Neher, and Ralf Schneggenburger. 2003. “Probing the Intracellular Calcium Sensitivity of Transmitter Release during Synaptic Facilitation.” *Neuron* 37 (5): 801–11. [https://doi.org/10.1016/S0896-6273\(03\)00085-0](https://doi.org/10.1016/S0896-6273(03)00085-0).

Fenoglio, C., E. Scherini, R. Vaccarone, and G. Bernocchi. 1995. “A Re-Evaluation of the Ultrastructural Localization of 5'-Nucleotidase Activity in the Developing Rat Cerebellum, with a Cerium-Based Method.” *Journal of Neuroscience Methods* 59 (2): 253–63. [https://doi.org/10.1016/0165-0270\(94\)00211-X](https://doi.org/10.1016/0165-0270(94)00211-X).

Feoktistov, Igor, and Italo Biaggioni. 1997. “Adenosine A_{2B} Receptors.” *Pharmacological Reviews* 49 (4): 381.

Ferré, Sergi, Marzena Karcz-Kubicha, Bruce T. Hope, Patrizia Popoli, Javier Burgueño, M. Angeles Gutiérrez, Vicent Casadó, Kjell Fuxe, Steven R. Goldberg, and Carme Lluis. 2002. “Synergistic Interaction between Adenosine A_{2A} and Glutamate mGlu5 Receptors: Implications for Striatal Neuronal Function.” *Proceedings of the National Academy of Sciences* 99 (18): 11940–11945.

Fiebich, Bernd L., Knut Biber, Kacin Gyufko, Mathias Berger, Joachim Bauer, and Dietrich Van Calker. 1996. “Adenosine A_{2B} Receptors Mediate an Increase in Interleukin (IL)-6 mRNA and IL-6 Protein Synthesis in Human Astrogloma Cells.” *Journal of Neurochemistry* 66 (4): 1426–1431. <https://doi.org/10.1046/j.1471-4159.1996.66041426.x>.

- Fields, R Douglas, and Geoffrey Burnstock. 2006. "Purinergic Signalling in Neuron–glia Interactions." *Nature Reviews. Neuroscience* 7 (6): 423–36. <https://doi.org/10.1038/nrn1928>.
- Fields, R.Douglas, and Beth Stevens. 2000. "ATP: An Extracellular Signaling Molecule between Neurons and Glia." *Trends in Neurosciences* 23 (12): 625–33. [https://doi.org/10.1016/S0166-2236\(00\)01674-X](https://doi.org/10.1016/S0166-2236(00)01674-X).
- Fioravante, Diasynou, and Wade G Regehr. 2011. "Short-Term Forms of Presynaptic Plasticity." *Current Opinion in Neurobiology* 21 (2): 269–74. <https://doi.org/10.1016/j.conb.2011.02.003>.
- Florenzano, F., P. Carrive, M.T. Visconti, F. Ferrari, L. Latini, D. Conversi, S. Cabib, C. Bagni, and M. Molinari. 2008. "Cortical and Subcortical Distribution of Ionotropic Purinergic Receptor Subunit Type 1 (P2X1R) Immunoreactive Neurons in the Rat Forebrain." *Neuroscience* 151 (3): 791–801. <https://doi.org/10.1016/j.neuroscience.2007.11.027>.
- Florenzano, F., M. T. Visconti, F. Cavaliere, C. Volonte, and M. Molinari. 2002. "Cerebellar Lesion up-Regulates P2X 1 and P2X 2 Purinergic Receptors in Precerebellar Nuclei." *Neuroscience* 115 (2): 425–434.
- Fonta, C. 2004. "Areal and Subcellular Localization of the Ubiquitous Alkaline Phosphatase in the Primate Cerebral Cortex: Evidence for a Role in Neurotransmission." *Cerebral Cortex* 14 (6): 595–609. <https://doi.org/10.1093/cercor/bhh021>.
- Fonta, C., L. Negyessy, I. Brun Heat, M. Ermonval, D. Czege, L. G. Nowak, B. Frances, J. S. Xiao, and J. L. Millán. 2012b. "TNAP in the Brain: Functions in Neurotransmission." *Bulletin Du Groupement International Pour La Recherche Scientifique En Stomatologie et Odontologie* 51 (1): 27.
- Fonta, Caroline, Laszlo Negyessy, Luc Renaud, and Pascal Barone. 2005. "Postnatal Development of Alkaline Phosphatase Activity Correlates with the Maturation of Neurotransmission in the Cerebral Cortex." *The Journal of Comparative Neurology* 486 (2): 179–96. <https://doi.org/10.1002/cne.20524>.
- Fredholm, B. B., and T. V. Dunwiddie. 1988. "How Does Adenosine Inhibit Transmitter Release?" *Trends in Pharmacological Sciences* 9 (4): 130–134.
- Fredholm, Bertil B. 2011. "Physiological and Pathophysiological Roles of Adenosine: Roles of Adenosine and Its Receptors." *Sleep and Biological Rhythms* 9 (February): 24–28. <https://doi.org/10.1111/j.1479-8425.2010.00460.x>.
- Fredholm, Bertil B., Jiang-Fan Chen, Rodrigo A. Cunha, Per Svenningsson, and Jean-Marie Vaugeois. 2005. "Adenosine and Brain Function." In *International Review of Neurobiology*, 63:191–270. Elsevier. [https://doi.org/10.1016/S0074-7742\(05\)63007-3](https://doi.org/10.1016/S0074-7742(05)63007-3).
- Fuchs, Jannon L. 1991. "5'-Nucleotidase Activity Increases in Aging Rat Brain." *Neurobiology of Aging* 12 (5): 523–30. [https://doi.org/10.1016/0197-4580\(91\)90083-V](https://doi.org/10.1016/0197-4580(91)90083-V).
- Gampe, Kristine, Jennifer Stefani, Klaus Hammer, Peter Brendel, Alexandra P?tzsch, Grigori Enikolopov, Keiichi Enyōji, Amparo Acker-Palmer, Simon C. Robson, and Herbert Zimmermann. 2015. "NTPDase2 and Purinergic Signaling Control Progenitor Cell Proliferation in Neurogenic Niches of the Adult Mouse Brain: NTPDase2 Controls Adult Neurogenesis." *STEM CELLS* 33 (1): 253–64. <https://doi.org/10.1002/stem.1846>.
- Gersdorff, Henrique von, and J. Gerard G. Borst. 2002. "Short-Term Plasticity at the Calyx of Held." *Nat Rev Neurosci* 3 (1): 53–64. <https://doi.org/10.1038/nrn705>.
- Gijsbers, Rik, Junken Aoki, Hiroyuki Arai, and Mathieu Bollen. 2003. "The Hydrolysis of

Lysophospholipids and Nucleotides by Autotaxin (NPP2) Involves a Single Catalytic Site." FEBS Letters 538 (1–3): 60–64. [https://doi.org/10.1016/S0014-5793\(03\)00133-9](https://doi.org/10.1016/S0014-5793(03)00133-9).

Girschick, Hermann J, Etienne Mornet, Meinrad Beer, Monika Warmuth-Metz, and Peter Schneider. 2007. "Chronic Multifocal Non-Bacterial Osteomyelitis in Hypophosphatasia Mimicking Malignancy." BMC Pediatrics 7 (1). <https://doi.org/10.1186/1471-2431-7-3>.

Gleizes, Marie, Simon P. Perrier, Caroline Fonta, and Lionel G. Nowak. 2017. "Prominent Facilitation at Beta and Gamma Frequency Range Revealed with Physiological Calcium Concentration in Adult Mouse Piriform Cortex in Vitro." Edited by Giuseppe Gangarossa. PLOS ONE 12 (8): e0183246. <https://doi.org/10.1371/journal.pone.0183246>.

Goding, James W., Bert Grobben, and Herman Slegers. 2003. "Physiological and Pathophysiological Functions of the Ecto-Nucleotide Pyrophosphatase/Phosphodiesterase Family." Biochimica et Biophysica Acta (BBA) - Molecular Basis of Disease 1638 (1): 1–19. [https://doi.org/10.1016/S0925-4439\(03\)00058-9](https://doi.org/10.1016/S0925-4439(03)00058-9).

Gonçalves, Francisco Q., Johny Pires, Anna Pliassova, Rui Beleza, Cristina Lemos, Joana M. Marques, Ricardo J. Rodrigues, et al. 2015. "Adenosine A_{2b} Receptors Control A₁ Receptor-Mediated Inhibition of Synaptic Transmission in the Mouse Hippocampus." European Journal of Neuroscience 41 (7): 878–88. <https://doi.org/10.1111/ejn.12851>.

Gottfried, Jay A. 2010. "Central Mechanisms of Odour Object Perception." Nature Reviews. Neuroscience 11 (9): 628–41. <https://doi.org/10.1038/nrn2883>.

Greene, R. W., and H. L. Haas. 1991. "The Electrophysiology of Adenosine in the Mammalian Central Nervous System." Progress in Neurobiology 36 (4): 329–341.

Griffith, Douglas A., and Simon M. Jarvis. 1996. "Nucleoside and Nucleobase Transport Systems of Mammalian Cells." Biochimica et Biophysica Acta (BBA)-Reviews on Biomembranes 1286 (3): 153–181.

Griffiths, R J, E J Stam, J T Downs, and I G Otterness. 1995. "ATP Induces the Release of IL-1 from LPS-Primed Cells in Vivo." *The Journal of Immunology* 154 (6): 2821.

Guo, W., X. Xu, X. Gao, G. Burnstock, C. He, and Z. Xiang. 2008. "Expression of P2X5 Receptors in the Mouse CNS." Neuroscience 156 (3): 673–92. <https://doi.org/10.1016/j.neuroscience.2008.07.062>.

Guzman, Segundo J., Hartmut Schmidt, Heike Franke, Ute Krügel, Jens Eilers, Peter Illes, and Zoltan Gerevich. 2010. "P2Y1 Receptors Inhibit Long-Term Depression in the Prefrontal Cortex." Neuropharmacology 59 (6): 406–15. <https://doi.org/10.1016/j.neuropharm.2010.05.013>.

Haberly, Lewis B., and Joseph L. Price. 1978. "Association and Commissural Fiber Systems of the Olfactory Cortex of the Rat II. Systems Originating in the Olfactory Peduncle." The Journal of Comparative Neurology 181 (4): 781–807. <https://doi.org/10.1002/cne.901810407>.

Hammarberg, Christian, Gunnar Schulte, and Bertil B. Fredholm. 2003. "Evidence for Functional Adenosine A3 Receptors in Microglia Cells: Adenosine A3 Receptors Activate ERK1/2 in Microglia." Journal of Neurochemistry 86 (4): 1051–54. <https://doi.org/10.1046/j.1471-4159.2003.01919.x>.

Hanics, János, János Barna, Jinsong Xiao, José Luis Millán, Caroline Fonta, and László Négyessy. 2012. "Ablation of TNAP Function Compromises Myelination and Synaptogenesis in the Mouse Brain." Cell and Tissue Research 349 (2): 459–71. <https://doi.org/10.1007/s00441-012-1455-z>.

- Haskó, György, Pál Pacher, E Sylvester Vizi, and Peter Illes. 2005. "Adenosine Receptor Signaling in the Brain Immune System." *Trends in Pharmacological Sciences* 26 (10): 511–16. <https://doi.org/10.1016/j.tips.2005.08.004>.
- Heinrich, Attila, Ágnes Kittel, Cecilia Csölle, E. Sylvester Vizi, and Beáta Sperlágh. 2008. "Modulation of Neurotransmitter Release by P2X and P2Y Receptors in the Rat Spinal Cord." *Neuropharmacology* 54 (2): 375–86. <https://doi.org/10.1016/j.neuropharm.2007.10.013>.
- Helmchen, F., J.G. Borst, and B. Sakmann. 1997. "Calcium Dynamics Associated with a Single Action Potential in a CNS Presynaptic Terminal." *Biophysical Journal* 72 (3): 1458–71. [https://doi.org/10.1016/S0006-3495\(97\)78792-7](https://doi.org/10.1016/S0006-3495(97)78792-7).
- Hindley, S., M. A. R. Herman, and M. P. Rathbone. 1994. "Stimulation of Reactive Astrogliosis in Vivo by Extracellular Adenosine Diphosphate or an Adenosine A2 Receptor Agonist." *Journal of Neuroscience Research* 38 (4): 399–406. <https://doi.org/10.1002/jnr.490380405>.
- Ho, Cheryl, Janice Hicks, and Michael W. Salter. 1995. "A Novel P2-Purinoceptor Expressed by a Subpopulation of Astrocytes from the Dorsal Spinal Cord of the Rat." *British Journal of Pharmacology* 116 (7): 2909–2918. <https://doi.org/10.1111/j.1476-5381.1995.tb15944.x>.
- Jacobson, Kenneth A., Olga Nikodijević, Dan Shi, Carola Gallo-Rodriguez, Mark E. Olah, Gary L. Stiles, and John W. Daly. 1993. "A Role for Central A3-Adenosine Receptors: Mediation of Behavioral Depressant Effects." *FEBS Letters* 336 (1): 57–60.
- Kang, Jian, Ning Kang, Ditte Lovatt, Arnulfo Torres, Zhuo Zhao, Jane Lin, and Maiken Nedergaard. 2008. "Cx43 Hemichannels Are Permeable to ATP." *The Journal of Neuroscience : The Official Journal of the Society for Neuroscience* 28 (18): 4702–11. <https://doi.org/10.1523/JNEUROSCI.5048-07.2008>.
- Kanjhan, Refik, Gary D. Housley, Lucille D. Burton, David L. Christie, Andree Kippenberger, Peter R. Thorne, Lin Luo, and Allen F. Ryan. 1999. "Distribution of the P2X2 Receptor Subunit of the ATP-Gated Ion Channels in the Rat Central Nervous System." *Journal of Comparative Neurology* 407 (1): 11–32.
- Katz, B, and R Miledi. 1968. "The Role of Calcium in Neuromuscular Facilitation." *The Journal of Physiology* 195 (2): 481–92.
- Kermer, Vanessa, Mathias Ritter, Boris Albuquerque, Christoph Leib, Matthias Stanke, and Herbert Zimmermann. 2010. "Knockdown of Tissue Nonspecific Alkaline Phosphatase Impairs Neural Stem Cell Proliferation and Differentiation." *Neuroscience Letters* 485 (3): 208–11. <https://doi.org/10.1016/j.neulet.2010.09.013>.
- Kerr, Michael I., Mark J. Wall, and Magnus J. E. Richardson. 2013. "Adenosine A1 Receptor Activation Mediates the Developmental Shift at Layer 5 Pyramidal Cell Synapses and Is a Determinant of Mature Synaptic Strength." *The Journal of Physiology* 591 (13): 3371–3380. <https://doi.org/10.1113/jphysiol.2012.244392>.
- Khakh, Baljit S., Daniel Gittermann, Debra A. Cockayne, and Alison Jones. 2003. "ATP Modulation of Excitatory Synapses onto Interneurons." *The Journal of Neuroscience* 23 (19): 7426.
- Khan, Ghous M., Ilse Smolders, Guy Ebinger, and Yvette Michotte. 2001. "2-Chloro-N6-Cyclopentyladenosine-Elicited Attenuation of Evoked Glutamate Release Is Not Sufficient to Give Complete Protection against Pilocarpine-Induced Seizures in Rats." *Neuropharmacology* 40 (5): 657–667.
- King, Brian F., and Geoffrey Burnstock. 2002. "Purinergic Receptors." *Understanding G Protein-Coupled Receptors and Their Role in the CNS*, 422–438.

- Kirschuk, S., J. Scherer, H. Kettenmann, and A. Verkhratsky. 1995. "Activation of P2-purinoreceptors Triggered Ca²⁺ Release from InsP₃-sensitive Internal Stores in Mammalian Oligodendrocytes." *The Journal of Physiology* 483 (1): 41–57. <https://doi.org/10.1113/jphysiol.1995.sp020566>.
- Klyuch, B. P., N. Dale, and M. J. Wall. 2012. "Deletion of Ecto-5'-Nucleotidase (CD73) Reveals Direct Action Potential-Dependent Adenosine Release." *Journal of Neuroscience* 32 (11): 3842–47. <https://doi.org/10.1523/JNEUROSCI.6052-11.2012>.
- Kuba, Hiroshi, Konomi Koyano, and Harunori Ohmori. 2002. "Synaptic Depression Improves Coincidence Detection in the Nucleus Laminaris in Brainstem Slices of the Chick Embryo." *European Journal of Neuroscience* 15 (6): 984–990.
- Kügelgen, Ivar von. 2006. "Pharmacological Profiles of Cloned Mammalian P2Y-Receptor Subtypes." *New Developments in Receptor Pharmacology* 110 (3): 415–32. <https://doi.org/10.1016/j.pharmthera.2005.08.014>.
- Kukulski, F., S. A. Lévesque, E. G. Lavoie, J. Lecka, F. Bigonnesse, A. F. Knowles, S. C. Robson, T. L. Kirley, and J. Sévigny. 2005. "Comparative Hydrolysis of P2 Receptor Agonists by NTPDases 1, 2, 3 and 8." *Purinergic Signalling* 1 (2): 193–204.
- Kulesskaya, Natalia, Vootele V?ikar, Marjaana Peltola, Gennady G. Yegutkin, Marko Salmi, Sirpa Jalkanen, and Heikki Rauvala. 2013. "CD73 Is a Major Regulator of Adenosinergic Signalling in Mouse Brain." Edited by Tobias Eckle. *PLoS ONE* 8 (6): e66896. <https://doi.org/10.1371/journal.pone.0066896>.
- Langer, D., Y. Ikebara, H. Takebayashi, R. Hawkes, and H. Zimmermann. 2007. "The Ectonucleotidases Alkaline Phosphatase and Nucleoside Triphosphate Diphosphohydrolase 2 Are Associated with Subsets of Progenitor Cell Populations in the Mouse Embryonic, Postnatal and Adult Neurogenic Zones." *Neuroscience* 150 (4): 863–79. <https://doi.org/10.1016/j.neuroscience.2007.07.064>.
- Langer, David, Klaus Hammer, Patrycja Koszalka, Jürgen Schrader, Simon Robson, and Herbert Zimmermann. 2008. "Distribution of Ectonucleotidases in the Rodent Brain Revisited." *Cell and Tissue Research* 334 (2): 199–217. <https://doi.org/10.1007/s00441-008-0681-x>.
- Latini, Serena, and Felicita Pedata. 2001. "Adenosine in the Central Nervous System: Release Mechanisms and Extracellular Concentrations." *Journal of Neurochemistry* 79 (3): 463–484.
- Lazarowski, Eduardo R. 2012. "Vesicular and Conductive Mechanisms of Nucleotide Release." *Purinergic Signalling* 8 (3): 359–73. <https://doi.org/10.1007/s11302-012-9304-9>.
- Lian, Lu-Yun, Sravan R Pandalaneni, Paul A C Todd, Victoria M Martin, Robert D Burgoyne, and Lee P Haynes. 2014. "Demonstration of Binding of Neuronal Calcium Sensor-1 to the Ca(v)2.1 P/Q-Type Calcium Channel." *Biochemistry* 53 (38): 6052–62. <https://doi.org/10.1021/bi500568v>.
- Little, Joshua W, Amanda Ford, Ashley M Symons-Liguori, Zhoumou Chen, Kali Janes, Timothy Doyle, Jennifer Xie, et al. 2015. "Endogenous Adenosine A(3) Receptor Activation Selectively Alleviates Persistent Pain States." *Brain* 138 (1): 28–35. <https://doi.org/10.1093/brain/awu330>.
- Lloyd, H.G.E., and B.B. Fredholm. 1995. "Involvement of Adenosine Deaminase and Adenosine Kinase in Regulating Extracellular Adenosine Concentration in Rat Hippocampal Slices." *Neurochemistry International* 26 (4): 387–95. [https://doi.org/10.1016/0197-0186\(94\)00144-J](https://doi.org/10.1016/0197-0186(94)00144-J).
- Lopes, Luísa V., Nelson Rebola, Paulo C. Pinheiro, Peter J. Richardson, Catarina R. Oliveira, and Rodrigo A. Cunha. 2003. "Adenosine A3 Receptors Are Located in Neurons of the Rat Hippocampus." *Neuroreport* 14 (12): 1645–1648.

- Lovatt, D., Q. Xu, W. Liu, T. Takano, N. A. Smith, J. Schnermann, K. Tieu, and M. Nedergaard. 2012. "Neuronal Adenosine Release, and Not Astrocytic ATP Release, Mediates Feedback Inhibition of Excitatory Activity." *Proceedings of the National Academy of Sciences* 109 (16): 6265–70. <https://doi.org/10.1073/pnas.1120997109>.
- MacLean, Paul D., Burton S. Rosner, and Franklin Robinson. 1957. "Pyriform Responses to Electrical Stimulation of Olfactory Fila, Bulb and Tract." *American Journal of Physiology—Legacy Content* 189 (2): 395–400.
- Manabe, Hiroyuki, and Kensaku Mori. 2013. "Sniff Rhythm-Paced Fast and Slow Gamma-Oscillations in the Olfactory Bulb: Relation to Tufted and Mitral Cells and Behavioral States." *Journal of Neurophysiology* 110 (7): 1593. <https://doi.org/10.1152/jn.00379.2013>.
- Marangos, Paul J., Andrea M. Martino, Steven M. Paul, and Philip Skolnick. 1981. "The Benzodiazepines and Inosine Antagonize Caffeine-Induced Seizures." *Psychopharmacology* 72 (3): 269–73. <https://doi.org/10.1007/BF00431829>.
- Matveev, Victor, Robert S Zucker, and Arthur Sherman. 2004. "Facilitation through Buffer Saturation: Constraints on Endogenous Buffering Properties." *Biophysical Journal* 86 (5): 2691–2709.
- Mendonça, Alexandre de, and J.A. Ribeiro. 1996. "Adenosine and Neuronal Plasticity." *Life Sciences* 60 (4): 245–51. [https://doi.org/10.1016/S0024-3205\(96\)00544-9](https://doi.org/10.1016/S0024-3205(96)00544-9).
- Mendoza-Fernández, Victor, R. David Andrew, and Carlos Barajas-López. 2000. "ATP Inhibits Glutamate Synaptic Release by Acting at P2Y Receptors in Pyramidal Neurons of Hippocampal Slices." *Journal of Pharmacology and Experimental Therapeutics* 293 (1): 172–179.
- Mochida, Sumiko, Alexandra P. Few, Todd Scheuer, and William A. Catterall. 2008. "Regulation of Presynaptic CaV2.1 Channels by Ca²⁺ Sensor Proteins Mediates Short-Term Synaptic Plasticity." *Neuron* 57 (2): 210–16. <https://doi.org/10.1016/j.neuron.2007.11.036>.
- Moody, Catherine J., Parviz Meghji, and Geoffrey Burnstock. 1984. "Stimulation of P1-Purinoceptors by ATP Depends Partly on Its Conversion to AMP and Adenosine and Partly on Direct Action." *European Journal of Pharmacology* 97 (1): 47–54. [https://doi.org/10.1016/0014-2999\(84\)90511-9](https://doi.org/10.1016/0014-2999(84)90511-9).
- Moore, Kimberly A., Roger A. Nicoll, and Dietmar Schmitz. 2003. "Adenosine Gates Synaptic Plasticity at Hippocampal Mossy Fiber Synapses." *Proceedings of the National Academy of Sciences* 100 (24): 14397–14402.
- Morán-Jiménez, María-José, and Carlos Matute. 2000. "Immunohistochemical Localization of the P2Y1 Purinergic Receptor in Neurons and Glial Cells of the Central Nervous System." *Molecular Brain Research* 78 (1): 50–58. [https://doi.org/10.1016/S0169-328X\(00\)00067-X](https://doi.org/10.1016/S0169-328X(00)00067-X).
- Mulkey, RM, and RS Zucker. 1992. "Posttetanic Potentiation at the Crayfish Neuromuscular Junction Is Dependent on Both Intracellular Calcium and Sodium Ion Accumulation." *The Journal of Neuroscience* 12 (11): 4327.
- Muto, Junko, Hosung Lee, Hyunjin Lee, Akemi Uwaya, Jonghyuk Park, Sanae Nakajima, Kazufumi Nagata, Makoto Ohno, Ikuroh Ohsawa, and Toshio Mikami. 2014. "Oral Administration of Inosine Produces Antidepressant-like Effects in Mice." *Scientific Reports* 4: 4199. <https://doi.org/10.1038/srep04199>.
- Muzzi, Mirko, Elisabetta Coppi, Anna Maria Pugliese, and Alberto Chiarugi. 2013. "Anticonvulsant Effect of AMP by Direct Activation of Adenosine A1 Receptor." *Experimental Neurology* 250 (December): 189–93. <https://doi.org/10.1016/j.expneurol.2013.09.010>.

- Namba, Kazunori, Tokiko Suzuki, and Hiroyasu Nakata. 2010. "Immunogold Electron Microscopic Evidence of in Situ Formation of Homo- and Heteromeric Purinergic Adenosine A₁ and P2Y₂ Receptors in Rat Brain." *BMC Research Notes* 3 (1): 323. <https://doi.org/10.1186/1756-0500-3-323>.
- Namvar, Simin, Javad Mirnajafi-Zadeh, Yaghoub Fathollahi, and Maryam Zeraati. 2008. "The Role of Piriform Cortex Adenosine A₁ Receptors on Hippocampal Kindling." *The Canadian Journal of Neurological Sciences* 35 (02): 226–31. <https://doi.org/10.1017/S0317167100008684>.
- Narisawa, Sonoko, Nils Fröhlander, and José Luis Millán. 1997. "Inactivation of Two Mouse Alkaline Phosphatase Genes and Establishment of a Model of Infantile Hypophosphatasia." *Developmental Dynamics* 208 (3): 432–46. [https://doi.org/10.1002/\(SICI\)1097-0177\(199703\)208:3<432::AID-AJA13>3.0.CO;2-1](https://doi.org/10.1002/(SICI)1097-0177(199703)208:3<432::AID-AJA13>3.0.CO;2-1).
- Narisawa, Sonoko, Charlotte Wennberg, and José Luis Millán. 2001. "Abnormal Vitamin B₆ Metabolism in Alkaline Phosphatase Knock-out Mice Causes Multiple Abnormalities, but Not the Impaired Bone Mineralization." *The Journal of Pathology* 193 (1): 125–33. [https://doi.org/10.1002/1096-9896\(2000\)9999:9999<::AID-PATH722>3.0.CO;2-Y](https://doi.org/10.1002/1096-9896(2000)9999:9999<::AID-PATH722>3.0.CO;2-Y).
- Nascimento, Francisney P., Sonia M. Figueiredo, Rodrigo Marcon, Daniel F. Martins, Sérgio J. Macedo, Denise A. N. Lima, Rúbia C. Almeida, Rosana M. Ostroski, Ana Lúcia S. Rodrigues, and Adair Roberto Soares Santos. 2010. "Inosine Reduces Pain-Related Behavior in Mice: Involvement of Adenosine A₁ and A_{2A} Receptor Subtypes and Protein Kinase C Pathways." *Journal of Pharmacology and Experimental Therapeutics* 334 (2): 590. <https://doi.org/10.1124/jpet.110.166058>.
- Nascimento, Francisney Pinto, Sérgio José Macedo-Júnior, Fabrício Alano Pamplona, Murilo Luiz-Cerutti, Marina Machado Córdova, Leandra Constantino, Carla Inês Tasca, et al. 2015. "Adenosine A₁ Receptor-Dependent Antinociception Induced by Inosine in Mice: Pharmacological, Genetic and Biochemical Aspects." *Molecular Neurobiology* 51 (3): 1368–78. <https://doi.org/10.1007/s12035-014-8815-5>.
- Neher, Erwin, and Takeshi Sakaba. 2008. "Multiple Roles of Calcium Ions in the Regulation of Neurotransmitter Release." *Neuron* 59 (6): 861–72. <https://doi.org/10.1016/j.neuron.2008.08.019>.
- Neher, Jonas J, Urte Neniskyte, Tamara Hornik, and Guy C Brown. 2014. "Inhibition of UDP/P2Y(6) Purinergic Signaling Prevents Phagocytosis of Viable Neurons by Activated Microglia in Vitro and in Vivo." *Glia* 62 (9): 1463–75. <https://doi.org/10.1002/glia.22693>.
- Neville, Kevin R., and Lewis B. Haberly. 2003. "Beta and Gamma Oscillations in the Olfactory System of the Urethane-Anesthetized Rat." *Journal of Neurophysiology* 90 (6): 3921. <https://doi.org/10.1152/jn.00475.2003>.
- Noji, Tohru, Akira Karasawa, and Hideaki Kusaka. 2004. "Adenosine Uptake Inhibitors." *European Journal of Pharmacology* 495 (1): 1–16. <https://doi.org/10.1016/j.ejphar.2004.05.003>.
- Nörenberg, Wolfgang, and Peter Illes. 2000. "Neuronal P2X Receptors: Localisation and Functional Properties." *Naunyn-Schmiedeberg's Archives of Pharmacology* 362 (4): 324–39. <https://doi.org/10.1007/s002100000311>.
- Nousiainen, Heidi O., Ileana B. Quintero, Timo T. Myöhänen, Vootele Voikar, Jelena Mijatovic, Mikael Segerstråle, Annakaisa M. Herrala, et al. 2014. "Mice Deficient in Transmembrane Prostatic Acid Phosphatase Display Increased GABAergic Transmission and Neurological Alterations." Edited by Anna-Leena Sirén. *PLoS ONE* 9 (5): e97851. <https://doi.org/10.1371/journal.pone.0097851>.

- Ongini, Ennio, and Bertil B. Fredholm. 1996. "Pharmacology of Adenosine A_{2A} Receptors." *Trends in Pharmacological Sciences* 17 (10): 364–72. [https://doi.org/10.1016/S0165-6147\(96\)80010-1](https://doi.org/10.1016/S0165-6147(96)80010-1).
- Pankratov, Yuri, Ulyana Lalo, Alexei Verkhratsky, and R. Alan North. 2006. "Vesicular Release of ATP at Central Synapses." *Pflügers Archiv - European Journal of Physiology* 452 (5): 589–97. <https://doi.org/10.1007/s00424-006-0061-x>.
- Pankratov, Yuriy, Ulyana Lalo, Alexei Verkhratsky, and R. Alan North. 2007. "Quantal Release of ATP in Mouse Cortex." *The Journal of General Physiology* 129 (3): 257–65. <https://doi.org/10.1085/jgp.200609693>.
- Pascual, Olivier, Kristen B. Casper, Cathryn Kubera, Jing Zhang, Raquel Revilla-Sanchez, Jai-Yoon Sul, Hajime Takano, Stephen J. Moss, Ken McCarthy, and Philip G. Haydon. 2005. "Astrocytic Purinergic Signaling Coordinates Synaptic Networks." *Science* 310 (5745): 113. <https://doi.org/10.1126/science.1116916>.
- Pelegrin, Pablo, and Annmarie Surprenant. 2006. "Pannexin-1 Mediates Large Pore Formation and Interleukin-1 β Release by the ATP-Gated P2X(7) Receptor." *The EMBO Journal* 25 (21): 5071–82. <https://doi.org/10.1038/sj.emboj.7601378>.
- Pellerin, L, and P J Magistretti. 1994. "Glutamate Uptake into Astrocytes Stimulates Aerobic Glycolysis: A Mechanism Coupling Neuronal Activity to Glucose Utilization." *Proceedings of the National Academy of Sciences of the United States of America* 91 (22): 10625–29.
- Picher, Maryse, Lauranell H. Burch, Andrew J. Hirsh, Josef Spychala, and Richard C. Boucher. 2003. "Ecto 5'-Nucleotidase and Nonspecific Alkaline Phosphatase: TWO AMP-HYDROLYZING ECTOENZYME WITH DISTINCT ROLES IN HUMAN AIRWAYS." *Journal of Biological Chemistry* 278 (15): 13468–79. <https://doi.org/10.1074/jbc.M300569200>.
- Puchałowicz, Kamila, Maciej Tarnowski, Irena Baranowska-Bosiacka, Dariusz Chlubek, and Violetta Dziedziejko. 2014. "P2X and P2Y Receptors—Role in the Pathophysiology of the Nervous System." *International Journal of Molecular Sciences* 15 (12): 23672–704. <https://doi.org/10.3390/ijms151223672>.
- Puerto, Ana del, Francisco Wandosell, and Juan José Garrido. 2013. "Neuronal and Glial Purinergic Receptors Functions in Neuron Development and Brain Disease." *Frontiers in Cellular Neuroscience* 7. <https://doi.org/10.3389/fncel.2013.00197>.
- Quiroz, César, Rafael Luján, Motokazu Uchigashima, Ana Patrícia Simões, Talia N. Lerner, Janusz Borycz, Anil Kachroo, et al. 2009. "Key Modulatory Role of Presynaptic Adenosine A_{2A} Receptors in Cortical Neurotransmission to the Striatal Direct Pathway." *The Scientific World JOURNAL* 9: 1321–44. <https://doi.org/10.1100/tsw.2009.143>.
- Ralevic, Vera, and Geoffrey Burnstock. 1998. "Receptors for Purines and Pyrimidines." *Pharmacological Reviews* 50 (3): 413.
- Rebola, N., R.J. Rodrigues, L.V. Lopes, P.J. Richardson, C.R. Oliveira, and R.A. Cunha. 2005. "Adenosine A₁ and A_{2A} Receptors Are Co-Expressed in Pyramidal Neurons and Co-Localized in Glutamatergic Nerve Terminals of the Rat Hippocampus." *Neuroscience* 133 (1): 79–83. <https://doi.org/10.1016/j.neuroscience.2005.01.054>.
- Rebola, Nelson, Catarina R. Oliveira, and Rodrigo A. Cunha. 2002. "Transducing System Operated by Adenosine A_{2A} Receptors to Facilitate Acetylcholine Release in the Rat Hippocampus." *European Journal of Pharmacology* 454 (1): 31–38.
- Rebola, Nelson, Paulo C. Pinheiro, Catarina R. Oliveira, João O. Malva, and Rodrigo A. Cunha. 2003. "Subcellular Localization of Adenosine A₁ Receptors in Nerve Terminals and Synapses of the

Rat Hippocampus.” *Brain Research* 987 (1): 49–58. [https://doi.org/10.1016/S0006-8993\(03\)03247-5](https://doi.org/10.1016/S0006-8993(03)03247-5).

Regehr, W. G. 2012. “Short-Term Presynaptic Plasticity.” *Cold Spring Harbor Perspectives in Biology* 4 (7): a005702–a005702. <https://doi.org/10.1101/cshperspect.a005702>.

Rétey, J V, M Adam, E Honegger, R Khatami, U F O Luhmann, H H Jung, W Berger, and H-P Landolt. 2005. “A Functional Genetic Variation of Adenosine Deaminase Affects the Duration and Intensity of Deep Sleep in Humans.” *Proceedings of the National Academy of Sciences of the United States of America* 102 (43): 15676–81. <https://doi.org/10.1073/pnas.0505414102>.

Ribeiro, J. A. 1995. “Purinergic Inhibition of Neurotransmitter Release in the Central Nervous System.” *Pharmacology & Toxicology* 77 (5): 299–305. <https://doi.org/10.1111/j.1600-0773.1995.tb01031.x>.

Rittiner, Joseph E., Ilia Korboukh, Emily A. Hull-Ryde, Jian Jin, William P. Janzen, Stephen V. Frye, and Mark J. Zylka. 2012. “AMP Is an Adenosine A₁ Receptor Agonist.” *Journal of Biological Chemistry* 287 (8): 5301–9. <https://doi.org/10.1074/jbc.M111.291666>.

Robson, Simon C., Jean Sévigny, and Herbert Zimmermann. 2006. “The E-NTPDase Family of Ectonucleotidases: Structure Function Relationships and Pathophysiological Significance.” *Purinergic Signalling* 2 (2): 409–30. <https://doi.org/10.1007/s11302-006-9003-5>.

Rodrigues, R. J. 2005. “Dual Presynaptic Control by ATP of Glutamate Release via Facilitatory P2X1, P2X2/3, and P2X3 and Inhibitory P2Y1, P2Y2, And/Or P2Y4 Receptors in the Rat Hippocampus.” *Journal of Neuroscience* 25 (27): 6286–95. <https://doi.org/10.1523/JNEUROSCI.0628-05.2005>.

Rubio, Maria E., and Florentina Soto. 2001. “Distinct Localization of P2X Receptors at Excitatory Postsynaptic Specializations.” *Journal of Neuroscience* 21 (2): 641–653.

Russell, R. G. G. 1965. “Excretion of Inorganic Pyrophosphate in Hypophosphatasia.” *The Lancet* 286 (7410): 461–464.

Sala-Newby, Graciela B., Andrzej C. Skladanowski, and Andrew C. Newby. 1999. “The Mechanism of Adenosine Formation in Cells CLONING OF CYTOSOLIC 5'-NUCLEOTIDASE-I.” *Journal of Biological Chemistry* 274 (25): 17789–17793.

Sanchez-Vives, Maria V., and David A. McCormick. 2000. “Cellular and Network Mechanisms of Rhythmic Recurrent Activity in Neocortex.” *Nature Neuroscience* 3 (10): 1027.

Savaskan, N. E., L. Rocha, M. R. Kotter, A. Baer, G. Lubec, L. A. van Meeteren, Y. Kishi, et al. 2007. “Autotaxin (NPP-2) in the Brain: Cell Type-Specific Expression and Regulation during Development and after Neurotrauma.” *Cellular and Molecular Life Sciences* 64 (2): 230–43. <https://doi.org/10.1007/s00018-006-6412-0>.

Sawada, Keisuke, Noriko Echigo, Narinobu Juge, Takaaki Miyaji, Masato Otsuka, Hiroshi Omote, Akitsugu Yamamoto, and Yoshinori Moriyama. 2008. “Identification of a Vesicular Nucleotide Transporter.” *Proceedings of the National Academy of Sciences* 105 (15): 5683–5686.

Say, JoséC., Katia Ciuffi, Rosa P.M. Furriel, Pietro Ciancaglini, and Francisco A. Leone. 1991. “Alkaline Phosphatase from Rat Osseous Plates: Purification and Biochemical Characterization of a Soluble Form.” *Biochimica et Biophysica Acta (BBA) - General Subjects* 1074 (2): 256–62. [https://doi.org/10.1016/0304-4165\(91\)90161-9](https://doi.org/10.1016/0304-4165(91)90161-9).

Scemes, Eliana, David C Spray, and Paolo Meda. 2009. “Connexins, Pannexins, Innexins: Novel Roles of ‘hemi-Channels.’” *Pflugers Archiv: European Journal of Physiology* 457 (6): 1207–26.

<https://doi.org/10.1007/s00424-008-0591-5>.

- Schoen, S. W., and G. W. Kreutzberg. 1995. "Evidence That 5'-Nucleotidase Is Associated with Malleable Synapses—an Enzyme Cytochemical Investigation of the Olfactory Bulb of Adult Rats." *Neuroscience* 65 (1): 37–50.
- Sim, Joan A., Mark T. Young, Hye-Youn Sung, R. Alan North, and Annmarie Surprenant. 2004. "Reanalysis of P2X₇ Receptor Expression in Rodent Brain." *The Journal of Neuroscience* 24 (28): 6307. <https://doi.org/10.1523/JNEUROSCI.1469-04.2004>.
- Sippy, Tanya, Alberto Cruz-Martín, Andreas Jeromin, and Felix E Schweizer. 2003. "Acute Changes in Short-Term Plasticity at Synapses with Elevated Levels of Neuronal Calcium Sensor-1." *Nature Neuroscience* 6 (10): 1031–38. <https://doi.org/10.1038/nn1117>.
- Song, Xianmin, Wei Guo, Qiang Yu, Xiaofeng Liu, Zhenghua Xiang, Cheng He, and Geoffrey Burnstock. 2011. "Regional Expression of P2Y4 Receptors in the Rat Central Nervous System." *Purinergic Signalling* 7 (4): 469–88. <https://doi.org/10.1007/s11302-011-9246-7>.
- Sperlágh, Beáta, Attila Heinrich, and Cecilia Csölle. 2007. "P2 Receptor-Mediated Modulation of Neurotransmitter Release—an Update." *Purinergic Signalling* 3 (4): 269–84. <https://doi.org/10.1007/s11302-007-9080-0>.
- Sperlágh, Beáta, and E. Sylvester Vizi. 2011. "The Role of Extracellular Adenosine in Chemical Neurotransmission in the Hippocampus and Basal Ganglia: Pharmacological and Clinical Aspects." *Current Topics in Medicinal Chemistry* 11 (8): 1034–46. <https://doi.org/10.2174/156802611795347564>.
- Sperlágh, Beáta, E. Sylvester Vizi, Kerstin Wirkner, and Peter Illes. 2006. "P2X₇ Receptors in the Nervous System." *Progress in Neurobiology* 78 (6): 327–46. <https://doi.org/10.1016/j.pneurobio.2006.03.007>.
- Stevens, C F, and T Tsujimoto. 1995. "Estimates for the Pool Size of Releasable Quanta at a Single Central Synapse and for the Time Required to Refill the Pool." *Proceedings of the National Academy of Sciences of the United States of America* 92 (3): 846–49.
- Stout, Charles E., James L. Costantin, Christian C. G. Naus, and Andrew C. Charles. 2002. "Intercellular Calcium Signaling in Astrocytes via ATP Release through Connexin Hemichannels." *Journal of Biological Chemistry* 277 (12): 10482–88. <https://doi.org/10.1074/jbc.M109902200>.
- Strecker, R. E., Porkka-Heiskanen, T., Thakkar, M. M., Dauphin, L. J., Stenberg, D., and McCarley, R. W. 1999. Recent evidence that the sleep-promoting effects of adenosine are site specific. *Sleep* 22, S32.
- Street, S. E., N. J. Kramer, P. L. Walsh, B. Taylor-Blake, M. C. Yadav, I. F. King, P. Vihko, R. M. Wightman, J. L. Millan, and M. J. Zylka. 2013. "Tissue-Nonspecific Alkaline Phosphatase Acts Redundantly with PAP and NT5E to Generate Adenosine in the Dorsal Spinal Cord." *Journal of Neuroscience* 33 (27): 11314–22. <https://doi.org/10.1523/JNEUROSCI.0133-13.2013>.
- Suadicani, Sylvia O, Celia F Brosnan, and Eliana Scemes. 2006. "P2X(7) Receptors Mediate ATP Release and Amplification of Astrocytic Intercellular Ca(2+) Signaling." *The Journal of Neuroscience: The Official Journal of the Society for Neuroscience* 26 (5): 1378–85. <https://doi.org/10.1523/JNEUROSCI.3902-05.2006>.
- Sugimura, K., and A. Mizutani. 1979. "Histochemical and Cytochemical Studies of Alkaline Phosphatase Activity in the Synapses of Rat Brain." *Histochemistry* 61 (2): 123–29. <https://doi.org/10.1007/BF00496524>.

- Surprenant, A., F. Rassendren, E. Kawashima, R. A. North, and G. Buell. 1996. "The Cytolytic P_{2Z} Receptor for Extracellular ATP Identified as a P_{2X} Receptor (P_{2X}₇).” *Science* 272 (5262): 735. <https://doi.org/10.1126/science.272.5262.735>.
- Suzuki, N., and J. M. Bekkers. 2006. "Neural Coding by Two Classes of Principal Cells in the Mouse Piriform Cortex." *Journal of Neuroscience* 26 (46): 11938–47. <https://doi.org/10.1523/JNEUROSCI.3473-06.2006>.
- Suzuki, Norimitsu, and John M. Bekkers. 2012. "Microcircuits Mediating Feedforward and Feedback Synaptic Inhibition in the Piriform Cortex." *The Journal of Neuroscience* 32 (3): 919. <https://doi.org/10.1523/JNEUROSCI.4112-11.2012>.
- Taliaz, D, N Stall, D E Dar, and A Zangen. 2010. "Knockdown of Brain-Derived Neurotrophic Factor in Specific Brain Sites Precipitates Behaviors Associated with Depression and Reduces Neurogenesis." *Molecular Psychiatry* 15 (1): 80–92. <https://doi.org/10.1038/mp.2009.67>.
- Tang, Yun-gui, and Robert S. Zucker. 1997. "Mitochondrial Involvement in Post-Tetanic Potentiation of Synaptic Transmission." *Neuron* 18 (3): 483–91. [https://doi.org/10.1016/S0896-6273\(00\)81248-9](https://doi.org/10.1016/S0896-6273(00)81248-9).
- Thomson, L. F., J. M. Ruedi, A. Glass, G. Moldenhauer, P. Moller, M. G. Low, M. R. Klemens, M. Massaia, and A. H. Lucas. 1990. "Production and Characterization of Monoclonal Antibodies to the Glycosyl Phosphatidylinositol-Anchored Lymphocyte Differentiation Antigen Ecto-5'-Nucleotidase (CD73)." *Tissue Antigens* 35 (1): 9–19. <https://doi.org/10.1111/j.1399-0039.1990.tb01750.x>.
- Tonazzini, I., M. L. Trincavelli, J. Storm-Mathisen, C. Martini, and L. H. Bergersen. 2007. "Co-Localization and Functional Cross-Talk between A1 and P2Y1 Purine Receptors in Rat Hippocampus." *Eur J Neurosci* 26. <https://doi.org/10.1111/j.1460-9568.2007.05697.x>.
- Torres, Gonzalo E., Terrance M. Egan, and Mark M. Voigt. 1999. "Hetero-Oligomeric Assembly of P2X Receptor Subunits Specificities Exist with Regard to Possible Partners." *Journal of Biological Chemistry* 274 (10): 6653–6659.
- Tosh, Dilip K, Francesca Deflorian, Khai Phan, Zhan-Guo Gao, Tina C Wan, Elizabeth Gizewski, John A Auchampach, and Kenneth A Jacobson. 2012. "Structure-Guided Design of A(3) Adenosine Receptor-Selective Nucleosides: Combination of 2-Arylethynyl and Bicyclo[3.1.0]hexane Substitutions." *Journal of Medicinal Chemistry* 55 (10): 4847–60. <https://doi.org/10.1021/jm300396n>.
- Trieu, Brian H, Enikö A Kramár, Conor D Cox, Yousheng Jia, Weisheng Wang, Christine M Gall, and Gary Lynch. 2015. "Pronounced Differences in Signal Processing and Synaptic Plasticity between Piriform-Hippocampal Network Stages: A Prominent Role for Adenosine." *The Journal of Physiology* 593 (Pt 13): 2889–2907. <https://doi.org/10.1113/JP270398>.
- Trincavelli, Maria L., Matteo Marroni, Daniela Tuscano, Stefania Ceruti, Alessia Mazzola, Nico Mitro, Maria P. Abbracchio, and Claudia Martini. 2004. "Regulation of A2B Adenosine Receptor Functioning by Tumour Necrosis Factor α in Human Astroglial Cells." *Journal of Neurochemistry* 91 (5): 1180–1190. <https://doi.org/10.1111/j.1471-4159.2004.02793.x>.
- Trussell, Laurence O., Su Zhang, and Indira M. Ramam. 1993. "Desensitization of AMPA Receptors upon Multiquantal Neurotransmitter Release." *Neuron* 10 (6): 1185–96. [https://doi.org/10.1016/0896-6273\(93\)90066-Z](https://doi.org/10.1016/0896-6273(93)90066-Z).
- Tsodyks, Misha, Klaus Pawelzik, and Henry Markram. 1998. "Neural Networks with Dynamic Synapses." *Neural Computation* 10 (4): 821–35. <https://doi.org/10.1162/089976698300017502>.

- Tsodyks, Misha V., and Henry Markram. 1997. "The Neural Code between Neocortical Pyramidal Neurons Depends on Neurotransmitter Release Probability." *Proceedings of the National Academy of Sciences* 94 (2): 719–23.
- Vogel, M, H Kowalewski, H Zimmermann, N M Hooper, and A J Turner. 1992. "Soluble Low-Km 5'-nucleotidase from Electric-Ray (*Torpedo Marmorata*) Electric Organ and Bovine Cerebral Cortex Is Derived from the Glycosyl-Phosphatidylinositol-Anchored Ectoenzyme by Phospholipase C Cleavage." *Biochemical Journal* 284 (Pt 3): 621–24.
- Vongtau, H.O., E.G. Lavoie, J. Sévigny, and D.C. Molliver. 2011. "Distribution of Ecto-Nucleotidases in Mouse Sensory Circuits Suggests Roles for Nucleoside Triphosphate Diphosphohydrolase-3 in Nociception and Mechanoreception." *Neuroscience* 193 (October): 387–98. <https://doi.org/10.1016/j.neuroscience.2011.07.044>.
- Wang, Guan, James Gilbert, and Heng-Ye Man. 2012. "AMPA Receptor Trafficking in Homeostatic Synaptic Plasticity: Functional Molecules and Signaling Cascades." *Neural Plasticity* 2012: 825364. <https://doi.org/10.1155/2012/825364>.
- Wang, Ting-Fang, and Guido Guidotti. 1996. "CD39 Is an Ecto-(Ca, Mg)-Apyrase." *Journal of Biological Chemistry* 271 (17): 9898–9901.
- Waymire, Katrina G., J. Dennis Mahuren, J. Michael Jaje, Tomas R. Guilarte, Stephen P. Coburn, and Grant R. MacGregor. 1995. "Mice Lacking Tissue Non-Specific Alkaline Phosphatase Die from Seizures due to Defective Metabolism of Vitamin B-6." *Nat Genet* 11 (1): 45–51. <https://doi.org/10.1038/ng0995-45>.
- Weisman, Gary A, Lucas T Woods, Laurie Erb, and Cheikh I Seye. 2012. "P2Y Receptors in the Mammalian Nervous System: Pharmacology, Ligands and Therapeutic Potential." *CNS & Neurological Disorders Drug Targets* 11 (6): 722–38.
- Whyte, M P, J D Mahuren, K N Fedde, F S Cole, E R McCabe, and S P Coburn. 1988. "Perinatal Hypophosphatasia: Tissue Levels of Vitamin B6 Are Unremarkable despite Markedly Increased Circulating Concentrations of Pyridoxal-5'-phosphate. Evidence for an Ectoenzyme Role for Tissue-Nonspecific Alkaline Phosphatase." *Journal of Clinical Investigation* 81 (4): 1234–39.
- Whyte, M. P. 1995. Hypophosphatasia. In: Scriver, C. R., Beaudet, A. L., Sly, W. S., Valle, D. (Eds). *The Metabolic and Molecular Basis of Inherited Disease*, 7th edn. New York: McGraw-Hill, 4095–4111.
- Whyte, Michael P, Deborah Wenkert, William H McAlister, M Zulf Mughal, Anthony J Freemont, Richard Whitehouse, Eileen M Baillie, Stephen P Coburn, Lawrence M Ryan, and Steven Mumm. 2009. "Chronic Recurrent Multifocal Osteomyelitis Mimicked in Childhood Hypophosphatasia*." *Journal of Bone and Mineral Research* 24 (8): 1493–1505. <https://doi.org/10.1359/jbm.090308>.
- Wittendorp, Maria C., Hendrikus W.G.M. Boddeke, and Knut Biber. 2004. "Adenosine A3 Receptor-Induced CCL2 Synthesis in Cultured Mouse Astrocytes." *Glia* 46 (4): 410–418. <https://doi.org/10.1002/glia.20016>.
- Xu, Ji, Alexander M Bernstein, Angela Wong, Xiao-Hong Lu, Sheraz Khoja, X William Yang, Daryl L Davies, Paul Micevych, Michael V Sofroniew, and Baljit S Khakh. 2016. "P2X4 Receptor Reporter Mice: Sparse Brain Expression and Feeding-Related Presynaptic Facilitation in the Arcuate Nucleus." *The Journal of Neuroscience* 36 (34): 8902–20. <https://doi.org/10.1523/JNEUROSCI.1496-16.2016>.
- Xu, Jianhua, and Ling-Gang Wu. 2005. "The Decrease in the Presynaptic Calcium Current Is a Major Cause of Short-Term Depression at a Calyx-Type Synapse." *Neuron* 46 (4): 633–45. <https://doi.org/10.1016/j.neuron.2005.03.024>.

XU-FRIEDMAN, MATTHEW A., and WADE G. REGEHR. 2004. "Structural Contributions to Short-Term Synaptic Plasticity." *Physiological Reviews* 84 (1): 69. <https://doi.org/10.1152/physrev.00016.2003>.

Yaar, R., M.R. Jones, J.-F. Chen, and Katya Ravid. 2005. "Animal Models for the Study of Adenosine Receptor Function." *Journal of Cellular Physiology* 202 (1): 9–20. <https://doi.org/10.1002/jcp.20138>.

Yegutkin, Gennady G. 2008. "Nucleotide- and Nucleoside-Converting Ectoenzymes: Important Modulators of Purinergic Signalling Cascade." *Biochimica et Biophysica Acta (BBA) - Molecular Cell Research* 1783 (5): 673–94. <https://doi.org/10.1016/j.bbamcr.2008.01.024>.

Yoshioka, K., O. Saitoh, and H. Nakata. 2001. "Heteromeric Association Creates a P2Y-like Adenosine Receptor." *Proc Natl Acad Sci USA* 98. <https://doi.org/10.1073/pnas.121587098>.

Zhang, Dali, Wei Xiong, Stephanie Chu, Chao Sun, Benedict C. Albensi, and Fiona E. Parkinson. 2012. "Inhibition of Hippocampal Synaptic Activity by ATP, Hypoxia or Oxygen-Glucose Deprivation Does Not Require CD73." Edited by Steven Barnes. *PLoS ONE* 7 (6): e39772. <https://doi.org/10.1371/journal.pone.0039772>.

Zhang, Qi, Tina Pangršič, Marko Kreft, Mojca Kržan, Nianzhen Li, Jai-Yoon Sul, Michael Halassa, Elisabeth Van Bockstaele, Robert Zorec, and Philip G. Haydon. 2004. "Fusion-Related Release of Glutamate from Astrocytes." *Journal of Biological Chemistry* 279 (13): 12724–33. <https://doi.org/10.1074/jbc.M312845200>.

Zhou, Q Y, C Li, M E Olah, R A Johnson, G L Stiles, and O Civelli. 1992. "Molecular Cloning and Characterization of an Adenosine Receptor: The A3 Adenosine Receptor." *Proceedings of the National Academy of Sciences of the United States of America* 89 (16): 7432–36.

Zimmermann, Herbert. 2001. "Ectonucleotidases: Some Recent Developments and a Note on Nomenclature." *Drug Development Research* 52 (1–2): 44–56. <https://doi.org/10.1002/ddr.1097>.

Zimmermann, Herbert, Matthias Zebisch, and Norbert Sträter. 2012. "Cellular Function and Molecular Structure of Ecto-Nucleotidases." *Purinergic Signalling* 8 (3): 437–502. <https://doi.org/10.1007/s11302-012-9309-4>.

Zucker, Robert S., and Wade G. Regehr. 2002. "Short-Term Synaptic Plasticity." *Annual Review of Physiology* 64 (1): 355–405. <https://doi.org/10.1146/annurev.physiol.64.092501.114547>.

Zylka, Mark J, Nathaniel A Sowa, Bonnie Taylor-Blake, Margaret A Twomey, Annakaisa Herrala, Vootele Voikar, and Pirkko Vihko. 2008. "Prostatic Acid Phosphatase Is an Ectonucleotidase and Suppresses Pain by Generating Adenosine." *Neuron* 60 (1): 111–22. <https://doi.org/10.1016/j.neuron.2008.08.024>.

ABSTRACT

The functions of Tissue Nonspecific Alkaline Phosphatase (TNAP) in the brain are not clearly identified. The localization and expression of TNAP at the neuronal level, however, suggests that it plays a prominent role in the development and the function in the brain. This is supported by the presence of severe epileptic seizures in humans carrying TNAP mutation. These epileptic seizures are lethal in TNAP KO mice. Studies in mice show that TNAP could regulate GABA-mediated postsynaptic inhibition and may be involved in presynaptic inhibition mediated by adenosine. Adenosine is, partly, synthesized via the successive dephosphorylation of ATP to ADP and then to AMP by ectonucleotidases. Among them TNAP and ecto-5'-nucleotidase (NT5E) are able to hydrolyze AMP into adenosine. Adenosine acts mainly at the presynaptic level via A1 receptors activation. Adenosine has an influence on synaptic transmission and thus on synaptic plasticity. This could partly explain the epileptic seizures observed in TNAP knock-out mice. The two main purposes of my thesis were: (1) to evaluate the contribution of TNAP in adenosine production in the brain; (2) to study the influence of adenosine on synaptic plasticity.

Firstly, the study of the contribution of TNAP in adenosine production in the brain was carried out using two complementary approaches. A metabolomic approach (proton NMR spectroscopy) on whole brains of TNAP KO mice showed that TNAP is involved in adenosine synthesis in the brain. In a second approach, *in vitro* electrophysiological recordings on mouse brain slices allowed us to examine the consequences of the inhibition of the ectonucleotidases involved in adenosine synthesis. This revealed that inhibition of ectonucleotidases (TNAP and NT5E) did not suppress the inhibitory effect of AMP mediated by A1 receptors.

Secondly, we studied the influence of adenosine on short-term synaptic plasticity. Field potentials were recorded in response to electrical stimulations (3.125 to 100 Hz) applied with frequencies encompassing the range of physiological oscillation. Our results show that, with high adenosine concentrations, the facilitation is emphasized compared to that observed in the control situation. This effect is observed for frequencies greater than or equal to 25 Hz. In addition, the higher the frequency, the greater the facilitation. Finally, by blocking the action of endogenous adenosine, the opposite effect was observed: a deficient facilitation with respect to the control, whose defect was increasing with stimulation frequency.

All these results converge towards the hypothesis that TNAP deficiency, expressed by absence of adenosine, could contribute to the maintenance of the epileptic processes generated by an imbalance of the neuronal inhibition and the excitation due to a decrease of GABA. AMP inhibitory effect mediated by A1 receptors, would not be sufficient to counteract epileptic seizures observed in hypophosphatasic patients and TNAP KO mice.

Key-words: TNAP, adenosine, A1 receptors, plasticity, electrophysiology, AMP, ectonucleotidases, piriform cortex.

RESUME

Dans le cerveau, les fonctions de la phosphatase alcaline non spécifique des tissus (TNAP) ne sont pas clairement identifiées. La localisation et l'expression de cette enzyme au niveau neuronal suggère cependant, qu'elle joue un rôle important dans le développement et le fonctionnement du cerveau. Cela est supporté par la présence de graves crises d'épilepsie chez les humains porteurs d'une mutation de la TNAP. Ces crises d'épilepsie sont létales chez les souris KO pour la TNAP. Des études chez la souris montrent que la TNAP pourrait réguler l'inhibition postsynaptique médiée par le GABA et elle pourrait être impliquée dans l'inhibition présynaptique médiée par l'adénosine. L'adénosine est, en partie, synthétisée via la déphosphorylation successive de l'ATP en ADP puis en AMP par des ectonucléotidases. Parmi elles, la TNAP et l'ecto-5'-nucléotidase (NT5E) catalysent l'hydrolyse de l'AMP en adénosine dans le cortex cérébral. L'adénosine agit principalement au niveau présynaptique par l'intermédiaire des récepteurs A1. Ainsi l'adénosine a une influence sur la transmission synaptique et sur la plasticité synaptique. Ceci pourrait expliquer, en partie, les crises d'épilepsie observées chez les souris KO pour la TNAP. Les deux objectifs principaux de ma thèse ont été : (1) évaluer la contribution de la TNAP dans la production d'adénosine dans le cerveau ; (2) étudier l'influence de l'adénosine sur la plasticité synaptique.

Premièrement, l'étude de la contribution de la TNAP dans la production d'adénosine dans le cerveau a été réalisée au moyen de deux approches complémentaires. Une approche métabolomique (spectroscopie RMN du proton) sur des cerveaux entiers de souris KO pour la TNAP a permis de montrer que la TNAP participe, entre autre, à la synthèse d'adénosine dans le cerveau. Une deuxième approche, électrophysiologique sur tranches de cerveaux de souris *in vitro*, nous permet d'examiner les conséquences de l'inhibition des ectonucléotidases intervenant dans la synthèse de l'adénosine. Elle a révélé que l'inhibition des ectonucléotidases (TNAP et NT5E) ne supprime pas l'effet inhibiteur de l'AMP médiée par les récepteurs A1.

Deuxièmement, nous avons étudié l'influence de l'adénosine sur la plasticité synaptique à courte terme. Nous avons enregistré des potentiels de champs dans la couche la du cortex piriforme en réponse à des stimulations électriques (3,125 à 100 Hz) présentée avec des fréquences recouvrant la gamme d'oscillations physiologiques. Nos résultats montrent qu'avec de fortes concentrations d'adénosine, la facilitation est accentuée par rapport à celle observée en situation contrôle. Cet effet est observé pour des fréquences supérieures ou égales à 25 Hz. De plus, cette accentuation est d'autant plus grande que la fréquence est élevée (maximum atteint à 100 Hz pour 100 µM). En bloquant l'action de l'adénosine endogène, l'effet contraire est observé : une facilitation déficiente par rapport au contrôle et dont le défaut est croissant avec la fréquence de stimulation.

Tous ces résultats convergent vers l'hypothèse qu'une déficience en TNAP, traduite par une absence d'adénosine, pourrait contribuer au maintien des processus épileptiques générés par un déséquilibre de l'inhibition et de l'excitation dû à une diminution de GABA. L'effet inhibiteur de l'AMP médié par les récepteurs A1 ne serait pas suffisant pour contrecarrer les crises d'épilepsie observées chez les sujets hypophosphatasiques et les souris KO pour la TNAP.

Mots-clés : TNAP, adénosine, récepteur A1, plasticité, électrophysiologie, AMP, ectonucléotidases, cortex piriforme.